

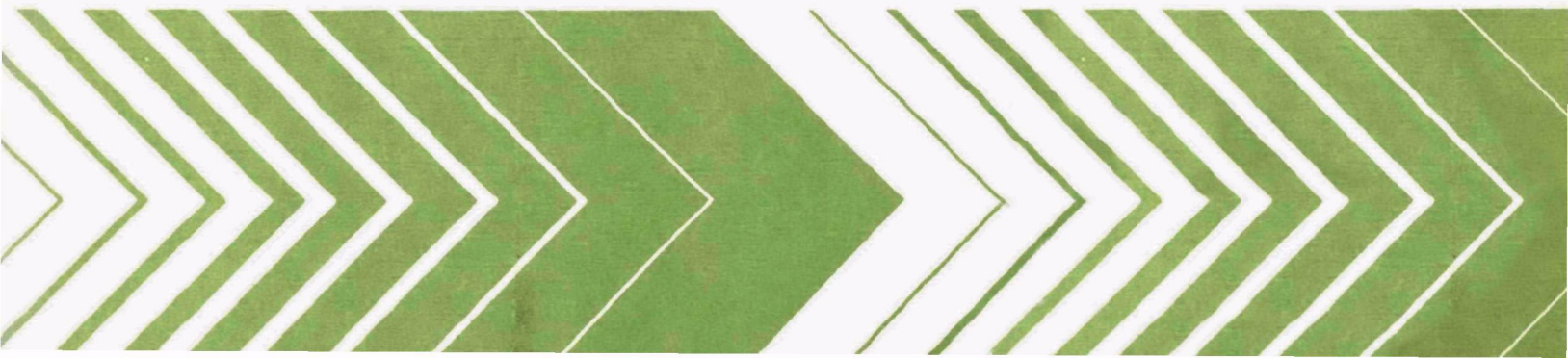
United States
Environmental Protection
Agency

Robert S. Kerr Environmental Research EPA 600/2-79-148
Laboratory
Ada OK 74820
August 1979

Research and Development



Irrigation Practices and Return Flow Salinity in Grand Valley



RESEARCH REPORTING SERIES

Research reports of the Office of Research and Development, U.S. Environmental Protection Agency, have been grouped into nine series. These nine broad categories were established to facilitate further development and application of environmental technology. Elimination of traditional grouping was consciously planned to foster technology transfer and a maximum interface in related fields. The nine series are:

1. Environmental Health Effects Research
2. Environmental Protection Technology
3. Ecological Research
4. Environmental Monitoring
5. Socioeconomic Environmental Studies
6. Scientific and Technical Assessment Reports (STAR)
7. Interagency Energy-Environment Research and Development
8. "Special" Reports
9. Miscellaneous Reports

This report has been assigned to the ENVIRONMENTAL PROTECTION TECHNOLOGY series. This series describes research performed to develop and demonstrate instrumentation, equipment, and methodology to repair or prevent environmental degradation from point and non-point sources of pollution. This work provides the new or improved technology required for the control and treatment of pollution sources to meet environmental quality standards.

EPA-600/2-79-148
August 1979

IRRIGATION PRACTICES AND RETURN FLOW SALINITY
• IN GRAND VALLEY

by

Gaylord V. Skogerboe
David B. McWhorter
James E. Ayars
Department of Agricultural and Chemical Engineering
Colorado State University
Fort Collins, Colorado 80523

Grant No. S-800687

Project Officer

James P. Law, Jr.
Source Management Branch
Robert S. Kerr Environmental Research Laboratory
Ada, Oklahoma 74820

ROBERT S. KERR ENVIRONMENTAL RESEARCH LABORATORY
OFFICE OF RESEARCH AND DEVELOPMENT
U.S. ENVIRONMENTAL PROTECTION AGENCY
ADA, OKLAHOMA 74820

DISCLAIMER

This report has been reviewed by the Robert S. Kerr Environmental Research Laboratory, U. S. Environmental Protection Agency, and approved for publication. Approval does not signify that the contents necessarily reflect the views and policies of the U. S. Environmental Protection Agency, nor does mention of trade names or commercial products constitute endorsement or recommendation for use.

FOREWORD

The Environmental Protection Agency was established to coordinate administration of the major Federal programs designed to protect the quality of our environment.

An important part of the Agency's effort involves the search for information about environmental problems, management techniques and new technologies through which optimum use of the Nation's land and water resources can be assured and the threat pollution poses to the welfare of the American people can be minimized.

EPA's Office of Research and Development conducts this search through a nationwide network of research facilities.

As one of these facilities, the Robert S. Kerr Environmental Research Laboratory is responsible for the management of programs to: (a) investigate the nature, transport, fate and management of pollutants in groundwater; (b) develop and demonstrate methods for treating wastewaters with soil and other natural systems; (c) develop and demonstrate pollution control technologies for irrigation return flows; (d) develop and demonstrate pollution control technologies for animal production wastes; (e) develop and demonstrate technologies to prevent, control or abate pollution from the petroleum refining and petrochemical industries; and (f) develop and demonstrate technologies to manage pollution resulting from combinations of industrial wastewaters or industrial/municipal wastewaters.

This report contributes to the knowledge essential if the EPA is to meet the requirements of environmental laws that it establish and enforce pollution control standards which are reasonable, cost effective and provide adequate protection for the American public.

William C. Galegar

William C. Galegar
Director
Robert S. Kerr Environmental
Research Laboratory

PREFACE

This report is the first in a series of two reports resulting from U.S. Environmental Protection Agency Grant No. S-800687, "Irrigation Practices, Return Flow Salinity and Crop Yields." This report focuses upon the prediction of subsurface irrigation return flow salinity. The second report, "Potential Effects of Irrigation Practices on Crop Yields in Grand Valley," focuses upon the impact of various irrigation practices in determining crop yields, with particular emphasis on corn and wheat. These reports have been used as input to another research project conducted in Grand Valley and largely funded by the U.S. Environmental Protection Agency under Grant No. S-802985, "Implementation of Agricultural Salinity Control Technology in Grand Valley."

Three reports have been produced under Grant No. S-802985. The first report, "Implementation of Agricultural Salinity Control Technology in Grand Valley," describes the design, construction and operation of a variety of salinity control technologies implemented on farmers' fields. The second report, "Evaluation of Irrigation Methods for Salinity Control in Grand Valley," is concerned with the evaluation of furrow, border, sprinkler and trickle irrigation as individual salinity control alternatives. The third report of this series, "Best Management Practices for Salinity Control in Grand Valley," develops the methodology for determining the cost-effectiveness of individual salinity control measures, as well as a complete package of salinity control measures that should be implemented in the Grand Valley.

ABSTRACT

This study was undertaken to evaluate the effects of the volume of leachate on the quality of the leachate. A numerical model of salt transport developed by Dutt et al. (24) was used in the study. Field data were collected on 63 research plots located in the Grand Valley and used to test and calibrate the model. The model was used in a series of hypothetical simulations designed to provide the required information.

From the calibration of the moisture flow model using infiltration data, water content profiles, and storage change data, it was concluded that water flow could be adequately modeled for the Grand Valley. The functional relations used for hydraulic conductivity and soil-water diffusivity and the method of averaging the values of the hydraulic parameters were developed during the course of the study.

From comparisons of simulated and field data used in evaluating the chemistry model, it was concluded that total dissolved solids (TDS) concentrations were adequately modeled but that individual ionic species concentrations were not. Comparison of calculated and measured data indicate that the $\text{CaSO}_4\text{-CaCO}_3\text{-Ca(HCO}_3)_2$ system is not properly modeled for the soils in the Grand Valley.

Data for single growing season simulations using 7- and 14-day irrigation schedules and 2%, 5%, 20% and 40% leaching increments, coupled with data from a 6-year simulation using a 14-day irrigation interval and 20% leaching increment, indicate that the salt concentration of the leachate at the bottom of the soil profile is independent of the volume of leachate. The TDS profile calculated at the beginning and end of the growing season show the concentration of salt in the profile below the root zone to be relatively constant. This region acts as a buffer and caused the salt concentration of the return flow to be relatively constant. This means the reductions in salt loading are directly proportional to reductions in the volume of return flow.

This report was submitted in fulfillment of Grant No. S-800687 by Colorado State University under the sponsorship of the U.S. Environmental Protection Agency. This report covers the period of February 18, 1974 to June 17, 1977 and was completed as of August 31, 1978.

CONTENTS

Foreword	iii
Preface	iv
Abstract	v
Figures	viii
Tables	x
List of Symbols	xii
Acknowledgements	xiv
1. Introduction	1
2. Conclusions	5
3. Recommendations	8
4. Experimental Design	10
Study Area	10
Locating a Project Site	12
Design of Irrigation and Drainage Systems	15
Construction of Plots	28
Installation of Vacuum Soil Moisture Extractors	32
Treatments	38
Data Collection and Instrumentation	40
5. Soil Moisture and Salt Transport Models	44
Solutions of Water Flow Equation	44
Sink Strength	50
Soil Properties	51
Salt Transport	52
6. Model Description	58
Moisture Flow Program	58
Biological-Chemical Program	68
7. Model Results	79
Moisture Flow Model	79
Chemical Model	89
Simulation of Hypothetical Cases	100
8. Prediction of Return Flow Salinity	125
Geology and Subsurface Hydrology	125
Prediction of Salt Load	142
References	143
Appendices	
A. Soil properties and evapotranspiration data	151
B. Simulated data	154
C. Analysis of field data	162
D. Listing of Program SORPT	163
E. Listing of Biological-Chemical Program	166

FIGURES

<u>Number</u>		<u>Page</u>
1	Geology of the Grand Valley	11
2	Map of the Grand Valley showing areas of positive site location	13
3	Pictures of the Giddings rig and jetting rig	14
4	Map showing location of the Matchett farm	16
5	Map showing the fields used for the study area	17
6	Plots in Field I	19
7	Plots in Field II	20
8	Plots in Field III	21
9	Plot cross-section with drain details	22
10	Plan view of drainage system detail	23
11	Typical manhole installation	25
12	Irrigation system control valves	27
13	Flow measurement structures containing 30° V-notch weir for measuring quantity of irrigation water applied to each plot	29
14	Pictures showing use of the grade rod	30
15	Placement of grade stakes in trench	31
16	Placement of rolled curtain on the trench floor	31
17	Unrolling of curtain and placement against trench wall	33
18	Sealing the PVC curtain at corners	33
19	Method of sealing the curtain around the drainage pipe	34
20	Field installation soil moisture vacuum extractors	36
21	Hydraulic ram used to auger and shape holes for lysimeter pans	37
22	Construction of lysimeter pans	37
23	Housing for vacuum units	39
24	Vacuum units	39
25	Grid system used for one-dimensional finite differencing	47
26	Spacial division of soil-plant water system along a flow line	59
27	Grid system used for finite differencing Richards' equation	61
28	Saturation domains used for fitting Su and Brooks parameters	66
29	Generalized block diagram of Moisture Flow model	69
30	Generalized block diagram of Biological-Chemical Program	71
31	Generalized block diagram of subroutine XCHANGE	72
32	Soil-water characteristic used in study	82
33	Moisture content profiles in Plot 30 used to calibrate the flow model	86
34	Moisture content profiles in Plot 25 used to calibrate the flow model	87
35	Computed and measured concentrations of Mg^{++} , Na^+ and Ca^{++} in soil solution at a depth of 1.1 m in Plot 23	93
36	Computed and measured concentrations of $SO_4^{=}$, HCO_3 , and Cl^- in soil solution at a depth of 1.1 m in Plot 23	94

<u>Number</u>		<u>Page</u>
37	Computed and measured TDS concentrations in soil solutions at a depth of 1.1 m in Plot 25	95
38	Cumulative leachate as a function of cumulative infiltration calculated by hypothetical simulations using a 7-day irrigation interval	105
39	Cumulative leachate as a function of cumulative infiltration calculated by hypothetical simulations using a 14-day irrigation interval	106
40	Chloride concentration profiles calculated by hypothetical simulations using 7-day irrigation interval	109
41	Chloride concentration profiles calculated by hypothetical simulations using a 14-day irrigation interval	110
42	TDS and chloride concentrations as a function of cumulative leachate at a depth of 2.1 m calculated by hypothetical simulations using a 7-day irrigation interval	113
43	TDS and chloride concentrations as a function of cumulative leachate at a depth of 2.1 m calculated by hypothetical simulations using a 14-day irrigation interval	114
44	(TDS-Cl) concentration as a function of cumulative leachate at a depth of 2.1 m calculated by 6-year hypothetical simulations using 20% leaching increment and 14-day irrigation interval	119
45	TDS and chloride concentration profiles at day 293 calculated by a 6-year hypothetical simulation using 20% leaching increment and 14-day irrigation interval	120
46	Chloride concentration profiles for second year of 2-year simulation calculated by hypothetical simulations using a 14-day irrigation interval, 20% leaching increment and 2 winter conditions	122
47	Chloride concentration profiles at day 293 calculated by hypothetical simulations using a 14-day irrigation interval, 20% leaching increment and 2 winter conditions	123
48	Natural washes, canals and boundary of irrigated lands in the Grand Valley	126 127
49	Cobble aquifer cross-section	
50	Monitoring network for the Grand Valley Salinity Control Demonstration Project	132
51	Calcium-magnesium ratios for selected ground and surface water samples in the Grand Valley	135
52	Location of wells installed by the Agricultural Research Service in western Grand Valley	140

TABLES

<u>Number</u>		<u>Page</u>
1	Moisture Content Profiles at a Depth of 1.52 to 2.13 meters for Selected Plots	80
2	Parameters Used in Hydraulic Conductivity and Diffusivity Functions	83
3	Moisture Content Profiles From Plot 30 Used for Model Calibration	85
4	Moisture Content Profiles From Plot 25 Used for Model Calibration	88
5	Simulated Volumetric Moisture Content at 2.13 meters Using 14-day Irrigation Schedule and 20 Percent Leaching Increment	89
6	1975 Irrigation Water Analysis (ppm)	90
7	Initial Chemical Profile and Soil Data for Plot 23, Matchett Farm, 1975	91
8	Irrigation Treatments on Plot 23 in 1975 Used to Calibrate Chemical Model	92
9	pK Analysis of Soil Solution Extract at 1.1 m on Plot 23, Matchett Farm, 1975	97
10	Concentrations Calculated at 1.1 m Depth With Gypsum - 25 meq/100 gm in all Horizons	98
11	pK Values for Selected Ions	98
12	Plot 23 Concentration at 2.13 m Predicted Using $P_{CO_2}=7$ matm	100
13	Chemical Composition of Drainage Water From Field II, Matchett Farm, 1975	101
14	Cumulative Infiltration for 150-day Hypothetical Simulations Using 7-day and 14-day Irrigation Schedules	103
15	Cumulative Leachate at 2.1 m for 150-day Hypothetical Simulations Using 7- and 14-day Irrigation Schedules	103
16	Leaching Fractions Computed for 7- and 14-day Irrigation Schedules	103
17	Variation of Volume of Solution in Soil Segment at the Lower Boundary for Simulations Used in the Study	111
18	TDS Concentration and Chloride Concentration in Cumulative Leachate at 2.13 m for 6-year Hypothetical Simulation Using 14-day Irrigation Schedule and 20% Leaching Increment	115
19	Chloride Concentration Profiles for 6-year Simulation Using 14-day Irrigation Schedule and 20% Leaching Increment	117
20	Average Water Equivalent Depth Used for Winter Simulations	121
21	Concentration of Salts in Soil Solution, Matchett Farm, 1976	129
22	Total Dissolved Solids of Drainage Water From Field III, Matchett Farm, 1975	131
23	Salinity of Natural Wash Discharges in the Grand Valley	131

<u>Number</u>		<u>Page</u>
24	Salinity of Open Drains in the Grand Valley Salinity Control Demonstration Project Area	133
25	Location, Depth and Top Elevation of Two-inch Diameter Wells In the Grand Valley Salinity Control Demonstration Project . .	137
26	Selected Salinity Data for CSU Well No. 12 Located Near the Intersection of 31 and F Roads in the Grand Valley Salinity Control Demonstration Project Area	137
27	Selected Salinity Data for Wells Located Along D Road in the Grand Valley Salinity Control Demonstration Project	138
28	Selected Salinity Data for Wells Installed by the Agricultural Research Service (SEA) in Western Grand Valley	141
A-1	Soil Properties for Billings Salty Clay Loam, Matchett Farm Soil Moisture Characteristic	151
A-2	Initial Soil Moisture Distribution Used for Simulations	151
A-3	Equations Used to Calculate Evapotranspiration	152
A-4	Irrigation Schedule for the Corn Crop Used in the Simulation 14-day Irrigation Schedule, 7-day Irrigation Schedule	153
B-1	Simulation Data for Plot 23, Matchett Farm with $P_{CO_2}=7$ matm Day 166-196, 1975	154
B-2	Simulation Data for Plot 23, Matchett Farm, Day 166-196, 1975 .	154
B-3	TDS Concentrations and Chloride Concentrations in Cumulative Leachate at 2.13 m for Hypothetical Simulation Using 7-day Irrigation Schedule	155
B-4	TDS Concentrations and Chloride Concentrations in Cumulative Leachate at 2.13 m for Hypothetical Simulation Using 14-day Irrigation Schedule	157
B-5	Chloride Concentration Profiles (ppm) for Hypothetical Simulations Using 14-day Irrigation Schedule	159
B-6	Chloride Concentration Profiles (ppm) for Hypothetical Simulations Using 7-day Irrigation Schedule	160
B-7	Chloride Concentration Profiles (ppm) for Day 293 of 2nd Year in a 2-year Hypothetical Simulation Using 20% Leaching Increment and 14-day Irrigation Schedule	161
B-8	TDS Concentration Profiles (ppm) for 6-year Simulation	161
C-1	Chemical Analysis of Soil Solution Extracted at a Depth of 1.1 Meters in Plot 23 on the Matchett Farm in 1975	162
C-2	pK Analysis of Drainage Water Samples Collected on Matchett Farm, 1975	162

LIST OF SYMBOLS

<u>Symbol</u>	<u>Description*</u>
a	domain of saturation associated with concave portion of soil-water characteristic
A	area (L^2)
A(Z)	plant root extraction term (L)
b	domain of saturation associated with convex portion of soil-water characteristic
c	solute concentration (m/L^3)
C	specific water capacity (1/L)
D	diffusion-dispersion coefficient (L^2/T)
D(θ)	soil-water diffusivity (L^2/T)
E_t^+	evapotranspiration = volume per unit area (L)
ET^+	evapotranspiration = volume per unit area (L)
FR'	solution flux computed using Darcy's law (L/T)
g	acceleration due to gravity (L/T^2)
h	soil-water pressure head (L)
H	piezometric head (L)
i	finite difference index
I	infiltration rate (L/T)
j	finite difference index
K(θ)	hydraulic conductivity as function of water content (L/T)
K_s	saturated hydraulic conductivity (L/T)
K_{sp}	solubility product for chemical species
m^\ddagger	shape factor used in Su and Brooks representation of soil-water characteristic
P	volume of precipitation per unit area ($L^3/L^2 = L$)

*The units given in parenthesis are: m for mass, L for length, and T for time.

^+E_t and ET are used interchangeably.

‡ Although this symbol usually represents mass, it has been used in the text as a shape factor to conform with the original work by Su and Brooks.

<u>Symbol</u>	<u>Description</u>
P_a	Pascal (m/LT^2)
P_b	bubbling pressure (m/LT^2)
P_c	capillary pressure (m/LT^2)
P_i	inflection capillary pressure (m/LT^2)
q	solution flux (L/T)
S	water-content saturation
S_e	effective saturation
S_r	residual saturation
t	time (T)
v	volumetric flux (L/T)
V_i	volume of intercepted water (L^3)
V_L	volume of leakage (L^3)
V_r	volume of runoff (L^3)
V_s	volume of water stored in a partially saturated zone (L^3)
V_w	volume of ground water storage (L^3)
β	volume of water stored in soil segment (L)
γ_1	monovalent activity coefficient
γ_2	divalent activity coefficient
θ	volumetric water content (L^3/L^3)
θ_R	water content at residual saturation (L^3/L^3)
θ_s	water content at saturation (L^3/L^3)
λ	pore-size distribution index
ρ	density of solution (m/L^3)
Z	depth (L)

ACKNOWLEDGEMENTS

The extreme 1972-1973 winter conditions in Grand Valley prevented the site selection process from being undertaken until the last half of March 1973. The cooperation and public-spirited attitude of the landowner, Mr. Kenneth Matchett, in leasing the necessary site was deeply appreciated. A high degree of cooperation and support facilitated the undertaking and completion of the construction process.

In order to get construction under way required the swift cooperation and efforts by the Project Officer, Dr. James P. Law, Jr.; the Colorado State University (CSU) College of Engineering purchasing agent, Mr. O. K. Warren; and Mr. Ronald Jaynes, salesman for Grand Junction Pipe and Supply Company, who submitted the low bids for the drainage and irrigation system materials. The construction of the drainage system was accomplished by Smith Welding and Construction Company of Grand Junction. Mr. Delbert Smith, President, was extremely cooperative in meeting the special construction requirements of this project. The construction, field installation, and successful operation of the vacuum soil moisture extractors resulted from the conscientious efforts of Mr. John Brookman of CSU.

Numerous project personnel worked long and hard hours during the construction of facilities and during cultivating, planting and field data collection. The assistance in the collection of field data by Messrs. George Bargsten, John Bargsten, Robert Evans and Berry Treat and the remaining staff and field personnel of the Grand Junction office is deeply appreciated. In addition, the diligent efforts of Ms. Barbara Mancuso and Mr. Sam Marutzky in the laboratory were very important to the project.

Much of this report resulted from the efforts of James E. Ayars in completing a Ph.D. dissertation. The authors wish to thank the other members of Mr. Ayars' committee; Dr. Arnold Klute and Dr. Harold Duke, for their extensive review of this work. Also, the discussion with Dr. Sterling Olsen and Dr. John Laronne have been very helpful.

Finally, the authors appreciate very much the efforts of Ms. Diane English and Ms. Mary Lindburg in typing the drafts and final copy of this report.

Gaylord V. Skogerboe
David B. McWhorter
James E. Ayars

SECTION 1

INTRODUCTION

BACKGROUND

The Colorado River Basin typifies the problems and the future needs for river management. The Colorado River currently provides irrigation water to seven states: Colorado, Wyoming, Utah, Arizona, New Mexico, California, Nevada, as well as to the Republic of Mexico. In addition to agricultural uses, the Colorado River also provides water to the cities of Los Angeles, San Diego, Denver, and many others.

Holburt (40) estimates that unless salinity control measures are instituted, the salinity levels at Imperial Dam, the lowest diversion point in the United States, will have increased from their current 870 parts per million (ppm) to over 1300 ppm by the turn of the century. To maintain the current concentration of salinity, roughly 2.7×10^9 kilograms (kg) of salt will have to be removed yearly from the Colorado River to offset the projected growth in the basin.

These growth projections were made before the energy shortage raised the spectre of supplying large quantities of water to various energy complexes; water which would be taken from the headwaters of the Colorado River and be of the highest quality possible. The challenge facing agriculture in the Colorado River Basin is to minimize return flow while maintaining a productive industry.

PROBLEM

The Colorado River Basin lies in the arid and semi-arid west and exemplifies the problems of production faced by irrigated agriculture in arid areas. As irrigation was introduced to virgin lands and an irrigated agriculture developed, leaching of salts from the soils occurred. As new irrigation projects were developed, the return flows increased and the salinity loading of the river increased due to two factors. The first, salt-loading, is due to the mineral dissolution occurring in the soil profile. The second effect, concentration of salts, is the result of the consumption of pure water through evaporation and transpiration.

In the Colorado River Basin there are several irrigated valleys which contribute large salt loads to the river. One of the largest of these is the Grand Valley located in western Colorado. Irrigation started in the Grand Valley in the 1880's and developed over the years until roughly 30,350

hectares (ha) were developed for irrigation. Of the total developed land, about 12,000 ha have been damaged due to salinization and urbanization.

As irrigation developed on the higher lands away from the river, excess water from deep percolation, low soil hydraulic conductivity and a soil of marine origin combined to destroy the productive capability of the land. High water tables near the river contributed to the upward movement of water which evaporated from the soil surface leaving a deposit of salt, thus taking the land out of production.

Studies have been conducted in the Grand Valley since 1908 on methods to alleviate the high water tables and restore the land to a productive state. The most recent series of studies began in 1968 with the Grand Valley Salinity Control Demonstration Project. In this study, seepage of water from the canals and laterals in the demonstration area was investigated. The resulting seepage data, along with hydraulic and hydrologic data for the region, were used to estimate salt loading of the Colorado River due to irrigation in the Grand Valley. Skogerboe and Walker (75) found that the diversion of water into the canals of Grand Valley's irrigation system amount to 27,420 cubic meters (m^3) of water diverted for each hectare under cultivation of which 10,050 m^3 was spilled. They estimated a salt loading of 6.35×10^5 to 9.07×10^5 metric tons of salt annually from the Grand Valley. The salt originates in the marine soils of the valley and in salt lenses found in the Mancos shale which underlies this region. It is dissolved by percolation water from irrigation and seepage from canals and laterals and is carried to the river. The final step in the investigation was to line portions of the canals studied and again estimate losses due to seepage. From these data, the effect of a program of canal lining was evaluated and estimates of the cost of control were made.

On-farm water management practices were studied next. These studies included installing drainage for salinity control and irrigation scheduling to improve water management. It was believed that drainage would intercept return flows from irrigation before they reached chemical equilibrium with the underlying shale. Since concentrations of deep percolation beneath the soil profile are about 3000 ppm salt while salinity levels leaving the shale are as high as 9000 ppm salts, it was theorized that a significant reduction in salt load could be made by intercepting the subsurface return flow before it picked up additional salt from the underlying shale. Due to the low hydraulic conductivities of the soil, the required spacings for the subsurface drains are 30 meters (m). This means that parallel relief drains as a salinity control measure are quite expensive (1).

Irrigation scheduling was investigated to evaluate the effect of supplying water as needed to meet crop needs plus the required leaching fraction. These studies indicated that, at the time of the study, irrigation scheduling for salinity control had only a marginal effect because of poor on-farm control of water. However, irrigation scheduling was found to be essential in a program of total water management in the valley which has as its goal the reduction of saline return flows (81).

PROJECT OBJECTIVES

Previous studies conducted on methods of salinity control in the Grand Valley assumed that the concentration of salt in the subsurface return flow was dependent of the volume of the return flow. This implied that any method which reduced the volume of return flow would effect a similar reduction in the salt load. The current study was designed to evaluate the validity of this assumption.

A total of eight objectives were outlined for this research project:

1. Evaluate the effects of various irrigation practices and chemical quality of return flows.
2. Evaluate the effects of various irrigation practices on crop yields and fertilizer requirements.
3. Demonstrate that improved farm management of irrigation water can reduce the mineral content of return flows.
4. Demonstrate that improving the chemical quality of irrigation return flows through better farm irrigation practices is profitable due to increased crop yields and reduced fertilizer expense.
5. Provide a better understanding of the manner in which water quality degradation takes place as a result of irrigation.
6. Develop recommendations regarding irrigation systems, methods, and practices which will minimize the chemical quality of return flows while maintaining a good crop environment and maximum benefits from the consumed water.
7. Develop procedures for projecting the findings of this study to basin-wide evaluations.
8. Provide useful information for future salinity studies concerned with farm management.

This particular report addresses objectives 1, 3, 5, 7, and 8. An accompanying report, "Potential Effects of Irrigation Practices on Crop Yields in Grand Valley," will address the remaining objectives. The results of these two reports were utilized in preparing the reports, "Evaluation of Irrigation Methods for Salinity Control in Grand Valley" and "Best Management Practices" for Salinity Control in Grand Valley" under EPA Grant No. S-802985. The results of this particular report regarding the methodology for soil moisture-chemistry simulation has been incorporated into an "Environmental Planning Manual for Salinity Management in Irrigated Agriculture" under EPA Grant No. R-804672.

SCOPE

Before a valley-wide action salinity control program can be implemented in Grand Valley, it becomes essential that salt load reductions occurring in

the Colorado River can be predicted as a result of reducing subsurface irrigation return flows by constructing physical facilities and improving water management practices to insure that the program will be cost-effective.

In order to relate chemical quality to reduced subsurface return flows, this particular study focused upon the adaptation and evaluation of a numerical model which could be used to characterize the salt transport occurring in the soils of the Grand Valley. A numerical model developed by Dutt et al. (24), which is currently being used by the Bureau of Reclamation, USDI, was selected for use in the study. The method of calculating the value of hydraulic conductivity and diffusivity used in the difference equation of the soil-water flow program was changed from that found in Dutt's model (24). Also, the functional relationships used to calculate hydraulic conductivity and diffusivity were changed. The soil-water flow and soil-chemistry data used in the evaluation of the model were collected as part of an on-going study in which the effect of irrigation on crop yields and salinity of deep percolation was investigated.

The research was conducted on 63 research plots located on a 9.3 ha site in the Grand Valley. Eight irrigation treatments, four crops, and two fertilization treatments were used to generate the moisture flow and salt transport data required to calibrate the numerical model.

Once the evaluation was completed, the model was used to simulate a series of hypothetical irrigation treatments. The irrigation schedules in the hypothetical simulations used either 7- or 14-day irrigation intervals and a depth of irrigation equal to the evapotranspiration in the interval plus a leaching increment which ranged from 1% to 40% of estimated evapotranspiration. The evapotranspiration for the simulations was estimated using meteorological data collected in the Grand Valley in conjunction with the irrigation scheduling program of the Agricultural Research Service (42). Data from these simulations were used to evaluate the effect of the volume of return flow on the concentration of ionic species in the soil solution, both in the soil profile and leaving the soil profile. If the soil solution became saturated with a particular ionic species, then further salt pickup could be prevented as the return flow moved over the shale bed.

Data from these studies were used to evaluate the effects of on-farm irrigation water management on return flow quality and quantity. These results could then be used in conjunction with the field data collected under the Grand Valley Salinity Control Demonstration Project in order to predict the impact of constructing new irrigation facilities and improved irrigation practices upon the salt load reaching the Colorado River. In turn, sufficient field data has been collected throughout the Grand Valley under EPA Grant No. S-802985 to allow the results found in the demonstration project area to be expanded to valley-wide predictions. The final objective of the research reported herein was to develop an irrigation return flow model (later referred to as soil moisture-chemistry simulation) which can be used as a tool in water resources planning and management.

SECTION 2

CONCLUSIONS

1. From the calibration of the moisture flow model using infiltration data, water content profiles and storage change data, it was concluded that the water flow through the soil profile could be adequately modeled for the Grand Valley. Several modifications were made to Dutt's original program before the above conclusion could be made.
2. The functions originally used to calculate hydraulic conductivity, $K(\theta)$, and soil-water diffusivity, $D(\theta)$, in the model did not permit accurate computation of soil-water flux at water contents close to full saturation for the conditions of this study. A functional relationship developed by Brooks and Corey (9) was used in the program to calculate hydraulic conductivity. The function used in the model to calculate soil-water diffusivity was developed using the Brooks-Corey (9) relationship for $K(\theta)$ and the Su-Brooks (78) relationship for the soil-water characteristic.
3. The method used to compute the average values of hydraulic conductivity, $K(\theta)$, and soil-water diffusivity, $D(\theta)$, required to solve the difference form of Richards' equation was also changed. The average values of $K(\theta)$ and $D(\theta)$ were originally computed using the average water content of the two nodes being considered. The averaging in the flow model was modified so the conductivity is now calculated by using the moisture content at each node and then the calculated conductivities are averaged. The diffusivity is now calculated as an integrated average diffusivity between the water contents at adjacent nodes.
4. After making the changes described above, it was possible to predict infiltration, water content distributions and changes in storage that agreed satisfactorily with field measurements. Since the model assumed a homogeneous profile, it was necessary to calibrate the flow model so as to incorporate the variability of field properties into the simulations. The soil-water characteristic was calculated as an average from water-content pressure head data gathered through the entire depth of the soil profile in a small area of the test site. This average characteristic was then used to calculate $K(\theta)$ and $D(\theta)$ in the calibration simulations.
5. From comparisons of simulated and field data used in evaluating the chemistry component of Dutt's model, it was concluded that TDS concentrations were adequately modeled but that individual ionic species concentrations were not. The simulations used to compare computed and field chemistry data were made using field data for initial and boundary conditions in both the chemistry and flow models. Field data on the chemical composition of the soil solution

extracted at a depth of 1.1 m for a 30-day period was used to compare with calculated salt concentrations.

6. Comparisons of calculated and measured data indicate that the $\text{CaSO}_4\text{-CaCO}_3\text{-Ca(HCO}_3)_2$ system is not adequately modeled for the soils in the Grand Valley.³ The model computed calcium ions (Ca^{++}) concentrations at a depth of 1.1 m that were greater than theoretical maximum values expected for this soil system. A study of the $\text{CaSO}_4\text{-CaCO}_3\text{-Ca(HCO}_3)_2$ equilibrium equations indicated that the solubility product of $\text{Ca(HCO}_3)_2$ calculated using ion activities was incorrect. The solubility of calcium bicarbonate [$\text{Ca(HCO}_3)_2$] was then calculated based on the partial pressure of carbon dioxide (CO_2). A reasonably good agreement between computed and measured total dissolved solids (TDS) was obtained using a value of 7 milli-atmospheres (matm) for the partial pressure of CO_2 in the simulations.

7. Data for single growing season simulations using 7- and 14-day irrigation schedules and 2%, 5%, 20%, and 40% leaching increments, coupled with data from a 6-year simulation using a 14-day irrigation schedule and 20% leaching increment, indicate that the salt concentration of the leachate is independent of the volume of leachate. TDS profiles calculated at the beginning and end of the 6-year simulation show the concentration of salt in the profile below a depth of 122 centimeters (cm), which is the bottom of the root zone in the simulation, to be relatively constant.

8. Since chloride ions (Cl^-) are relatively inert in soils, Cl^- concentration profiles were used to evaluate the calculation of salt transport by the model. Concentration profiles for the hypothetical simulations indicate that salt transport is modeled adequately at least on a qualitative basis.

9. Simulations were made for a winter condition which included the addition of pure water. The Cl^- concentration profiles calculated from this simulation show the effectiveness of pure water in reducing Cl^- concentrations. This simulation also shows the necessity for properly accounting for precipitation when computing leaching fractions based on Cl^- concentrations. The simulation shows that the leaching fraction would be overestimated if precipitation is not included in the computation.

10. These studies showed that the salinity concentration of the deep percolation losses were independent of the volume of deep percolation, because the concentration of salt below the root zone produces a saturated gypsum and lime condition which is relatively constant. Groundwater chemistry data also show that the concentration of salt in the cobble aquifer, although double the concentration of deep percolation immediately below the crop root zone, is still relatively constant owing to the solubility limits of the major salts. Thus, the salt loading due to irrigation return flow can be calculated from a knowledge of water balance for the Grand Valley. The reductions in salt loading which reach the Colorado River will be directly proportional to reductions in subsurface irrigation return flows (seepage and deep percolation losses).

11. The results of this study show that a strong emphasis should be placed on achieving high irrigation application efficiencies in a salinity control program for the Grand Valley in order to minimize deep percolation losses. Also,

improvements in present irrigation methods and practices in the valley should be sought that will result in more uniform irrigation applications. Consequently, advanced irrigation methods such as sprinkler or trickle irrigation, or automation of surface irrigation methods, are highly desirable because of their potential for more uniform irrigation applications while reducing deep percolation losses.

12. These research results can be incorporated into the detailed water budgets (hydro-salinity model) for the Grand Valley Salinity Control Demonstration Project, which in turn can be used in combination with the inflow-outflow analysis for the entire valley, in order to predict the impact of any proposed salinity control technologies upon the salt load in the Colorado River.

13. Based upon the results of this study and EPA funded research conducted in Ashley Valley by Utah State University (93), it is expected that other irrigated areas in the Upper Colorado River Basin having soils derived from erosion and weathering of the Mancos shale formation would also exhibit a nearly constant salinity concentration of the deep percolation losses immediately below the crop root zone.

14. The soil moisture-chemistry model used in this study has general utility and can be used in other irrigated areas. This model has been incorporated into an "Environmental Planning Manual for Salinity Management in Irrigated Agriculture" under EPA Grant No. R-804672.

SECTION 3

RECOMMENDATIONS

1. Although it has been shown that the groundwater (subsurface) return flows to the Colorado River are in chemical equilibrium, this research was not able to describe the higher level (second order) chemical reactions that are taking place during the movement of water through the shallow groundwater aquifer. To describe such complex phenomena will require the best expertise available in the fields of soil chemistry and water chemistry. Such knowledge would be beneficial in extending our capability to model and predict the chemical changes occurring during the movement of subsurface irrigation return flows.
2. These research results should be incorporated into the development of best management practices for the Grand Valley. The effectiveness of each proposed salinity control technology in reducing the salt load in the Colorado River can now be evaluated using the results of this study.
3. A strong emphasis should be placed on achieving high irrigation application efficiencies and more uniform irrigation applications in the salinity control program for the Grand Valley to be implemented by the U.S. Bureau of Reclamation (USBR) and the Soil Conservation Service (SCS). Advanced irrigation methods, such as sprinkler or trickle irrigation, or automation of surface irrigation methods, should be incorporated into the best management practices because of their potential for more uniform irrigation applications while reducing deep percolation losses.
4. These research results should be incorporated into the irrigation scheduling program presently being conducted by the USBR in the Grand Valley. The irrigation scheduling program should make every attempt to minimize deep percolation losses through improved irrigation methods and practices, as well as insuring that irrigation is terminated as soon as possible so as to maximize the available soil moisture storage for winter precipitation.
5. The economic advantages to farmers in adopting more advanced irrigation methods, such as sprinkler or trickle, should be documented in a style that is meaningful to farmers. These irrigation methods have definite advantages for reducing the salt loads reaching the Colorado River. Salt loads will be reduced primarily because of significant reductions in deep percolation losses early in the season. Increased fertilizer use efficiency resulting from reduced deep percolation losses should also be included in this documentation.

6. The results of this study, and EPA funded research conducted in Ashley Valley by Utah State University (93), show that other irrigated areas in the Upper Colorado River Basin having soils derived from erosion and weathering of the Mancos shale formation should be investigated to determine whether they also exhibit a nearly constant salinity concentration of the deep precolation losses immediately below the crop root zone. If this is the case, then the development of best management practices for each irrigated area in the Upper Colorado River Basin will be a much simpler task.

SECTION 4

EXPERIMENTAL DESIGN

STUDY AREA

The geologic formations throughout the Colorado River Basin were laid by an inland sea which covered the area. After the retreat of the sea, the land masses were uplifted and subsequent erosion has created the mountains and plateaus as they are today. As shown in Fig. 1, the upper formations are sandstones and marine shales which are underlain by the marine Mancos Shale and the Mesa Verde formations. These formations occur in about 23% of the basin in such locations as the Book Cliffs, Wasatch, Aquarius and Kaiparowits Plateaus, the cliffs around Black Mesa and areas in the San Juan and Rocky Mountains. The Grand Valley was created by erosion, which cut through the upper formations creating the valley in the Mancos Shale. This formation is the main source of the salt contribution to the Colorado River. Due to its marine origin, the shale contains lenses of salt which are easily dissolved as water moves over the shale beds. Water moving over and through the shale originates as leakage from the canals, laterals and over-irrigation. Since the overlying soil is derived from the shale, it is also high in salts and contributes significantly to the salinity of return flows.

The desert climate of the area has restricted the growth of native vegetation, thereby causing the soils to be very low in nitrogen content due to the absence of organic matter. The mineral soil is high in lime, carbonates, gypsum and sodium, potassium, magnesium and calcium salts. Although natural phosphate exists in the soils, it becomes available too slowly to supply the needs of cultivated crops. Other minor elements such as iron are available, except in areas where drainage is inadequate. The soils in the Grand Valley are of relatively recent origin and contain no definite concentration of lime or clay in the subsoil as might be expected in weathered soils.

The climate is marked by a wide seasonal range of temperature with sudden or severe weather changes occurring infrequently. The ring of mountains around the valley moderates weather changes but also contributes to the relatively low annual precipitation of approximately 20 cm. Moisture is removed from the air masses originating in the Pacific Ocean or Gulf of Mexico as these air masses move over the mountains. Precipitation during the growing season is minimal and comes from thunderstorms which develop over the western mountains. The valley location, coupled with west to east valley breezes, provides some spring and fall frost protection resulting in an average growing season of 190 days from April to October. Temperatures range as high as 40°C, with summer temperatures normally in the middle to low 30's in the daytime

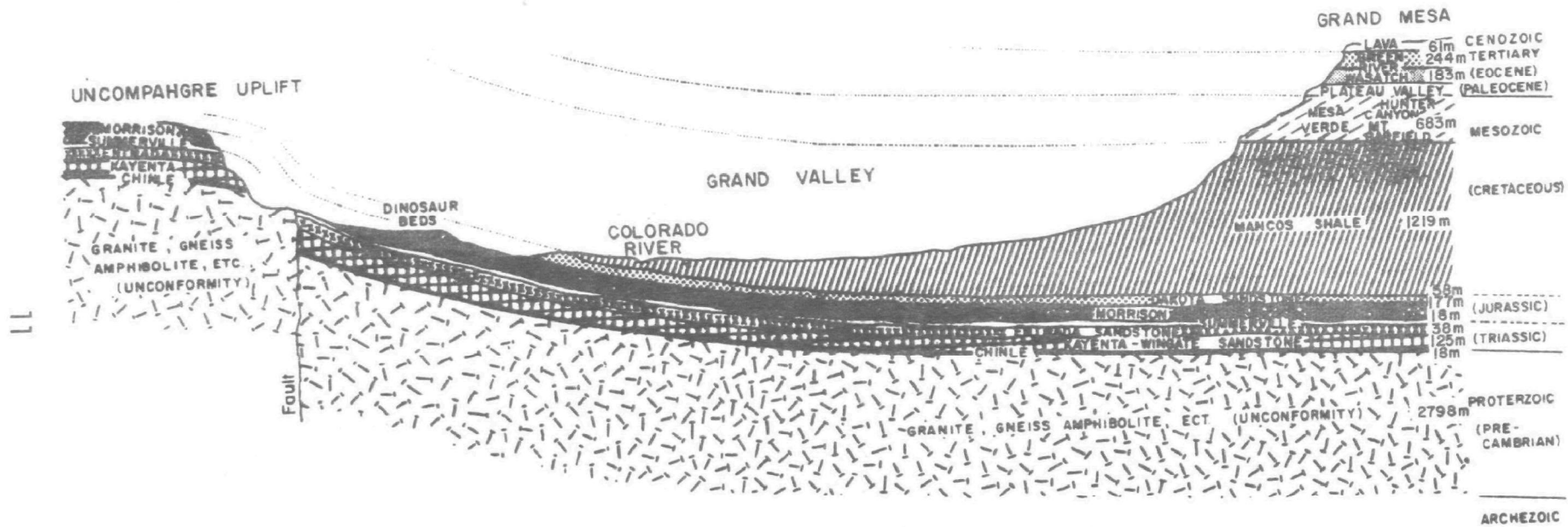


Figure 1. Geology of the Grand Valley.

and about 20°C at night. Relative humidity is usually low during the growing season, which is common throughout the semi-arid Colorado River Basin.

LOCATING A PROJECT SITE

The effects of an ancient sea are evident from the large amount of Mancos shale prevalent in the area. Nearly all of the valley is underlain by this shale at varying depths below the present shallow alluvial soil surface. The shale is at or near the ground surface in the area along the north side of the valley and along the south bank of the Colorado River. The lands along the north side of the valley were considered desirable for a possible project site (Fig. 2).

The site requirements for the project were quite restrictive. An area of approximately 10 ha was required for the research plots and buffer zones. The field had to be located in an area such that all subsurface flows presently crossing the area could be intercepted and removed. A smooth, fairly level topography over the farm land with slopes not exceeding 1% was necessary for furrow irrigation to be used successfully. However, a drainage channel, either natural or man made, was needed nearby and of sufficient depth to allow the water removed by the subsurface drains to leave the area under gravity flow. For construction purposes, a continuous layer of shale underlying the area at a depth of between 6 and 12 feet was required. Preferably the slope of the shale would not exceed the slope of the ground surface.

The first step in the location procedure was to carefully study the aerial photographs of the valley to locate fields of suitable size that were contained in the desired area. Land lying above and below the Government High-line Canal was considered. Virgin, as well as cultivated, lands were initially considered; however, it was soon decided that, due to the lack of soil development and the possibility of higher salt levels in the unfarmed lands, the virgin lands would not be suitable for the study area.

Having thoroughly studied the photographs, a field survey of the area was undertaken. Starting at the upper end of the valley, each field was located and evaluated using the criteria previously mentioned. Many of the possible sites were eliminated because they lacked suitable drainage outlets, sufficient water supplies, or were too saline to grow the required crops. Changes in land use since the date of the aerial photos also eliminated some of the possibilities. Several possible sites were found during the field survey that had not been evident on the photos. Following the field survey, the sites which met the surface requirements were probed to determine the depth to the underlying shale layer. This was accomplished using the Giddings Soil Sampling Rig shown in Fig. 3. The Giddings unit consists of a small gasoline engine which powers a hydraulic pump. The unit is capable of operating either a 4-inch screw auger or a 2-inch coring tube to depths of 8 m. Since the primary interest at this time was in determining the depth to shale, the 4-inch screw auger was used. These preliminary holes were dug mainly on public rights-of-way such as in borrow pits or on canal banks beginning in mid-March. The purpose of this was twofold: first, the severity of the winter (one of the coldest on record in Grand Valley) did not allow access to the

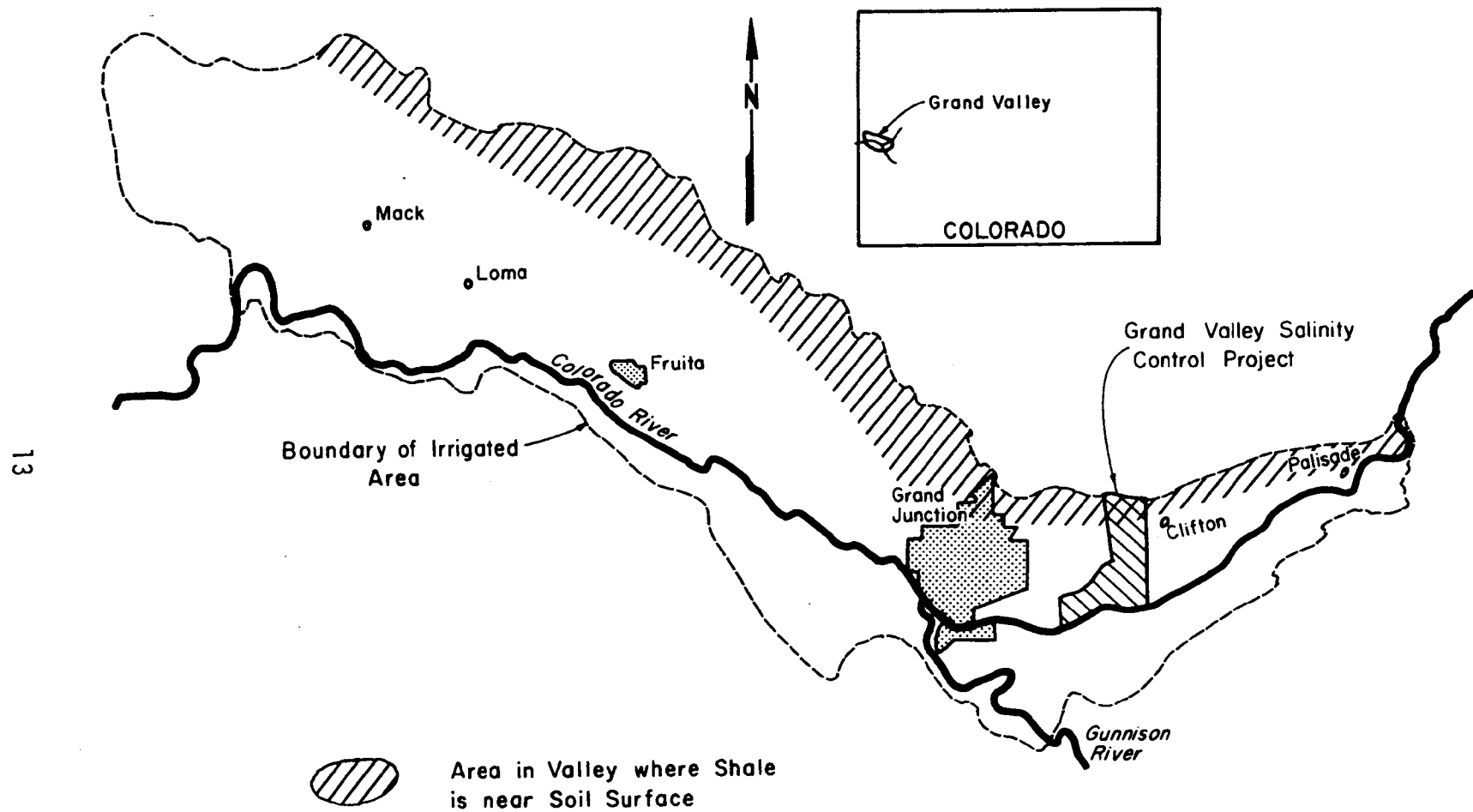


Figure 2. Map of the Grand Valley showing areas of positive site location.

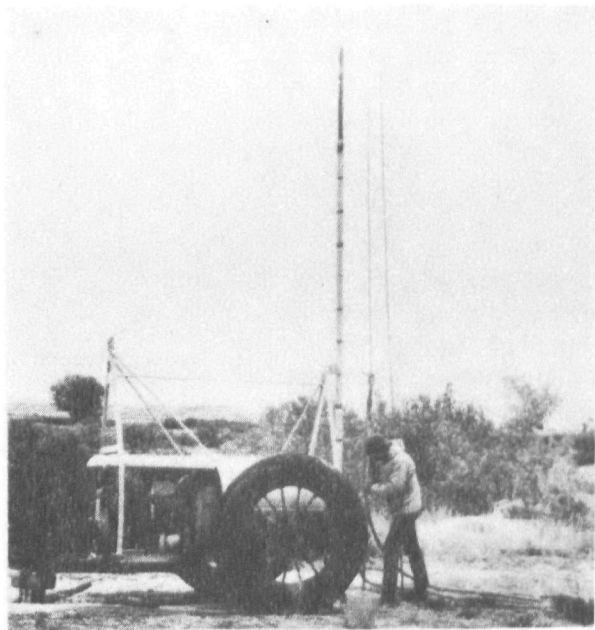
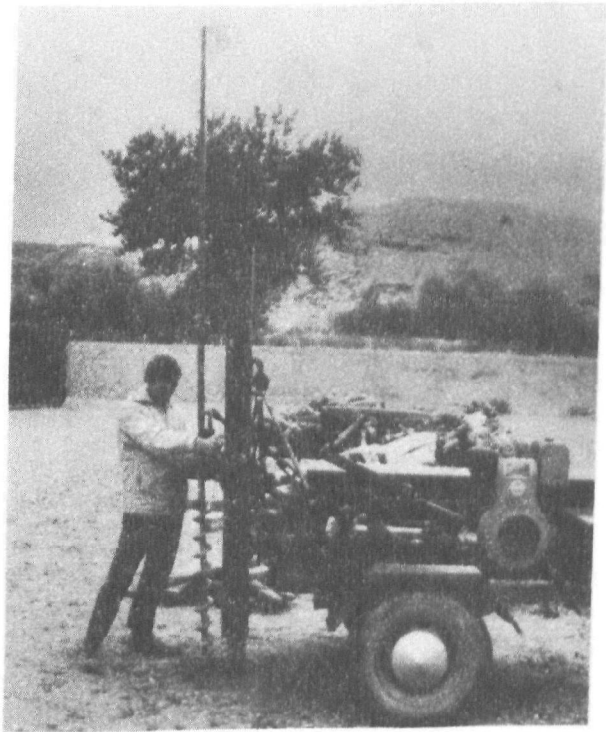


Figure 3. Pictures of the Giddings rig and jetting rig.

fields as early as planned; and secondly, contact with the owners was not considered desirable until it could be ascertained that the field might be suitable for this project. Initially, many of the sites were thought to be suitable. However, as the drilling process was begun, it was soon discovered that in most areas the shale layer was more undulating than had been expected. Approximately 100 holes were drilled to depths ranging from 1 to 8 m before a site was located.

Upon locating the site which was ultimately used, the process of mapping the shale elevations in detail was begun. The field was staked using a standard 30.5 m by 30.5 m (100 ft by 100 ft) pattern. Using an engineer's level, the ground surface elevation above mean sea level at each stake was determined. These elevations were also used in preparing topographic maps of the area. The depth to the shale layer was then determined using the jetting technique. Since the shale is similar to a layer of soft rock material, the pipe, which is being jetted into the ground, cannot penetrate the shale layer. Therefore, by measuring the length of the pipe which entered the ground and subtracting this from the ground surface elevation, the elevation of the shale layer can be determined. The pipe is then removed from the ground and the process repeated at the next station. The jetting technique is more accurate than drilling because it is difficult to tell exactly when the shale is encountered using a drill rig. Having completed the topographic maps of both the shale and the ground surface, a preliminary design of the project was prepared. This not only included a tentative layout of the plots, but also the tentative location of the drains and the irrigation lines. Upon deciding that the site was suitable, negotiations were begun on March 28, 1973, with the land owner for a lease agreement.

DESIGN OF IRRIGATION AND DRAINAGE SYSTEMS

The intensive study area was constructed on 9.3 ha of land owned by Kenneth Matchett. The farm is located north of the city of Grand Junction and just below the Government Highline Canal (Fig. 4). A natural waste channel known as Indian Wash runs along the east boundary of the area, then turns to the west and cuts diagonally across the top of the land which was used for the study area (Fig. 5). The wash averages approximately 8 m in depth and is cut into the shale, thereby effectively intercepting any subsurface flows originating in the lands above and seepage losses from the Government Highline Canal.

Water is supplied to the area by a lateral which is operated by the Grand Valley Water Users Association. Because of this lateral, the required acreage is divided into three fields instead of one as was originally planned. However, having three fields does have the advantage of better accessibility to the plots. Also, there are four points of water diversion, thereby providing more flexibility in the supply of irrigation water.

The depth to shale over the fields ranged mostly between 2 and 4 m with isolated areas as shallow as 0.4 m and as deep as 7 m. The deep areas were not used for plots. The plane of the shale slopes to the southwest with some undulation. However, it was possible to construct the system with all of the perforated drain lines lying on top of the shale with only a minimum of

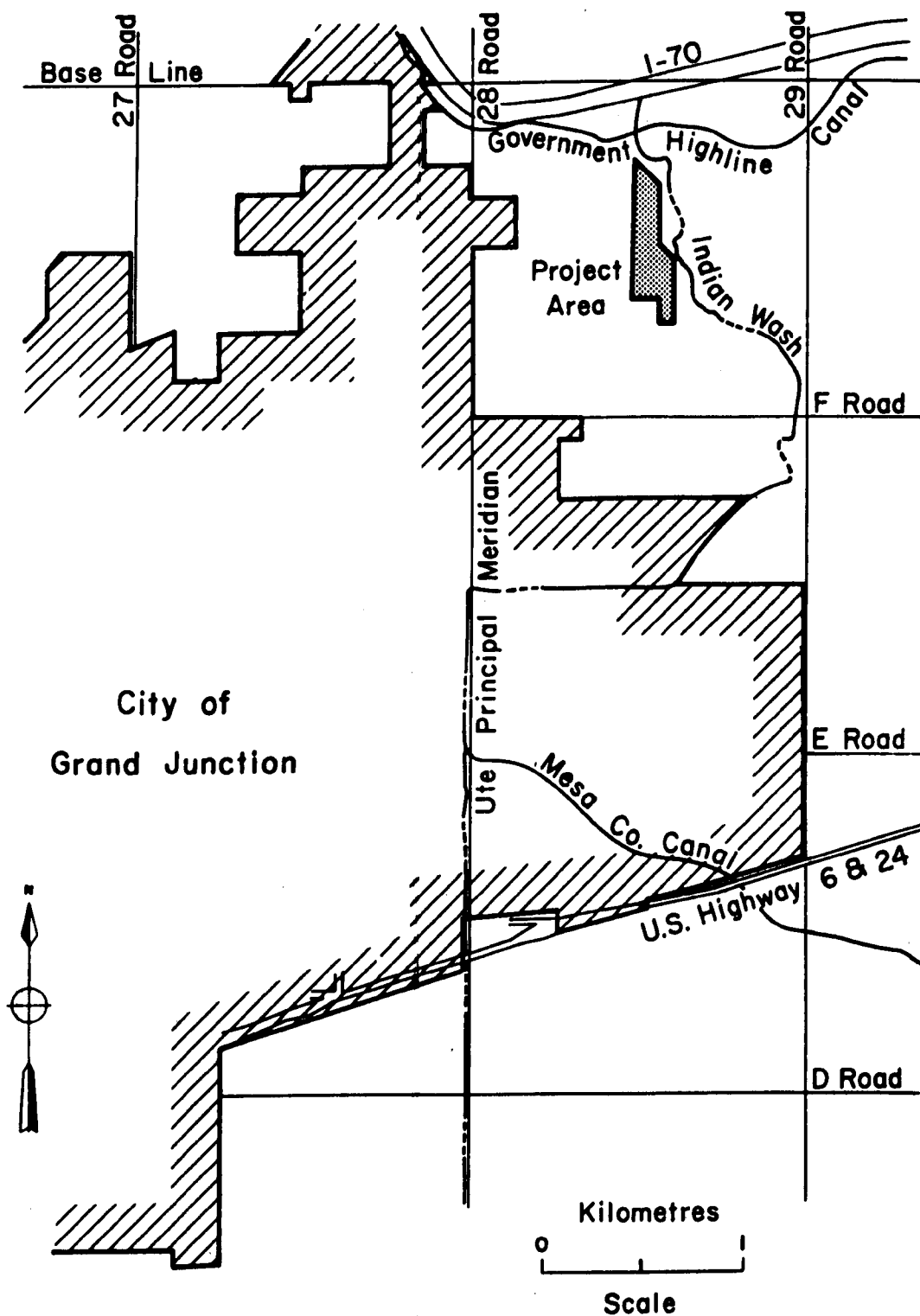


Figure 4. Map showing location of the Matchett farm.

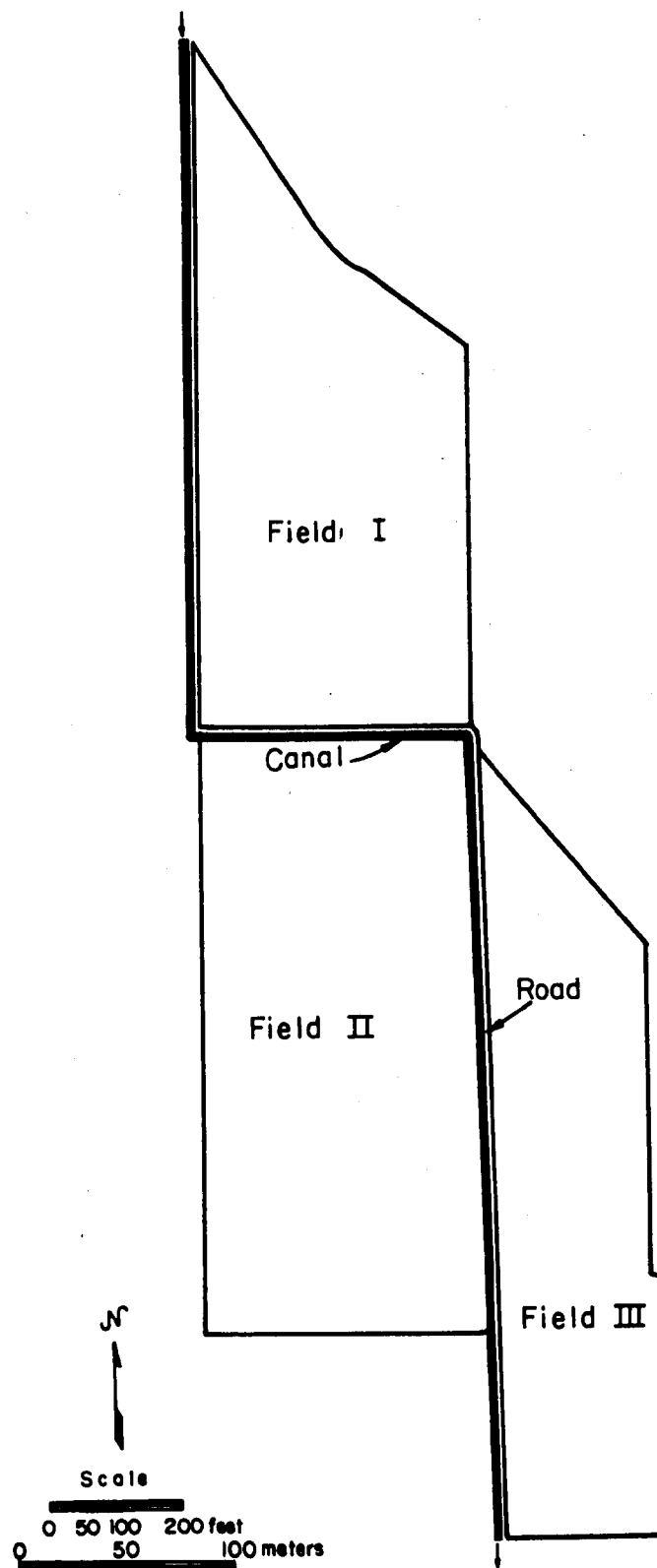


Figure 5. Map showing the fields used for the study area.

excavation into the shale for the main outlet lines.

Having located a suitable site for the project and upon the closing of the lease agreement, work was begun on the final design of the system. Since the area was divided into three fields because of the lateral, the first problem was to lay out the plots to use the ground most effectively and to avoid the areas of deep shale. The final drawings showing plot boundaries for the three fields are shown in Fig. 6, 7, and 8. The reader should note that these figures show the proposed boundary locations. The final curtain locations are offset slightly because the curtains were attached to the trench walls. Also, due to higher than anticipated construction costs, only plots 11, 12, 13, 14, 15, and 16 were constructed on Field I during the spring of 1973, with plots 1 to 10 being constructed during the early spring of 1974.

The plots on Field III which are 12.2 m (40 ft) wide and either 61, 91.5, or 152.4 m (200, 300, or 500 ft) long were constructed to evaluate the effects of long period contact with shale on the chemical water quality of subsurface irrigation return flows. In these areas, the depth to shale ranges from 0.4 to 1.2 m (1.3 to 4 ft).

Plastic barriers were installed between each of the plots and "sealed" to the shale as indicated in Fig. 9. A drainage line was installed across the lower end of each plot as indicated in Fig. 10. Water applied to these plots percolated normally through the soil until it encountered the shale. The flow path was then along the top of the shale until the drain was reached, which collected and conveyed the water from the field to a collection box where quality and quantity samples could be taken. The variations in plot lengths allowed comparison of the change in water quality with the distance the water traveled in contact with shale. These data were then compared with that collected from the standard plots.

Drainage System

The drainage system for this project was unique in that the usual factors of depth, spacing, and size of the drains were not the limiting constraints in the design of the system. These factors were adequately met by the criteria required for the plots. The depth of the drain was dictated by the fact that the drain must be placed on the shale barrier (Fig. 9). The spacing and size of the lines were limited by the plot size. In a 30 m by 30 m plot, the greatest distance that water must travel to a drain was 15 m and the drainage pipe had the capacity to convey the water draining from such a small area.

The deciding factors in the choice of the type of pipe used for the drain lines were ease of installation and cost. The fact that a plastic curtain had to be used to divide the plots (Fig. 9 and 10) pointed to the need for a pipe that was easy to install because of congestion in the trenches, while the large footage of pipe required that the material be low in cost. The new plastic drainage pipe materials were found to fit both requirements. The 10-cm (4-in) diameter pipe came in 75-m (250 ft) rolls which made it easier to install than short lengths of tile or cement pipe would have been. The price for this material was 59 cents per m (18 cents per ft), which was considerably less than the cost of clay or cement pipe.

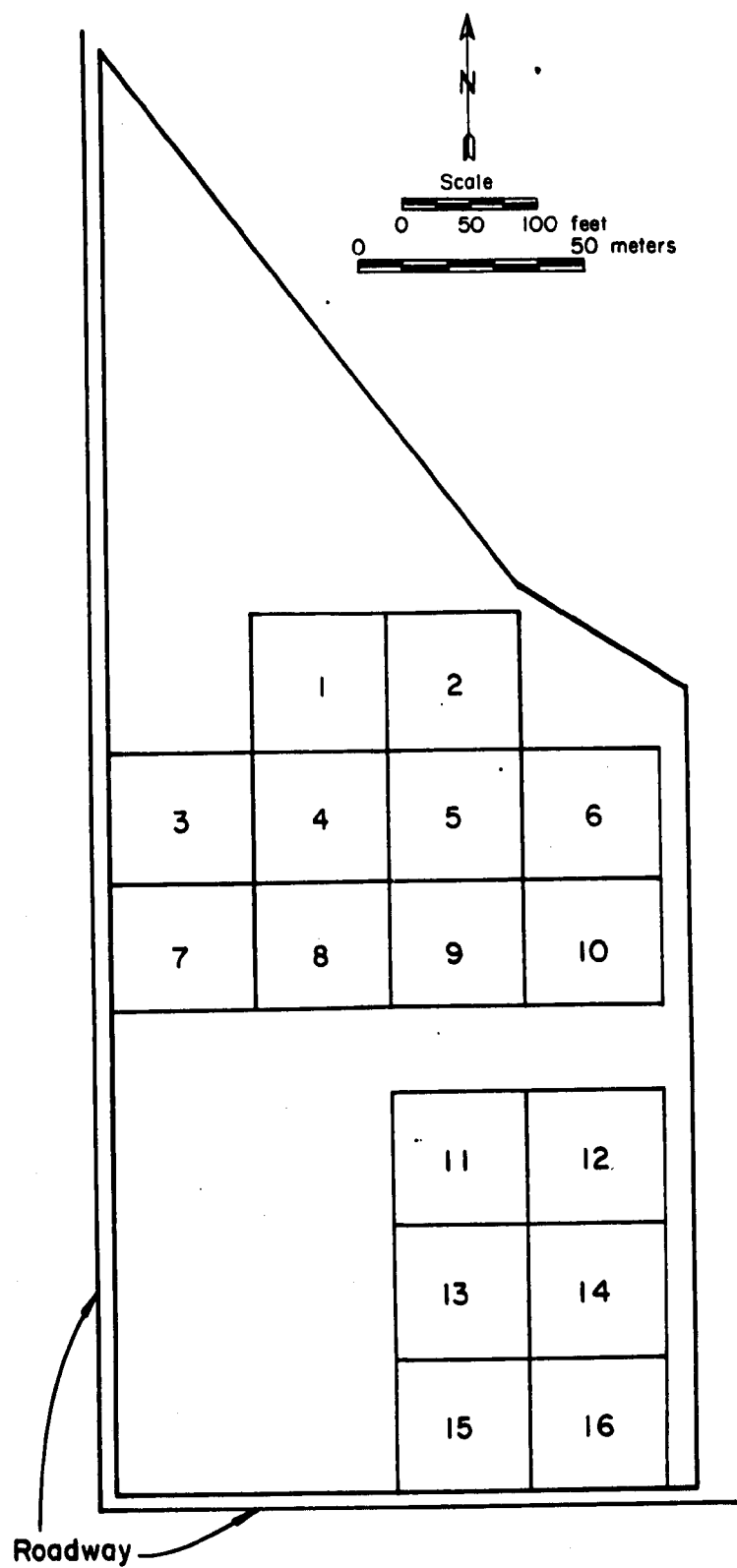
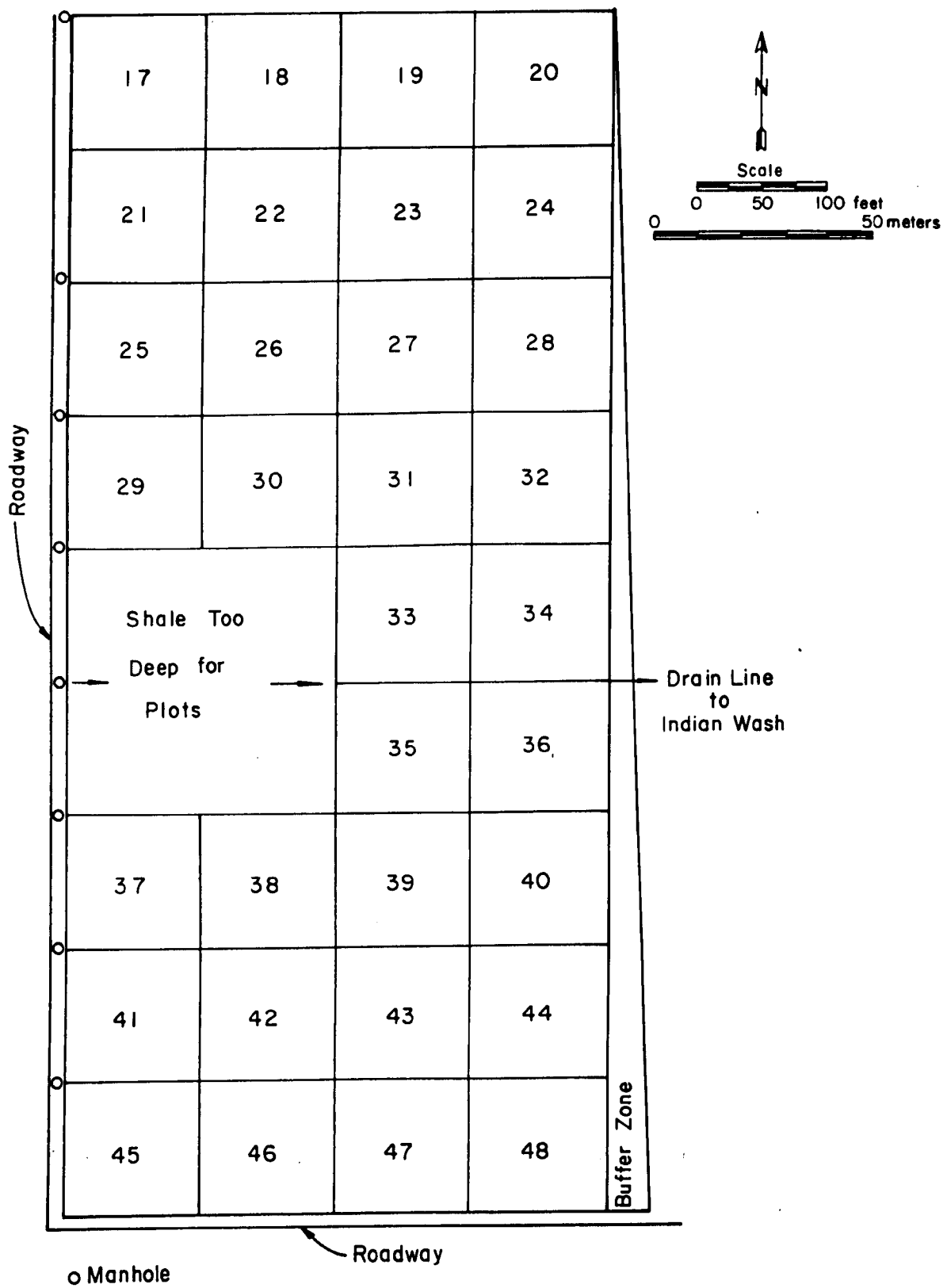


Figure 6. Plots in Field I.



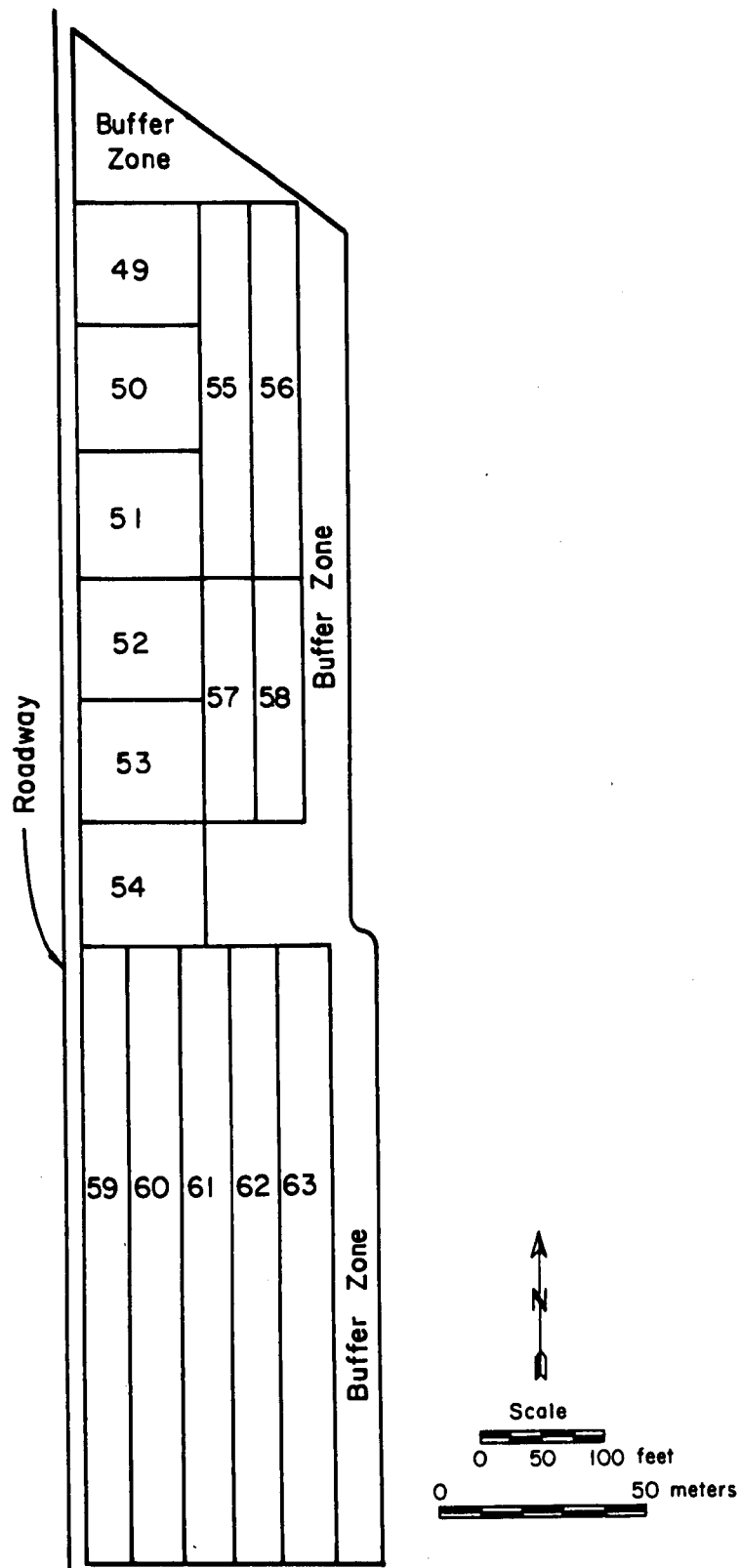


Figure 8. Plots in Field III.

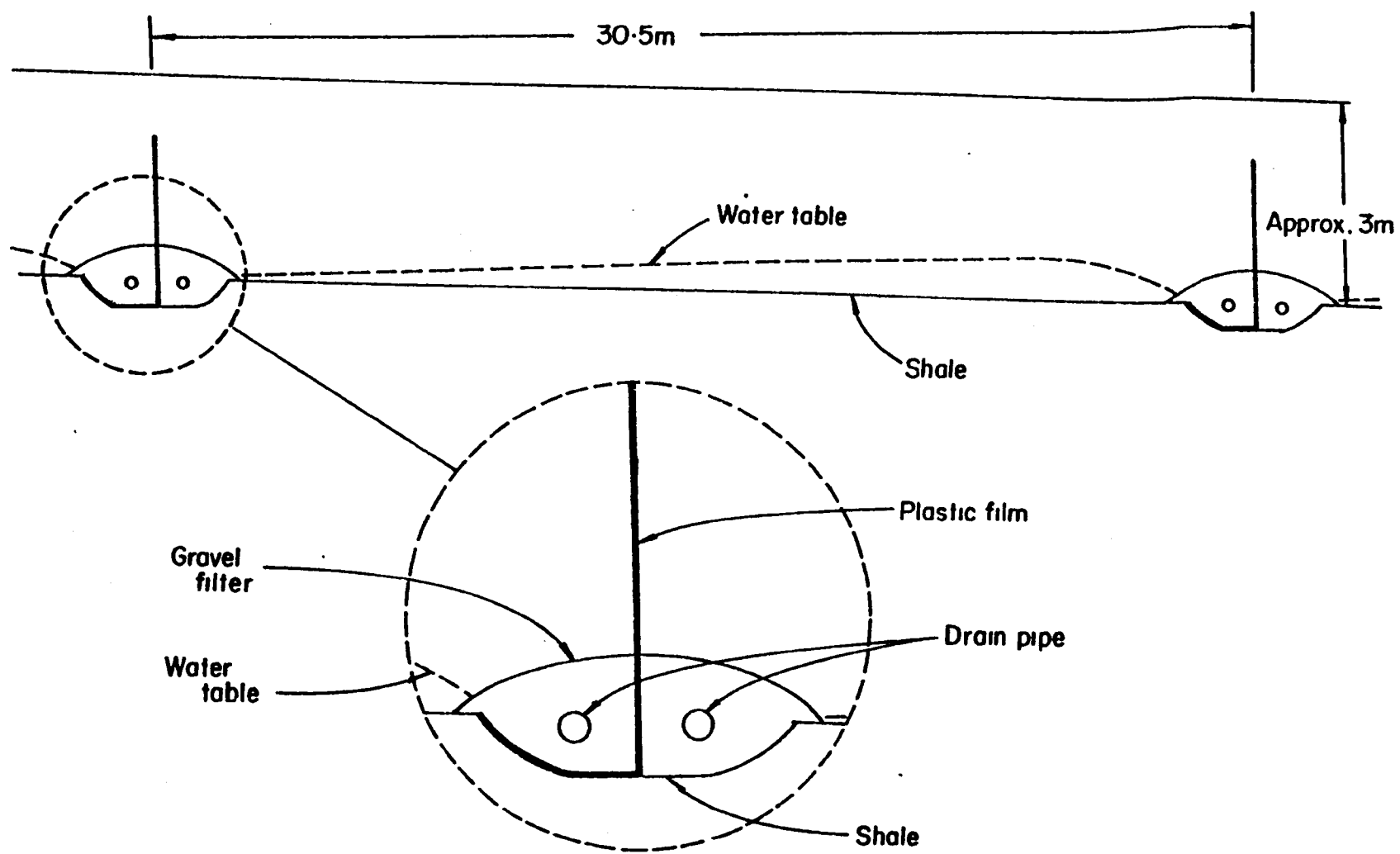


Figure 9. Plot cross-section with drain details.

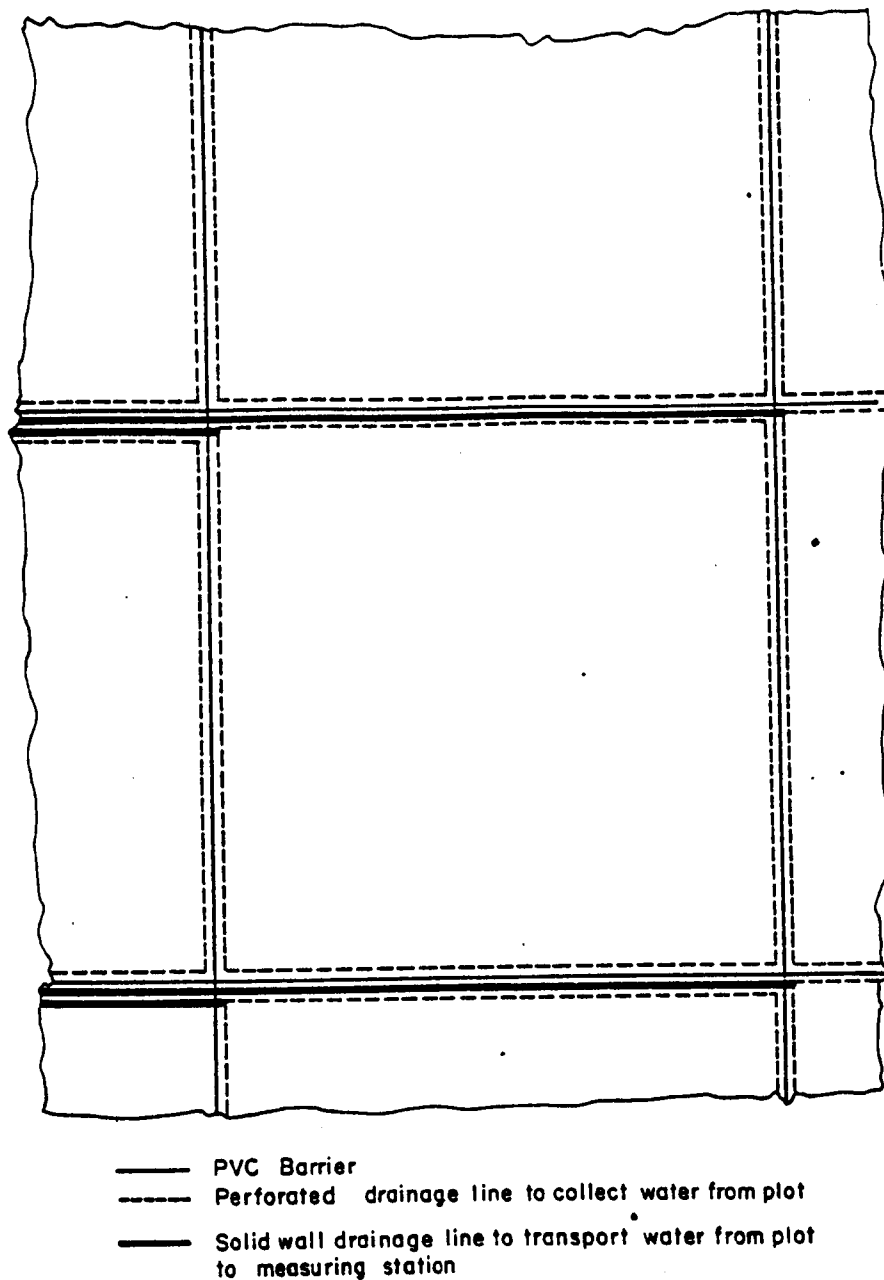


Figure 10. Plan view of drainage system detail.

Originally, plans called for using polyethylene film for the membrane to divide the plots. However, upon further research into the materials available it was found the PVC vinyl was much better suited to the requirements of this project. The PVC is much stronger than the polyethylene film with the same thickness. The problem of connecting the sheets of material in the field was also solved since the PVC material could be bonded together using solvent cement, whereas the polyethylene had to be taped. Furthermore, the cement bond on the PVC was much stronger and more water tight. After considering the suitability and cost of the various materials, the decision was made to use PVC vinyl membrane with a 10 mil thickness.

Selection of the proper gravel filter material for encasing the drain lines was possibly the key to the successful operation of the entire drainage system. The soils in the project area are classified as Billings Clay loam, which is a very fine-grained soil. The filter material surrounding the perforated drainage pipe had to be selected so that a minimum amount of these fine materials would be permitted to pass through the filter and into the drain line. Five gravel sources of sufficient volume were found in the valley: (a) 2-cm (0.75 in) washed crusher waste; (b) 4-cm (1.5 in) washed crusher waste; (c) pit run; and (d) two different sources of unwashed 2-cm (0.75 in) crushed material. The pit run, or uncrushed, gravel in the Grand Valley contained a large percentage of very large cobble rocks ranging from 15 to 30 cm (6 to 12 in) in diameter. Samples were taken from each of the sources and a standard mechanical analysis performed on each sample. After carefully comparing the particle size distribution curves of the filter material with that of the soil, a 2-cm (0.75 in) unwashed crushed material located at the upper end of the valley was selected.

The slope of the drain lines was dictated by the slope of the shale layer. However, the minimum slope required to prevent salt accumulation was calculated to be 0.5 m per 100 m. Whenever the slope of the shale exceeded the minimum slope required, which was the case at most locations, the drain lines were laid at the slope of the shale. When the slope of the shale was less than the minimum required slope, the trenches were excavated at a slope of 0.5%.

Since the only barrier between adjacent plots was the vinyl membrane, when the drain line from one plot passed through the membrane it was in another plot and, therefore, had to be a closed conduit to prevent water from moving either in or out of the conduit. Original plans called for a pipe of reduced size to be used to carry the water from each plot to a centrally located water monitoring station. After considering the total length of pipe required and its cost, the use of a number of smaller monitoring stations was found to be the most desirable method.* Since the Indian Wash waste channel runs close to the east boundaries of Fields I and III, a number of control box structures were used along the wash.

The location of Field II presented a different problem. A system for using concrete manholes was developed to cope with this problem (Fig. 11). By setting the base and the outlet of the manhole below the grade of the incoming drain lines, as shown in Fig. 11, the water entered the manhole and fell freely to the floor. This free outfall made it possible to collect both quality and quantity samples of the water being removed from each plot. The water

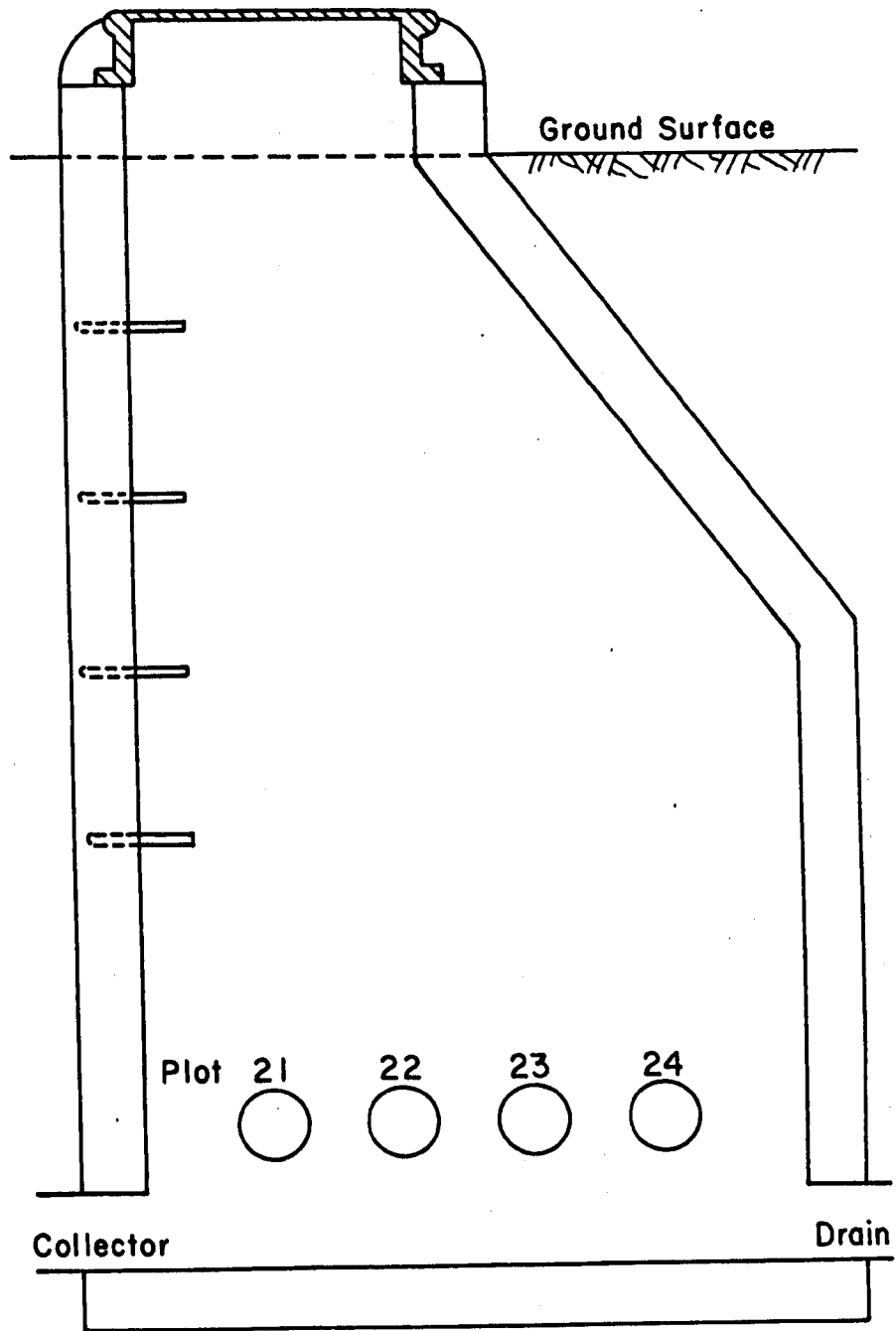


Figure 11. Typical manhole installation.

then entered a 15-cm (6 in) diameter pipe which collected the water from each manhole and transported it to Indian Wash. The use of the manholes eliminated the need for several miles of pipe. The manholes chosen for use were standard concrete sewer manholes 122-cm (48 in) in diameter, which provided ample room in which to conduct the sampling procedures.

Irrigation System

The furrow method of irrigation was used in the study area. Due to the nature of this study, the delivery system used had to meet certain requirements, which included: (a) the water applied must be accurately measured; (b) tail-water runoff must be minimized or eliminated; (c) the water application must be carefully controlled; (d) there must not be any water applied to the plots that is not measured including seepage losses, leakage, or water running from the plot above; and (e) flow rates in the furrows must be small due to the short length of run (30 m). The delivery of water to each plot with zero losses required that a system of lined or closed conduits be used. A network of lightweight aluminum gated pipe was found to be ideally suited to this purpose.

The system was designed so that a line of gated pipe was laid across the upper end of each plot. Since none of the fields were more than four plots wide, the ability to water one plot on each line per day allowed a complete irrigation every four days, which was more than sufficient. Calculations from previous studies conducted by the authors showed that a flow rate of 4 liters per minute (1/m) [1 gallon per minute (gpm)] in each furrow was adequate for runs of 30 m. Using row spacings of 75 cm (30 in), which are fairly standard in this area, a total of forty furrows on each pipeline could be irrigated at once. Therefore, the design capacity of the system in liters per minute equaled forty times the number of lines served. It was found that 15-cm (6-in) diameter pipe was needed for the gated pipe lines since pipes of smaller diameters have a tendency to leak around the gates. Supply lines of 20-cm (8-in) diameter were required to carry the needed flows under the available hydraulic head.

The ability to control the flow rate entering each line of gated pipe from the main supply line was very critical. This was accomplished by using a hydrant valve assembly to connect the gated pipe to the supply line as shown in Fig. 12. A "butterfly" valve placed immediately downstream from each turnout was used to control the amount of head available at the hydrant.

Flow Measurement

The accurate measurement of the irrigation water applied to each plot was of utmost importance. This measurement also posed one of the more difficult problems encountered on this project. During the first year, the flow rate into each furrow was determined volumetrically using a 2-l (0.5 gal) container and a stop watch. While this method was highly accurate, the time needed to perform this task for approximately 400 to 500 furrows daily became enormous.



Figure 12. Irrigation system control valves.

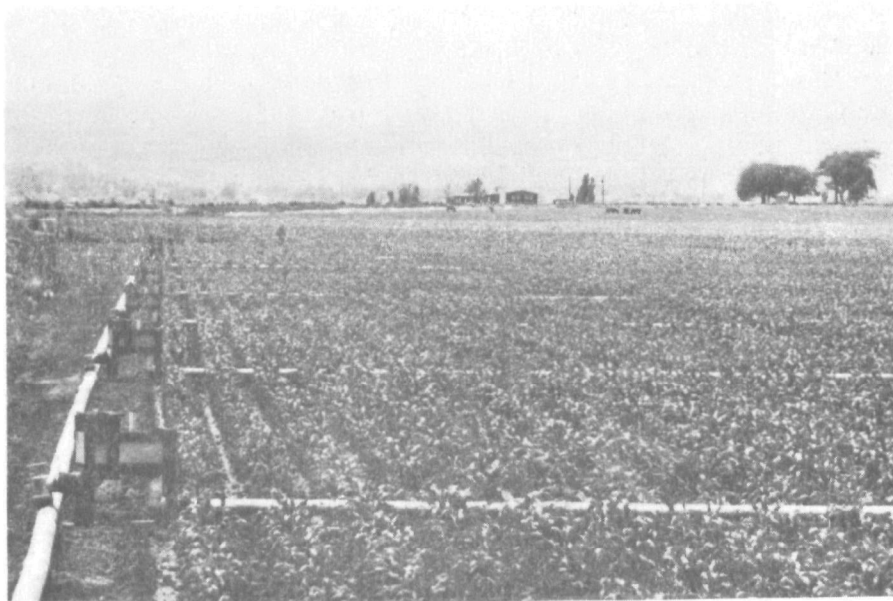
Prior to the 1974 irrigation season, flow measurement structures were constructed. As mentioned earlier, a 20-cm aluminum main line was used to deliver water along one side of each field. At the upper end of a series of plots, a combination control valve and riser were used, with the water discharging from the riser into a weir box. The weir box contained a gravel-filled screen which reduced the flow turbulence. The water then passed over a 30° V-notch weir which had been rated. After flowing over the weir, the water discharged into a lateral of 15-cm gated pipe which conveyed the water across the top of a series of plots (usually four). This system of flow measurement is illustrated in Fig. 13.

CONSTRUCTION OF PLOTS

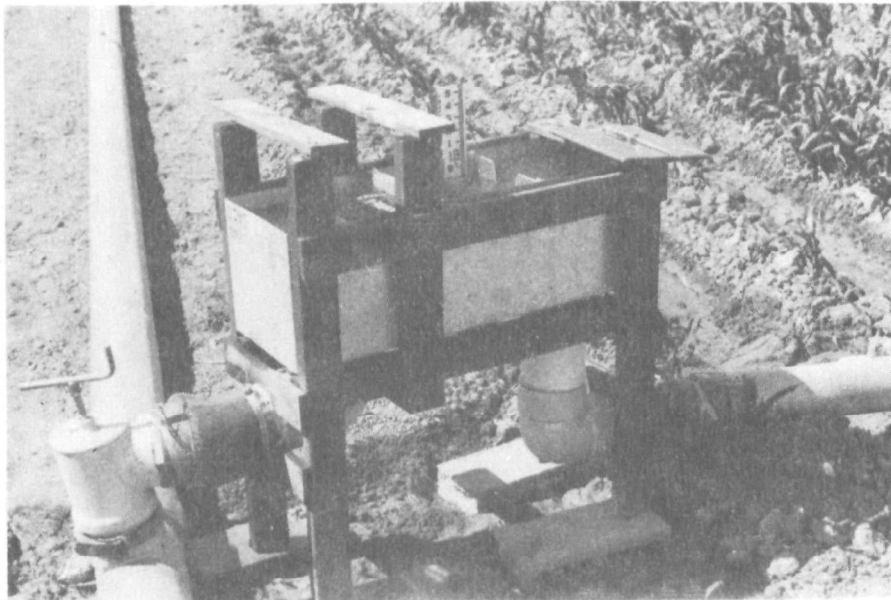
After completing the design and obtaining the materials, construction on the drainage system was begun on May 9, 1973. In order to gain experience in handling the plastic curtains, the 12 m by 30 m plots in the shallow portions of Field III were undertaken first. A small bucket type wheel trencher was used in this shallow area. The trench was dug so that the bottom was slightly below the top of the shale layer. The loose material in the bottom of the trench was removed by hand to provide a smooth flat surface. The curtain was then secured inside the trench. Sufficient curtain material was left at the bottom of the trench to be laid across the trench floor and covered with the moist clay soil. Workmen compacted this soil to "seal" the plastic curtain to the shale layer. The trenches were then backfilled, making certain that the curtain remained in place. Two large hydraulic crawler backhoes were required to excavate the deeper trenches. Since most of the trench work was to depths of 2 to 5 m, the trenches had to be "shelved" so that the top was much wider than the bottom in order to prevent the banks from caving.

To obtain the proper grade to the trenches, lines of hub stakes were set on a 3 m (10 ft) offset from the center line of the trench. The elevation of the hubs was then determined using an engineer's level. A grad rod, consisting of two boards, a hinge and a carpenter's level, as shown in Fig. 14, was used to determine when the trench had been excavated to the proper depth. The trenches were cut 15 cm (0.5 ft) below the depth specified for the drain invert placement. This was necessary to provide for a clay layer of 7.5 cm (0.25 ft) on top of the curtain and a 7.2 cm (0.25 ft) layer of gravel filter material underneath the drain. After placement of the 10-cm diameter plastic drainage pipe, additional gravel was placed on the sides and over the top of the pipe to ensure that the drainage pipe was completely surrounded with the gravel filter.

Upon completion of the trenching operation, wooden stakes were driven into the side of the trench at the elevation of the invert of the drainage pipes (Fig. 15). The plastic curtain was then laid in the bottom of the trench and a strip about 30 cm wide along the bottom edge covered with compacted clay soil. The entire curtain was coiled and placed on the floor of the trench as shown in Fig. 15. The gravel and pipes were then laid into position with the gravel completely surrounding the pipeline. Upon completion of the drain installation, the curtain was then unrolled upward from the bottom of the trench (Fig. 16) and secured to the wall of the trench, opposite from the soil



(a) Watering of corn plots using gated pipe.



(b) Measurement of water applied to the plots using a V-notch weir.

Figure 13: Flow measurement structures containing 30° V-notch weir for measuring quantity of irrigation water applied to each plot.

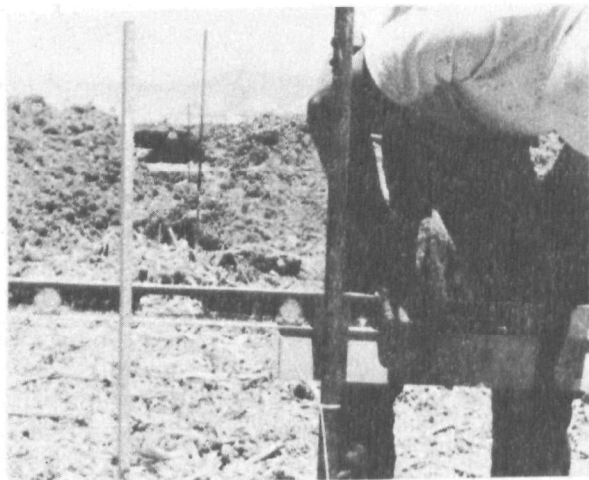


Figure 14. Pictures showing use of the grade rod.



Figure 15. Placement of grade stakes in trench.



Figure 16. Placement of rolled curtain on the trench floor.

bank, using large nails (Fig. 17). A means of supporting the curtains across the open ends of the trenches while completing the backfilling operation was needed. This was accomplished by suspending the curtain with baler twine which was connected to wooden stakes driven into the wall of the trenches as shown in Fig. 18. This method also provided a means of holding the curtains in position during the glueing operation.

The drainage lines, used to convey the water from the plots to the measuring stations, had to pass through the plastic curtain upon leaving the plot. Since this required making a hole through the curtain, a possible point of leakage of water between plots was introduced, which had to be sealed. This was solved by glueing another piece of PVC material around the hole through the curtain and allowing it to extend perpendicular to the curtain, forming a "boot" around the pipe (Fig. 19). By wrapping this boot around the pipe and securing it with plastic materials, a virtually leak-proof seal was formed.

Whenever possible, the pipes running from the plots to the measuring stations were installed using a continuous section of pipe. However, this was not always possible since the distance was sometimes greater than 75 m (250 ft). In standard drainage systems, a water-tight conduit is not needed; therefore, the couplers used with the Certiflex pipe are not water tight. When water-tight joints were required, the couplers were coated with a tar-like asphaltic mastic that completely sealed the joint.

The backfilling operation was performed in much the same manner as on the 12-m plots except that the deeper trenches produced much larger soil banks. This larger bank required that a D-8 dozer be used to backfill the trenches. The curtain was again held in place by a workman until the fill dirt was in place. The corner areas of the plots, where the curtain was exposed from all sides, presented a special backfilling problem. Unless dirt was evenly deposited on all sides of the curtain, the weight of the soil would tear the curtain material. The use of a small tractor-mounted backhoe proved very successful for this purpose. A laborer assisted in the careful placement of the backfill material against the curtain. The dirt was placed carefully on all sides until the curtain was completely buried. The remainder of the trench was then filled using the dozer.

INSTALLATION OF VACUUM SOIL MOISTURE EXTRACTORS

To aid in modeling the ground water and salt movement in the soil, data were required on the total flux of solute and soil solution leaving the root zone, as well as that leaving through the drains. Since the root zone is an unsaturated zone, the soil-water is under suction and a vacuum is required to collect a soil moisture sample. This can be accomplished by applying a vacuum to a ceramic tube which has been isolated from the total soil mass by a box which is open only to percolation from the ground surface. The total flux of soil-water can be collected and measured. Knowing the vertical contribution of flow, a more accurate water balance can be computed for the entire ground-water system. Sources of salt contribution are also more accurately identified by knowing the solute concentration leaving the root zone. The vacuum



Figure 17. Unrolling of curtain and placement against trench wall.



Figure 18. Sealing the PVC curtain at corners.

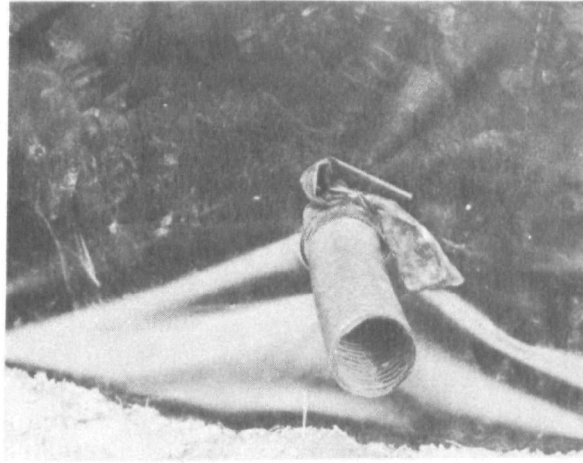


Figure 19. Method of sealing the curtain around the drainage pipe.

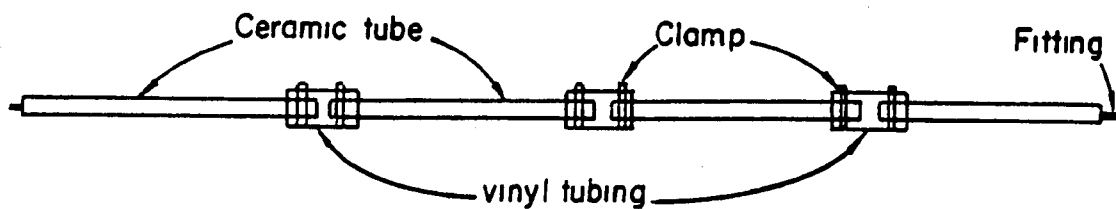
lysimeter used in this study was patterned after the equipment developed by Duke and Haise (21).

The equipment represents an extension of the techniques used for on-site collection of the soil solution described by Reeve and Doering, (67) and Brooks et al. (8). The early studies simply used porous ceramic cups connected to vacuum lines. The intent of these investigators was to extract soil water at various depths to investigate soil salinity variations with depth. Since total flux was not being measured, the pan required to collect percolating water was not required. In the current application, the cups were replaced by a 135-cm (4.5 ft) "string" of porous ceramic tubes which were enclosed within a pan. These "strings" were made by joining four 30-cm (1 ft) long by 1.27-cm (0.5 ft) diameter tubes with 5 cm pieces of polyethylene tubing. Glue inside the tubing and clamps on the outside insured that the joint would not leak when a vacuum was applied [Fig. 20(a)]. Each "string" had a fitting on each end which was used for connecting the tubing needed to collect samples and to flush the ceramics with chemicals in order to prevent the growth of microorganisms. The ceramic strings were treated with 0.1 N hydrochloric acid and flushed with deionized water prior to being installed for use in the field.

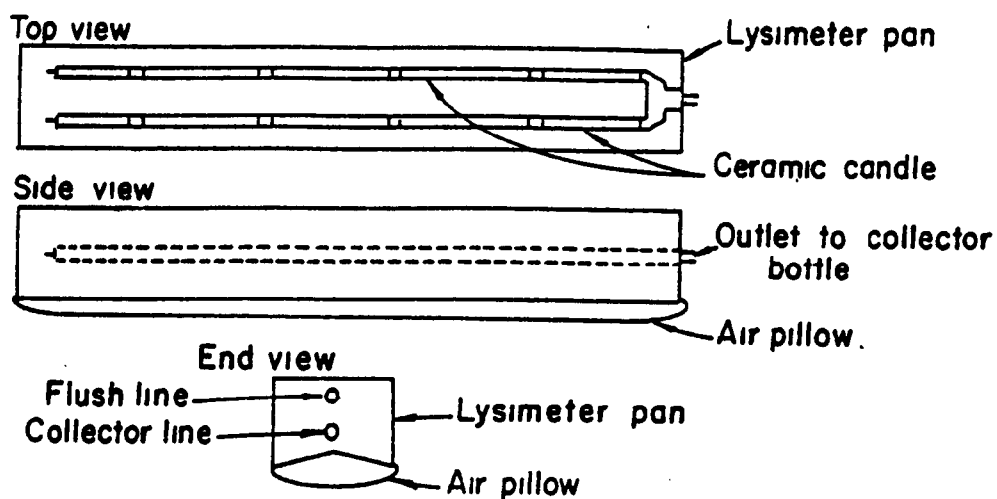
Two ceramic strings were placed in each lysimeter pan which was constructed of sheet metal and measured 150 cm long by 12.7 cm wide and 17.8 cm deep. When ready for installation, the ceramics were placed in this pan and covered with soil. The candles were placed 5 to 8 cm above the bottom of the pan so that they were surrounded by soil. The soil was mounded above the upper edge of the pan.

A heavy gauge rectangular rubber pillow was glued to the bottom of the pan. Inflating the pillow after installation of the unit in the field pushed the pan up against the soil above it and the mounded soil in the pan ensured a positive contact between the lysimeter and soil matrix above. A schematic of a completed lysimeter pan is given in Fig. 20 (b). Four pan lysimeters were placed in each of two test plots. They were located at the corners of a 3 m by 4 m rectangle which had been centered in the plot as shown in Fig. 20 (c).

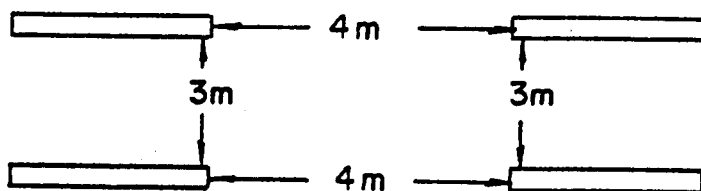
The pan lysimeters were installed during the construction of the test plots. First, a rectangular pit (3m by 4.5 m by 1.5 m) was excavated in the center of the plot. Then, holes to house the lysimeter pans were augered into the sides of this pit roughly 1 to 1.3 m below the ground surface. These holes were augered using a hydraulic ram (Fig. 21) which was mounted on a steel frame. The ram was then used to push a box-shaped bit into the soil which formed a shaped hole the size of the lysimeter pan (Fig. 22). After the four holes were shaped and the pans inserted, the flush lines, air pillow lines, collector lines, vacuum lines and collection bottles were placed two to a well, which was 0.6 m in length and made of 30-cm diameter plastic pipe. Various sizes of polyethylene and plastic tubing were used to make the connections of the lysimeter pans to the collection bottles, to the vacuum unit, to the flushlines and to the air supply. Vacuum, air, flush and dump lines running to the edge of the test field were housed in 3-cm polyethylene tubing. After completing the installation, the site was backfilled.



(a) Ceramic Candle Detail



(b) Lysimeter Pan Detail



(c) Plan View of Lysimeter Pan Locations in Research Plot

Figure 20. Field installation soil moisture vacuum extractors.

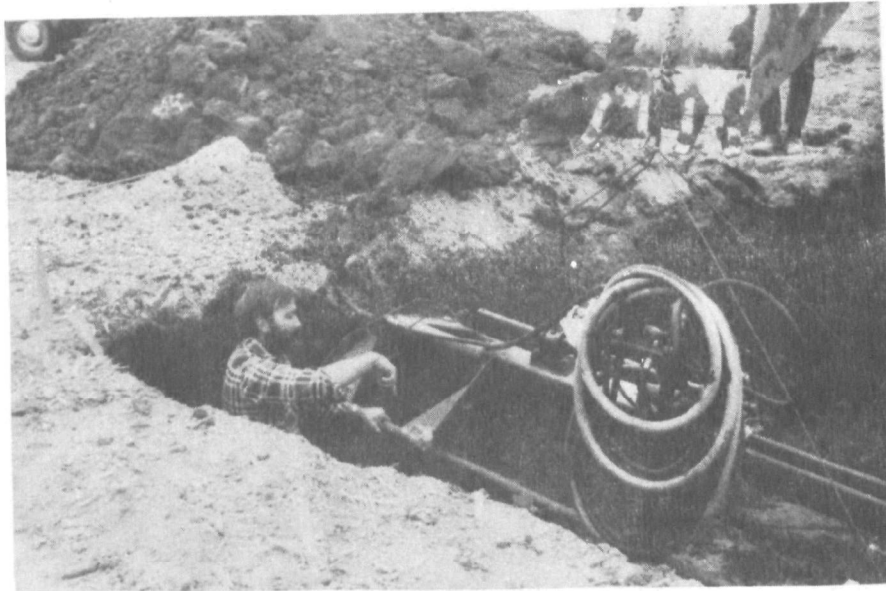


Figure 21. Hydraulic ram used to auger and shape holes for lysimeter pans.



Figure 22. Construction of lysimeter pans.

Vacuum was applied continuously to the ceramics and samples were collected weekly or more frequently as required. The proper operating vacuum was attained by using two tensiometers; one placed in the lysimeter pan and one in the soil at the same depth in a region close to the pan. The vacuum was then adjusted so approximately the same soil suction was present on each tensiometer.

The ceramic strings were connected to a 4-l (1-gal) jar which collected and held the soil solution between sampling periods. There were collection bottles for each pan. The 4-l (1-gal) jar was connected to a vacuum source located at the edge of the test field (Fig. 23). A vacuum unit (Fig. 24) consisted of a vacuum pump, vacuum tank, manometer and pressure switches to control and maintain the vacuum in the collectors. One vacuum unit was used to run a set of four pans.

TREATMENTS

Crops

The agricultural industry in the Grand Valley is comprised mainly of fruit crops, pears, peaches, cherries, and field crops such as corn, small grains, sugar beets, alfalfa, and other hay crops. The crops selected for use in the experiment were corn, alfalfa, wheat, and a crested wheat grass. These were selected because they represent the predominant crops and require a minimum amount of special equipment for production. The alfalfa was planted as a permanent stand in Field I (Fig. 6), corn was planted in Field II (Fig. 7), and wheat in the north one-half of Field III (Fig. 8). The south one-half of Field III was planted with a permanent stand of Jose Tall Wheat grass.

Fertilization Treatment

The fertilization treatments were designed to ensure a good stand of the crop and to evaluate nutrient losses due to excess irrigation. After an initial fertilization to establish the crop, the alfalfa received no additional fertilizer. The wheat crop received the recommended quantities of nitrogen, potassium and phosphate based on a nutrient analysis of the surface soils in the test area. The recommendation was based on a yield goal of 32.656 mg/ha for wheat and comes from the Colorado State Publication, "Guide to Fertilizer Recommendation in Colorado" (51). The Jose Tall Wheat grass in Field III-S received a uniform application of fertilizer based on soil analysis and yield goals found in the fertilizer guide.

The corn test plots received fertilization such that two levels of nitrogen were achieved in the soil. The goal was to achieve an equivalent of either 100 ppm nitrogen or 50 ppm nitrogen in the surface soils on a plot. To do this, the surface soils were analyzed for nutrients and then, based on existing nitrate levels, one-half of the plots was selected to be fertilized to 50 ppm nitrogen, while the other one-half was fertilized to 100 ppm nitrogen. By using the approximation (51) that 10 ppm nitrogen is roughly equivalent to 40 kg/ha of nitrate-nitrogen in the top 30 cm of soil, the nitrogen required to achieve a specified fertilization level was computed. The potassium and phosphate fertilizations were based on the surface soil analysis and



Figure 23. Housing for vacuum units.

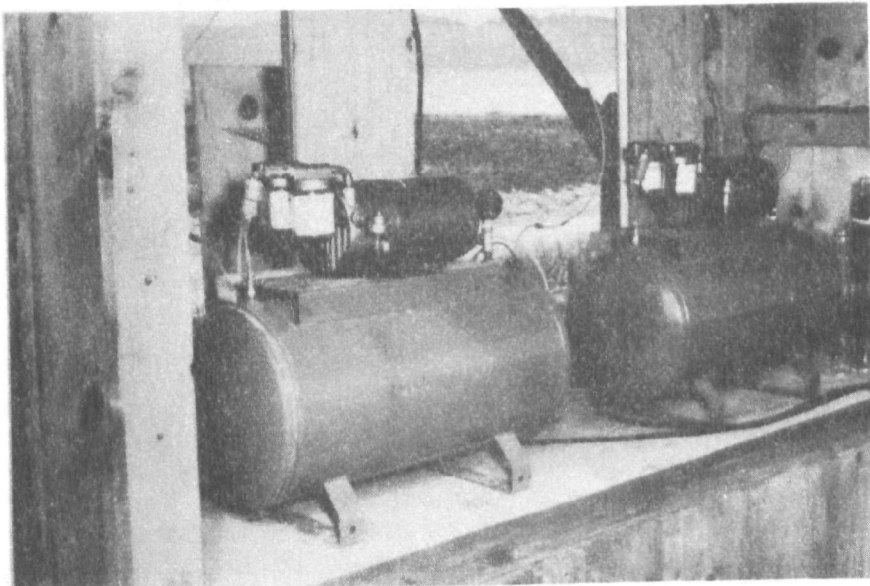


Figure 24. Vacuum units.

recommendations found in the fertilization guide [Ludwick and Soltanpour (51)]. The treatment design was random in that no specific pattern of plots within the test area was chosen for the fertilization treatment.

Irrigation Treatment

The irrigation treatments were developed based on the levels of depletion and replenishment of available water in a plot. The available water, as used in this study, was defined as the soil water stored between 33 kilopascals (kPa) and 1.5×10^3 kPa. The water content at 33 kPa and 1.5×10^3 kPa was computed as a percentage of the dry soil weight. The levels of depletion selected were 70% and 50% of available moisture. Four levels of replenishment, 75%, 100%, 150%, and 200% of the depleted moisture were used. This resulted in a total of eight irrigation treatments. Specific irrigation treatments assigned to a plot depended on both plot location and fertilizer treatment. For operation purposes, replicate plots were irrigated using the same schedule. This meant that replicates could not be supplied by the same lateral.

In Field I, the irrigation treatments were replicated because there were sixteen test plots. The plot assignments were made based solely on the operational requirements. In Field II, all eight irrigation treatments were replicated four times, twice on the plots containing 50 ppm nitrogen and twice on those plots containing 100 ppm nitrogen. This design used all available test plots in Field II. Field III-N contained only ten plots and each irrigation treatment was used once. Two treatments were replicated using the remaining plots. The plots in Field III-S were used to evaluate the pickup of salts by water moving over the shale layer. The irrigation treatment for these plots was different from the rest of the research area. Irrigation water was applied when the crop required moisture and was run for either 24 or 48 hours on a plot.

Initiation of Irrigation

Since the design of the irrigation treatment was based on depleted soil-water, a method was established to monitor this depletion. Because of the large number of test plots, it was impossible to monitor all plots for their existing water content. Plots having the same irrigation treatments were paired and one plot of each pair was monitored for depletion. Monitoring was accomplished using a neutron probe. The decision to irrigate was based on the depleted water computed as the difference between the 33 kPa water content (field capacity) for that plot and the existing water content. Depletions were computed from graphical plots of soil moisture with depth, using a planimeter to measure the area on the curves between the field capacity moisture and the existing moisture profile. Once a monitor plot was depleted to the desired level, both plots were irrigated.

DATA COLLECTION AND INSTRUMENTATION

Data needed as input to the model and for use in calibrating the model were collected. This included irrigation depths and timing, soil-water storage, soil-water fluxes, drainage, chemical analysis of soil-water, evapotranspiration data and chemical analysis of soil profiles. Other data needed to

extend the results of this report to predicting changes in salinity of sub-surface irrigation return flows in the Grand Valley Salinity Control Demonstration Project area and the entire Grand Valley are presented in Section 8.

Irrigation

The depth of irrigation for a specific plot was computed based on the assigned irrigation treatment and the available moisture on the plot. After the decision to irrigate was made, the irrigation was scheduled as soon as practicable. Irrigation water was delivered to the plots via 20-cm aluminum pipe strung along one edge of a field. From the 20-cm line the water came up through a riser into a weir box containing a 30° V-notch weir; where the flow was measured. After flowing over the weir, the water dropped into a lateral of 15-cm gated pipe which conducted the water to the upper end of the plot. Plots were isolated by constructing an earthen berm around the perimeter of each plot. As a practical matter, the rate and duration of flow for an irrigation treatment were specified for a plot prior to initiating the irrigation.

Soil Moisture Measurements

Soil moisture measurements were required to monitor moisture levels for irrigation, compute water stored with each irrigation and estimate soil hydraulic properties. These measurements were made gravimetrically and with neutron attenuation equipment, see van Bavel et al. (87).

Neutron probes used in the study were field-calibrated to the soils and access tubes used in this project (87). Neutron access tubes centered in each quadrant (4 tubes per plot) of all the test plots were used to establish an average moisture profile. Neutron readings taken at 6 in. intervals beginning at 6 in. below the soil surface over the entire soil depth were taken in each quadrant of a plot and then averaged to give a single profile. A count interval of 0.5 min per reading was used instead of the 1 and 2 min counts usually preferred. Rogerson (72) found that for practical purposes 0.5 min counts are adequate for probe systems with 100 millicuries (mc) Americium-Beryllium (AmBe) sources, which were the sources used in this study. Moisture profiles of each plot were made the day before irrigation and four days subsequent to an irrigation with the difference in moisture profiles being the water stored from that irrigation.

Vacuum Extractors

Data on the total flux of soil solution leaving the root zone was gathered using two sets of vacuum extractors developed by Duke and Haise (21). Since the root zone is generally a partially saturated zone, the soil water is under suction and vacuum is required to extract it from the soil. The vacuum was applied through a ceramic tube that was isolated from the total soil mass by a box that could only receive percolation from the ground surface.

Four lysimeter pans (comprising one unit) were placed in each of two test plots in Field II and located at the corners of a 3 m by 4 m rectangle centered in the plot as shown in Fig. 20. The pans were installed during the construction of the test plots and were connected by polyethylene tubing to control

units housed at the edge of Field II. The polyethylene tube was used to supply vacuum, air pressure and provide dump lines to collect accumulated samples. Extracted water was held in 3.9 l jars buried in wells in the test plots which were emptied as required. Each pan was equipped with a separate collection bottle.

The control unit consisted of a vacuum pump, vacuum tank, manometer and pressure switches to control and maintain the vacuum at a specific level on the ceramic tube. One vacuum unit was used to run a set of four lysimeter pans. Water samples collected were used to estimate total flux below the root zone and as samples for water quality analysis.

Drainage

The collection boxes for the drains from Fields I and III-N were located in Indian Wash on the east side of the test area. These boxes were compartmentalized (one drain per compartment) and fitted with 30° V-notch weirs so discharge from each drain could be measured. The depth and duration of flow were measured. The drains were checked daily and depth of flow was measured twice each day if flowing. The drains from the plots in Field II and their outfall in the manholes in Field II also were checked each day and flows were measured twice each day as required. Water for quality analysis was collected at the same time that flows were being measured.

Evapotranspiration

A weather station consisting of a Class A evaporation pan, a tipping bucket rain gage, an anemometer, a recording hygrothermograph, two grass lysimeters and a pyranometer were located in Field III-S for use in evapotranspiration studies. These instruments provided daily values of humidity, maximum and minimum temperature, net daily solar radiation, evaporation from free water surface, rainfall, and daily evapotranspiration from a well-watered grass. By using the pan evaporation and a crop coefficient (84), the daily loss of soil moisture was estimated and used in scheduling irrigations.

The grass lysimeters consist of a 1.2 m by 1.2 m by 0.5 m box containing a layer of coarse gravel covered by a layer of soil on which sod was grown. Water was supplied to the sod in the box lysimeter from a reservoir. A constant water level was maintained in the sod box using a float valve. The drop in water level in the reservoir supplying the sod box was recorded using a water stage recorder.

Soil and Water Chemistry

Soil chemical profiles were determined annually for each plot by taking soil samples at 30-cm intervals through the first 1.8 m of the profile and then at 60-cm intervals from 1.8 m until shale was encountered. Within each plot, samples were taken from the center of the upper and lower one-half of the plot, composited by depth, and prepared for laboratory analysis.

In addition to the water samples gathered from the vacuum extractor and drains, water samples were taken daily from the irrigation supply lateral for

chemical analysis. Analyses conducted by the project laboratory included determinations of pH, electrical conductivity (EC), total dissolved solids (TDS), and the concentration of the following ions: Calcium (Ca^{++}), Magnesium (Mg^{++}), Sodium (Na^+), Potassium (K^+), carbonate ($\text{CO}_3^{=}$), bicarbonate (HCO_3^-), chloride (Cl^-), sulfate ($\text{SO}_4^{=}$), and nitrate (NO_3^-). Additional chemical studies were done at the Colorado State University Soil Testing Laboratory to determine soil texture, percent of organic matter, lime, total nitrogen, cation exchange capacity, and concentration of gypsum in the soils in the study area.

Soil Properties

Soil-water characteristic curves for the research plots were developed from undisturbed soil samples using a pressure plate apparatus. Two undisturbed samples were taken at 30-cm intervals through a 2.1-m soil profile. New samples were taken for use with each value of pressure used to compute the characteristic curves. Fourteen values of moisture content were averaged at each value of pressure head (ranging from 29 cm of water pressure to 1.5×10^3 kPa) used to construct the characteristic curves. Saturated flow through short columns of undisturbed soil and values of hydraulic conductivity from previous studies (1) were used to estimate saturated hydraulic conductivity. Bulk densities for the soil in the research area were calculated from the dried soil samples used to develop the soil moisture characteristic curves.

SECTION 5

SOIL MOISTURE AND SALT TRANSPORT MODELS

Salt transport studies should include not only a consideration of the movement of salts or dissolved constituents, but also the displacement of the solvent as well. Biggar and Nielsen (3) have stated that "such considerations become particularly important in irrigated agriculture when it is desirable to know the concentration and location of a dissolved constituent in the soil profile, the reactions of constituents with each other, and the soil matrix during the displacement and transport of water and solutes to plant roots."

The research described in this report considered salt transport and solution displacement. A field study was conducted in the Grand Valley of Colorado where data were collected to calibrate a numerical model which describes the salt and solvent transport process occurring in the soils in the Grand Valley.

To meet the objectives of the research, the solution flow segment of the model simulated transient one-dimensional infiltration and redistribution, and evapotranspiration by crops. The boundary condition in the field at the soil surface was that imposed by intermittent irrigation from a gravity system. It was also required that the model calculate the dissolution and precipitation of salts and cation exchange of ions commonly found in soils and compute the transport of these ionic species in response to the solution displacement computed in the solution flow segment. In the remaining portions of this section the literature pertinent to each of the components of the model is reviewed.

SOLUTIONS OF WATER FLOW EQUATION

The equation describing the vertical flow of water in soils is

$$\frac{\partial \theta}{\partial t} = \frac{\partial}{\partial z} \left[K(\theta) \frac{\partial H}{\partial z} \right] + S \quad (1)$$

where θ is volumetric water content, t is time, z is depth, H is piezometric head, and $K(\theta)$ is hydraulic conductivity as a function of water content. This formulation without the sink term is attributed to Richards (70) and is commonly called the Richards' equation. The equation is valid for flow in saturated and unsaturated flow regimes. Water is added or subtracted from the soil at "points" in some problems and a sink or source term (S) is used to handle these cases. Many investigators have found it more convenient to

write Equation 1 with θ as the dependent variable, a form known as the water content form, i.e.,

$$\frac{\partial \theta}{\partial t} = \frac{\partial}{\partial z} \left[D(\theta) \frac{\partial \theta}{\partial z} \right] + \frac{\partial K(\theta)}{\partial z} + S \quad (2)$$

where $D(\theta)$ is the diffusivity. (However, the water content form is applicable to partially saturated flow only because $D(\theta)$ is not defined in saturated soils.)

Analytic Solutions to Richards' Equation

Analytic solutions have found considerable application as tools for investigating and understanding particular aspects of flow phenomena. However, they have a very limited applicability for direct use in this study because of their lack of generality imposed by limiting assumptions. These assumptions are not generally satisfied in the field problem of interest in this research. The analytic solutions do, however, play a role in model studies because they provide a standard for comparison against which numerical models can be checked. It is for this reason that several solutions for one-dimensional flows are described briefly.

Few exact solutions to the Richards' equation exist due to the nonlinearity of the equation. The water content form of the equation for horizontal and vertical infiltration has been studied extensively, experimentally and mathematically. Philip (65), Brutsaert (13,15) and Parlange (62,63) have developed analytic solutions for Richards' equation.

Philip (65) developed numerical solutions for horizontal imbibition and vertical infiltration of water. For vertical infiltration, the solution is given as an infinite series

$$Z = \sum_{n=1}^{\infty} f_n(\theta) t^{n/2} \quad (3)$$

where Z is depth to a particular water content, t is time. The coefficient $f_n(\theta)$ is calculated from a knowledge of diffusivity and conductivity functions.

Brutsaert (13,15) also used Richards' equation which had been transformed into an ordinary differential equation using the Boltzmann transformation to arrive at his solutions. He developed functional forms for the conductivity and soil moisture characteristic and substituted an approximation for the transformed terms on the right-hand-side of the equation. He was then able to integrate the equation and arrive at an analytic solution for θ versus depth.

Parlange (62,63) transformed the water content form of Richards' equation into an equation with Z as the dependent variable and approximated the water content profile by integration while neglecting the unsteady-state term. The unsteady-state term was calculated using this approximation and was reinserted into the differential equation which was then integrated to derive a second

approximation (52). Numerical comparisons of water content profiles calculated using Parlange's method with Philip's analysis were quite good as was Brutsaert's comparison for cumulative infiltration.

Gardner et al. (33) developed an approximate solution to the Richards' equation for redistribution behind a wetting front. By assuming functional forms for conductivity and diffusivity as power functions of water content, and assuming that the matric potential is proportional to $\exp(-B\theta)$, where B is a constant, they solved the equation by separation of variables with the solution assumed to be of the form $\theta = T(t)Z(z)$ where t is time and z is depth. Solutions were given for cases of redistribution with and without gravity terms included, and good agreement was attained between the theory and experimental results for stored water and drainage from column studies.

Numerical Solutions to Richards' Equation

Because the complexity of the flow system often makes an analytic solution to the Richards' equation impossible, recent investigators have turned to numerical methods to study flow systems. The object of a numerical method is to solve a differential equation using an equation which approximates the original equation. Numerical methods to solve Richards' equation were developed many years ago (44), but only with the advent of high speed digital computers did they become feasible as a method to solve complex problems. Currently, finite difference techniques are probably the most widely used numerical method. The finite element method and dynamic simulation languages have been investigated and, due to their versatility, will probably gain more acceptance in the future. A finite difference technique was used in this investigation to model soil-water flow.

When using finite differences, the derivatives in the equation are approximated by Taylor series expansion of the dependent variable as a function of the independent variable. Depending on the expansion used, the differencing is known as a "forward-difference," "backward-difference," or "central-difference." When the function f is expanded into a Taylor series about x in the positive direction, $f(x+\Delta x)$, the expression for df/dx is

$$\frac{df}{dx} = \frac{f(x+\Delta x) - f(x)}{\Delta x} + o(\Delta x) \quad (4)$$

where $o(\Delta x)$ represents the remaining terms in the series. The forward approximation for df/dx is given by dropping the $o(\Delta x)$ term. The backward approximation is derived in the same fashion as the forward approximation except that the function is expanded in the negative direction $f(x-\Delta x)$. When the Taylor series expansion for f in the negative direction is subtracted from the Taylor series for f in the positive direction, the resulting expression is the central-difference approximation for the derivative. A geometrical interpretation can be given to these differences. The approximation can be represented by the slope of the line connecting the two values of the function used to describe the difference. If the approximation of the function is being made at a point x , then the "backward-difference" is represented by the slope of the line between x and $x-\Delta x$. The "forward-difference" is represented by the slope of the line between x and $x+\Delta x$, and the "central-difference" is

represented by the slope of the line between $x-\Delta x$ and $x+\Delta x$. Approximations for both first and second derivatives can be made using Taylor series expansions.

To apply a numerical technique, the algebraic equations which approximate the differential equation are solved at a series of points or nodes which denote the time and space domains. For instance, in one dimension, domains are represented as a rectangular grid system with the indices i and j (Fig. 25) denoting the principal axes of the system. The j index indicates the time domain and the i index corresponds to the space domain.

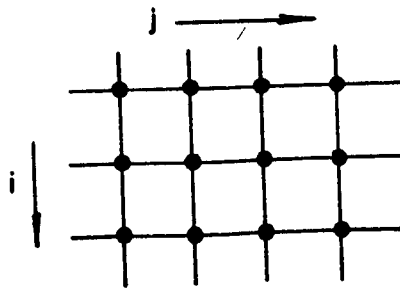


Figure 25. Grid system used for one-dimensional finite differencing.

The difference equations for the nodes between the boundaries, along with the equations for the boundary conditions, create a system of n algebraic equations in n unknowns. The series of algebraic equations used to approximate the Richards' equation in one-dimension form a tridiagonal matrix for which many solution schemes have been developed (69).

The solution techniques which have been developed are classified as either implicit or explicit. The implicit methods solve the equations simultaneously for each new time interval using a value of the variable at each node from the previous time interval. The implicit method provides a stable but not necessarily accurate solution regardless of the size of the time interval used to advance the solution.

Because of the approximation, the unknown in the "forward-difference" equation is given explicitly in terms of three known values for a previous time step. Thus, the terminology explicit arises and the solution is capable of being marched forward in time. For this technique to be convergent and stable, the time increments can be no larger than one-half the square of the space increments (69). In many practical situations this criterion can be very restrictive and can require large amounts of computer time for very short simulation periods. However, it also requires less storage than implicit techniques and solution methods for problems in subsurface hydrology, the reader is referred to Remson et al. (69).

One of the earliest and most widely known numerical solutions of the Richards' equation was developed by Hanks and Bowers (37). They solved the pressure head form of the equation, including a gravity term, for infiltration

into a layered soil using a Crank-Nicholson numerical technique. They considered the critical part of the solution of the system of difference equations to be the selection of the hydraulic parameters, K (conductivity), and C (specific moisture capacity), and Δt , the time interval. The parameters K and C were considered constant for a given time interval but were allowed to vary with time.

The time interval varied and was dependent upon the infiltration of a constant volume of water. The relationship was:

$$(\Delta t)^{j+1/2} = \frac{Q}{I^{j-1/2}} \quad (5)$$

where Q is a constant volume approximated as $Q = 0.035\Delta z$, where Δz is depth increment and $I^{j-1/2}$ is the infiltration rate from the previous time step. The superscript j indicates the time step being used in the computation.

The hydraulic conductivity at each grid for each time step was estimated from a difference form of the definition of diffusivity

$$K(\theta) = D(\theta) \frac{d\theta}{dh} \quad (6)$$

where the diffusivity had been estimated as an integrated average. This averaging was done to minimize the effect of water content changes on the computed value of $K(\theta)$, since small changes in water content can cause large changes in hydraulic conductivity. Since the diffusivity $D(\theta)$ does not vary as widely as $K(\theta)$ with moisture content, they found that better results in their simulation were obtained when using an average $D(\theta)$ to compute an average $K(\theta)$.

Hanks and Bowers (37) obtained better results when the specific moisture capacity was calculated using a value of moisture content estimated at the end of the time interval. The expression used for this estimation is

$$\theta^{j+1} \text{ (estimated)} = (\theta_i^j - \theta_i^{j-1}) B + \theta_i^j \quad (7)$$

where B is a constant equal to 0.7 or $t/(t+3-1/3)$, whichever is greater. The moisture content, pressure head and diffusivity data were entered as tabular data. Good agreement was achieved between calculated and experimental water content profiles for horizontal infiltration when compared with Philip's (66) work. The work of Hanks and Bowers has been used extensively in the development of the flow model used in this investigation.

Hysteresis of the soil moisture characteristic has been considered by several investigators (25,38,73,77,92) and has been found to be a significant factor in calculating all phases of flow, i.e., infiltration, redistribution and drainage. Also air entrapment by infiltrating water has been shown to significantly affect the advance of the water front (70). The effects of hysteresis and air entrapment were not included in the current study since

such a detailed description of flux was not needed to complete the analysis for this research project.

Characterization of soils is a major problem encountered in modeling soil-water systems. In most studies (39,62,73), it has been assumed that the soils were homogeneous and isotropic throughout the profile. If layered soils were to be modeled, then the properties were considered uniform through each layer (36). Wang and Lakshminarayana (90) used numerically averaged field data for the entire profile for the conductivity water content relationship and the soil-water characteristics. Comparisons between computed and field measured water content profiles in a nonhomogeneous soil were good.

Freeze (26,27) investigated saturated-unsaturated flow systems in both one and three dimensions. The models were used to analyze the interaction between surface water and groundwater as influenced by partially saturated flow in basin-wide hydrologic response studies. For the one-dimensional case, the pressure-head form of Richards' equation was solved using a recurrence relation developed by Richtmyer (71). The solution was initiated at the bottom boundary and proceeded to the surface boundary. The procedure applies as long as the soil is partially saturated. At saturation the recursion relationships are no longer defined and an alternate solution is required. The functional relationships for the hydraulic parameters and soil-moisture characteristic, including hysteresis, are entered as tabular values.

Bhuiyan et al. (2) and van der Ploeg (89) have used a dynamic simulation language to model vertical and horizontal infiltration in one-dimension as well as two- and three-dimensional infiltration problems. Using this method, the flux is calculated through a series of soil layers with conservation of mass principles and Darcy's law. Water content is calculated by integrating net flux using a fourth order Runge-Kutta scheme (2). The method gave excellent comparisons for horizontal infiltration studies when compared to Philip's numerical studies. The method is easily programmed and mathematically straight-forward which makes it easy to use.

Soil Moisture Extraction

The models discussed have not included the sink term as part of the solution. In investigations where a sink was included, the focus of the study was the sink, its functional form, and how it could be incorporated into the numerical solution for moisture flow. Plant roots are the most important water sink in the soil profile. The first approach to simulating water extraction by roots, termed microscopic, considers flow to a single root while the second approach, labeled macroscopic, considers evapotranspiration as a sink distributed over the total depth of the root zone.

Gardner (31), Molz et al. (57), and Cowan (16) have used a microscopic model to study the effect of soil water availability on transpiration by plants. Gardner's (31) idealized root model consists of an infinitely long cylinder of uniform radius and water absorbing properties placed in an infinite two-dimensional medium in which flow occurs in the radial direction only. Studies of root models such as the one proposed by Gardner (31) are necessary in developing an understanding of the microscopic aspects of flow in soil-water

systems. However, the description of the macroscopic or bulk flow of the soil solution is required for the research in this study.

The next type of model to be considered treats the root-zone extraction process as a whole without considering flow to individual roots. Molz and Remson (56) have labeled these macroscopic extraction models. A macroscopic root model developed by Gardner (32) distributed the roots through the soil profile and determined the water uptake pattern based on soil hydraulic properties. To apply the model, the root zone was segmented into layers, osmotic effects were neglected, and gravity was accounted for in terms of head. The total withdrawal (q) is computed for a cross-sectional area. Other macroscopic models are constructed from the Richards' equation coupled with a sink term and the resulting equations are solved with the sink included. Molz and Remson (56) and Nimah and Hanks (59) have developed models of this type which differ in the functional expression of the sink.

Molz and Remson (56) developed a model which was a function of a fixed rooting depth and pattern and plant transpiration rate. They approximated the distribution of root extraction as 40%, 30%, 20%, and 10% of the total transpiration coming from each successively deeper quarter of the root zone. The depth of the root zone remained fixed throughout the simulation. Soil moisture flux computed with the model compared well to experimental values of flux measured in a steady-state system, in which Birdsfoot trefoil (*Lotus coniculatus* var. *Tennuifolius*) was being grown in Pachappa fine sandy loam. Molz and Remson (56) and Nimah and Hanks (59) have proposed macroscopic models which are functions of moisture content, root depth and distribution, and crop transpiration rate. In each of the above models, the sink term was finite differenced and solved as part of the Richards' equation. All the models mentioned require that the magnitude of the sink (rate of withdrawal of water by the root system) be specified.

SINK STRENGTH

The magnitude of the sink strength is usually correlated with a value of evapotranspiration. The measurement of evapotranspiration was divided into three categories by Tanner (80) and provided convenient groups for consideration of the methods used to calculate evapotranspiration.

The first method considers a water balance for the region to be studied. Mathematically the balance is given as:

$$ET = P - (V_r + V_i + V_L + \Delta V_w + \Delta V_s) / A \quad (8)$$

where P is the volume of precipitation or applied water per unit area, and V represents volume elements of moisture accounting for intercepted water (i), leakage (L), runoff and drainage (r), stored water above the water table (s), and ground-water storage (w), and area of interception (A). The size of the region which can be studied varies from an entire watershed to a lysimeter. In general, as the area under investigation is reduced, the accuracy of the estimates improves because the measured variables begin to more closely

reflect the environment of a specific area. Lysimeter studies are very precise since the variables in the water balance can be controlled and measured accurately. Field studies have less precision because several of the variables must be estimated. The problem in field studies is to accurately estimate changes in storage and total drainage losses. Soil moisture changes can be estimated using either gravimetric methods or neutron scattering techniques; the second method is preferred since the same soil mass is measured each time and relatively large masses are considered. This ability or inability to measure or estimate accurately the drainage component from the profile can seriously affect the accuracy of the evapotranspiration estimate. Soil-water depletion studies, coupled with measurements of soil suction, have been used by Reicosky et al. (68) to estimate the uptake of water by plant roots.

The second classification of equations are those which use micrometeorological data. In this group are the equations which have been developed using mass transfer and wind profile theories or energy balances. Also included in this category are the equations which combine profile and energy balance methods. The assumptions basic to all the equations are steady-state adiabatic conditions, one-dimensional transport (no horizontal gradients), and a homogeneous surface. These conditions are difficult to achieve, and factors have been developed to account for deviation from the assumed condition. There still is the problem of deciding where to measure the variables and how many measurements to make. This becomes particularly difficult when measuring the environment around agricultural surfaces. Combination equations by Penman and van Bavel (64,86) are used frequently in evapotranspiration studies.

The remaining methods are empirical equations which have been developed by relating specific climatological parameters to evapotranspiration. Parameters used in the development of these equations include radiation, temperature, vapor pressure, humidity and percentage of monthly daylight hours. These equations have been developed for specific climatic conditions and their applicability is limited to these conditions. The Jensen-Haise and Blaney-Criddle equations (41), which are examples of empirical formulas, were developed in the western United States and are best suited for use in regions with a climate similar to this area. Correlation of pan evaporation and crop evapotranspiration is another method for estimating E_t (evapotranspiration). Again, this is site-specific, but has the advantage of being easily measured and applied. The equations mentioned predict potential evapotranspiration, thus requiring an adjustment for actual evapotranspiration. This adjustment can be made using crop coefficients which account for crop growth stage.

SOIL PROPERTIES

Characterization of the soil hydraulic properties and soil moisture characteristics is probably the most difficult part of modeling, particularly in a field study. Stable (77) attributed much of the error in his comparison between field data and computed results to the difficulty inherent in measuring conductivity and diffusivity over the entire range of moisture content occurring in the field. One alternative is to create a hypothetical soil with "reasonable" properties and use this data to conduct a theoretical study (92). Since the current research was a field investigation, the collection of soil

data from the research plot was part of the study. A knowledge of the conductivity versus moisture content relationship and the soil moisture characteristic is sufficient to develop the parameters needed for a flow model. The techniques which are currently used to measure these properties fall into one of two categories: In-situ or laboratory.

In-Situ Method

To calculate soil properties using in-situ methods, water flow and soil water suction data are collected in the field and used to solve the Richards' equation in one dimension. The hydraulic conductivity can be calculated once the soil-water flux and head are known. In-situ methods are attractive conceptually since the properties are measured in conditions which are representative of the soil profile and in large volumes of soil which are relatively undisturbed. In-situ methods have been used by several investigators (18,39,58), but were of no use in the current investigation. The inability to measure small changes in water content and suction occurring in the soils in the test plots prevented the use of these methods in characterizing the soils.

Laboratory Methods

Extensive literature exists on laboratory methods to measure hydraulic conductivity, diffusivity and soil moisture characteristics. The hydraulic properties are measured by experiments which have been devised to collect data to solve Richards' equation (11,12,30) or Darcy's law (9). Other investigators have explored the use of the soil moisture characteristic as a means to estimate hydraulic conductivity from the implied pore-size distribution data (9,10,35,55). Bruce (10) and Green and Corey (35) have evaluated these equations and found them acceptable provided a matching factor is used to match the computed value of conductivity to a measured value of conductivity at a specific moisture content, usually at or near saturation. Brutsaert (14) applied probability laws to the pore-size distribution to arrive at permeabilities, while Brooks and Corey (9) developed a power relationship for the permeability as a function of capillary pressure based on extensive experimental data.

Pressure plate (85) and hanging water column devices (45) have been used to develop the moisture characteristic needed to complete either of the above studies. Sample sizes and the use of disturbed samples are the major criticisms of laboratory methods. Collection of a number of samples sufficient to characterize a field is particularly important since, as Nielsen et al. (58) concluded, "The most important laboratory measurements for predicting the soil-water behavior in the field are the soil-water characteristic curve and a steady-state hydraulic conductivity." Steady-state methods for measuring hydraulic conductivity using short columns and other techniques have been discussed in detail by Klute (45).

SALT TRANSPORT

Salt transport occurs in soils as part of a miscible displacement process resulting from irrigation water or precipitation infiltrating and displacing

the soil solution. The salt transport process can be described using the diffusion convection equation. The equation in one dimension is

$$\frac{\partial(\theta c)}{\partial t} = \frac{\partial}{\partial z} \left(\theta D \frac{\partial c}{\partial z} \right) - \frac{\partial(vc)}{\partial z} + S \quad (9)$$

where D is an apparent diffusion coefficient which accounts for diffusion and dispersion, c is solute concentration, v is volumetric flux given by Darcy's law, and S is a sink term for the chemical species. The other parameters have the same definition as in the Richards' equation. When solute concentration changes occur at "points" in the system as the result of precipitation, dissolution or cation exchange, the source or sink term on the right-hand side of equation (9) handles these cases. As the displacement occurs, mixing of the two solutions occurs and a zone develops which is a mixture of the solutions. Within this zone in nonreactive porous media, mixing is the result of two phenomena which occur simultaneously. The first effect, mechanical dispersion, occurs because of the nonuniform velocity distribution in soils due to the variation in the shape and size of the pore spaces. The second effect, diffusion, is the mixing due to random motion of ions occurring in response to chemical potential gradients (3, 28). Even though the processes occur simultaneously, the effects of the processes cannot be superimposed and are generally treated as a single process because each is affected by the geometry of porous media, the properties of the fluid and water flux. Ion exchange between the soil solution and soil matrix, and dissolution and precipitation of species occur in soils and complicate the mathematical description of the transport process.

Chromatographic Theories

Initially, investigators tried to adapt the chromatographic theories used in column separations in the chemical industry to soil systems. Frissel and Poelstra (29) have discussed these theories and their application in much detail. The theories can be broken into two classifications; rate and plate.

The rate theories were developed assuming a kinetic exchange process. Theories of de Vault and Hiester and Vermeulen have been used to study transport in soils (29). Generally, rate theories have not been satisfactory for use in soil systems and all the flow and exchange parameters are required for the successful application of these methods.

Plate theories have been used by several investigators (24, 83, 88) with varying degrees of success. Dutt's model (24), which is used in the current study, is based on plate theory. The plate theory uses the height of the plate as the unit of calculation. The plate height is defined as the distance required for the mobile phase to come to equilibrium with the stationary phase. Application of plate theories requires an experiment to determine the plate height for each flow system. This is a limitation since each flow rate requires a different plate height. In some cases (24), the plate height has been fixed for convenience' sake to complete the computations.

Thomas and Coleman (83) investigated the leaching of fertilizer salts in soils using a chromatographic equation. They found poor agreement between concentrations of fertilizer salt found in the soil and those predicted by the model. They attributed the poor agreement to the lack of adequate data to

describe the soil characteristics. Van der Molen (88) studied the reclamation of Dutch soils which had been inundated with sea water using Glueckauf's (34) theory and found good qualitative agreement.

Lai and Jurinak (50) developed a numerical solution of a material balance equation which included a nonlinear exchange function. The isotherms were developed from column studies. They found from comparisons of numerical results with column studies that better agreement was obtained using nonlinear exchange isotherms. They also found that applicability of the equilibrium assumption used in the analysis depended on the flow velocity of the fluid and the cation exchange properties of the soil.

Bresler (5) and Terkletaub and Babcock (82) have developed plate models for use in investigating the movement of non-interacting solutes in response to irrigation water. Bresler (5) developed a linear model based on conservation of mass principles which he used to study the vertical downward flow of non-adsorbed ion species. Input data required for application of Bresler's model included the soil moisture characteristic, initial salinity and water content in each layer and the quantity and quality of applied water. Bresler (5) found good agreement between measured and predicted Cl^- profiles for a series of field experiments using varying irrigation treatments.

Terkletaub and Babcock (82) developed an algebraic expression to model the mixing process occurring during infiltration of a solution containing a non-interacting ionic species. They found a reasonably good prediction of concentration profiles when compared to column studies using ten sections. They also found that increasing the number of sections used in the computation had a marginal effect in improving the accuracy of the simulation.

The mixing cell concept is another technique which has been used to model dispersion in porous media. It is assumed that the solution in the cell is completely mixed and has a uniform concentration. The simple cell model is developed using the material balance equation

$$C_{i-1} - C_i = \frac{dC_i}{d\tau} \quad i=1,2,3,\dots,N \quad (10)$$

where C_i is the concentration of a component, τ is dimensionless time, and N is the number of cells. The advantages of the model are: (a) a serial solution of ordinary differential equations is required rather than a solution of a boundary-value partial differential equation; and (b) transport phenomena, chemical reactions or flow profiles can be easily added without changing the mathematical form or difficulty (19). It does not predict the observed tailing and asymmetry for pulsed systems. To account for this behavior, more complex models which include stagnant zones have been developed (49).

Numerical Solutions

In addition to the methods previously discussed, many investigators (6,7, 76,91) have attempted to solve the diffusion convection equation. These solutions are generally numerical solutions. Analytic solutions are possible, i.e., when pure diffusion is considered (28).

Warrick et al. (91) arrived at an approximate analytic solution for the diffusion-convection equation which describes the simultaneous transfer of a non-interacting solute and water during infiltration. He assumes one-dimensional steady flow in homogeneous soils. The finite difference method of Hanks and Bowers (37) was used by Warrick (91) to simulate the water infiltration. Warrick felt that comparisons of predicted moisture contents and concentration profiles and field measured data were reasonable considering the lack of homogeneity in the field.

Bresler and Hanks (7) combined the flow model of Hanks and Bowers (37) and the salt model of Bresler (5) to develop a new model capable of describing salt transport of non-interacting solutes in unsaturated soils under transient conditions. They found that the computed concentration profiles had shapes which were similar to profiles found in the experimental columns used for comparison.

In the solution of the diffusion convection equation, the magnitude of diffusion-calculated by the solution is often much smaller than the dispersion (numerical dispersion) due to differencing of the convective term. Bresler (6) eliminated the numerical dispersion by including higher than second order differences. He found agreement in the shape and concentration values between calculated and field measured water and salt profiles. Bresler (6) concluded that the apparent agreement suggests that macro-scale theoretical approaches were generally satisfactory for analysis and prediction.

Davidson et al. (17) solved the transport equation including a sink term for simultaneous transport of water and exchangeable solutes through soil under transient flow conditions. Water movement was simulated using an implicit-explicit technique and the salt transport equation was solved using an explicit method. Dispersion was calculated using the methods described by a Freundlich relation. Separate equations were used to describe either adsorption or desorption. Equilibrium conditions were assumed to exist between exchanging phases.

In addition to Dutt et al. (24), whose model is used in this study and discussed in detail in Section 6, King and Hanks (43) have also developed a salt transport model. King and Hanks (43) developed a detailed transport model which combined the water and salt flow model of Bresler and Hanks (7) and the inorganic chemistry model of Dutt et al. (24). The moisture flow model of Hanks et al. (38) was modified to include a plant root extraction $A(Z)$ term. The moisture flow equation solved by King and Hanks (43) was

$$\frac{\partial \theta}{\partial t} = \frac{\partial}{\partial Z} \left[K(\theta) \frac{\partial H}{\partial Z} \right] + A(Z) \quad (11)$$

where θ is volumetric water content, $K(\theta)$ is hydraulic conductivity, Z is distance, t equals time, H is piezometric head and $A(Z)$ is plant root extraction term.

The transport of salts in one dimension was expressed as

$$\left[\frac{\partial(\theta c)}{\partial t} \right]_Z = - \left[\frac{\partial(\bar{v}c)}{\partial Z} \right]_Z \quad (12)$$

where θ is volume water content, c is concentration of solute, \bar{v} is solution flux, Z equals depth and t equals time.

In the derivation of Eq. 12, it was assumed that dispersion was absent and no sources or sinks existed. The sink or source was treated implicitly as a change of concentration of the salts present at each depth due to chemical reactions occurring at that depth. The dispersion, which occurred in the results of the simulations, was due to the method of computing salt flow. The change in salt concentration within a depth increment was calculated using the net solution flux. The concentrations of the influent and the solution remaining in the depth increment were averaged to give the concentration for the space and time increment.

Reactions included in King and Hanks' model (43) were: (a) the dissolution or precipitation of gypsum; (b) the formation of undissociated calcium and magnesium sulfates (CaSO_4 and MgSO_4); (c) the dissolution or precipitation of lime; and (d) cation exchange reactions for Ca^{++} and Mg^{++} and Na^+ . The shapes and values of field measured moisture profiles and computed moisture profiles beneath an established stand of alfalfa compared quite well. The comparisons of the profiles for computed and measured values of concentrations of ionic species were found to be better for TDS than for individual species. With the exception of King and Hanks' model, most of the transport models discussed considered either the transport of non-interacting solutes or adsorption of a single solute. For the research in this investigation, it was required that the chemistry portion of the transport model calculate: (a) the dissolutions or precipitation of gypsum and/or lime; and (b) cation exchange reactions for Ca^{++} , Mg^{++} and Na^+ .

The fundamental chemical reactions and the stoichiometric relations describing the aforementioned reactions have been known and studied for some time. The application of computers to solve a system of equations which describe a combination of these reactions has occurred only recently. Several researchers (22,23,60,61,79) have investigated the chemistry of soil systems which included gypsum and lime equilibria and cation exchange reactions.

Dutt (22) predicted the equilibrium concentration of Mg^{++} and Ca^{++} in the soil solution and adsorbed phase in a Ca^{++} - Mg^{++} -soil containing excess gypsum. The concentration of Mg^{++} and Ca^{++} were predicted for the case of wetting the soil with either distilled water or a solution containing Mg^{++} and/or Ca^{++} salts. The equations used to describe the exchange of the cation and the dissolution of gypsum were solved by a computer using a series of successive approximations. Comparisons of measured and calculated values of Ca^{++} and Mg^{++} concentrations in the soil solution were generally good. Dutt and Doneen (23) used a computer to solve the equations to predict the concentrations of Ca^{++} , Mg^{++} and Na^+ in saturated extracts of soils undergoing salinization with waters containing Cl^- and SO_4^{--} salts and one or more of the cations, Ca^{++} , Mg^{++} and Na^+ .

Tanji (79) developed a computational scheme to predict ion association and solubility of gypsum in simple and mixed aqueous electrolyte systems. This computed model accepted as input data nonequilibrium solute concentrations and considered simultaneously the Debye-Huckel theory, the solubility product of gypsum and the dissociation constant of CaSO_4 , MgSO_4 , and sodium sulfate (NaSO_4) to predict equilibrium concentrations without prior measurement in the equilibrium state (79). Predicted cation activities and solubility of gypsum were in agreement with values found in the study.

Oster and McNeal (60) used three models to compute the variation of soil solution composition with water content for partially saturated soils. The calculation began using laboratory data on the composition of the soil-saturation extract, the cation exchange capacity of the soil, the percent water at saturation, the field water content and the estimated partial pressure of carbon dioxide in the laboratory atmosphere during the analytical determinations. These data were used to calculate the concentrations and activity coefficients of ion and ion pairs and the degree of supersaturation with respect to calcite and gypsum. Sulfate-gypsum equilibria and HCO_3^- - CO_3^{2-} -pH equilibria were computed as subgroups. Cation exchange was not included. The composition of the exchange phase was then initialized. Saturation-extract data were related to field-water contents by multiplying the calculated dissociated concentrations of each dissolved species by the ratio of the water content at saturation to the field water. The calculations used to calculate the concentrations in saturation extract were then repeated with cation exchange included. Calculated values of electrical conductivity compared well with field measured values.

Oster and Rhoades (61) used irrigation water compositions, leaching fractions, aragonite and gypsum solubilities and the partial pressure of CO_2 to calculate drainage water compositions. The model assumed: (a) steady conditions for chemical equilibria; (b) soil solution was saturated by lime; (c) water was in equilibrium with 0.13 atmospheres (atm) CO_2 ; and (d) the Debye-Huckel theory applied to mixed salt solutions when ion pair chemistry was considered. The initial input to the model was the concentration of salt in the drainage water obtained by concentrating the salts in the irrigation water using the experimental leaching fractions. Equilibrium drainage water compositions were determined by successive calculations of the concentrations of each chemical species using appropriate equilibrium constants (61). Comparisons of measured and calculated concentrations of salts in drainage water from lysimeters maintained at steady-state leaching were reasonably good. The model was used to predict the salinity, sodic and pollution hazards of irrigation waters in terms of minimum leaching fractions needed to maintain satisfactory salinity and sodic levels.

In each of the models presented, the major problem encountered in the simulation was developing the set of chemical reactions and constants which properly described the soil system under investigation. Many of the reactions discussed in the review of literature were included in the Dutt et al. (24) chemistry model, i.e., Ca^{++} - Na^+ exchange, dissolution and precipitation of gypsum and lime.

SECTION 6

MODEL DESCRIPTION

The salt transport model used in this study was developed by Dutt et al. (24) and has subsequently been modified by the Bureau of Reclamation, USDI. Salt transport is computed by assuming that soluble species move freely with water contained in the segment. The mass of salt moved into a segment from adjacent segments is computed by multiplying solute concentrations (assumed constant for any segment) by the appropriate flow volumes (24). The model is composed of two primary components. The first component computes soil solution flux using the Richards' equation. The flux from the first component is input to the second section and is used to compute the flow volume in the chemical transport model. The second submodel computes the concentration of the solution with depth needed to complete the transport calculation.

The spatial division of the soil-plant water system used in the computations is shown in Fig. 26. The segment sizes used in the simulations differ between models; and an interfacing program has to be written to adjust for these differences.

MOISTURE FLOW PROGRAM

Mathematical Basis

Soil homogeneity, air entrapment, hysteresis, thermal and chemical gradients all affect the flow of water through soil. Incorporation of these factors into a model requires extensive data and a degree of complexity not warranted in a study of the scope being considered here.

In the flow program, the Richards' equation was used to solve one-dimensional flow assuming a homogeneous soil profile, isothermal conditions, no air entrapment and no hysteresis.

For the one-dimensional case with distance measured as positive downward, Richards' equation is

$$\frac{\partial \theta}{\partial t} = \frac{\partial}{\partial z} \left[K(\theta) \frac{\partial H}{\partial z} \right] \quad (13)$$

Substituting the sum of suction head (h) and elevation head (z) for the piezometric head (H) and completing the differentiation, Eq. 13 becomes

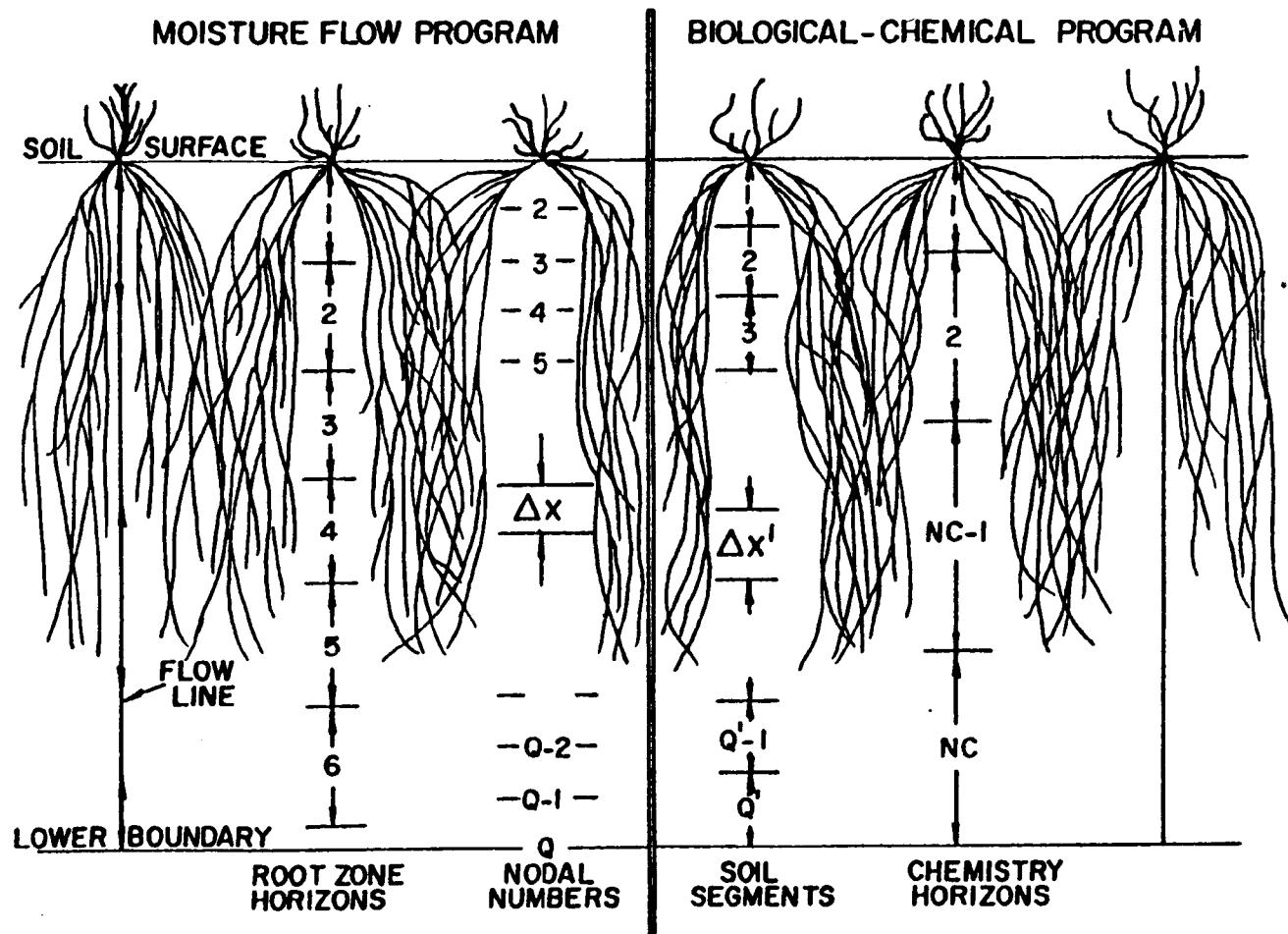


Figure 26. Spacial division of soil-plant-water system along a flow line.
(After Dutt et al., 24)

$$\frac{\partial \theta}{\partial t} = \frac{\partial}{\partial z} \left[K(\theta) \left(\frac{\partial h}{\partial z} - 1 \right) \right] \quad (14)$$

Equation 14 is transformed to an equation with θ as the dependent variable by first applying the chain rule of differentiation to the gradient of suction,

$$\frac{\partial h}{\partial z} = \frac{dh}{d\theta} \frac{\partial \theta}{\partial z} \quad (15)$$

and defining the diffusivity $D(\theta)$

$$D(\theta) = K(\theta) \frac{dh}{d\theta} \quad (16)$$

After substitution of these expressions into Richards' Eq. 14, the result is

$$\frac{\partial \theta}{\partial t} = \frac{\partial}{\partial z} \left[D(\theta) \frac{\partial \theta}{\partial z} - K(\theta) \right] \quad (17)$$

A sink term (S) was added to the right-hand side and the equation used in the model is

$$\frac{\partial \theta}{\partial t} = \frac{\partial}{\partial z} \left[D(\theta) \frac{\partial \theta}{\partial z} - K(\theta) \right] - S \quad (18)$$

where θ is volumetric moisture content, $D(\theta)$ is soil moisture diffusivity, $K(\theta)$ is hydraulic conductivity, S is a sink term (volume of water consumed per unit volume of soil per unit time), t equals time, and z is the space coordinate in vertical direction.

Solution Technique

The finite difference approximation used in the model is

$$\frac{\theta_j^{i-\theta_j^{i-1}} - \theta_j^{i-1}}{t} = [D_{j-1/2}^{i-1/2} (\theta_{j+1}^i + \theta_{j+1}^{i-1} - \theta_j^i - \theta_j^{i-1}) - 2\Delta z K_{j+1/2}^{i-1} - D_{j-1/2}^{i-1/2} (\theta_j^i + \theta_j^{i-1} - \theta_{j-1}^i - \theta_{j-1}^{i-1}) - 2\Delta z K_{j-1/2}^{i-1}] / 2\Delta z^2 - S_j^i \quad (19)$$

where the superscript "i" specifies the time step used to evaluate the variable and the subscript "j" specifies the depth increment used to evaluate the variable.

Using the grid system in Fig. 27, the combination of superscripts and subscripts in Eq. 19 specifies the node and the value of water content used in the calculation. The value of water content being calculated is specified as θ_j^i and integer or fractional values of the indices specify the step size used to select the values of water content needed for the calculation. For example, θ_j^{i+1} specifies the value of moisture for the next time step at depth j.

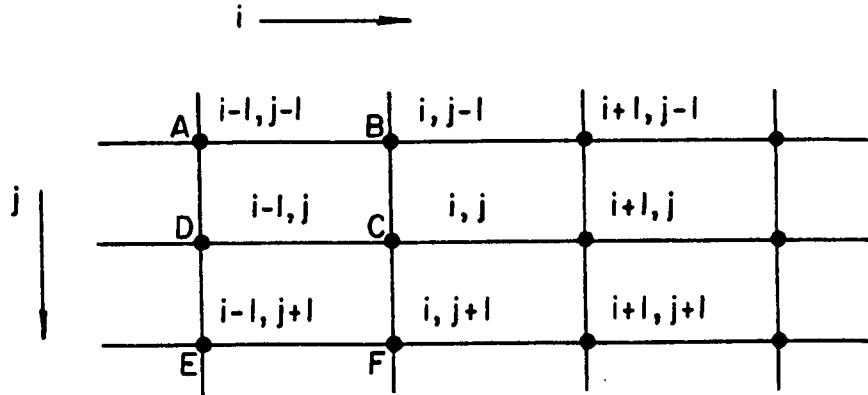


Figure 27. Grid system used for finite differencing of Richards' equation.

The finite difference approximation used for Richards' equation computes the moisture content for the center of the grid as the average of the moisture content occurring at the nodes of the grid, ABCD and CDEF in Fig. 27. The approximation is backwards in time, which means that values of moisture content from the previous time step are used to calculate values for the present time.

When the algebraic Eq. 19 is applied to each grid point, along with the equations for the boundaries, a system of n equations in n unknowns is formed. When the system of equations is put into a matrix, a tridiagonal matrix is created which can be solved efficiently.

An implicit solution method developed by Richtmyer (71), which is a special adaptation of the Gauss elimination procedure, uses a series of recursion relationships and is the solution method used in the model. The algebraic Eq. 19 to be solved by the model can be written in the form

$$-A_j \theta_{j+1} + B_j \theta_j - C_j \theta_{j-1} = D_j \quad (20)$$

where A , B , and C are the coefficients of the water contents given on the left-hand side of the matrix equation. D is the right-hand side of the matrix equation and contains known values of moisture content. Richtmyer (71) provided a solution to the system of equations as

$$\theta_j = E_j \theta_{j+1} + F_j \quad (21)$$

where

$$E_j = \frac{A_j}{B_j - C_j E_{j-1}} \quad j \geq 1 \quad (22)$$

$$F_j = \frac{D_j + C_j F_{j-1}}{B_j - C_j E_{j-1}} \quad j \geq 1 \quad . \quad (23)$$

Equations 22 and 23 and the condition $E_0=0$ and $F_0=0$ are used to complete the solution. E_j and F_j can be calculated inductively in order of increasing j ($j=0,1,\dots,k$). The value of U_{j+1} is given for $j=k$ by the right-hand boundary condition (in the model this corresponds to the lower boundary). The value for θ_j in Eq. 21 can be calculated inductively in order of decreasing j ($j=k,k-1,\dots,1$).

Initial and Boundary Conditions

The previous discussion shows that the initial moisture content distribution and the upper and lower boundary conditions must be specified. The initial soil moisture profile can be uniform or nonuniform. The saturated water content and lower limit of available water are also required.

Attempts to accurately simulate the boundary conditions in the field resulted in a modification by the authors of the original program. The bottom boundary was originally specified as a constant moisture content. If water content at complete saturation is used, then the boundary condition represents a water table fixed at that position. If no water table exists, the moisture content can be specified. In any case, to complete the solution, the moisture content must be known at the lower boundary.

Little or no drainage water from tile drains located in the test area was evidence that a water table condition did not exist in the area being modeled. Neutron probe data indicated that the moisture content at the lower boundary was not constant. Plots of the moisture profiles showed that relatively uniform values of moisture content existed below a depth of 1.5 m. This indicated that the gradient of piezometric head was near unity in this region.

Dutt's program was modified to permit the moisture content at the bottom boundary to vary in response to flow through the soil profile by forcing the gradient of piezometric head to be unity. This was done by adding a node below the bottom boundary of the profile and assigning the moisture content of the bottom node to the extra node. The moisture content of the bottom node is now computed using the same recursion relations as are used in the solution of the remaining internal nodes. As a result, the moisture content can fluctuate in response to the drainage and redistribution occurring in the soil profile.

The upper boundary condition can be specified to simulate infiltration, evaporation and zero flux. The evaporation and zero flux conditions can be simulated by applying the sink term to the first node inside the upper boundary. Infiltration is calculated as the flux between the boundary node and second node using the diffusivity form of Darcy's equation:

$$q = K(\theta) - D(\theta) \, d\theta/dz \quad (24)$$

In the model, when infiltration is calculated, the upper boundary is given as moisture content until the water ponded on the surface has been infiltrated. Dutt et al. (24) stated that the use of the moisture content boundary condition was not expected to introduce significant error in the infiltration computation. Philip (66) found that an error in the calculated values of infiltration rate and cumulative infiltration of 2% /cm of ponded water resulted if the depth of ponding was not considered. If the model is used to simulate the infiltration under conditions where the depth of ponding is minimal, or ponding does not occur, then the approximation of Dutt et al. (24) is adequate.

Time Step

The simulation is advanced in time using time increments selected in two ways. When infiltration is not occurring, the time interval is specified as input data. When infiltration is occurring, the time interval used is computed internally using a relationship suggested by Hanks and Bowers (37), i.e.,

$$\Delta t^{i+1} = \frac{0.035\Delta z}{FR'} \quad (25)$$

where Δt^{i+1} is the interval for the next time step, Δz is the segment size, and FR' is the largest value of flux occurring between any two nodes for the previous time step. Flux (FR') is calculated using the diffusivity form of Darcy's law.

Hydraulic Parameters

The hydraulic parameters used in the model are assumed to be single valued functions of moisture content (no hysteresis). Data available for computing the soil hydraulic parameters included a soil moisture characteristic and an estimate of saturated hydraulic conductivity. Attempts to collect in-situ field data and laboratory studies of steady flow in short columns were unsuccessful. As a result, the Brooks-Corey (9) relationship for conductivity was selected for use in this study. The relationship used is

$$K(S_e) = K_s(S_e)^{\frac{2+3\lambda}{\lambda}} \quad (26)$$

where K_s is the saturated hydraulic conductivity, λ is the pore-size distribution index, and S_e is the effective saturation. The effective saturation (S_e) is defined by

$$S_e = \left(\frac{\theta - \theta_R}{\theta_S - \theta_R} \right)^\lambda, \quad (27)$$

where θ_R is water content at residual saturation and θ_S is water content at saturation. Substituting Eq. 27 in Eq. 26, the expression for the conductivity becomes

$$K(\theta) = K_S \left(\frac{\theta - \theta_R}{\theta_S - \theta_R} \right)^{\frac{2+3\lambda}{\lambda}}, \theta_r < \theta \leq \theta_S \quad (28)$$

$$K(\theta) = 0, \quad \theta \leq \theta_r$$

which is the form used in the model. The pore-size distribution index (λ) is the negative slope of the straight line drawn through a plot of $\log S_e$ as a function of $\log P_c/\gamma$, where P_c is the capillary pressure and γ is the specific weight of water.

The value of conductivity in the difference Eq. 19 is given by $K_{j+1/2}$.

The value indicated is that which occurs midway between nodes j and $j+1$. The value for K was calculated by evaluating the function at each node (j and $j+1$) and then averaging the computed values, i.e., $K_{j+1/2} = (K_j + K_{j+1})/2$. This method of computing the value for the conductivity is another modification the authors applied to Dutt's model.

During the preliminary testing of the moisture flow model, it was found that accurate simulation of field infiltration data and water content profiles was not possible for the case under consideration. The functions $K(\theta)$ and $D(\theta)$ used to compute flow were studied to determine their effect on the calculation of infiltration and flow. Originally in Dutt's (24) model, the conductivity function (Eq. 28) was computed using the average value of water content of adjacent nodes. For example, if the conductivity is calculated for two nodes which have volumetric water contents of 0.45 and 0.20, using the average value 0.325, the conductivity is 0.075 cm/day. If the conductivity is calculated as the average of the values of conductivity at each node, the conductivity is 10 cm/day. Because of the nonlinearity of the conductivity-water content relationship, averaging water contents before computing conductivities gives too much weight to the lower water contents.

Infiltration is computed in the model using the diffusivity form of Darcy's law. One can expect, therefore, that the time of infiltration will be sensitive to the flux computations. Using the above example of nodes with water contents of 0.45 and 0.20 and $\Delta x = 15$ cm, there is a 17% difference in the calculated value of flux, assuming the same value for the term $[D(\theta) \partial \theta / \partial x]$ in the flux calculations. If $K(\theta)$ is 0.075 cm/day, the flux equals 53 cm/day and if $K(\theta)$ is 10 cm/day, the flux equals 63 cm/day. Therefore, the method of computing $K(\theta)$ has a significant effect in the flow computation. After the method of computing $K(\theta)$ and $D(\theta)$ (which will be discussed later) was changed, it was possible to more nearly simulate field data. Computed infiltration times and water content profiles were roughly equal to measured values.

Hanks and Bowers (37) found, in their model studies, that better results for horizontal infiltration into homogeneous soil were obtained when compared to Philip's work, if the specific water capacity (C) was selected using a value of moisture content estimated to occur at the end of the time step. This procedure was adopted to calculate the diffusivity. Hanks and Bowers' (37) water content equation is

$$\theta_{est}^{i+1} = (\theta_j^i - \theta_j^{i-1}) Y + \theta_j^i \quad (29)$$

where Y equals 0.7 or $t/(t+3-1/2)$, whichever is larger.

The diffusivity has been previously defined as

$$D(\theta) = +K \frac{dh}{d\theta} \quad (30)$$

where K is the conductivity and $dh/d\theta$ is the derivative of the capillary pressure head with respect to water content. For the diffusivity to be consistent with the theory used to develop the conductivity relationship, the value for the derivative $dh/d\theta$ should also be computed using Brooks-Corey theory. Pressure head can be derived from the Brooks-Corey theory using the functions:

$$\begin{aligned} S_e &= (P_b/P_c)^\lambda & P_b &\leq P_c \\ S_e &= 1.0 & P_b &\geq P_c \end{aligned} \quad (31)$$

where P_b is bubbling pressure, P_c is capillary pressure and S_e is effective saturation. The equation for capillary pressure head is

$$\frac{P_c}{\rho g} = \frac{P_b}{\rho g} (S_e)^{-1/\lambda} \quad P_b \leq P_c \quad (32)$$

Without modification, these functions cannot be used to define $dh/d\theta$, since the derivative of the function is not continuous over the entire range of pressure. A functional relationship proposed by Su and Brooks (78), which gives pressure head as a function of saturation over the entire pressure range, was used therefore instead of the Brooks-Corey relation.

The relation proposed by Su and Brooks (78) is a combination of two Pearson Type VIII distributions that were found to match a soil moisture characteristic. The function is

$$P_c = P_i \left[\frac{S - S_r}{a} \right]^{-m} \left[\frac{1 - S}{b} \right]^{bm/a} \quad (33)$$

where P_c is capillary pressure, P_i is capillary pressure at inflection point, S is water content saturation, S_r is residual saturation, m is shape factor of the curve, a is the domain of saturation associated with concave portion of the curve and b is the domain of saturation associated with convex portion of the curve. The relation of the domains specified by the constants a , b , and S_r is given in Fig. 28. If b in Eq. 33 goes to zero, Eq. 33 becomes

$$P_c = P_i \left[\frac{S - S_r}{a} \right]^{-m} \quad (34)$$

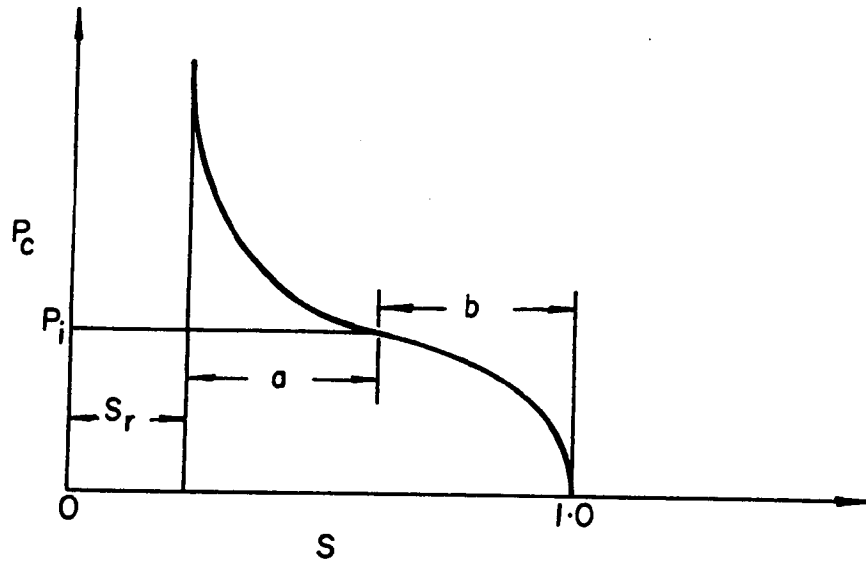


Figure 28. Saturation domains used for fitting Su and Brooks' parameters.

For this case, $a = 1 - S_r$, $m = 1/\lambda$, $P_c = P_b$ and Eq. 33 reduces to

$$\frac{P_c}{\rho g} = \frac{P_b}{\rho g} [S_e]^{-1/\lambda} \quad (35)$$

which is the Brooks-Corey equation for capillary pressure head.

Values of moisture content, not saturation, are calculated by the model. It becomes necessary, therefore, to make Eq. 33 a function of moisture content (θ). This conversion was accomplished by defining the saturation as

$$S = \frac{\theta}{\theta_s} \quad (36)$$

where θ_s is the moisture content at saturation. This expression was substituted into Eq. 33 to give the pressure head as a function of moisture content. The resulting equation was differentiated with respect to θ to give $dh/d\theta$, i.e.

$$\frac{dh}{d\theta} = - \frac{P_i}{\rho g} \frac{m}{\theta_s^a} \left[\frac{\theta - \theta_r}{\theta_s^a} \right]^{-m} \left[\frac{\theta_s - \theta}{\theta_s^b} \right]^{bm/a} \left[\frac{\theta_s^b}{\theta_s - \theta} + \frac{\theta_s^a}{\theta - \theta_r} \right] \quad (37)$$

Equations 28 and 37 for conductivity and the gradient of pressure head are substituted into the definition for diffusivity. The resulting relationship defining diffusivity is

$$D(\theta) = K_S \left[\frac{1}{(\theta_s - \theta_r)} \right]^{\frac{2+3\lambda}{\lambda}} \frac{\rho_i m}{\rho g} \left[\frac{1}{a\theta_s} \right]^{-m} \left[\frac{1}{b\theta_s} \right]^{bm/a} \\ \left[(\theta - \theta_r)^{\left(\frac{2+3\lambda}{\lambda} - m\right)} (\theta_s - \theta)^{bm/a} \right] \left[\left(\frac{\theta - \theta_r}{\theta_s - \theta} \right) \frac{b}{a} + 1 \right] \quad (38)$$

The value for diffusivity ($D_{j+1/2}$) used in the difference form of Richards' equation corresponds to a value of moisture midway between nodes. The method used to calculate the value of diffusivity is another modification of the Dutt et al. (24) program. Originally, the model of Dutt et al. (24) computed an average water content between 2 nodes and used the average value of water content to compute the diffusivity. We replaced Dutt's average $D(\theta)$ with an integrated average value. The change was required to properly model infiltration. Hanks and Bowers (37) found that cumulative infiltration was changed markedly for small changes of diffusivity computed at water contents near saturation. Their infiltration studies showed the need for weighted diffusivity values which include the effect of the diffusivity at saturation on the average value of diffusivity. Since the diffusivity - water content relationship is also nonlinear, averaging the water contents at two adjacent nodes prior to computing $D(\theta)$ does not properly weight the value of $D(\theta)$ at higher levels of saturation. Using the example for two nodes at water contents 0.45 and 0.20, the integrated average value of $D(\theta)$ is 3194 cm²/day, while the value of $D(\theta)$ for θ equal to 0.325 is 6.35 cm²/day. Calculating flux without considering the contribution from gravity ($q = D d\theta/dx$) with $\Delta x = 15$ cm, for water content equal to 0.325, the computed flux is 0.1 cm/day and with $D(\theta)$ computed as an integrated average, the computed flux is 53 cm/day.

For this example, using water contents of 0.45 and 0.20 at adjacent nodes, if the average value of water content 0.325 is used to compute $K(\theta)$ and $D(\theta)$, the calculated values of flux between these two nodes will be 0.175 cm/day. Using the $K(\theta)$ and $D(\theta)$ functions included in the model by the authors, the computed value of flux is 63 cm/day. Even though the example used shows an extreme case, it serves to point out the importance of properly accounting for the water content when computing the hydraulic functions $K(\theta)$ and $D(\theta)$.

The integrated average diffusivity was computed using the expression

$$D(\theta)_{\text{ave}} = \int_{\theta_j}^{\theta_{j+1}} \frac{D(\theta) d\theta}{\theta_{j+1} - \theta_j} \quad (39)$$

[a form used by other investigators (37, 77)]. The integration is completed numerically, using Simpson's rule, between the values of moisture content θ_j and θ_{j+1} occurring at adjacent nodes. If the moisture content is less than the value of moisture content at residual saturation (θ_r), the integration is divided into two parts. For $\theta \leq \theta_r$ the integrated average diffusivity is

$$D(\theta)_{\text{ave}} = \frac{\int_{\theta_1}^{\theta_r} D(\theta) d\theta + \int_{\theta_r}^{\theta_2} D(\theta) d\theta}{\theta_2 - \theta_1} \quad (40)$$

and the value of the integral for water contents below residual saturation is zero. The diffusivity is not defined at saturation ($\theta = \theta_s$). Therefore, the upper limit of the integration is a value of $\theta = \theta_s - \Delta\theta$ where $\Delta\theta$ is small.

Subroutine CONUSE

Subroutine CONUSE is called by the main program described above to provide values for the sink term (S). The value of evapotranspiration (ET) used for the sink is either input data given as semi-monthly or daily (ET), or semi-monthly values computed within the program using the Blaney-Criddle formula. The sink is a macroscopic root model which is distributed according to a user supplied distribution. In this work, the distribution of the sink was given as 40%, 30%, 20%, and 10% in 30 cm increments. Water is withdrawn from the root zone in proportion to the fixed distribution. Extraction is assumed to occur according to this fixed distribution until the lower limit of available water content is reached. The limit simulates the water content below which extraction by roots cannot occur. The model has no mechanism to increase withdrawal from wetter portions of the root zone as do the models of Nimah and Hanks (59), Gardner (32), and Molz and Remson (56), and thus, it lacks some realism available in other models. For studies which include the presence of a water table, this could represent a serious weakness. There are two other subroutines included in this program which are used as bookkeeping routines to record the results of the simulation and control the flow of data required for the simulation. The generalized program is given in block form in Fig. 29.

BIOLOGICAL-CHEMICAL PROGRAM

This section is a summary of the work of Dutt et al. (24) and is provided as source material. For a complete discussion of the chemistry and related works, the reader is referred to Dutt et al. (24).

The biological-chemical model, as constructed, includes two major areas of soil chemistry. The first area, nitrogen chemistry, was developed using reaction kinetics so that the nitrogen transformations, including microbial activity, could be included. While nitrogen is an important element affecting soil fertility and plant nutrition, it will not be considered as a pollutant in this study. The major pollutants in the Grand Valley are salts, and for this reason only the salt chemistry is considered.

The other area of chemistry considered, inorganic chemistry, includes reactions involving ion exchange, solution-precipitation of slightly soluble salts and formation of undissociated ion-pairs. In contrast to the nitrogen species, the equations describing these reactions are based on equilibrium chemistry, since the reaction times involved are assumed to be on the order

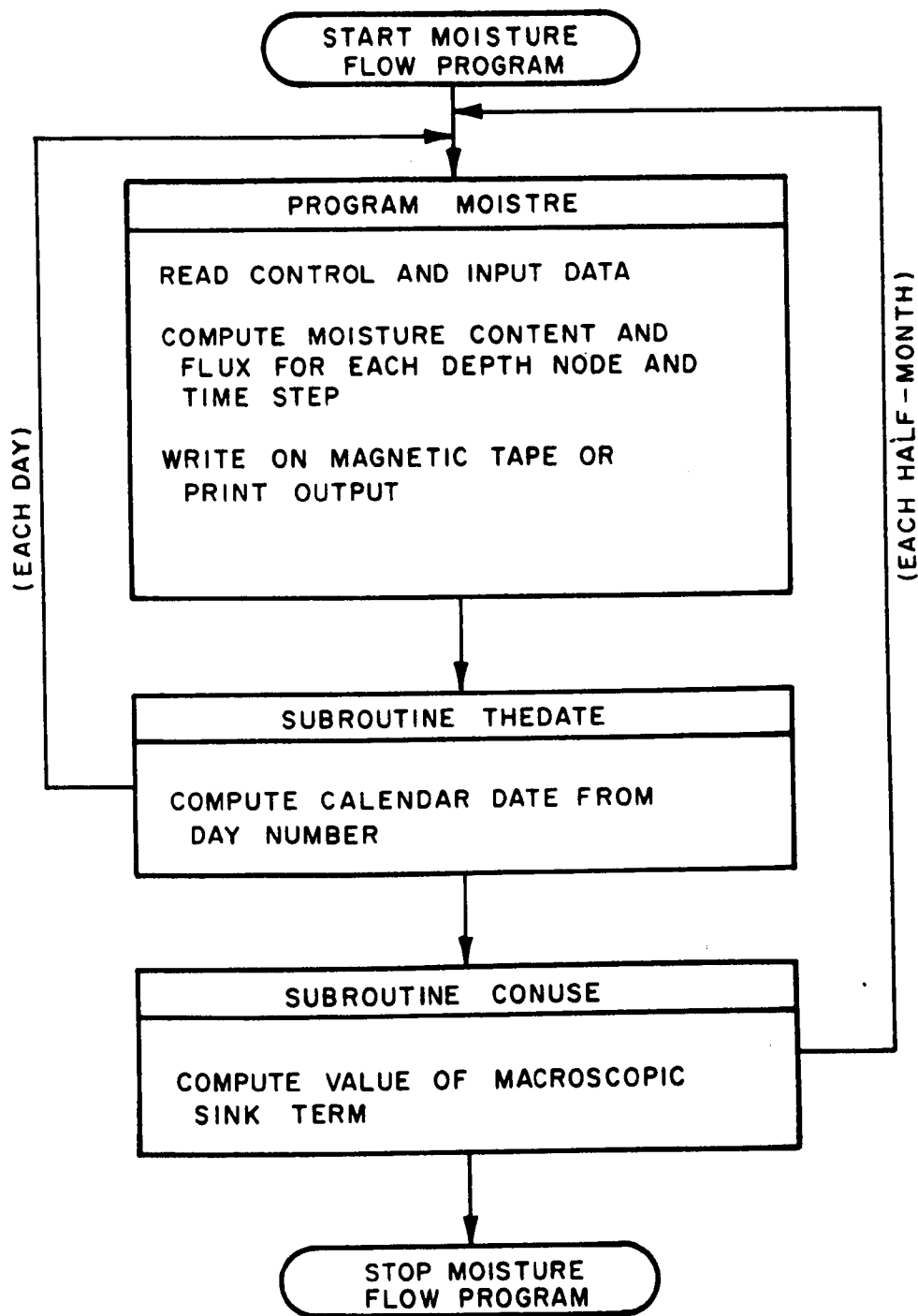


Figure 29. Generalized block diagram of Moisture Flow model.
(After Dutt et al.,24).

of minutes or seconds (times which are less than the residence time of water in a soil segment).

The chemical component of the Dutt et al. (24) model was developed assuming that water flow and content are independent of any chemical process. However, chemical process (dissolution, precipitation, etc.) depended on water flow and water content in a soil segment. From a computation standpoint, the water flow can be simulated independent of the chemistry and the results of the simulations used in the chemical component. The mixing cell concept is used with the water flow data to simulate solute dispersion and movement. It is assumed that: (1) complete mixing occurs at each increment in time and space; (2) each chemical process is independent of other processes over a time step with respect to availability of component masses; and (3) the rate of change of mass for each component is constant over a time step.

A generalized block diagram of the biological-chemical program is given in Fig. 30. The program consists of three control routines (MAIN, EXECUTE, COMBINE), five computational subroutines (TRNSFM, UPTAKE, XCHANGE, FL, EQEXCH) and several subroutines which serve as accounting and input-output devices. The routines of interest in this discussion include, MAIN, EXECUTE, COMBINE, XCHANGE, FL (flow) and EQEXCH (equilibrium exchange).

The program sequence begins with program MAIN reading control and input data and printing the same data, if desired. From MAIN, control is transferred to routine EXECUTE which initiates the computations in the biological-chemical program for each time step, monitors application of fertilizer and organic matter and reads daily moisture flow values which were computed by the moisture flow program. EXECUTE calls the COMBINE subroutine which controls the computation of chemical analyses for each depth increment and updates the masses of salt in storage in a segment using moisture flow data from routine FL.

Routine XCHANGE includes chemical reactions in base saturated soils which affect the solute composition of percolating waters. The primary assumptions used in this routine are: (1) that the reaction rates of the chemical process considered are much less than the residence times; and (2) that water entering a segment equilibrates with any remaining solution, the slightly soluble salts, and exchangeable ions on the exchange complex. A generalized block diagram of the logic of this routine is included as Fig. 31. During the initial time step, the subroutine EQEXCH calculates the exchangeable ion concentration from the initial soil analysis. The iteration process implied in Fig. 31 represents a method of successive approximations which is used to solve the equations describing the chemical reactions. The computation is initiated with an approximation of the concentration of an ionic constituent and is completed when the equilibrium constants of the involved reactions are satisfied within a tolerance established by the program user.

The chemical constituents and the mathematical relationship used to describe the chemical reactions included in the program are given below. The justification and development of these relationships can be found in Dutt et al. (24).

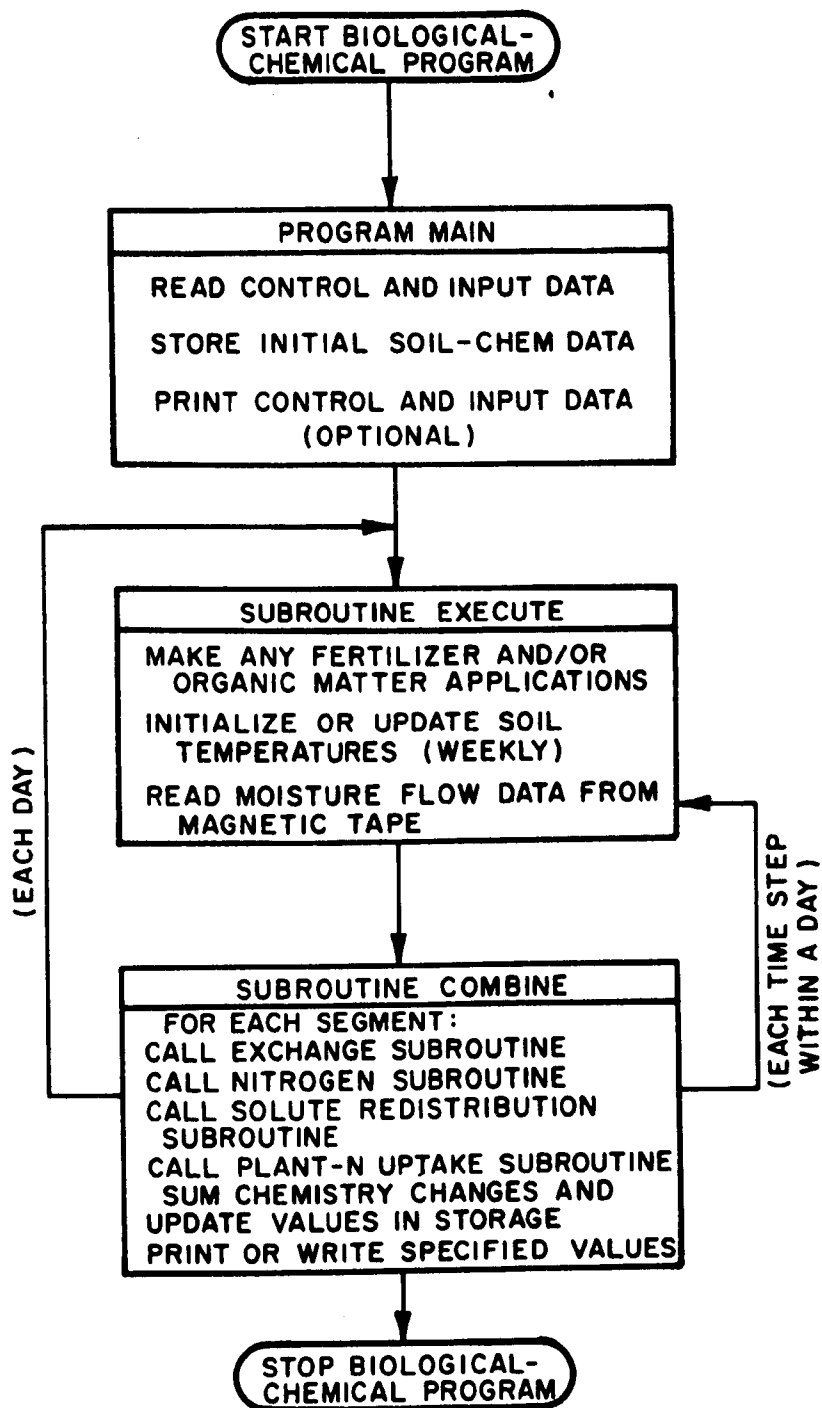


Figure 30. Generalized block diagram of Biological-Chemical Program.
(After Dutt et al., 24)

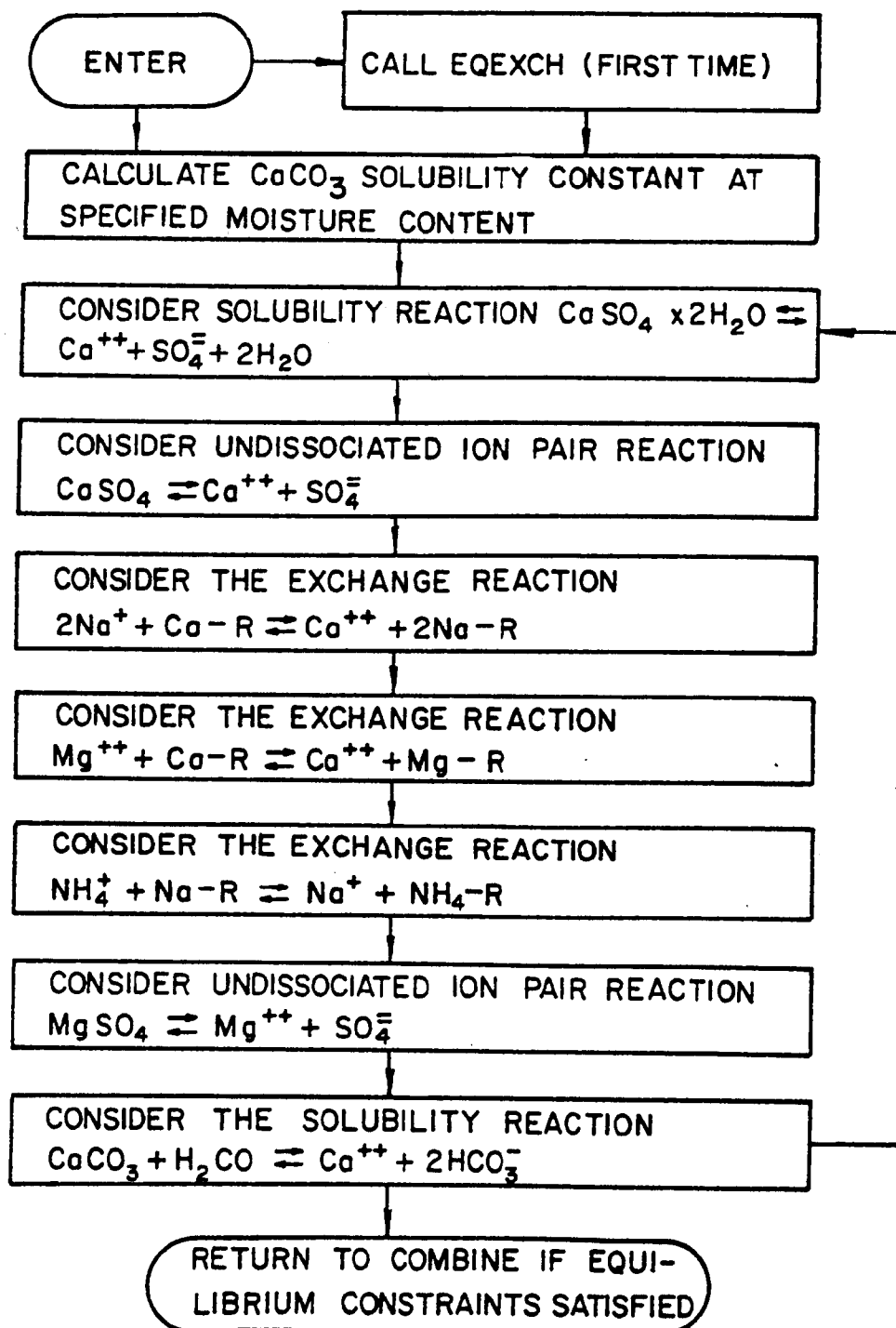
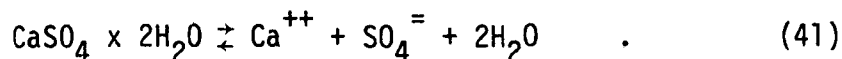


Figure 31. Generalized block diagram of subroutine XCHANGE.
(After Dutt et al., 24)

Subroutine XCHANGE

Solubility and Precipitation of Gypsum --

Gypsum is a slightly soluble salt found in many soils in the western United States and often included as a soil amendment in reclaiming sodic soils. It is found in the soils of the Grand Valley and is of interest in this study. The equilibrium equation for gypsum is



The equilibrium concentrations for Eq. 41 in soil-water systems given either initial concentrations or approximations of the constituent concentrations are calculated using

$$x^2 + Bx + C = 0 \quad (42)$$

where x equals the change in concentration of Ca^{++} and $\text{SO}_4^{=}$ to reach equilibrium. The coefficients are given as

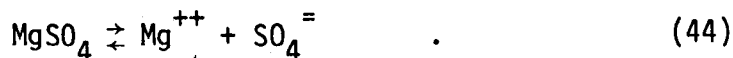
$$B = C'_{\text{Ca}} + C'_{\text{SO}_4}$$

$$C = C'_{\text{Ca}} C'_{\text{SO}_4} - K_{\text{SP}}/\gamma_2^2$$

where C' is initial or approximate concentration of the ion indicated by subscripts, K_{SP} is the solubility product equal to 2.4×10^{-5} and γ_2 is the divalent activity coefficient.

Undissociated Ca^{++} and Mg^{++} Sulfate --

Since the chemistries for undissociated CaSO_4 and MgSO_4 in solution are similar, the reactions will be considered together. The chemical reactions occurring in water are



The equation used to calculate equilibrium concentrations of the above reactions is

$$Ax^2 + Bx + C = 0 \quad (45)$$

where x is the change in $\text{SO}_4^{=}$ and Ca^{++} or Mg^{++} concentrations to reach equilibrium; A equals γ_2^2 (divalent activity coefficient); B equals $(K_D + \gamma_2^2 C'_{\text{Ca}} \text{ or } \text{Mg} + \gamma_2^2 C'_{\text{SO}_4})$; C equals $(\gamma_2^2 C'_{\text{Ca}} \text{ or } \text{Mg} C'_{\text{SO}_4} - K_D C_{\text{CaSO}_4} \text{ or } \text{MgSO}_4)$; and K_D is the appropriate dissociation constant. When the system contains gypsum, the undissociated CaSO_4 becomes a constant

$$C'_{CaSO_4} = K_{SP}/K_D \quad (46)$$

Ca⁺⁺ - Mg⁺⁺ Exchange --

The equation used to calculate the Ca⁺⁺ - Mg⁺⁺ exchange process is

$$Ay^2 + By + C = 0 \quad (47)$$

where y is the change in concentration of Mg⁺⁺ and Ca⁺⁺ to reach equilibrium. The constants and coefficients are defined as

$$A = \beta(1 - K_{Mg-Ca})$$

$$B = \beta(N'_{Mg} + K_{Mg-Ca}N'_{Ca}) + C'_{Ca} = K_{Mg-Ca}C'_{Mg}$$

$$C = C'_{Ca}N'_{Mg} - K_{CaMg}C'_{Mg}N'_{Ca}$$

β is the liters of water per grams of soil; K_{Mg-Ca} is the Ca-Mg exchange constant; and N' is the approximation of initial concentration of exchangeable ion indicated by the subscript.

Ca⁺⁺ - Na⁺ Exchange --

The Gapon equation was used to describe the Na⁺-Ca⁺⁺ exchange. The equation for the equilibrium condition is

$$Ax^4 + Bx^3 + Cx^2 + Dx + E = 0 \quad (48)$$

where x equals change in concentration of Ca⁺⁺ to reach equilibrium.

$$A = -4K_{Ca-Na}^2\beta^2$$

$$B = 4\beta(\gamma_{1/2} + 2K_{Ca-Na}^2N'_{Ca}\beta + K_{Ca-Na}^2C'_{Na})$$

$$C = 4\gamma_{1/2}(C'_{Ca} + N'_{Na}\beta) - 4K_{Ca-Na}^2\beta N'_{Ca}(\beta N'_{Ca} + 2C'_{Na}) - K_{Ca-Na}^2C'_{Na}^2$$

$$D = N'_{Na}\gamma_{1/2}(4C'_{Ca} + N'_{Na}\beta) + 2K_{Ca-Na}^2N'_{Ca}C'_{Na}(2\beta N'_{Ca} + C'_{Na})$$

$$E = N_{Na}^2C'_{Ca}\gamma_{1/2} - K_{Ca-Na}^2C'_{Na}^2N_{Ca}^2$$

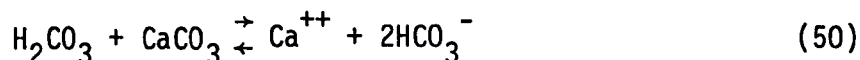
where $\gamma_{1/2} = \gamma_1/\gamma_2$ γ_1 = monovalent activity coefficient.

Dissociation of CaCO₃ in Water --

The dissociation of CaCO₃ is given as



Dutt et al. (24) state that the $\text{CO}_3^{=}$ concentration is a function of CO_2 partial pressure and HCO_3^- is usually the predominant form of CO_3 occurring in soil-water systems. The following reaction is considered in the model:



with

$$KK = \frac{a_{\text{Ca}} a_{\text{HCO}_3}^2}{a_{\text{H}_2\text{CO}_3}} \quad (51)$$

or

$$KK = \frac{K_{\text{SP}} K_1}{K_2} \quad (52)$$

where a is the activity coefficient of subscripted ion; KK is the thermodynamic equilibrium constant; K_1 and K_2 are the first and second acid dissociation constants for H_2CO_3 ; and, K_{SP} is the thermodynamic solubility product.

If an equilibrium system is at constant CO_2 pressure and the activity of the uncharged species is unity, Eq. 51 becomes

$$\frac{K'}{\gamma_1^2 \gamma_2} = \frac{KK C_{\text{H}_2\text{CO}_3}}{\gamma_1^2 \gamma_2} = C_{\text{Ca}}' C_{\text{HCO}_3}^2 \quad (53)$$

where γ_1 is the monovalent activity coefficient; γ_2 is the divalent activity coefficient; and C is the equilibrium concentration of subscripted species. The equation describing the dissociation of CaCO_3 was developed by substituting the stoichiometric relations

$$C_{\text{Ca}} = C_{\text{Ca}}' + Z \quad (54)$$

$$C_{\text{HCO}_3} = C_{\text{HCO}_3}' + 2Z \quad (55)$$

into Eq. 53. Where C_x' are concentrations of species before equilibria existed or approximate concentrations of indicated species, and Z is the change in moles to reach equilibrium. The resulting equations are

$$AZ^3 + BZ^2 + CZ + E = 0.0 \quad (56)$$

where,

$$A = 4.0; B = 4.0(C_{\text{HCO}_3}' + C_{\text{Ca}}'); C = C_{\text{HCO}_3}' + 4.0C_{\text{Ca}}' C_{\text{HCO}_3}'; E = C_{\text{HCO}_3}^2 C_{\text{Ca}}' - K'/\gamma_1^2 \gamma_2.$$

Dutt et al. (24) investigated the change in CaCO_3 solubility with changes in soil moisture and included this representation in the model. Through laboratory determination of Ca^{++} , $\text{CO}_3^{=}$ and HCO_3^- concentration in extracts

at three moisture levels (saturation, 100% and 500%) from six calcareous soils, a functional relationship was derived to describe the solubility. The derived relationship was then assumed to hold at field moisture levels and was used in the model.

Activity Coefficients--

Debye-Huckel theory was used in the model to calculate activity coefficients. To calculate single ion activities the equation is

$$\log \gamma_i = \frac{-0.509 Z_i^2 \mu^{1/2}}{1 + \mu^{1/2}} \quad (57)$$

where Z is the valence of ion i and

$$\mu = 1/2 \sum_{i=1}^n C_i Z_i^2,$$

and n is the total number of species present. Only two activity coefficients are needed since only mono and divalent ion species are considered in the model.

Subroutine EQEXCH

Dutt et al. (24) included in EQEXCH the effects of sulfate as an ion ($\text{SO}_4^{=}$) and undissociated CaSO_4 and MgSO_4 on the exchangeable Na^+ , Ca^{++} , and Mg^{++} in the system. The total sulfate, Ca^{++} and Mg^{++} in solution are given by:

$$C_{\text{SO}_4\text{T}} = C_{\text{SO}_4} + C_{\text{CaSO}_4} + C_{\text{MgSO}_4} \quad (58)$$

$$C_{\text{CaT}} = C_{\text{Ca}} + C_{\text{CaSO}_4} \quad (59)$$

$$C_{\text{MgT}} = C_{\text{Mg}} + C_{\text{MgSO}_4} \quad (60)$$

The thermodynamic equilibrium constants for equilibrium between the undissociated species in solution and the appropriate ions are

$$K_{\text{CaSO}_4} = a_{\text{Ca}} a_{\text{SO}_4} / a_{\text{CaSO}_4} \quad (61)$$

$$K_{\text{MgSO}_4} = a_{\text{Mg}} a_{\text{SO}_4} / a_{\text{MgSO}_4} \quad (62)$$

Combining Eqs. 59, 60, 61, and 62, the concentrations of CaSO_4 and MgSO_4 can be calculated. When these expressions are entered into Eq. 58 and assuming the divalent activity coefficients of MgSO_4 and CaSO_4 equal, the equation necessary to calculate the concentration of Ca^{++} and Mg^{++} is derived. The equation is

$$Ax^3 + Bx^2 + Cx + D = 0 \quad (63)$$

where

$$x = C_{SO_4}$$

$$A = \gamma_2^2 = (\gamma_{Ca} \gamma_{SO_4}) = (\gamma_{Mg} \gamma_{SO_4})$$

$$B = \gamma_2 \left[(K_{CaSO_4} + K_{MgSO_4}) + \gamma_2 (C_{MgT} + C_{CaT} - C_{SO_4T}) \right]$$

$$C = K_{CaSO_4} K_{MgSO_4} + \gamma_2 \left[C_{MgT} K_{CaSO_4} + C_{CaT} K_{MgSO_4} - C_{SO_4T} (K_{CaSO_4} + K_{MgSO_4}) \right]$$

$$D = - C_{SO_4T} K_{MgSO_4} K_{CaSO_4} .$$

The Ca-Mg exchange is given by

$$\frac{a_{Ca}}{a_{Mg}} = K_1 \frac{N_{Ca}}{N_{Mg}} \quad (64)$$

where N is the concentration of the subscripted exchangeable ion.

The Gapon equation

$$\frac{a_{Na}}{\sqrt{a_{Ca}}} = K_2 \frac{N_{Na}}{N_{Ca}} \quad (65)$$

is used for the Na-Ca exchange. The total concentration of exchangeable ions (N_T) then is

$$N_T = N_{Na} + N_{Ca} + N_{Mg} . \quad (66)$$

Using Eqs. 64, 65, and 66, the equation for exchange of calcium is

$$N_{Ca} = \frac{N_T a_{Ca}^{1/2} K_2}{a_{Na}} + \frac{K_1 a_{Mg}}{a_{Ca}} + 1 . \quad (67)$$

Once the activity coefficients, ionic concentrations for an equilibrium extract for Ca^{++} , Mg^{++} , Na^+ and the total exchangeable bases are known, the exchangeable Ca^{++} can be calculated and, in turn, the exchangeable Na^+ from Eq. 65 and the exchangeable Mg^{++} from Eq. 66. In practice the exchange capacity is assumed to equal N_T .

Exchangeable NH_4^+ is computed using

$$\frac{C_{\text{NH}_4}}{C_{\text{Na}}} = K_o \frac{N_{\text{NH}_4}}{N_{\text{Na}}} \quad (68)$$

with K_o assumed equal to 0.22.

The equilibrium exchange routine was tested (24) using the experimental data of Paul, Tanji and Anderson. Plots of measured values for exchangeable Ca^{++} , Mg^{++} and Na^+ against calculated values showed a good correlation between the experimental and calculated results. The favorable correlation between the observed and calculated values indicated the procedure for calculating the exchangeable ions is of use in the model (24).

The preceding discussion has outlined the chemical reactions and the equations considered in the model. Once these computations have been made for all segments for a time interval, the time is incremented. The moisture movement for the next time is read, and the new values for the equilibrium concentrations are computed.

Subroutine FL

The mixing cell concept is used to calculate salt transport in the model. The soluble species are assumed to move with the soil solution and to be at their equilibrium concentrations throughout the entire length of the cell. The length of the cell corresponds to the segment size used for the computations and remains constant. Flow data from the moisture flow program supply this subroutine with the volume of water remaining in the segment and the volume of water transferred between the segments for each time step.

Subroutine FL combines concentration and flows to compute the incremental transfer of salts into or out of a segment. Once the transfer is complete, the value of the mass of ion in storage per segment is computed. After the transfer and update of salt mass is completed, time is incremented and the solution proceeds.

The lower boundary condition of the flow model assumes that the solute concentration in the water adjacent to the lowermost segment is the same as in the lowermost soil segment for the last time step. Surface inputs are simulated by assuming that surface additions of chemicals mix completely with the applied water. The infiltrating water and its dissolved constituents are then treated as inputs to the first segment.

Input data required to run this model include chemical analysis of irrigation water, chemical analysis of soil profile, fertilization and organic matter treatment and soil temperature when nitrogen chemistry is considered. The required soil chemical analysis includes concentrations of NH_4^+ , NO_3^- , UREA, Ca^{++} , Na^+ , Mg^{++} , HCO_3^- , Cl^- , CO_3^{--} , and gypsum plus the exchange capacity, bulk density, the presence of lime and the moisture content of the saturation extract. The soil analysis is required for each horizon identified within the soil profile. The irrigation water analysis includes the concentrations of NH_4^+ , NO_3^- , Ca^{++} , Na^+ , Mg^{++} , HCO_3^- , Cl^- , CO_3^{--} , and SO_4^{--} .

SECTION 7

MODEL RESULTS

This section is divided into three topics. The first topic discusses the calibration and adaptation of the moisture flow model. The second topic deals with the comparison of the chemical model with field data and the selection of the parameters used for the final simulations. The last topic presents the results of the simulations of hypothetical irrigation treatments used to evaluate the effect of irrigation on salt transport.

MOISTURE FLOW MODEL

The flow model, which was discussed in Section 6, computes flow in one dimension assuming homogeneous isotropic soils, isothermal conditions and no hysteresis. Data required as initial input to run the program include: (1) upper and lower boundary conditions; (2) an initial soil moisture distribution; (3) the hydraulic conductivity and diffusivity as functions of water content; and (4) values for the crop evapotranspiration, root distribution, and rooting depth.

To calibrate the flow model, the upper boundary conditions were formulated to simulate the depth of water applied, duration of application and frequency of application that were observed in the field during selected irrigation intervals. The desired lower boundary condition required a modification of the original program. The lower boundary condition was originally given in the model as a fixed moisture content, which could be used to simulate a water table or any moisture content desired by the user. Lack of drainage water from the test plot and neutron probe data taken on the test plot indicated that a water table condition did not exist in the area being modeled. Field data given in Table 1 for the moisture content profile over the 1.5 to 2.13 m depth exhibited fairly uniform values. This uniformity of moisture content indicated that the hydraulic gradient which existed in the field was probably close to unity. The data in Table 1 show that the values of moisture content over the 1.5 to 2.13 m depth interval fluctuated slowly over the season. A method of treating the boundary condition was developed which forced a unit gradient to exist at the lower boundary between the bottom node and an imaginary node. This boundary condition permitted the moisture content at the bottom boundary to vary with time in response to irrigation. The suitability of the modified boundary condition and some alternative boundary conditions will be discussed in conjunction with the calibration.

TABLE 1. MOISTURE CONTENT PROFILES AT A DEPTH OF 1.52 TO 2.13 METERS FOR SELECTED PLOTS

Plot	Date	θ 1.52m	θ 1.83m	θ 2.13m	Plot	Date	θ 1.52m	θ 1.83m	θ 2.13m
17	6/9	0.32	0.30	0.31	29	6/21	0.31	0.29	0.33
	8/6	0.35	0.31	0.32		6/27	0.32	0.31	0.33
	8/18	0.35	0.31	0.32		7/10	0.34	0.32	0.34
	9/3	0.33	0.31	0.31		7/20	0.34	0.32	0.34
	9/15	0.33	0.31	0.31	30	7/30	0.35	0.32	0.35
18	7/17	0.30	0.29	0.31		8/11	0.35	0.32	0.35
	7/23	0.30	0.31	0.31		8/18	0.34	0.32	0.36
	8/5	0.30	0.32	0.33		8/28	0.36	0.33	0.36
	8/15	0.32	0.32	0.33		9/4	0.32	0.31	0.35
	9/2	0.29	0.30	0.32		9/11	0.35	0.32	0.37
	9/18	0.29	0.30	0.32	31	6/17	0.30	0.32	0.36
19	7/8	0.30	0.31			7/4	0.36	0.38	0.40
	7/14	0.32	0.33			7/28	0.35	0.33	0.36
	7/22	0.31	0.33			8/18	0.36	0.36	0.39
	8/8	0.32	0.34		33	6/19	0.29	0.30	0.33
	8/18	0.31	0.32			6/24	0.33	0.30	0.35
	8/25	0.31	0.32			7/9	0.34	0.33	0.38
	9/10	0.30	0.31			7/17	0.34	0.33	0.38
21	6/20	0.32	0.29	0.33		7/21	0.35	0.33	0.37
	6/24	0.32	0.29	0.33		7/28	0.35	0.33	0.37
	7/11	0.36	0.31	0.35	34	6/21	0.28	0.32	0.32
	7/19	0.36	0.31	0.32		6/28	0.31	0.34	0.33
	7/29	0.36	0.30	0.34		7/23	0.30	0.33	0.33
	8/8	0.36	0.30	0.34		8/1	0.31	0.34	0.33
	8/12	0.33	0.30	0.33		8/26	0.31	0.34	0.36
	8/27	0.35	0.32	0.33	35	6/17	0.30	0.32	0.34
	9/4	0.35	0.30	0.34		6/23	0.35	0.36	0.34
	9/15	0.35	0.33	0.34		7/21	0.33	0.34	0.35
25	7/9	0.33	0.29	0.32		7/27	0.35	0.34	0.35
	7/18	0.36	0.33	0.35		7/30	0.33	0.34	0.35
	7/25	0.34	0.32	0.35		8/5	0.33	0.34	0.35
	8/12	0.35	0.32	0.35		8/19	0.33	0.34	0.35
	8/15	0.35	0.32	0.36		8/28	0.33	0.34	0.35
27	6/19	0.28	0.32	0.32	39	6/18	0.30	0.33	0.35
	6/23	0.28	0.32	0.32		6/27	0.35	0.33	0.35
	7/18	0.31	0.34	0.35		7/9	0.33	0.34	0.36
	8/22	0.32	0.34	0.35		7/17	0.33	0.34	0.36
						7/25	0.34	0.31	0.31
						8/4	0.34	0.35	0.34
						8/12	0.34	0.34	0.38
						8/24	0.34	0.34	0.38

The sink strength equaled the estimated daily values of evapotranspiration for the corn grown in the test plot. Evapotranspiration estimations were made using pan evaporation data which had been modified by the crop coefficient to account for the crop growth stage. The assumed extraction pattern for the roots was 40% from the top foot, 30% from the second foot, 20% from the third foot and 10% from the fourth foot of the soil profile. The 4-ft rooting depth was assumed fixed for the entire season.

The initial moisture distribution was specified using field data collected with neutron probe equipment. The initial moisture content profile used for calibration corresponded to the field moisture content which existed at the beginning of the calibration period.

The hydraulic conductivity and diffusivity functions used in the study were Eqs. 26 and 38, which were developed using empirical relationships derived from the soil-water characteristic. The hydraulic conductivity function was developed from the Brooks-Corey relationships and the diffusivity was developed using both Brooks-Corey and Su-Brooks representation of the soil-water characteristic. To complete the development of the hydraulic properties, the parameters in the Brooks-Corey empirical representation of the soil-water characteristic and in the Su-Brooks equations were determined by fitting to field data. The Brooks-Corey representation of the soil moisture characteristic is defined by Eq. 31, where S_e is the effective saturation defined by Eq. 27, θ_r is water content at residual saturation, θ_s is water content at full saturation and θ is water content. The values of λ , S , and $P_b/\rho g$ (bubbling pressure head) were calculated using a computer program (SORPT) developed at Colorado State University by Dr. A. T. Corey. Values of capillary pressure head and corresponding values of saturation taken from the measured soil-water characteristic were used by program SORPT to calculate λ , S_r , and $P_b/\rho g$. The graphical representations of the field data and the Brooks-Corey curves are given in Fig. 32. Field data for the soil-water characteristic are given in Appendix A. The computed parameters for the Brooks-Corey equations represent the shape and values of field water content well over the concave portion of the curve and diverge over the convex portion of the curve, as would be expected.

The definition of diffusivity $\{D = K [d(P_c/\rho g)]/d\theta\}$ requires that both the hydraulic conductivity and the derivative of the capillary pressure be known. The Brooks-Corey functions can not be used to define the diffusivity entirely, because the derivative of the function is not continuous over the full range of capillary pressure head. The expression for capillary pressure head developed by Su and Brooks was used to compute the derivative of the capillary pressure head.

The equation for the capillary pressure head used in the study

$$\frac{P_c}{\rho g} = \frac{P_i}{\rho g} \left(\frac{S - S_r}{a} \right)^{-m} \left(\frac{1 - S}{b} \right)^{bm/a}, \quad S = \frac{\theta}{\theta_s} \quad (69)$$

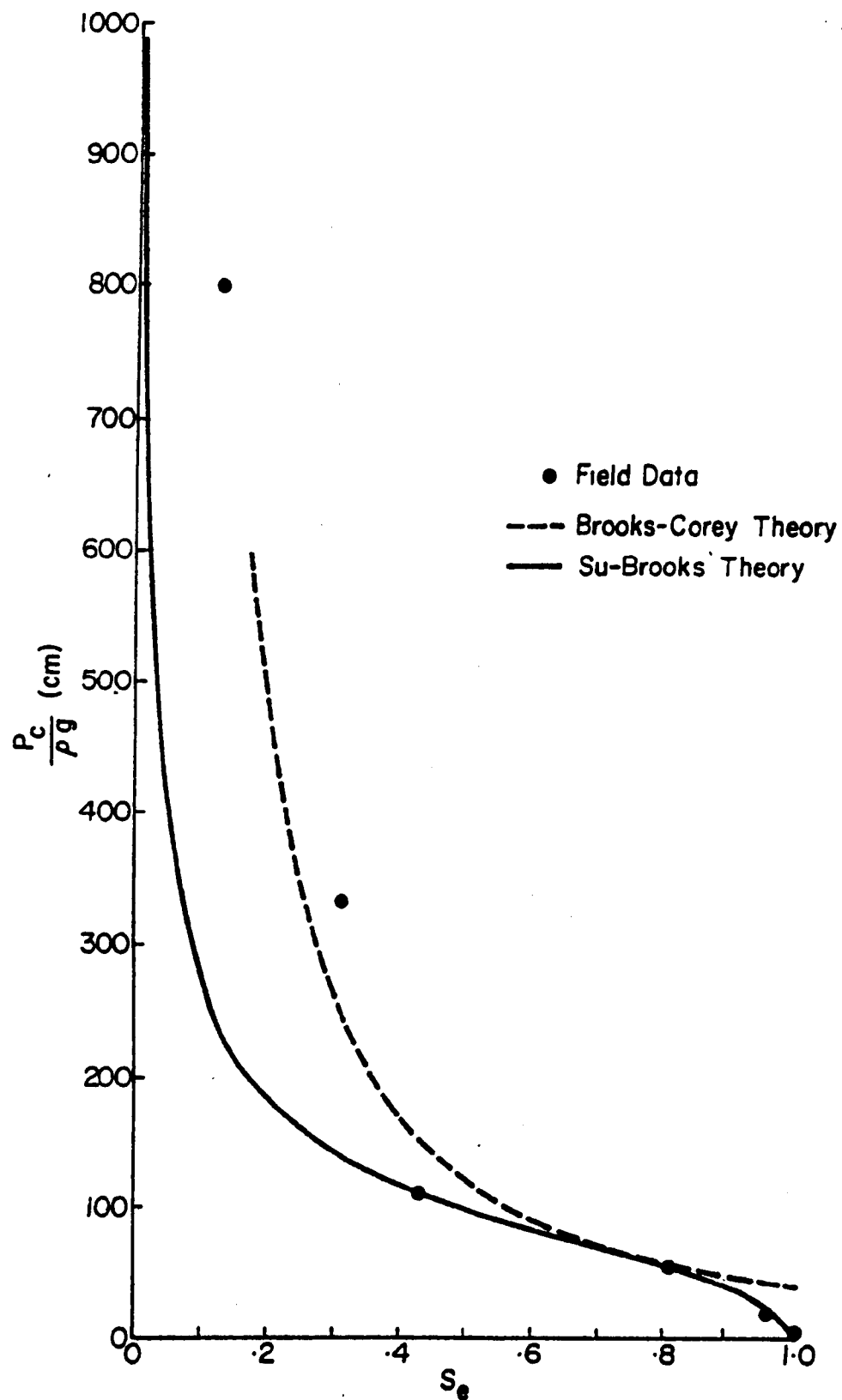


Figure 32. Soil-Water characteristic used in study.

was fitted to the soil-water characteristic by a trial and error process. First, the inflection pressure head (P_i) was selected and then, from the relationship for the parameters

$$a + b + S_r = 1.0 \quad (70)$$

in Fig. 28, the values for a and b were calculated. The value of m was computed by selecting a value for S , and its corresponding value of capillary pressure head, $P_c/\rho g$, substituting them in Eq. 69 and solving for the value of m which satisfied the equation. The first approximate characteristic was checked by entering values of saturation, S , calculated values of a , b and m , and an estimate of P_i into Eq. 69 and computing values of $P_c/\rho g$. The computed values of $P_c/\rho g$ were compared to the corresponding values of $P_c/\rho g$ at the same water content from the field soil-water characteristic. Values of P_i were adjusted and the above process was repeated until the fit was considered satisfactory. The graphical representation of the function used in this study is given in Fig. 32. The value of residual saturation, S_r , used in Eq. 69 was computed at program SORPT. Hanks and Bowers (36) found that values of diffusivity at or near saturation were most important in calculating infiltration. Therefore, the convex section of the characteristic was given the most weight in fitting the curve. This gave the best approximation of the derivative ($d(P_c/\rho g)/d\theta$) in the regions of higher saturation, and, we hope, the best values for the diffusivity. The curve fits the field data quite well over the convex section of the curve, but diverges on the concave side of the inflection point (to where $K(\theta)$ and $D(\theta)$ are quite low).

The values of parameters, for the Brooks-Corey and Su-Brooks functions used in this study, are given in Table 2.

TABLE 2. PARAMETERS USED IN HYDRAULIC CONDUCTIVITY AND DIFFUSIVITY FUNCTIONS

Brooks-Corey	Su-Brooks
$\lambda = 0.651$	$a = 0.24$
$S_r = 0.538$ $\theta_r = 0.242$	$b = 0.222$
$P_b/\rho g = 41 \text{ cm}$	$m = 0.428$
	$P_i/\rho g = 96 \text{ cm}$
	$\theta_s = 0.45$

The calibration of the model was necessary to implicitly incorporate the variability of field soil properties in the simulation. Field variation of properties occur both horizontally and vertically throughout the profile. The variation can be measured by extensive sampling and testing in the field. However, this was not done in the current study. Instead, the soil-water characteristic was calculated using undisturbed soil samples taken in only a small area on a single plot and the saturated hydraulic conductivity, K_s , was adjusted until calculated infiltration depth and time agreed with field observation.

The soil-water characteristic was calculated using two undisturbed soil samples taken at each 30 cm depth through the profile. Fourteen samples were used at each value of pressure head to calculate the water content. The calculated values of water content at a given pressure head were averaged to give a single representative water content. By averaging in this manner, the soil-water characteristic incorporated, in an approximate way, the vertical variability occurring in this region of the field. The area selected to gather data for the characteristic is similar to the remainder of the field with respect to soil type, and it is believed that the soil-water characteristic should be reasonably representative of the average characteristic for the field.

The average soil-water characteristic was used to develop the hydraulic functions $K(\theta)$ and $D(\theta)$, except for the value K_s , which was selected during the calibration procedure. Field observations of water content profiles and irrigation data were used with different values of K_s in a series of simulations to select a value for K_s .

The procedure was to select a value for K_s (the only hydraulic parameter remaining unspecified) and to calculate the cumulative infiltration and distribution of water content in the soil. The calculated time required to infiltrate a prescribed depth of water was compared to the observed time required in the field. Also, the calculated and observed water-content distributions were compared during infiltration and in the subsequent period of redistribution. The observed water-content distribution was an average one; obtained by averaging measured water contents for corresponding depths at four locations in the field plot.

The above procedure was repeated several times, and the value of K_s was determined which gave the most satisfactory agreement between calculated and observed water-content distributions, infiltration, and changes in soil-water storage. Even though a completely objective method for expressing the optimum agreement for all three comparisons was not derived, it was possible to select K_s so that all three comparisons were considered satisfactory, as will be shown in subsequent paragraphs.

Any effects on infiltration and soil-water distribution caused by spatial variability of the soil-water characteristic and not included in the characteristic used in the calculations was lumped into the adjusted value of K_s by this procedure. Strictly speaking, therefore, it is not certain that either the soil-water characteristic or K_s are actually the appropriate averages. On the other hand, the fact that, by adjusting K_s only, satisfactory comparisons for water balance, water distribution, and infiltration strongly suggests that the soil-water characteristic and K_s used in the calculation are nearly the correct, spatially weighted parameters.

The initial soil moisture distribution, field moisture distribution four days after irrigation, and corresponding data from the calculations for the values of K_s used in the calibration are given in Table 3. Infiltration data for the test plot are also given in Table 3. A value of $K_s = 20$ cm/day was found to yield calculated infiltration times that most nearly matched the measured infiltration time. The moisture profiles for the field data and the

TABLE 3. MOISTURE CONTENT PROFILES FROM PLOT 30 USED FOR MODEL CALIBRATION

Depth (cm)	Volumetric Moisture Content				
	Initial Field Moisture (1 day before irrigation)	Final Field Moisture (4 days after irrigation)	Final Model $K_s = 20 \frac{\text{cm}}{\text{day}}$	Final Model $K_s = 15 \frac{\text{cm}}{\text{day}}$	Final Model $K_s = 10 \frac{\text{cm}}{\text{day}}$
0			0.298	0.302	0.308
15			0.310	0.315	0.323
30	0.248	0.32	0.321	0.326	0.334
46	0.268	0.34	0.328	0.334	0.342
61	0.253	0.32	0.332	0.337	0.344
76	0.217	0.28	0.332	0.337	0.341
92	0.191	0.27	0.275	0.246	0.205
107	0.240	0.29	0.236	0.236	0.230
122	0.289	0.31	0.283	0.283	0.280
137	0.260	0.29	0.269	0.269	0.269
152	0.283	0.31	0.282	0.282	0.282
168	0.246	0.26	0.247	0.246	0.246
183	0.282	0.29	0.288	0.287	0.286
198	0.330	0.33	0.309	0.312	0.314
214	0.322	0.33	0.316	0.318	0.321
229	0.326	0.33	0.320	0.321	0.323
244	0.329	0.33	0.323	0.320	0.325
Time of Infiltration (Days)		0.2	0.2	0.3	0.4
Total Change in Storage (cm)		5.0	4.3	4.5	6.37
Simulated Date - Day 170-175					
$E_t = 1.48 \text{ cm}$					
Depth of Irrigation 9.65 cm Day 171					

simulation with $K_s = 20 \text{ cm/day}$ are plotted in Fig. 33. While the profile shapes do not match exactly, the fit is reasonable considering the soil is not homogeneous and hysteresis was not included in the calculations. The change in storage was computed using the plot of moisture content versus depth in Fig. 33. The field change in storage was 5 cm of water and the storage change for the simulation was 4.3 cm, using a value of $K_s = 20 \text{ cm/day}$. Field data from another plot were selected and used with a value of $K_s = 20 \text{ cm/day}$. The initial data are presented in Table 4 and the graphical presentation is given in Fig. 34. Again, the moisture distribution is not an exact match, but it is reasonable. In this simulation, water storage change in the field was 8.61 cm and the model simulated a storage change of 8.26 cm. On the basis of these simulations, a value of $K_s = 20 \text{ cm/day}$ was selected for use in the final simulations.

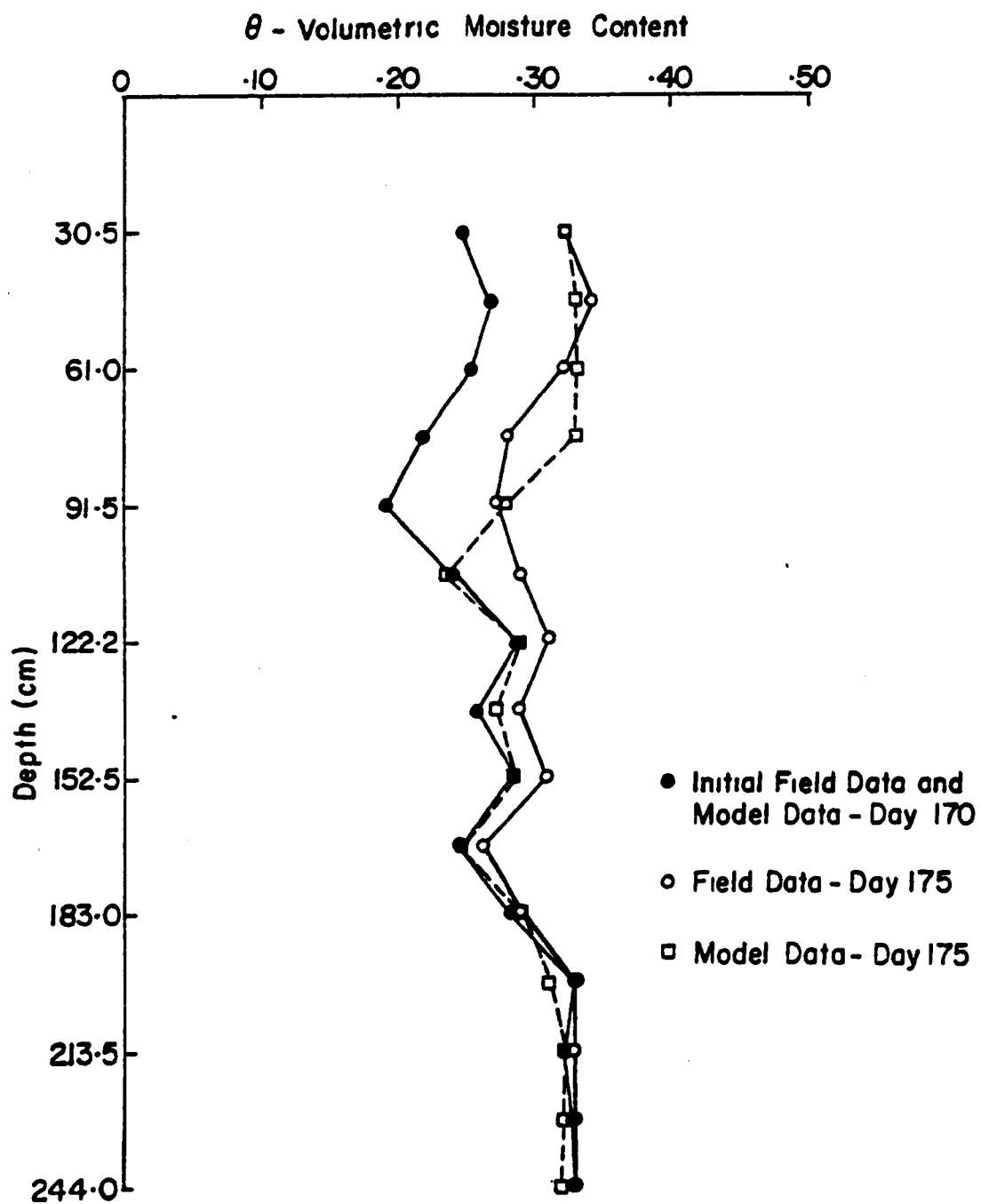


Figure 33. Moisture content profiles in Plot 30 used to calibrate the flow model.

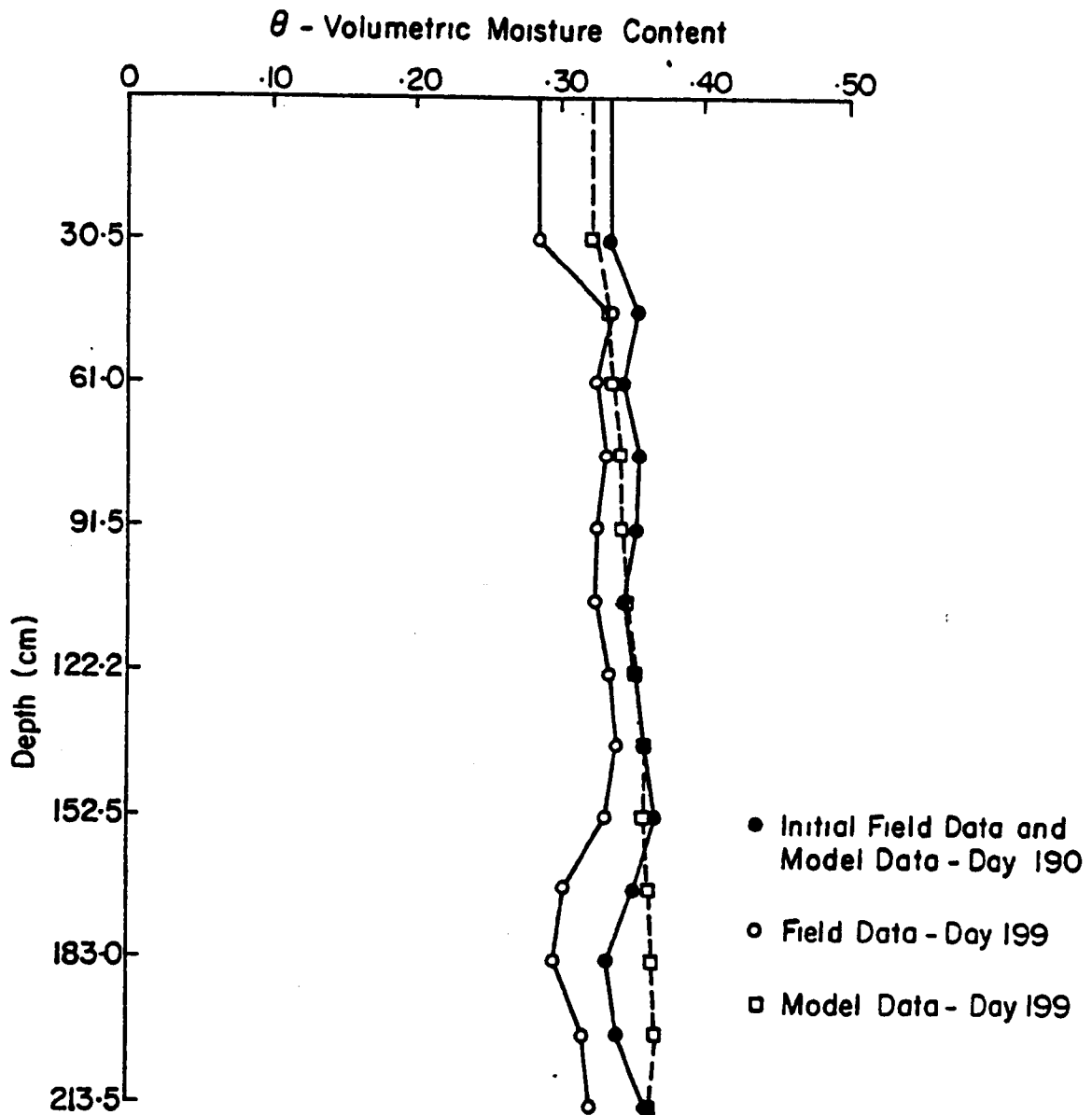


Figure 34. Moisture content profiles in Plot 25 used to calibrate the flow model.

TABLE 4. MOISTURE CONTENT PROFILES FROM PLOT 25 USED FOR MODEL CALIBRATION

Depth (cm)	Volumetric Moisture Content		
	Initial	Field Final	Model Final
15			0.315
30	0.283	0.332	0.324
45	0.333	0.355	0.331
61	0.323	0.344	0.337
76	0.331	0.356	0.342
91	0.325	0.352	0.346
106	0.325	0.342	0.349
122	0.333	0.352	0.352
137	0.339	0.356	0.355
152	0.331	0.364	0.358
167	0.302	0.350	0.360
183	0.292	0.331	0.362
198	0.318	0.339	0.365
213	0.318	0.357	0.367
<hr/>			
Time of Infil- tration (Days)		0.2	0.2
<hr/>			
Change in Stor- age (cm)		8.61	8.26
<hr/>			
Simulation Dates - Day 190-199			
$K_s = 20$ cm/day			
Depth of Irrigation 10.44 cm Day 191			
8.48 cm Day 193			
$E_t = 7.92$ cm			

The field moisture profiles plotted in Figs. 33 and 34 show that the assumption of a unit hydraulic gradient existing at the lower boundary condition was quite good. The agreement between the field moisture profiles and the simulated profile in Figs. 33 and 34 indicates that a unit gradient lower boundary condition was a good representation of the actual boundary condition. The effect of the unit gradient boundary condition on values of moisture content at the lower boundary was checked for a 150-day simulation period. Data for the moisture content at 2.13 m from a simulation using a 14-day irrigation interval and a 20% leaching increment are given in Table 5. The depth of the irrigation was calculated as the sum of the water depleted by evapotranspiration during the 14 days preceding the irrigations plus the leaching increments. Data in Tables 1 and 5 show that the fluctuations in moisture content at 2.13 m for field and simulated data are small.

Other boundary conditions considered were: (1) fixing the value of moisture content at the lower boundary; and (2) specifying a time varying moisture content for the lower boundary. Field data indicated that the moisture

TABLE 5. SIMULATED VOLUMETRIC MOISTURE CONTENT AT 2.13 METERS USING 14-DAY IRRIGATION SCHEDULE AND 20 PERCENT LEACHING INCREMENT

Day	θ	Day	θ
144	0.35	230	0.33
155	0.34	250	0.33
170	0.33	270	0.33
190	0.32	293	0.33
210	0.32		

content changed at the lower boundary during an irrigation season and a fixed value of moisture content would not be an accurate representation of the field situation.

Changing moisture content with time was also considered as a lower boundary condition. This method would provide an accurate representation of field conditions provided that the moisture content on the boundary was known as a function of time. A condition specifying a value of moisture content at the lower boundary as a function of time has one serious drawback, however. The values of moisture content at the lower boundary will not be known as a function of time unless they are measured under all conditions used in the simulation. This would require extensive experimentation and obviate the need for the model in the first place. The simulations of moisture flow used to calibrate the model indicated that the soils in the Grand Valley could be adequately modeled with the present program.

CHEMICAL MODEL

The chemical model calculates the chemistry of the soil solution and the transport of the salts. Computation of salt transport uses the moisture flow data generated by the moisture flow model. The data requirements for the chemistry subroutines in the model are: (1) the irrigation water chemical analysis; (2) the number and depth of the chemistry horizons in the soil profile; (3) the initial soil analysis of each horizon; and (4) fertilization and irrigation dates. The soil analysis required for each chemistry horizon includes the concentrations of NO_3^- , NH_4^+ , urea, Ca^{++} , Na^+ , Mg^{++} , HCO_3^- , Cl^- , $\text{CO}_3^{=}$, and $\text{SO}_4^{=}$ ions. Additional soil properties required include: (1) the cation exchange capacity of the soil; (2) the concentration of gypsum in the soil; (3) the bulk density of the soil; and (4) the presence of lime. The irrigation water analysis includes the same ions as does the soil analysis except for urea. If the partial pressure of CO_2 and the exchange constants for the $\text{Ca}^{++}\text{-Mg}^{++}$ and $\text{Ca}^{++}\text{-Na}^+$ exchanges are known, these values can be used in the chemistry portions of the model. Otherwise, estimates are supplied in the model for the $\text{Ca}^{++}\text{-Na}^+$ and $\text{Ca}^{++}\text{-Mg}^{++}$ exchange constants. The partial pressure of CO_2 is not needed to run the model; it is an optional data requirement.

The chemistry model was developed assuming that all chemical reactions reached equilibrium instantaneously. Since the reaction times for the processes considered in the model (ion exchange, solution-precipitation of slightly soluble salts, and formation of ion pairs) are on the order of seconds or minutes (13), the assumption of instantaneous equilibrium should be good. The validity of the equilibrium assumption as it applies to gypsum will be discussed later in this section.

Dutt et al. (24) validated the nitrogen portions of the model, but made no attempt to verify salt predictions of the model. Previous work indicated that the approach for the salt chemistry sections of the model was adequate.

Comparison of observed soil chemistry with predictions from the chemical model was accomplished as a single plot for which the available data included: (1) the initial soil chemistry for the soil profile; (2) the chemical analysis for a set of soil solution samples taken daily or at least weekly; (3) the initial and final soil moisture profiles; and (4) the irrigation treatment. Data from plot 23, taken from one of the vacuum extractors units, were used for the comparison.

The chemistry model uses a single chemical analysis for the irrigation water. Therefore, an average analysis of the water used for irrigation of the test plots in 1975 was used both for the calibration of the model and the hypothetical simulations. The average chemical analysis of the irrigation water used in the model and the analysis of June and October irrigation water for 1975 are given in Table 6. The data show a wide range of values for Cl^- and $\text{SO}_4^{=}$ concentrations.

TABLE 6. 1975 IRRIGATION WATER ANALYSIS (ppm)

Average			June	Oct.	Average			June	Oct.
Ca^{++}	-	43.5	34	63	$\text{SO}_4^{=}$	-	57.3	16	182
Na^+	-	47.25	17	110	NO_3^-	-	0.0	0	14
HCO_3^-	-	134.0	139	176	Mg^{++}	-	10.3	7	19
Cl^-	-	61.0	38	160	Total = 353.35				

The soil profile was divided into seven chemistry segments each 30-cm thick. The initial soil properties and soil chemical analyses were assumed uniform throughout each 30-cm segment. The segments were subdivided into segments 15 cm thick (using the field data for the 30-cm segments) to provide the computational segments used for the simulations and calibration of the model. The initial chemical profile and soil properties used to run the model for the investigation into its validity and, later, the hypothetical simulations are listed in Table 7. The irrigation, evapotranspiration and initial soil moisture data (taken from field data) used are presented in Table 8.

TABLE 7. INITIAL CHEMICAL PROFILE AND SOIL DATA FOR PLOT 23, MATCHETT FARM, 1975

Profile Chemical Analysis								
HZN or segment	Ca meq/l	Na meq/l	Mg meq/l	HCO ₃ meq/l	Cl ⁻ meq/l	CO ₃ meq/l	SO ₄ meq/l	NO ₃ meq/l
1	24.95	8.02	7.56	8.10	4.39	0.0	30.05	0.03
2	9.68	9.43	3.86	3.48	8.84	0.0	7.90	0.21
3	15.52	8.23	3.68	2.02	6.29	0.0	22.75	0.32
4	31.04	1.57	4.28	2.43	3.96	0.0	28.55	0.18
5	25.76	7.15	2.53	2.47	4.05	0.0	34.76	0.27
6	27.60	6.61	4.93	2.36	4.82	0.0	36.00	0.02
7	24.70	6.50	6.29	1.55	3.36	0.0	28.00	0.13

Soil Properties			
HZN or segment	Lime	Gypsum meq/100 gm	Cation exchange capacity meq/100 gm
1	yes	1	14
2	yes	1	15
3	yes	1	13
4	yes	5	16
5	yes	1	16
6	yes	15	16
7	yes	21	15

The data used for comparison covered a 30-day period from June 15 to July 14 (day 166-196). The computed concentrations of Ca⁺⁺, Mg⁺⁺, Na⁺, HCO₃⁻, SO₄⁼, Cl⁻ and TDS were compared to the soil solution extracted at 1.1 m depth. No drainage occurred from the drains which surround Plot 25 during the time period used in the comparison. Plot 25 had a treatment of L-5-4, which means low fertility (50 ppm of nitrogen in top 30 cm of soil), 50% allowable soil moisture depletion between field capacity (1/3 bar) and permanent wilting point (15 bars), and each irrigation to be 200% of the allowable depletion. However, it was not always possible to have sufficient irrigation water infiltrate into the soil in order to apply 200%. For the 1975 irrigation season, a total of 59.4 cm of water was applied (including rainfall), which was about 18 cm less than required to satisfy the experimental design. Water balance computations for the time period of June 15 to August 25, which encompasses the time period of the irrigations, showed that estimated evapotranspiration (43.7 cm) plus increased soil moisture storage (19.5 cm) exceeded the depth of water applied by 3.8 cm, which explains why there was no drainage except for a small event of 0.036 cm on July 14. The computed concentrations are presented graphically in Figs. 35 to 37 for the simulation period. The computer program is written so that TDS values are calculated as the sum of the concentrations of the ions in the soil solution samples extracted at a depth of 1.1 m in plot 23 for the time period of interest are presented in Figs. 35 to 37 and in Table C-1.

TABLE 8. IRRIGATION TREATMENTS ON PLOT 23 IN 1975 USED TO CALIBRATE CHEMICAL MODEL
Irrigation Treatment (H-3-2)

Irrigation Data		Initial Moisture Distribution				Evapotranspiration Data					
Date 1975 (Julian)	Depth (cm)	Depth	Vol.	Depth	Vol.	Date (Julian)	E _t (cm)	Date (Julian)	E _t (cm)	Date (Julian)	E _t (cm)
171	11.43	30.5	0.30	137.2	0.26	166	0.28	176	0.48	186	0.51
174	11.58	45.7	0.30	152.5	0.28	167	0.28	177	0.33	187	0.41
191	7.95	61.0	0.25	167.6	0.30	168	0.20	178	0.48	188	0.64
192	2.62	76.2	0.25	183.0	0.31	169	0.20	179	0.51	189	0.43
Total for 4 Irrigations	33.58	91.5	0.31	198.25	0.31	170	0.15	180	0.53	190	0.25
		106.7	0.32	213.50	0.34	171	0.18	181	0.48	191	0.30
		122.0	0.29			172	0.15	182	0.38	192	0.51
						173	0.23	183	0.38	193	0.43
						174	0.36	184	0.25	194	0.43
						175	0.48	185	0.36	195	0.41
										196	0.33

H - High fertility, 100 ppm of nitrogen in top 30 cm of soil.

3 - Allowable moisture depletion of 30% below field capacity as measured by difference between field capacity (1/3 bar) and permanent wilting point (15 bars).

2 - Replace 100% of depleted moisture so that soil moisture content after irrigation is at field capacity.

crop - Corn.

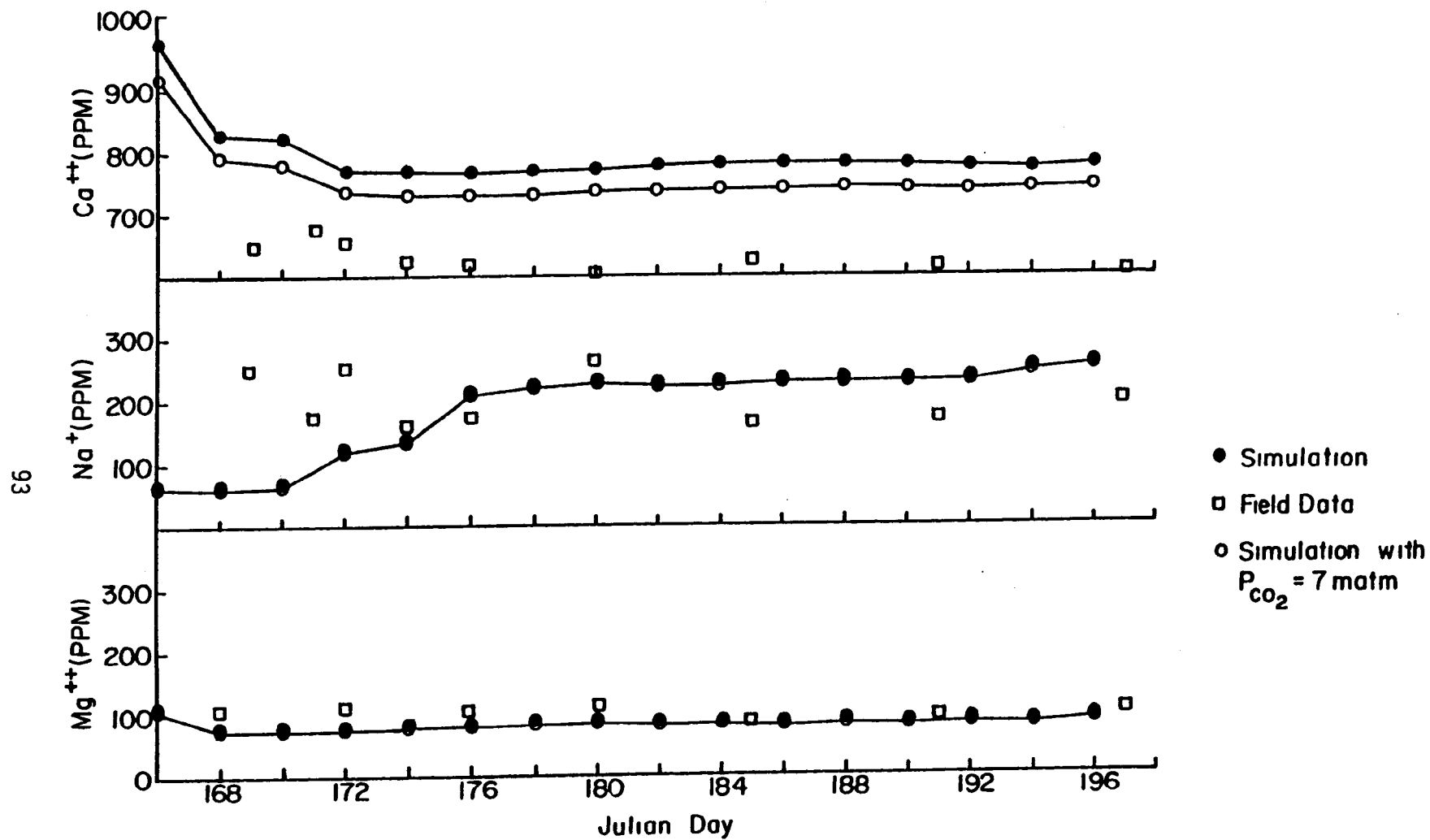


Figure 35. Computed and measured concentrations of Mg^{++} , Na^+ and Ca^{++} in soil solution at a depth of 1.1 m in Plot 23.

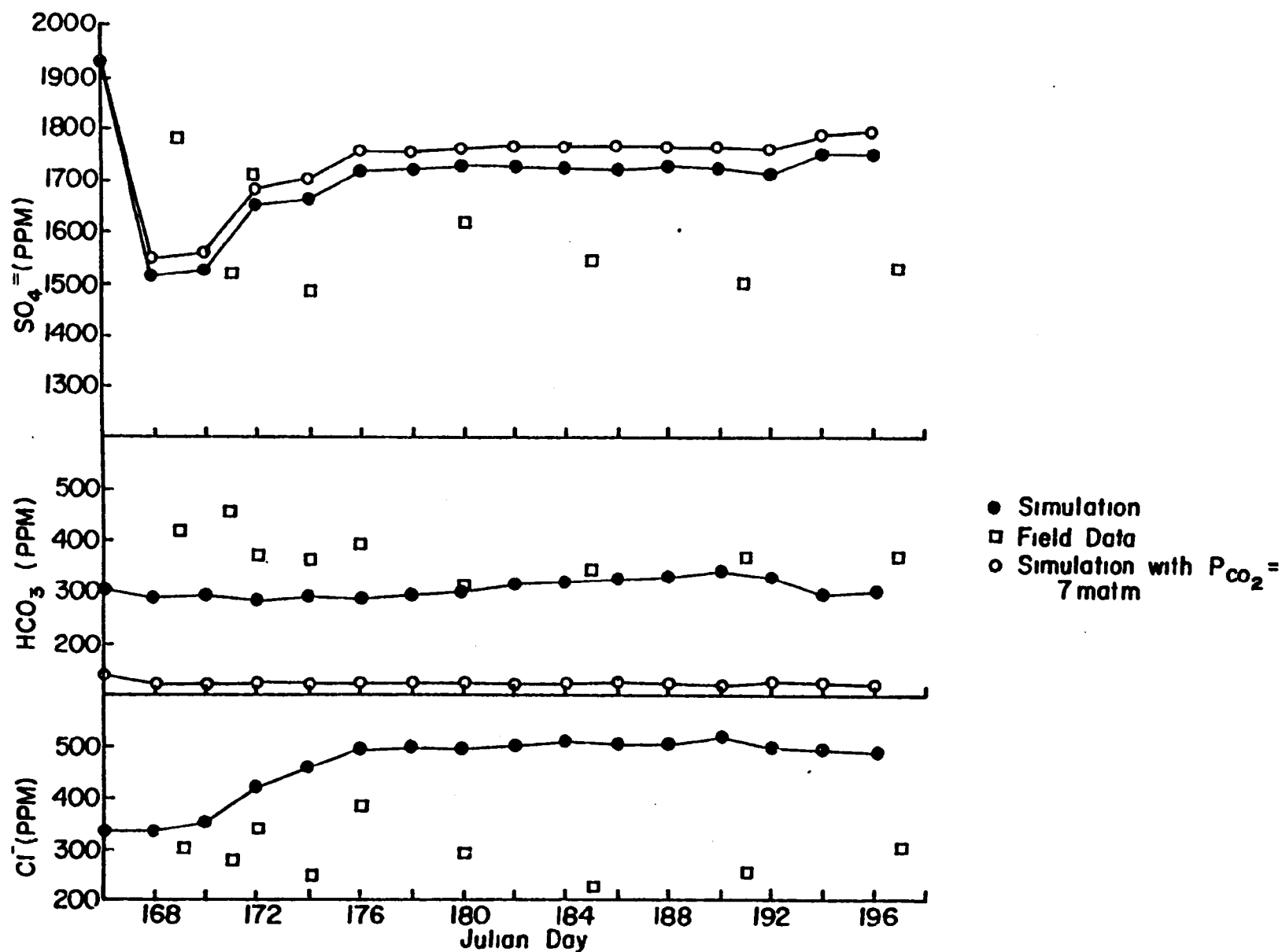


Figure 36. Computed and measured concentrations of SO_4^{2-} , HCO_3^- and Cl^- in soil solution at a depth of 1.1 m in Plot 23.

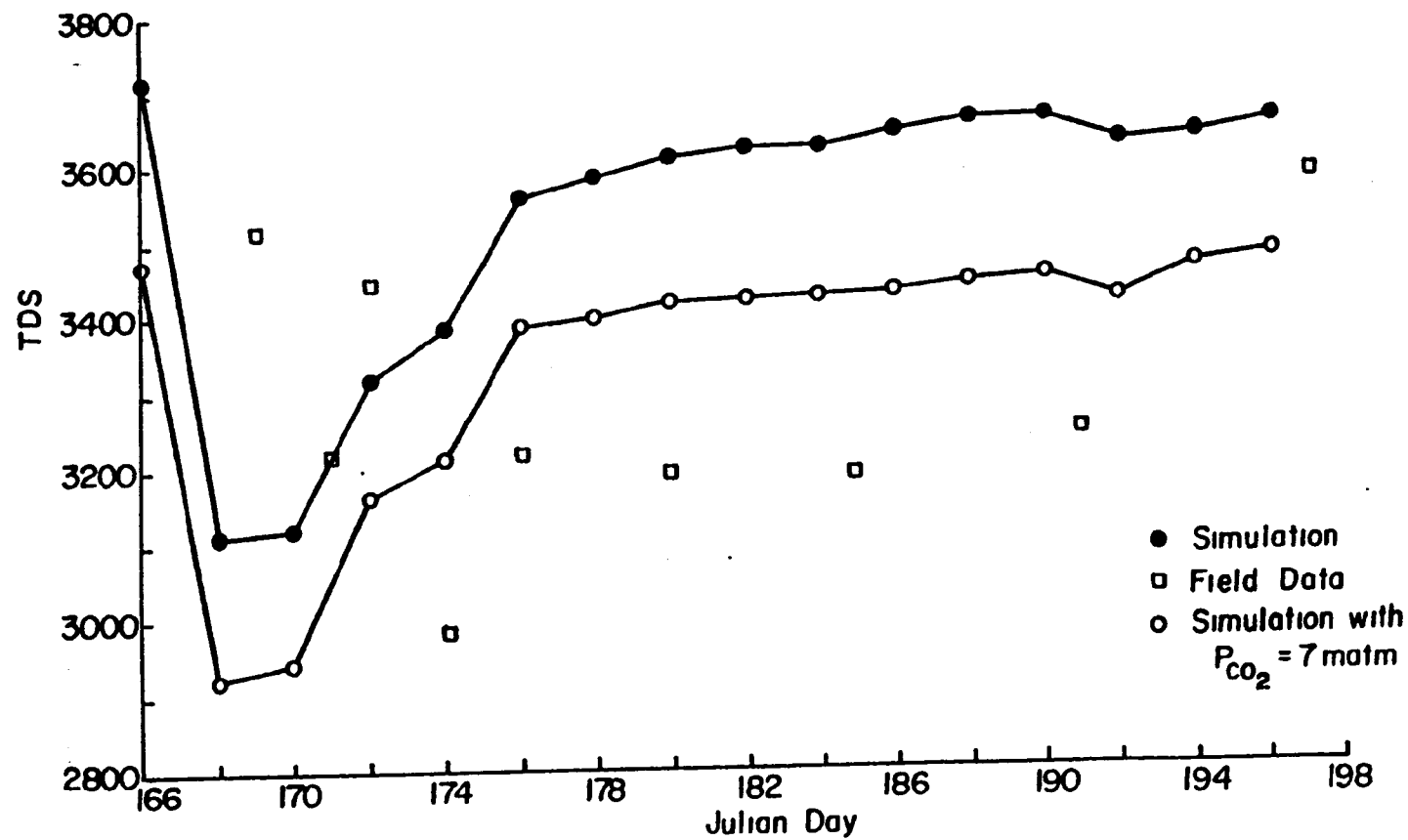


Figure 37. Computed and measured TDS concentrations in soil solutions at a depth of 1.1 m in Plot 25.

Inspection of the data presented in Figs. 35 to 37 shows that predicted values of Mg^{++} , HCO_3^- , Na^+ , $SO_4^{=}$, Ca^{++} , and TDS are within 25% of the field values, while the predicted values for Cl^- vary up to 100% from the measured values. With the exception of HCO_3^- and Mg^{++} ions, the predicted values are generally greater than the field values. These graphs reflect a calibration of the computer model and indicate the expected accuracy of any model predictions; however, some additional improvements will be made in the model as described in the following pages. The graphs of the Ca^{++} and $SO_4^{=}$ ions and TDS show sharp drops in concentration early in the simulation and then a tendency to level off. This effect probably results from the simulated chemical system adjusting to an equilibrium condition between the initial soil chemistry and the soil solution. The initial drop in the Ca^{++} and $SO_4^{=}$ would probably be eliminated by equilibrating the soil solution with the soil matrix before beginning the simulation. The lack of agreement points to the importance and need for further improvements in this soil chemistry model.

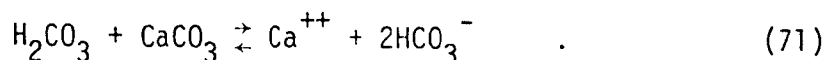
For soils containing gypsum, the upper limit of the concentration of Ca^{++} should be 630 to 650 ppm. This concentration is controlled by the solubility of gypsum. A saturated gypsum solution at 25 degrees C contains 30.5 meq/liters (85), which means the concentration of Ca^{++} at saturation is 610 ppm. Lower soil temperatures and the salts in the soil solution increase the solubility of $CaSO_4$ and increase the upper limit of Ca^{++} concentrations in the saturated solution. For the soil in the test plot, the program computed Ca^{++} concentrations of over 770 ppm. The analysis of the soil solution extracted in plot 23 (Table C-1) was used as a check to determine whether the concentration of Ca^{++} in the soil solution in the field was being controlled by the solubility of gypsum.

The check was made using a computer program developed by Dr. S.R. Olsen and Dr. H.R. Duke, Scientific Educational Administration-Agricultural Research, currently stationed at Colorado State University. The program computes the activity of each ion species in the solution and provides the negative logarithm (pK) of the computed activity for each species, K. If the Ca^{++} concentration is being controlled by the gypsum and is in an equilibrium condition, the pK of $CaSO_4$ should be 4.61, which is the pK value of pure $CaSO_4$. The pK analysis, using Dr. Olsen's program, of the soil solution (Table C-1) collected from plot 23 during the test period is given in Table 9. It can be seen from the $CaSO_4$ data that the concentration of Ca^{++} in the soil solution is in equilibrium with and being controlled by the gypsum in the soil.

One possible explanation of the discrepancy between field and simulation data was that the Ca^{++} concentration was not controlled by the gypsum solubility product, due to the absence of gypsum in the soil. If gypsum were not present, the Ca^{++} concentrations would be affected by the loss of water or other reactions occurring in the soil. To be sure the Ca^{++} concentration was controlled by the solubility product of gypsum, a simulation was made using a value for the gypsum concentration in the soil of 25 meq/100 gm of soil for all the chemistry horizons. The data for this simulation are presented in Table 10. The data show that the calculated values of Ca^{++} concentration were not improved, while the agreement between the field and predicted concentrations for the other ions did not differ significantly from the initial

simulation results. The check indicated that the value used for the concentration of gypsum in the soil was not the problem; therefore, additional investigation was required.

Other reactions considered in the model which include Ca^{++} are cation exchange and the dissociation of CaCO_3 . Dutt et al. (24) state that the HCO_3^- is usually the predominant form of $\text{CO}_3^{=}$ occurring in the soil-water system. The reaction used in the model for the $\text{CO}_3^{=}$ was



The system of equations used to describe the reaction(s) is given in Section 6. As part of the development of the equations describing the HCO_3^- system, Dutt et al. (24) proposed an equation to describe the solubility product of $\text{Ca}(\text{HCO}_3)_2$ as a function of moisture content. The solubility of $\text{Ca}(\text{HCO}_3)_2$ is computed in the program as the product of the activities of the Ca^{++} and HCO_3^- ions present in the soil solution. It is then modified using Dutt et al.'s (24) experimentally derived relationship for the solubility as a function of moisture content.

The effect of the value of the solubility product of $\text{Ca}(\text{HCO}_3)_2$ used in the simulation on the computed Ca^{++} concentrations was investigated using the measured and simulated data for plot 23. The simulated value for the $\text{Ca}(\text{HCO}_3)_2$ solubility can be compared to field values by using the pK values of the Ca^{++} and HCO_3^- ions. The pCa and pHCO₃ values for the field data for plot 23 are given in Table 9. The ion concentration data from the simulation using the initial soil analysis (Table 7) were used to calculate the pCa and pHCO₃ values for the simulations. The pK values for Ca^{++} , HCO_3^- , $\text{SO}_4^{=}$, and Mg^{++} for the simulated and measured data are given in Table 11.

TABLE 9. pK ANALYSIS OF SOIL SOLUTION EXTRACT AT 1.1 m ON PLOT 23, MATCHETT FARM, 1975

Julian Date	pCa	pMg	pSO ₄	pHCO ₃	pCO ₃	pCaCO ₃	pMgCO ₃	pCaSO ₄
169	2.3013	2.9167	2.2849	2.2976	4.9366	7.2280	7.7434	4.5862
171	2.2590	2.8696	2.3583	2.2493	5.0783	7.3374	7.9480	4.6173
172	2.2883	2.7873	2.3159	2.3522	4.8812	7.1696	7.6686	4.6043
174	2.2839	2.8763	2.3524	2.3506	4.5796	6.8635	7.4559	4.6363
176	2.2710	2.7909	2.4585	2.3198	4.6488	6.9199	7.4398	4.7295
180	2.3180	2.7733	2.3295	2.4213	4.8503	7.1684	7.6236	4.6476
185	2.2888	2.8956	2.3355	2.3801	4.9091	7.1979	7.8047	4.6244
185	2.2786	2.8196	2.3566	2.4119	4.9409	7.2196	7.7605	4.6353
197	2.3272	2.8824	2.3480	2.3294	5.0584	7.3856	7.9408	4.6752

TABLE 10. CONCENTRATIONS CALCULATED AT 1.1 m DEPTH WITH GYPSUM = 25 meq/100 gm IN ALL HORIZON.

Julian Date	Ca ppm	Na ppm	Mg ppm	HCO ₃ ppm	Cl ppm	SO ₄ ppm	TDS ppm
166	974	60	101	302	333	1938	3078
168	830	60	75	291	339	1521	3116
170	826	62	75	296	345	1526	3130
172	771	121	74	275	429	1656	3326
174	772	134	74	292	450	1665	3387
176	770	212	79	282	491	1725	3559
178	772	220	80	299	487	1727	3585
180	776	224	81	309	490	1730	3610
182	779	227	81	316	494	1727	3624
184	781	227	82	322	496	1727	3635
186	784	229	82	326	500	1727	3648
188	786	231	81	332	505	1726	3662
190	786	231	82	336	510	1721	3666
192	779	229	81	329	497	1718	3633
194	779	247	83	293	488	1755	3645
196	781	253	84	303	484	1756	3661

TABLE 11. pK VALUES FOR SELECTED IONS

Ion	Simulation	Field
Ca ⁺⁺	2.1929	2.2839
Mg ⁺⁺	2.9943	2.8763
HCO ₃ ⁻	2.4393	2.3500
SO ₄ ⁼	2.2390	2.3524

Using the pK values from Table 11, the pCa(HCO₃)₂ calculated by the simulation was 7.0715 and the field value was 6.9851. These pCa(HCO₃)₂ values correspond to solubility products of K_{sp} = 8.48x10⁻⁸ for the simulation and K_{sp} = 1.04x10⁻⁷ for the field data. The simulation predicts a lower solubility than exists in the field. The value of K_{sp} computed from the field data was inserted into the program as a fixed value, unaffected by moisture content, and the simulation was rerun. The predicted values of Ca⁺⁺ from the run using the field value of Ca(HCO₃)₂ solubility was larger than the Ca⁺⁺ concentrations predicted in the original simulation. Even though the solubility of gypsum (2.4x10⁻⁵) is significantly larger than the solubility of Ca(HCO₃)₂, the predicted values of Ca⁺⁺ concentration are sensitive to the value of the Ca(HCO₃)₂ solubility product used. Therefore, the problem was to select a value for the solubility of Ca(HCO₃)₂ which is characteristic of the field. Apparently, calculated field values for the solubility product can not be used in the model at this time. Dutt et al. (24) have provided another option to calculate the K_{sp} of Ca(HCO₃)₂.

Dutt et al. (24) assume "that at a given moisture content the H_2CO_3 concentration is constant at equilibrium, which is equivalent to assuming a constant CO_2 partial pressure at a constant moisture content." One option in the chemistry model specified a fixed value for the partial pressure of carbon dioxide (CO_2) for the soil solution and this fixes the solubility product of the $\text{Ca}(\text{HCO}_3)_2$.

A value of 3 milliatmospheres was used with the initial data in Table 7 to evaluate the effect of specifying the partial pressure of CO_2 on the computed Ca^{++} concentration. The computed values of Ca^{++} concentrations were lower than the values presented in Fig. 35. After discussions with Dr. Sterling Olsen, a value of 7 matm for the CO_2 partial pressure was selected as being representative of the soil system in the Grand Valley.

A 30-day simulation was made using the CO_2 partial pressure of 7 matm. The results are presented in Table B-1 and have been plotted in Figures 35 to 37. The use of a fixed value of CO_2 partial pressure improved the comparison between the field values and predicted values for the Ca^{++} concentration and had no effect on the comparison between the values of Na^+ , Mg^{++} , and Cl^- concentrations. The comparison of HCO_3^- concentrations is now quite poor, however. In this instance, the value of the solubility product was lower than the values used in previous simulations. The agreement between field and predicted values of TDS concentrations was improved when the CO_2 partial pressure was fixed. The comparison between the computed and measured $\text{SO}_4^{=}$ concentrations was poorer in this simulation.

Apparently, the reactions included in the model do not adequately describe the CaSO_4 , CaCO_3 - $\text{Ca}(\text{HCO}_3)_2$ system for the soils in the Grand Valley. However, the Ca^{++} , $\text{SO}_4^{=}$ and HCO_3^- concentrations appear to occur in the proper proportions so that TDS computations are valid even though the concentrations of Ca^{++} , $\text{SO}_4^{=}$, and HCO_3^- individually are incorrect. King and Hanks (43) used the salt portion of Dutt et al.'s (24) model in their studies and found that the TDS calculations were fairly good, but that the computations of the concentrations for single ion species were not adequate.

Comparisons of the data for Ca^{++} , HCO_3^- , and $\text{SO}_4^{=}$ concentrations for field and simulated data (Tables C-1 and B-1) show the predicted values of Ca^{++} and $\text{SO}_4^{=}$ to be higher than field values, and HCO_3^- concentrations for the field data being higher than predicted. The sums of the average concentrations of Ca^{++} , HCO_3^- and $\text{SO}_4^{=}$ ions in Tables B-1 and C-1 are 2556 ppm for the field data and 2624 ppm for the simulated data, a difference of 3%. While the predicted concentrations of Na^{++} and Mg^{++} fit field data fairly well (Fig. 25) the predicted Cl^- concentrations vary considerably from the field data.

The discussion has centered on comparisons of ion concentrations, computed and field, occurring at a depth of 1.1 m in the soil profile. However, the solution concentrations of interest in the final simulations are for the return flow at a depth of 2.13 m. As previously indicated, no drainage water was collected from plot 23, but chemical analyses of drainage water from other test plots are available.

Ion concentrations for the soil chemical profile occurring between depths of 1.2 to 2.1 m in all the field test plots are nearly equal regardless of irrigation treatment. Comparison of concentrations occurring from 1.2 to 2.1 m depth between plots shows that the values are nearly equal throughout the field. If the ion concentrations are the same throughout the field between depths of 1.2 to 2.1 m, then a reasonably good comparison should exist between concentration values computed using plot 23 and the field data for plot 23 or other plots. Comparison of the data simulated using a CO₂ partial pressure of 7 matm presented in Table 12 and field data in Table 13 show poor comparisons for individual ion concentrations, while TDS concentrations agree reasonably well. Based on the simulations used in the comparison of ion concentrations at 1.1 m and 2.13 m, a partial pressure of 7 matm was selected for use in the hypothetical simulations that follow.

TABLE 12. PLOT 23 CONCENTRATION AT 2.13 m PREDICTED USING P_{CO₂}=7 matm

Date	Ca ppm	Na ppm	Mg ppm	HCO ₃ ppm	Cl ppm	SO ₄ ppm	TDS ppm	TDS-Cl ppm
166	818	221	142	188	236	2136	3741	3505
168	731	218	118	122	247	1790	3226	2979
170	730	220	118	122	249	1786	3225	2976
172	717	213	115	123	236	1785	3189	2953
174	703	207	112	125	245	1834	3226	2981
176	659	197	104	131	294	1969	3354	3060
178	648	199	103	133	324	2010	3417	3093
180	646	200	102	134	337	2056	3475	3138
182	645	200	102	134	346	2042	3469	3123
184	644	200	102	134	350	2038	3470	3120
186	643	203	102	134	355	2047	3484	3129
188	642	203	102	134	358	2047	3486	3128
190	642	203	102	134	362	2048	3491	3129
192	643	204	102	135	363	2044	3491	3158
194	641	204	102	134	365	2056	3502	3137
196	641	204	102	135	365	2056	3503	3138

SIMULATION OF HYPOTHETICAL CASES

After the calibration of the moisture flow and chemistry models was completed, the chemistry and flow models were used as a single model to evaluate the effect of the volume of leachate on the salt concentration of the soil solution leaving the profile at the lower boundary. These simulations were undertaken to test the impact of a very small leaching fraction (e.g., 20%) and a large leaching fraction (40%). The long-term salinity impacts were tested by running the simulations for a six-year time period. The effect of winter precipitation on salt movement through the soil profile was also simulated. The hypothetical simulations in this part of the study were made using the initial chemistry profile data from Plot 23 (Table 7) and widely differing irrigation treatments. The irrigation treatments used were fixed

TABLE 13. CHEMICAL COMPOSITION OF DRAINAGE WATER FROM FIELD II, MATCHETT FARM, 1975.

Plot	Ca ppm	Mg ppm	Na ppm	HCO ₃ ppm	Cl ppm	SO ₄ ppm	TDS ppm	Date collected
25	612	88	147	616	268	1505	3464	7/14
28	619	90	151	624	274	1553	3436	7/14
28	644	114	228	622	278	1459	3532	7/15
28	573	95	187	436	247	1536	3392	7/16
29	634	102	152	754	308	1512	3608	7/14
29	653	125	234	736	323	1536	3720	7/15
29	653	131	237	826	320	1464	3748	7/15
32	607	112	736	736	296	1488	3580	7/14
33	636	172	223	501	304	1728	3804	7/25
33	597	166	159	118	79	2237	3736	8/08
33	481	109	131	490	198	1344	3144	8/25
33	525	99	138	432	178	1542	3040	8/26
34	603	118	155	634	293	1704	3104	7/14
34	572	162	179	476	294	1771	3756	7/24
34	592	162	136	459	265	1728	3300	7/25
34	601	18	223	458	211	1824	3928	7/28
34	575	29	136	94	78	1632	3816	8/08
35	560	118	126	573	238	1627	3460	7/14
40	482	121	205	252	255	1230	3125	6/24
40	506	125	186	389	180	1716	3492	7/22
40	593	106	196	379	137	1548	3456	7/31
40	611	102	185	365	131	1680	3368	8/15
40	619	85	144	420	172	1752	3064	8/20
41	613	88	150	450	171	1567	3428	6/22
41	544	90	137	423	192	1512	3148	6/26
41	570	100	152	490	177	1630	3276	7/15
41	607	93	148	336	148	1560	3016	7/25
41	566	79	125	309	140	1414	2936	7/24
41	525	99	144	315	150	1358	3124	8/22
42	688	110	200	529	230	1584	3348	6/22
42	578	99	162	455	198	1272	3304	6/29
42	659	99	168	490	174	1555	3308	7/15
42	569	121	179	521	189	1541	3512	7/17
42	590	107	184	388	198	1598	3408	7/19
42	578	93	148	348	162	1502	3180	7/25
42	578	93	136	307	112	1656	3136	7/26
43	494	106	181	407	221	1266	3292	6/24
43	545	119	150	476	85	1716	3508	7/14
43	594	108	184	379	189	1080	3252	7/19
43	547	107	168	386	60	1675	3420	7/21
44	589	100	166	451	206	1302	3264	6/24
44	603	106	166	492	186	1541	3384	7/15

irrigation schedules with varying depths of applied water. Daily 7-, 14-, and 28-day irrigation intervals were considered for use in the simulations. The depth of irrigation was set equal to the cumulative evapotranspiration occurring in the interval prior to irrigation plus an additional leaching increment equal to a percentage of the computed crop evapotranspiration. The leaching increments considered were 1%, 2%, 5%, 10%, 20%, and 40% of the computed evapotranspiration.

Simulations were made for a corn crop with a 150-day growing season beginning on May 24 and ending on October 20 (day 144-293). The crop was assumed to have a 120-cm rooting depth with a constant root distribution for the entire simulation period. The root distribution was assigned as a percentage of the total extraction with 40% occurring in the top 30 cm, 30% in the second 30 cm, 20% in the third 30 cm and 10% in the fourth 30 cm of soil.

The initial moisture distribution for the purpose of the simulations was assumed to be at 50% depletion of the available water, where available water is the difference between field capacity (1/3 bars) and permanent wilting point (15 bars). The initial moisture profile used in the simulations is given in Table A-2. The available water was defined as the water stored in the soil between a suction of 30 and 1500 kPa. From field data for the research plots, the value of available water used in the study was 13 cm of water in 1.2 m of soil.

Evapotranspiration (E_t) was computed using the method described by Kincaid and Heerman (42). The equations and measured climatic data used to compute E_t are given in Appendix A. The 7-day and 14-day irrigation schedules used in the study are listed in Appendix A.

Simulations were made using daily irrigations, but the data were not included in the final analysis. Daily values of irrigation equalled daily E_t values plus the leaching increment. The sum of E_t plus the leaching increment was consistently less than a depth of 1 cm. When daily irrigations were simulated, the computed depth of infiltration differed from the planned depth for a given day. Because of the poor representation of infiltration in this case, a daily schedule for irrigations was not used in the study.

The problem with modeling a small depth of infiltration is a result of the method used to compute infiltration. The upper boundary is specified as a saturated water content and the infiltration is computed using the flux between the upper two nodes. The depth of infiltration is equal to the flux multiplied by the time increment. The defining relation for the time interval is

$$\Delta t^{i+1} = \frac{0.035\Delta x}{FR'} \quad (72)$$

where FR' is the largest value of flux occurring in the previous time interval. Except when infiltration is occurring, the flux between any two nodes in the system will be small and the resulting time step will be relatively large (the maximum time interval used in the moisture flow calculations is 0.01 day

and was established as part of the input data). Therefore, the time step used to initiate infiltration will be large. The use of a large time step and the large flux values which occur during infiltration tends to over-predict infiltration in cases when the depth of infiltration is small. The infiltration computations do not create a significant error in the computed depth of infiltration when the depth of irrigation is large.

A 28-day schedule was also considered in the study, but it is not reported here. Estimates of water extracted by evapotranspiration between scheduled irrigations indicated that most of the available water would be removed between some irrigations. This irrigation practice would not normally occur in the field where irrigation water is abundant, and for that reason it was not included in the final analysis.

Irrigation intervals of 7 and 14 days and planned leaching increments of 2%, 5%, 20%, and 40% were used in the simulations needed for the study. Values for the total cumulative infiltration and leachate at 2.1 m resulting from the 7- and 14-day schedules for leaching increments of 2%, 5%, 20%, and 40% are given in Tables 14 and 15 for the 150-day irrigation season simulations.

TABLE 14. CUMULATIVE INFILTRATION FOR 150-DAY HYPOTHETICAL SIMULATIONS USING 7- AND 14-DAY IRRIGATION SCHEDULES

Irrigation Frequency (days)	Cumulative Infiltration (cm)			
	Leaching Increments			
	2%	5%	20%	40%
7	80.30	81.58	91.46	107.46
14	71.55	74.10	84.70	98.14

TABLE 15. CUMULATIVE LEACHATE AT 2.1 m FOR 150-DAY HYPOTHETICAL SIMULATIONS USING 7- AND 14-DAY IRRIGATION SCHEDULES

Irrigation Frequency (days)	Cumulative Leachate (cm)			
	Leaching Increment			
	2%	5%	20%	40%
7	8.17	9.19	19.25	33.8
14	7.84	8.95	17.74	30.9

TABLE 16. LEACHING FRACTIONS COMPUTED FOR 7- AND 14-DAY IRRIGATION SCHEDULES

Leaching Increment	Leaching Fractions			
	7-Day		14-Day	
	Actual	Adjusted	Actual	Adjusted
2%	0.102	0.027	0.109	0.026
5%	0.110	0.039	0.121	0.040
20%	0.210	0.178	0.209	0.186
40%	0.310	0.310	0.315	0.285

Leaching fractions at a depth of 2.1 m were calculated by two methods using data from Tables 14 and 15 and Figs. 38 and 39. The computed values of leaching fraction given in Table 16 are labeled actual and adjusted. The values labeled actual were calculated as the ratio of cumulative leachate at 2.1 m to cumulative infiltration. The leaching fractions labeled adjusted were computed using the data for cumulative infiltrations and leachate in Figs. 38 and 39. If the same boundary conditions were used to simulate water flow for many years, a plot of cumulative leachate vs. cumulative infiltration would become roughly linear. The slope of the linear portion of the plot would be equal to the leaching fraction for the simulation. The value of the adjusted leaching fraction is the slope of the line drawn through the linear segment of the data in Figures 38 and 39, and represents the long term leaching fraction.

Comparison of the data labeled actual and the planned leaching increments shows that with the exception of the 20% leaching increment, the planned values of the leaching fractions were not achieved. If the planned values of leaching had been attained, the values of the "actual" leaching fraction and the planned leaching increment would have been equal. The comparison shows that higher values of leaching were attained from the 2% and 5% leaching increments than were planned and that the leaching value was lower than planned for the 40% leaching increment.

The cumulative leachate was plotted versus the cumulative infiltration in Figs. 38 and 39 for each leaching increment and irrigation frequency used in the study. The plots in Figs. 38 and 39 show a sharp initial rise in the cumulative leachate values and then a transition to an approximately linear relationship.

The leaching fractions represented by the slopes of the linear portion of the plots of cumulative infiltration and cumulative leachate are given in Table 16 as the adjusted values of the leaching fraction. Comparison of the data in Table 16 shows the values of the adjusted leaching fraction to be much closer to the planned leaching increments for the 2% and 5% values for both the 7- and 14-day schedules. Comparison of the value of the planned increments and adjusted values for the 20% and 40% leaching fractions for the 7-day schedule shows a larger difference in value for the 20% than the one calculated as the actual value. The value of the adjusted leaching fraction is the same as the actual value for the 40% leaching increment and 7-day schedule. For the 14-day irrigation schedule, the adjusted leaching fractions for the 20% and 40% leaching increments are lower than the previously calculated "actual" value.

In the field, changes in soil moisture due to evapotranspiration and excess applications of irrigation water contribute to variations in the leaching fraction from day-to-day. Therefore, the concept of a leaching fraction is most appropriately applied over a long period of time. Storage in the profile and variation in computed flux due to the approximations used in the model also contribute to the differences between planned and computed leaching fractions.

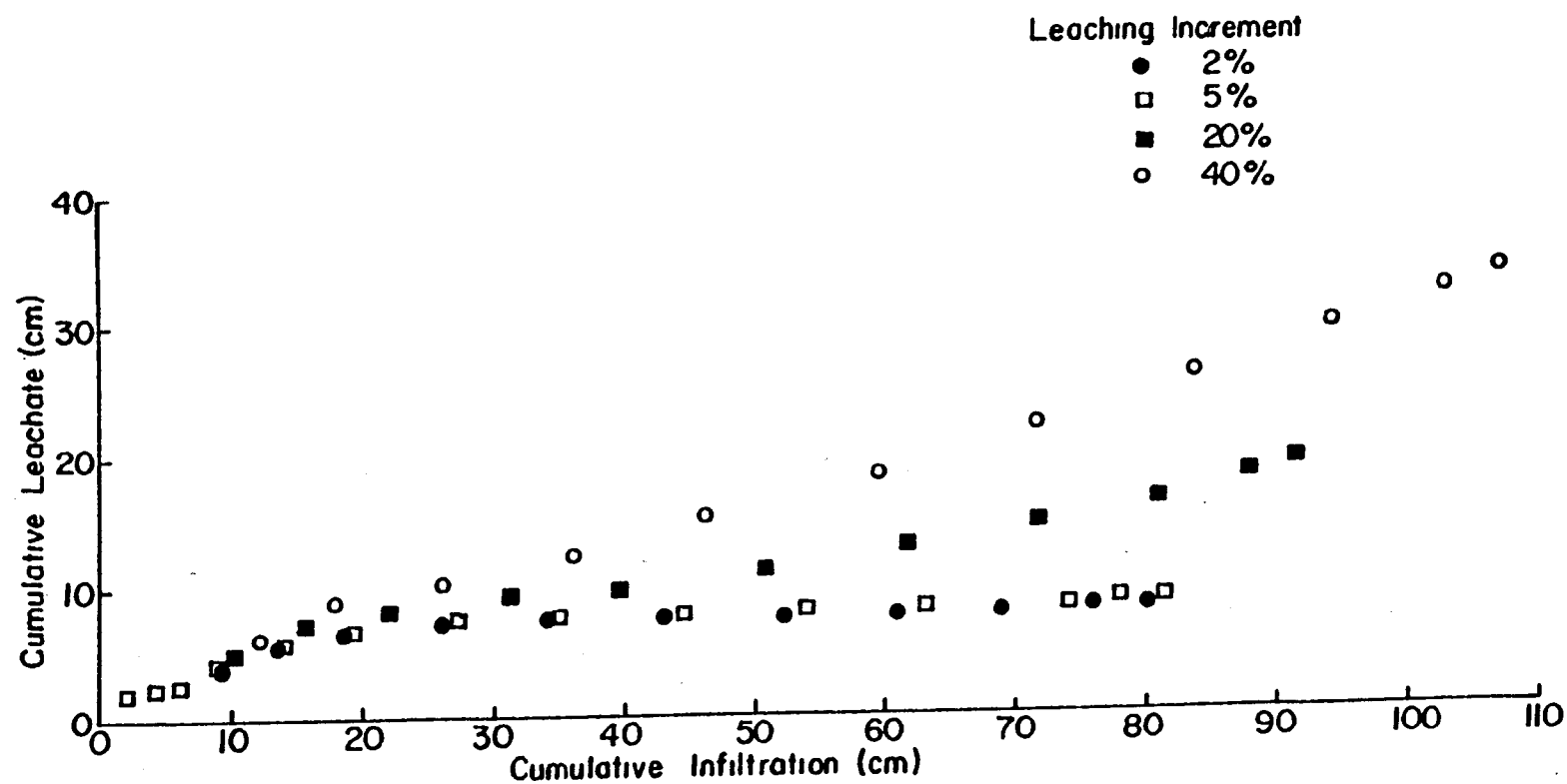


Figure 38. Cumulative leachate as a function of cumulative infiltration calculated by hypothetical simulations using a 7-day irrigation interval.

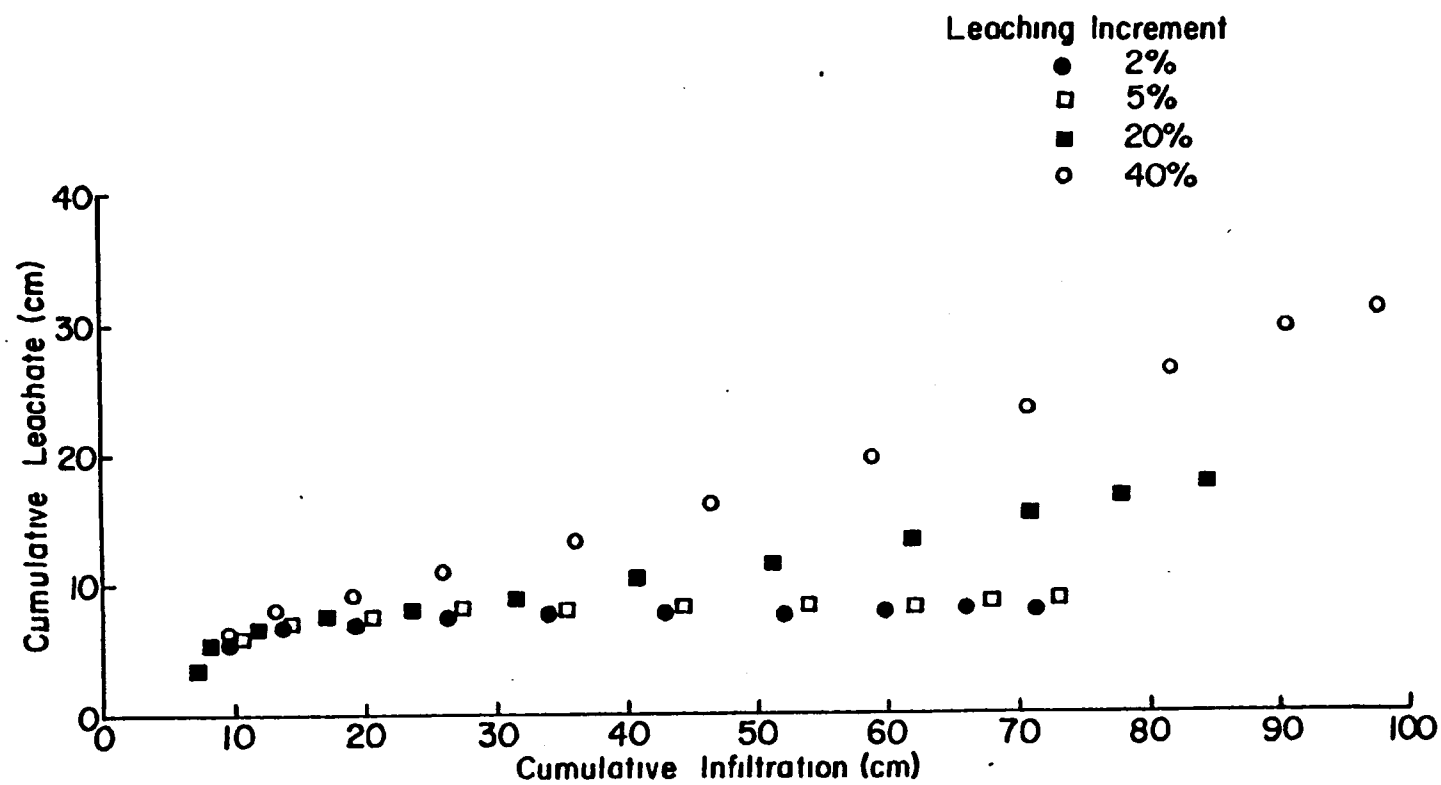


Figure 39. Cumulative leachate as a function of cumulative infiltration calculated by hypothetical simulations using a 14-day irrigation interval.

The first objective of this research was to measure the effect of the volume of return flow on the quality of return flow. The previous discussion of the leaching fraction points out the difficulty in characterizing the concept of leaching fraction. For the purposes of this research, a wide range of leachate was desired. Since the cumulative leachate data plotted as a nearly linear function over two-thirds of the simulation time (Figs. 38 and 39), the adjusted values obtained from the slope of the curves in Figs. 38 and 39 between a cumulative infiltration of 20 to 100 cm were used to characterize the leaching.

If an instantaneous equilibrium is assumed, the soil solution will always be in equilibrium with the salts in the soil, providing the salt exists in the profile, regardless of the volume of water passing through the soil. This means that the volume of leachate alone might not be the only significant parameter to use in evaluating the effect of the volume of leachate on the quality of the return flow. Another factor to be considered in relation to the salt concentration would be the water content in the soil segment. Inspection of the water content profiles for the soil below a depth of 1.2 m indicated that the water content values are nearly equal in this region. Therefore, the water contents at the lower boundary are representative of the water content in the soil profile below a depth of 1.2 m.

The values for the volume of solution in the last computation segment (bottom boundary) of the chemistry model are given in Table 17. Inspection of the results in Table 17 show about a 15% variation in the volume of soil solution in the final segment. The range of the volumetric water content at the lower boundary is 0.30 to 0.35. This range of water content probably encompasses values which are representative of field water contents below 1.2 m for the test plots, as well as areas where a shallow water table does not exist.

The calculated variation in water content for the lower boundary in the hypothetical simulations is large enough to evaluate the effect of water content on the salt concentration of the leachate. This is true because the concentration of salts in the leachate moving below the root zone is equal to the concentration occurring in the last soil segment. Therefore, any concentration changes due to the variation of water content should be reflected in the concentration of the leachate. The effect of moisture content on the concentration of salts in the return flow will be discussed in later sections.

Chloride Transport

The transport characteristics of the model can be evaluated qualitatively using profiles of Cl^- concentrations. Several investigators (3,54,91) have used Cl^- ions to study transport processes in soils since they are non-reactive in soils. Profiles of Cl^- concentrations for the 2%, 20% and 40% leaching increments and the 7- and 14-day schedules have been plotted in Figs. 40 and 41. The profiles were drawn for the Julian dates 157, 199, 255, and 293. Comparing the peak concentrations for each leaching increment in both the 7- and 14-day irrigation schedules shows that the peak concentrations decrease with increasing values of leaching increment. For the larger

leaching fractions, proportionately less water is extracted by evapotranspiration from the applied water than for the small leaching fractions. This means that the ionic concentration has been increased less by the larger leaching increments than for the smaller ones.

All of the profiles of Cl^- concentrations in Figs. 40 and 41 show an increase in peak concentration and an increase in depth to the peak concentration with time. The increases in Cl^- concentration result from the concentrating effect of evapotranspiration of the applied irrigation water. Evapotranspiration removes pure water from the solution and leaves the salts. The net effect is an increase in the concentration of salts. The movement of the peak results from the transport of the salts in the soil solution by infiltration of irrigation water, redistribution and drainage of the soil solution.

For both the 7- and 14-day irrigation schedules, the depth of penetration of the peak concentration is greatest for the largest leaching increment. Qualitatively, this would be expected. Excess water from the higher leaching increments moves deeper into the soil profile, since more water is available for redistribution. As the excess water moves, it transports the peak concentration deeper into the profile. Comparison of the depth to peak of the concentration profile for each leaching increment shows that the profiles were leached deeper with a given leaching increment for the 7-day irrigation schedule than for the 14-day schedule. For example, using the 2% leaching increment for the profile on day 255, the depth to the peak concentration is approximately 68 cm for the 14-day schedule and 83 cm for the 7-day schedule. Deeper penetrations of the peak chloride concentrations, using frequent small irrigations, have been reported by other investigators (3, 54). Results for the transport of Cl^- computed by the model indicate that salt transport is modeled in a manner which corresponds qualitatively to results described in experimental work on transport phenomena (3, 54).

TDS Studies

The TDS values at 2.1 m were plotted versus the cumulative leachate values (Figs. 42 and 43) for the 150 days, the four leaching increments and two irrigation frequencies used in the simulation. (Note: The scales of cumulative leachate in Figs. 42 and 43 have been extended over the range of 1 to 10 cm.) The data for both irrigation intervals show the same increasing values of TDS as a function of increasing values of cumulative leachate. Data for all leaching fractions are included in the initial portions of the curve. Since the values of cumulative leachate for the 2% and 5% leaching increment were less than 10 cm, only the data from the 20% and 40% leaching increment extend beyond 10 cm.

Some insight into the cause of the increase of the TDS concentration is available from the data for the Cl^- concentrations vs the cumulative leachate (Figs. 42 and 43). These data show the Cl^- concentrations rising, leveling off, and then showing a second increase in concentration.

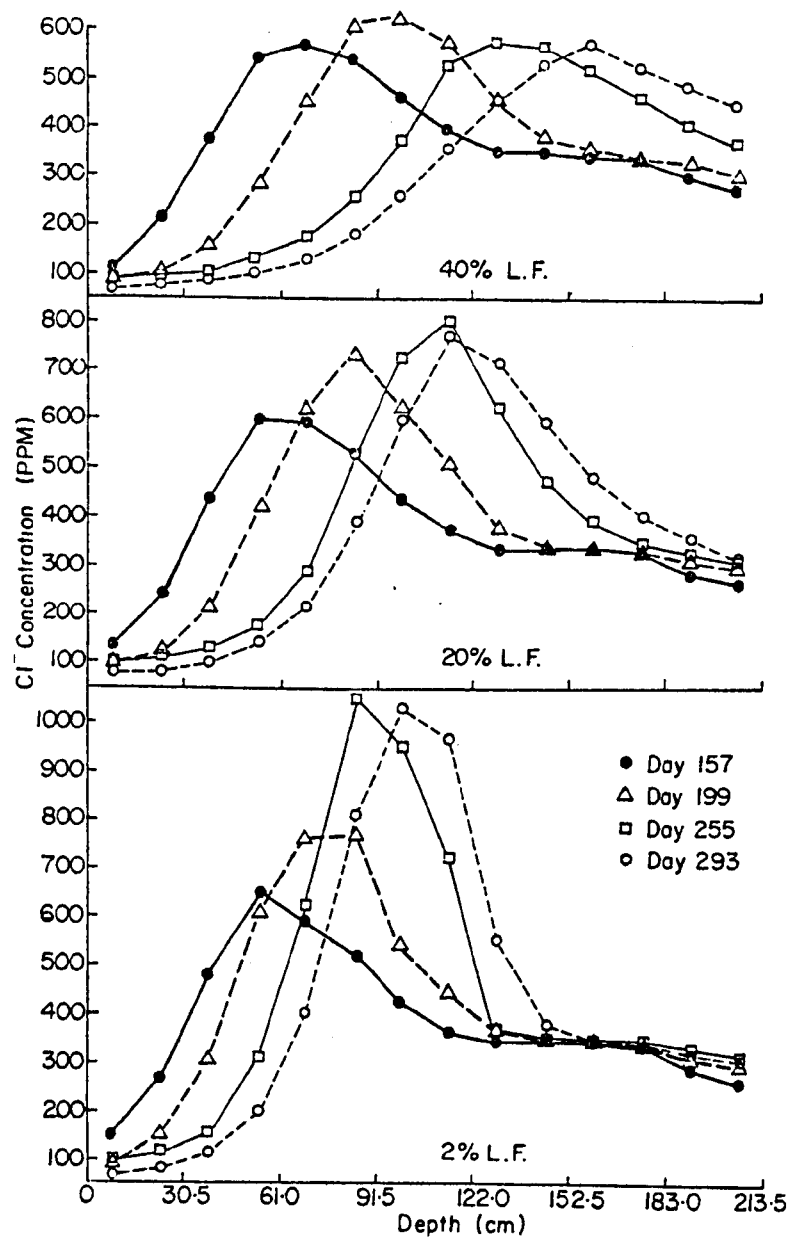


Figure 40. Chloride concentration profiles calculated by hypothetical simulations using 7-day irrigation interval.

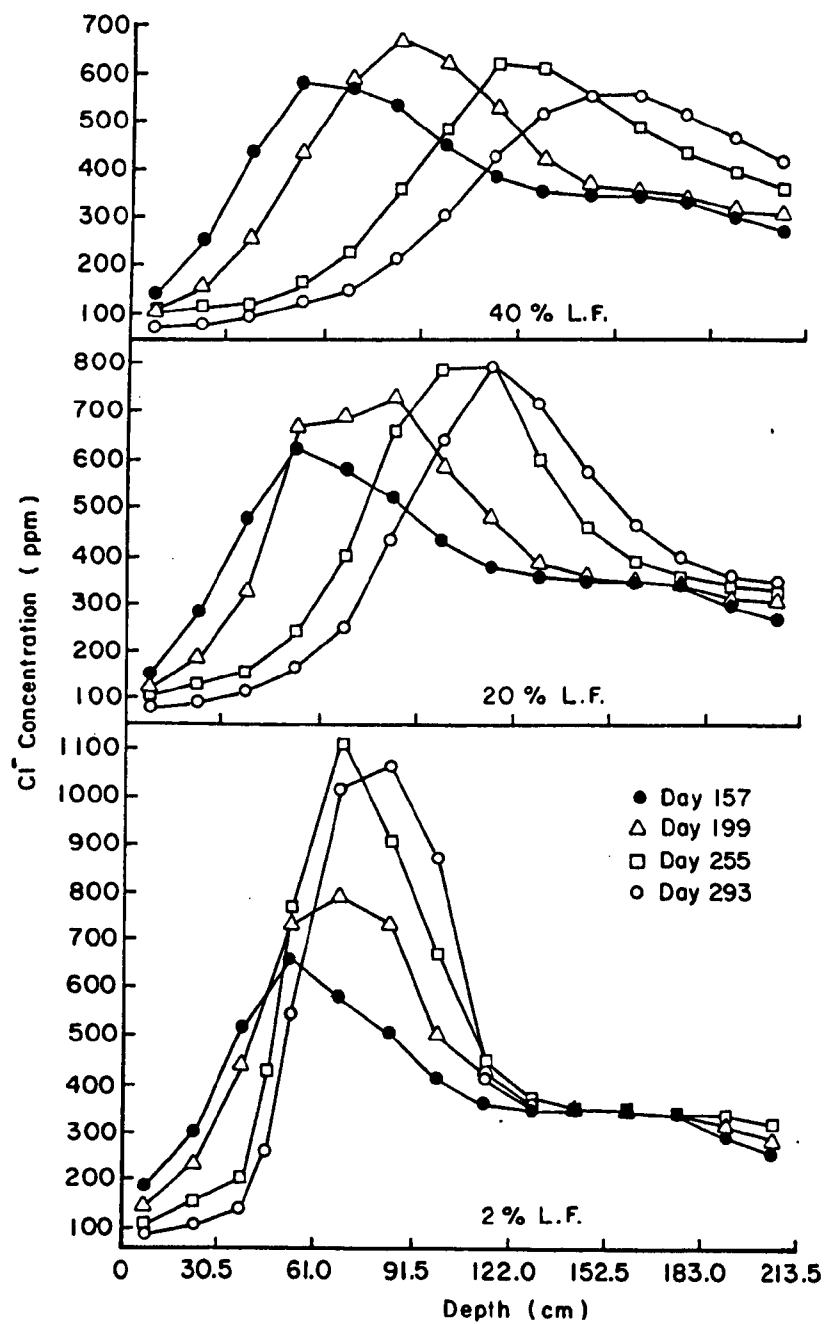


Figure 41. Chloride concentration profiles calculated by hypothetical simulations using a 14-day irrigation interval.

TABLE 17. VARIATION OF VOLUME OF SOLUTION IN SOIL SEGMENT AT THE LOWER BOUNDARY FOR SIMULATIONS USED IN THE STUDY

Date	Volume (cm ³ /soil segment)			
	Leaching Increment			
	2%	5%	20%	40%
<u>7-Day Schedule</u>				
157	5.11	5.12	5.12	5.15
171	4.92	4.93	5.02	5.05
185	4.80	4.81	4.86	4.88
199	4.71	4.72	4.75	5.07
213	4.65	4.65	4.84	5.11
227	4.59	4.60	4.94	5.18
241	4.55	4.57	4.96	5.17
255	4.52	4.57	5.01	5.14
269	4.50	4.61	4.98	5.12
283	4.48	3.69	4.94	5.08
293	4.49	4.71	4.92	5.03
<u>14-Day Schedule</u>				
157	5.11	5.12	5.12	5.13
171	4.90	4.90	4.90	4.95
185	4.79	4.79	4.79	4.90
199	4.70	4.70	4.76	5.02
213	4.64	4.64	4.88	5.07
227	4.59	4.59	4.92	5.05
241	4.55	4.56	5.00	5.07
255	4.52	4.53	5.02	5.08
269	4.40	4.54	5.00	5.08
283	4.47	4.63	4.98	5.08
293	4.46	4.69	4.91	5.09

The Cl^- and other ions moving through the soil are concentrated as water is removed by evapotranspiration. Repeated applications of irrigation water increase the mass of salts and transport the salts through the soil. As the salts are concentrated, reactions occur in the soil solution and between the salts in the solution and the soil matrix. Examples are $\text{Ca}^{++}\text{-Na}^+$ exchange, ion pair formation, and precipitation. Chlorides, however, do not participate in these reactions and changes in Cl^- concentrations are due to changes in irrigation water flux and the concentrating effect of the loss of pure water from the root zone. Since Cl^- ions are essentially inert in a soil system, the Cl^- concentrations were plotted against cumulative leachate (Figs. 42 and 43). This presentation more accurately reflects the results of the chemical reactions that occur. For example, Figs. 42 and 43 show that much of the increase in TDS values, particularly for the 20% and 40% increments, was due to the concentration of Cl^- in the soil solution.

The data for (TDS-Cl) in Fig. 42 and 43 show an initial rise to a peak value and then a slight decrease. The data follow the same trend and have approximately the same values of (TDS-Cl) concentrations as a function of cumulative leachate for each of the leaching increments used. The data seem to indicate that the concentration of salts in the leachate is independent of the volume of leachate. Since the data in Table 17 show a range of volumetric moisture content from 0.30 to 0.35 (corresponding to a solution volume of 4.5 to 5.2 cubic cm per soil segment), the salt concentration as computed by the model is relatively insensitive to moisture content.

The question does arise, however, as to the effect of the computed concentration of soil solution in the upper one-half of the profile on the salt concentrations of the leachate. To answer this, a simulation was extended for six years. A 14-day irrigation interval with a 20% leaching increment was used in the extended simulation. The data for this simulation are presented in Tables 18 and 19. A total of 482 cm of water was infiltrated during the simulation which resulted in 80 cm of leachate.

The (TDS-Cl) concentration at a depth of 2.13 m is plotted in Fig. 44. The data show the same pattern as was evidenced in Figs. 42 and 43. The concentrations rise to a peak value followed by a gradual decline and finally end in a constant value. The rise of (TDS-Cl) reflects the transport of salt from the profile above 2.13 m. The plot of the Cl⁻ profiles for the first, third and sixth years of the simulation show a steady advance of the peak chloride concentration (Fig. 45). The profile for year 6 is nearly a steady-state profile. The steady-state profile was calculated using the leaching fraction and the Cl⁻ concentration of the irrigation water,

$$C_{DW} = C_{IW} \frac{D_{IW}}{D_{DW}} = \frac{C_{IW}}{L.F.} \quad (73)$$

where C_{DW} is the concentration of the drainage water; C_{IW} is concentration of the irrigation water; D_{IW} is depth of irrigation water; D_{DW} is depth of drainage water; and L.F. is leaching fraction. The actual leaching fraction for the simulation was 0.166 and the Cl⁻ concentration was 61 ppm. For a steady-state system, the Cl⁻ concentration at the lower boundary should be 367 ppm and the computed value was 390 ppm. Since the hypothetical simulation was a perturbation on the field soil system, an extended simulation was required for the system to reach a steady-state condition. Once the steady-state condition was achieved, the data show uniform values of salt concentration.

After 63 cm of leachate, the (TDS-Cl) concentrations were 3028 ppm and the concentrations varied by less than 0.1% in the last 17 cm of leachate in the simulation. This is contrasted to a 5% variation in (TDS-Cl) concentration which occurred in the first 19 cm of leachate in the simulation. From the simulation results plotted in Figs. 42 to 45, it was concluded that the concentration of salts in the return flow is independent of the volume of leachate.

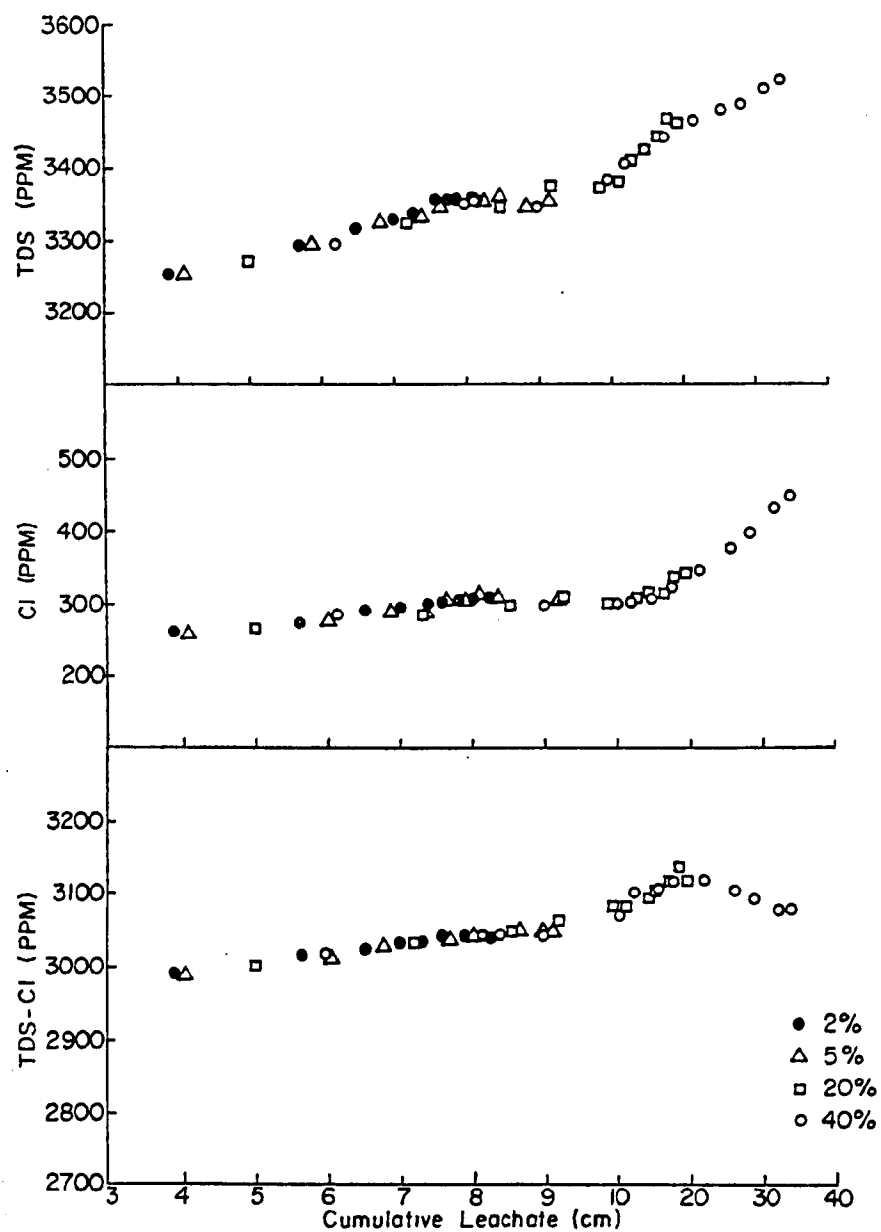


Figure 42. TDS and chloride concentrations as a function of cumulative leachate at a depth of 2.1 m calculated by hypothetical simulations using a 7-day irrigation interval.

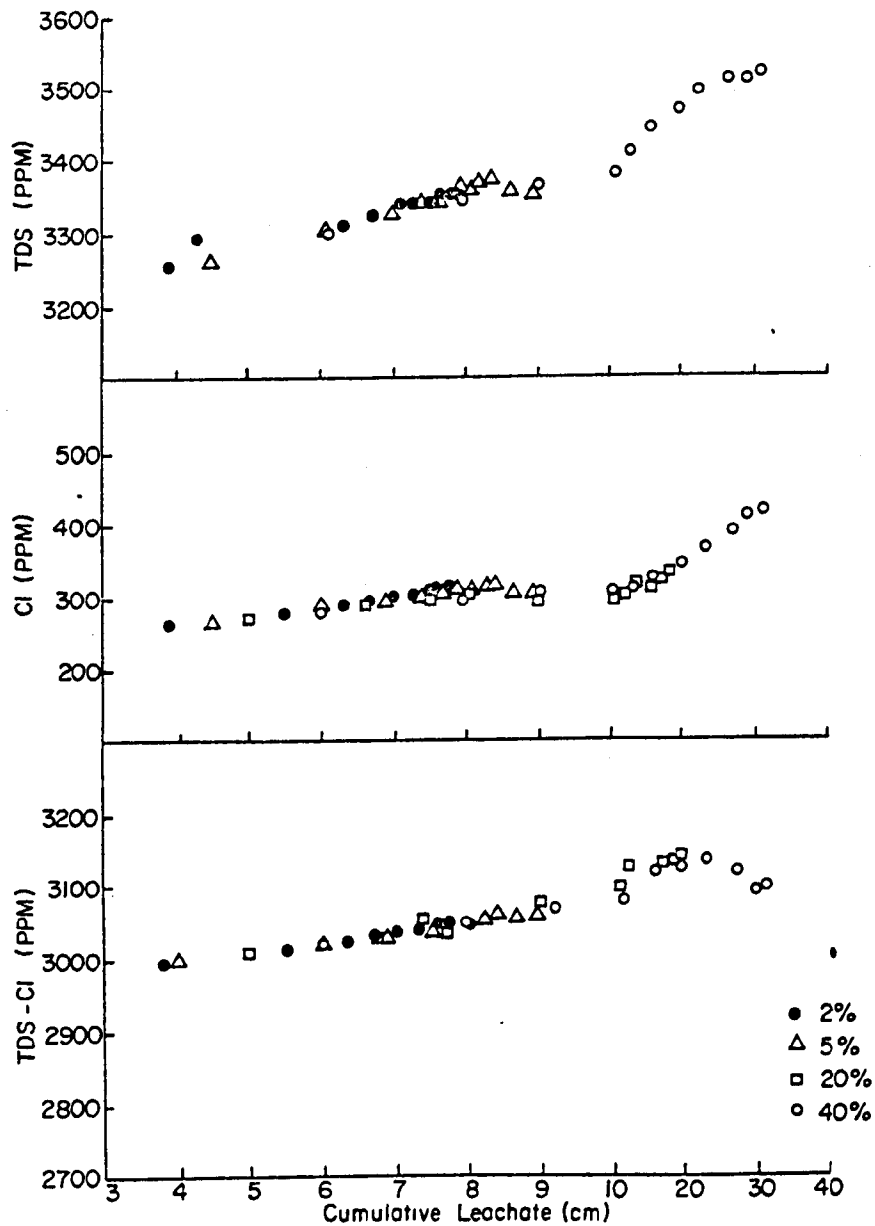


Figure 43. TDS and chloride concentrations as a function of cumulative leachate at a depth of 2.1 m calculated by hypothetical simulations using a 14-day irrigation interval.

TABLE 18. TDS CONCENTRATION AND CHLORIDE CONCENTRATION IN CUMULATIVE LEACHATE AT 2.13 m FOR 6-YEAR HYPOTHETICAL SIMULATION USING 14-DAY IRRIGATION SCHEDULE AND 20% LEACHING INCREMENT

Julian Date	Cumulative Infiltration (cm)	Cumulative Leachate (cm)	Cl ppm	TDS ppm	TDS-Cl ppm
<u>Year 1 of 6</u>					
157	8.33	5.02	269	3276	3007
171	11.45	6.70	290	3318	3028
185	16.46	7.48	298	3336	3038
199	23.50	8.05	302	3352	3050
213	31.64	8.92	297	3352	3055
227	40.55	10.11	299	3365	3066
241	51.25	11.93	302	3391	3089
255	60.49	12.86	317	3416	3099
269	68.36	13.66	323	3432	3109
283	75.11	14.31	327	3444	3117
293	80.55	14.75	327	3444	3117
<u>Year 2 of 6</u>					
157	88.52	19.20	357	3501	3144
171	91.64	19.96	338	3468	3130
185	96.77	20.65	348	3479	3131
199	103.71	21.21	353	3484	3131
213	111.84	22.16	351	3476	3125
227	120.80	23.25	362	3471	3109
241	131.49	24.85	378	3484	3106
255	140.73	26.02	405	3513	3108
269	148.60	26.76	421	3527	3106
283	155.36	27.47	434	3541	3107
293	160.79	27.91	438	3539	3101
<u>Year 3 of 6</u>					
157	168.76	32.37	525	3620	3095
171	171.88	33.12	504	3582	3078
185	177.01	33.81	522	3599	3077
199	183.95	34.37	531	3610	3079
213	192.18	35.22	531	3606	3075
227	201.04	36.41	546	3612	3066
241	211.73	38.01	562	3627	3065
255	220.97	39.18	594	3657	3063
269	228.84	39.97	608	3673	3065
283	235.60	40.63	618	3684	3066
293	241.03	41.07	620	3684	3064

(continued)

TABLE 18. (Continued)

Julian Date	Cumulative Infiltration (cm)	Cumulative Leachate (cm)	Cl ppm	TDS ppm	TDS-Cl ppm
<u>Year 4 of 6</u>					
157	249.00	45.53	656	3724	3068
171	252.12	46.28	612	3664	3052
185	257.25	46.97	618	3672	3054
199	264.19	47.53	620	3674	3054
213	272.33	48.38	604	3652	3048
227	281.28	49.57	596	3642	3046
241	291.97	51.17	584	3627	3043
255	301.21	52.34	595	3638	3043
269	309.08	53.13	596	3643	3047
283	315.84	53.79	591	3637	3046
293	321.27	54.23	587	3636	3043
<u>Year 5 of 6</u>					
157	329	58.69	563	3610	3047
171	332	59.44	519	3552	3033
185	337	60.12	518	3552	3034
199	344	60.69	515	3550	3035
213	353	61.54	497	3530	3033
227	361	62.73	484	3512	3028
241	372	64.33	466	3491	3025
255	381	65.50	471	3498	3027
269	389	66.29	470	3501	3031
283	396	66.95	467	3499	3032
293	401	67.39	463	3492	3029
<u>Year 6 of 6</u>					
157	409	71.85	446	3479	3033
171	413	72.60	411	3435	3024
185	418	73.29	413	3439	3026
199	425	73.85	412	3438	3026
213	433	74.71	398	3422	3024
227	442	75.89	390	3414	3024
241	452	77.49	382	3406	3024
255	462	78.69	391	3415	3024
269	470	79.45	392	3418	3026
283	476	80.10	392	3421	3029
293	482	80.55	390	3418	3028

TABLE 19. CHLORIDE CONCENTRATION PROFILES FOR 6-YEAR SIMULATION USING 14-DAY IRRIGATION SCHEDULE AND 20% LEACHING INCREMENT

Depth (cm)	Cl concentration (ppm)					
	Year					
	1	2	3	4	5	6
<u>Day 144</u>						
15	203	83	83	83	83	83
30	297	86	86	86	86	86
46	604	104	102	102	102	102
61	675	179	157	157	157	157
76	459	301	204	203	203	202
91	450	529	271	257	257	257
107	333	734	361	302	297	297
122	329	845	539	377	354	352
137	332	742	652	430	371	362
152	344	589	702	485	384	361
168	341	472	697	546	409	364
183	331	403	648	601	448	377
198	244	366	576	629	493	397
213	236	358	528	659	566	448
<u>Day 199</u>						
15	122	111	111	111	111	111
30	188	118	118	118	118	118
46	332	126	126	126	126	126
61	569	161	156	156	156	156
76	699	216	188	188	188	188
91	725	366	252	247	245	245
107	583	564	315	289	287	287
122	480	794	458	363	352	350
137	375	773	556	392	356	352
152	351	680	644	443	372	357
168	344	554	683	504	392	361
183	337	453	663	563	424	368
198	312	391	607	607	469	387
213	302	353	532	620	515	412
<u>Day 293</u>						
15	95	95	95	95	95	95
30	104	104	104	104	104	104
46	133	130	130	130	130	130
61	199	172	172	172	172	172
76	329	214	212	212	212	212
91	614	295	276	276	276	276
107	820	403	320	314	314	314
122	890	644	422	387	383	383
137	631	706	452	371	356	356
152	472	719	524	390	356	350
168	396	676	598	432	368	356

(continued)

TABLE 19. (Continued)

Cl concentration (ppm)						
Depth	Year					
(cm)	1	2	3	4	5	6
Day 293 (Continued)						
183	359	590	641	485	388	361
198	340	504	695	538	420	370
213	327	438	621	587	463	390
Day 365						
15	96	96	96	96	96	96
30	103	103	103	103	103	103
46	131	129	129	129	129	129
61	193	169	169	169	169	169
76	310	207	206	206	206	206
91	551	278	263	263	263	263
107	763	376	308	303	303	303
122	865	571	393	365	363	363
137	716	676	440	374	365	363
152	549	712	499	386	359	357
168	441	692	566	416	366	356
183	384	628	618	460	380	358
198	353	550	638	571	387	366
213	343	487	642	573	451	388

Winter Simulations

The data and analyses in the previous sections have been based on simulations made for a single growing season, or multiple growing seasons, without considering the effects of winter precipitation between irrigation seasons on salt transport below the root zone. One simulation using the 20% leaching increment and 14-day irrigation interval was extended over the winter months and through a second growing season. Two conditions were assumed for the winter portion of the simulation. The first condition assumed no water was applied during the winter months and no evapotranspiration occurred during the same period, which corresponds with the simulations described above wherein only the growing season was considered. The second condition assumed pure water (rainfall) was applied on the first day of each month during the winter, and again no evapotranspiration was assumed to occur. The water applied for each month in the winter was equal to the water equivalent resulting from the average depth of precipitation for the given month. The average water equivalent for each of the winter months was estimated from the Climatological Records for the Grand Valley. The data used in the simulation are given in Table 20.

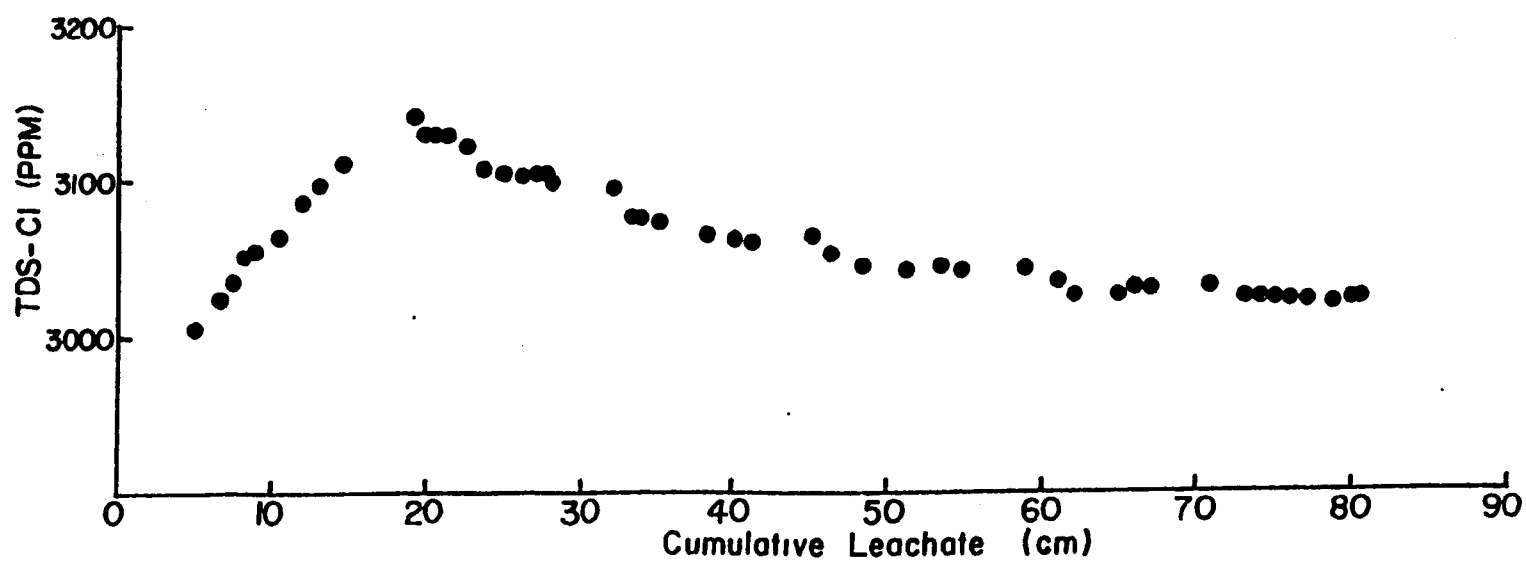


Figure 44. Total dissolved solids and chloride concentrations as a function of cumulative leachate at a depth of 2.1 m calculated by 6-year hypothetical simulations using 20% leaching increment and 14-day irrigation interval.

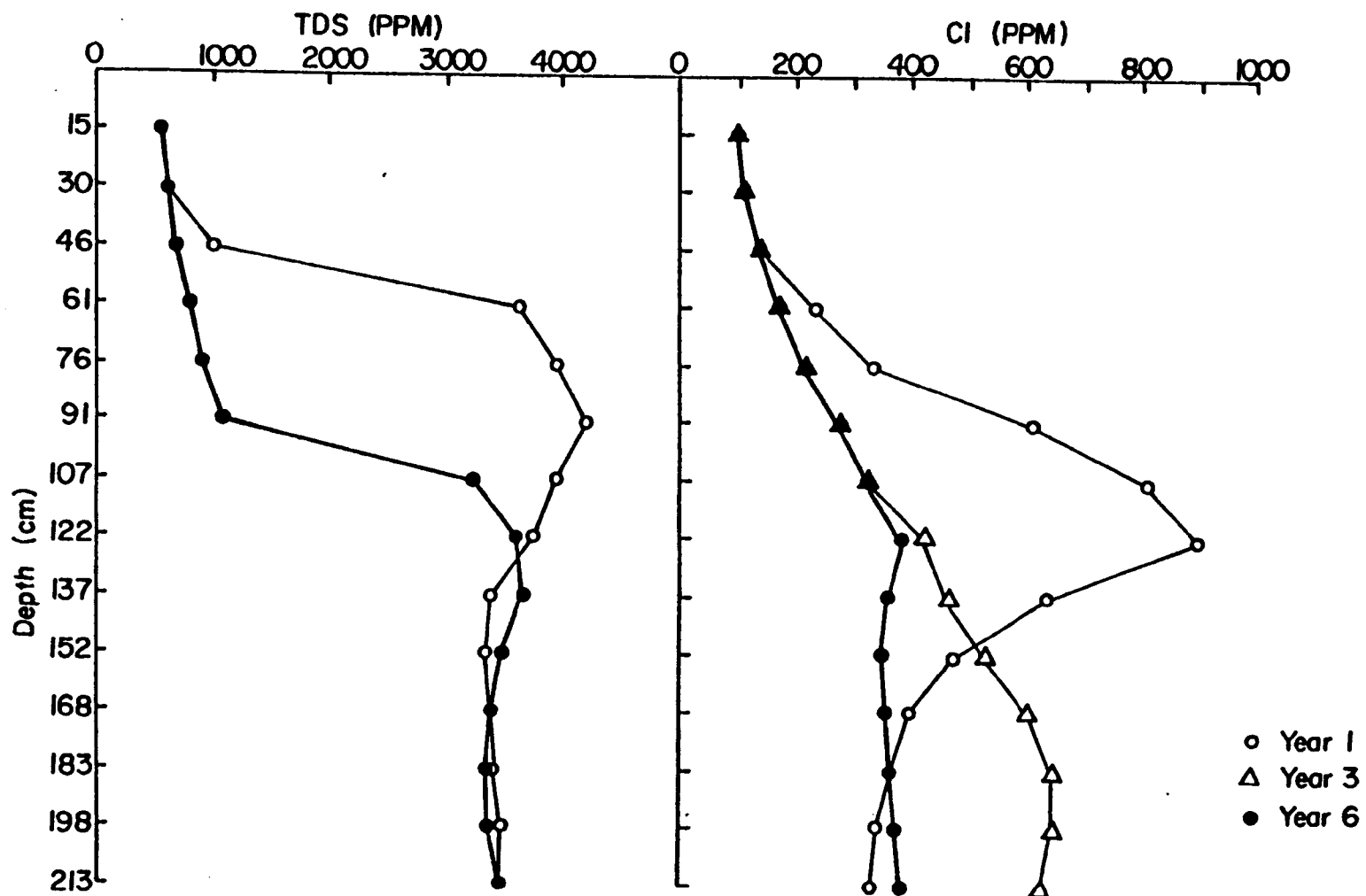


Figure 45. TDS and chloride concentration profiles at day 293 calculated by a 6-year hypothetical simulation using 20% leaching increment and 14-day irrigation interval.

TABLE 20. AVERAGE WATER EQUIVALENT DEPTH USED FOR WINTER SIMULATIONS

Month	Depth (cm)	Month	Depth (cm)
Nov.	1.55	Feb.	1.75
Dec.	1.45	March	1.90
Jan.	1.62	April	2.00

Two sets of Cl^- concentration profiles were plotted for these series of simulations. In the first set, Cl^- profiles were plotted for days 157, 199, 255, and 293 of the second year of the simulations for both conditions used (Fig. 46). In the second set, the plot (Fig. 47) shows the Cl^- profile on day 293 of the first and second year for each of the winter conditions simulated.

The effect of winter precipitation on the Cl^- concentration profile can be seen in Fig. 47. Below a depth of 75 cm the winter precipitation was quite effective in reducing the Cl^- concentration. The effectiveness of the winter precipitation results from the fact that the water contains no salts and the additional water maintained a larger water content over the winter. The larger water content in the soil contributed to the redistribution of the water and transport of chlorides.

Comparison of the Cl^- concentration profiles given in Fig. 46 shows a steady advance of the peak concentration through the soil profile. The data in Fig. 46 for the Cl^- advance during the second growing season show the benefit of the addition of the 10 cm of pure water. In the simulation where the pure water was added, by day 293 of the second season, the peak concentration had advanced 30 cm further than the simulation which did not include the pure water. Also, the peak concentration was reduced by 70 ppm for the simulation including the pure water as compared with the simulation which excluded the addition of precipitation.

These simulations serve to dramatize the effect of small quantities of pure water on leaching and transport of salts. For the simulations including winter precipitation, the pure water represented about 6% of the total applied water. The improvement in the efficiency of leaching by rain water has been noted by other investigators (3,54).

The Cl^- concentration profiles computed by including winter precipitation show one problem that arises in trying to use Cl^- concentrations to estimate leaching fractions. The leaching fraction can be estimated as the ratio of the Cl^- concentration of the applied water to the Cl^- concentration of the soil solution below the root zone. This calculation assumes that the Cl^- concentrations below the root zone represent a long-term average of the leaching from the upper portion of the profile. An idealized concentration profile would show gradually increasing Cl^- concentration with depth to the bottom of the root zone and then a uniform concentration to the bottom of the profile. This is the shape of the Cl^- profiles in the last year of the 6-year simulation (Fig. 45). Apparently, the Cl^- concentrations in this simulation have reached a steady state.

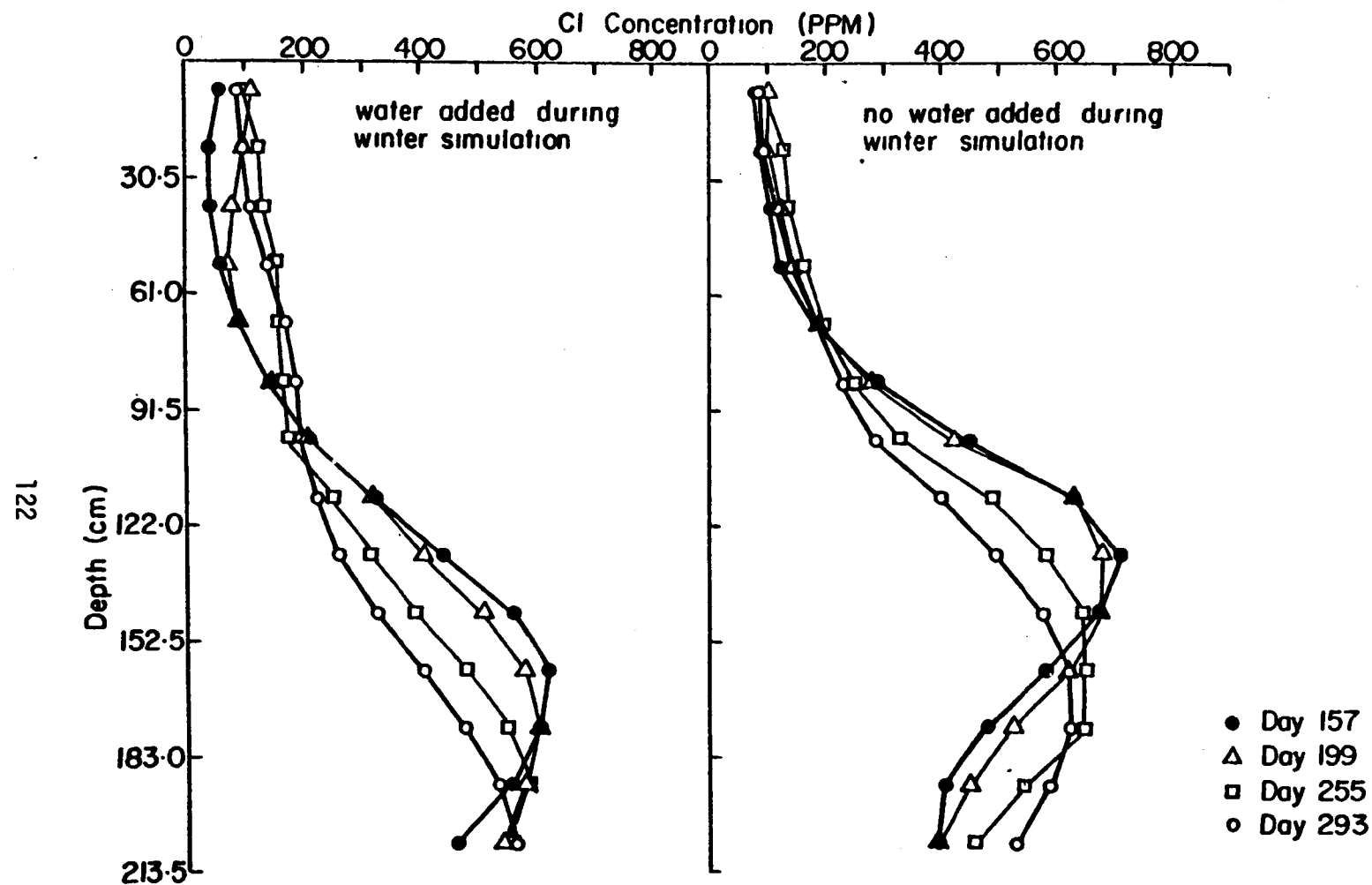


Figure 46. Chloride concentration profiles for second year of 2-year simulation calculated by hypothetical simulations using a 14-day irrigation interval, 20% leaching increment and 2 winter conditions.

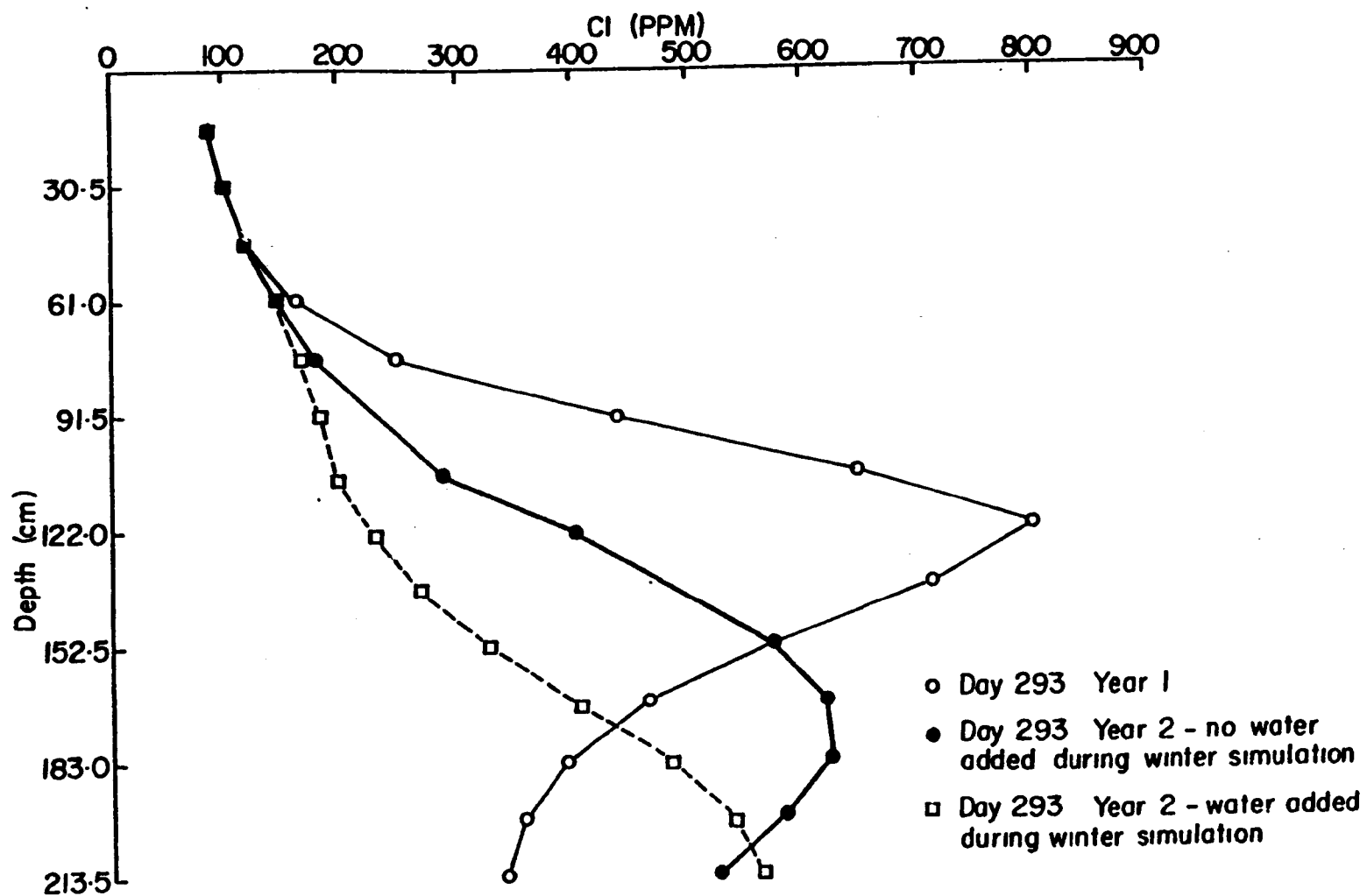


Figure 47. Chloride concentration profiles at day 293 calculated by hypothetical simulations using a 14-day irrigation interval, 20% leaching increment and 2 winter conditions.

Comparing the Cl^- concentrations at the bottom of the root zone at day 293 for year 6, and on the same day of the second year of the simulation which included the winter precipitation, shows the effect of the addition of pure water. The concentration profiles are roughly equal to a depth of 61 cm. Between a depth of 61 cm and 122 cm, the concentration where winter precipitation is considered is significantly lower after only two years than after six years when winter precipitation is not included. There is almost a 30% difference in concentrations at a depth of 120 cm with an addition of precipitation equal to only 6% of the total water applied to meet evapotranspiration and leaching requirements. If the leaching fraction were estimated using simulated Cl^- concentrations including winter precipitation, the leaching fraction would be over-estimated. Presumably, this would be the case in field sampling as well. As the volume of pure water included in the simulation is increased in relation to the irrigation water applied, the effect of pure water on the concentration profiles become even more significant.

TDS Profiles

The TDS profiles for day 293 of the first year and the sixth year in the 6-year simulation are plotted in Fig. 45. The data show that leaching is occurring in the region to a depth of 122 cm. This corresponds to the depth of the root zone used in the simulation. Below this depth, the concentration of salt is fairly constant. Irrigation water dissolves salts, such as gypsum and lime, and transports the ions through the profile until the concentration due to evapotranspiration causes precipitation. The region below the root zone acts as a buffer zone and controls the concentration of salts leaving the profile. Because of this buffering, the concentration of the leachate at 2.13 m remains relatively constant.

SECTION 8

PREDICTION OF RETURN FLOW SALINITY

The knowledge gained from the model results can be combined with the monitoring data collected in the Grand Valley Salinity Control Demonstration Project, as well as data collected by the Agricultural Research Service in the Grand Valley, to provide a picture of subsurface irrigation return flows and their corresponding salinity concentrations.

GEOLOGY AND SUBSURFACE HYDROLOGY

The general geologic characteristics (Fig. 1) of the Grand Valley have been briefly described in Section 4 of this report. The purpose of the additional discussion in this subsection is to provide a better background for understanding the irrigation return flow phenomenon in the valley.

The Grand Valley is underlain by the Mancos shale, a "dark-gray (black when wet) clayey and silty or sandy, calcareous gypsiferous" deposit of marine origin and upper Cretaceous in age (74). In the portion of the valley lying north of the Government Highline Canal (Fig. 48), Mancos shale is an exposed erosional surface. Almost no irrigation is practiced in this portion of the valley. Intermittent ridges of Mancos shale are exposed in the area bounded, approximately, by the Government Highline Canal on the north and the Grand Valley Canal on the south. These shale ridges have a general north-south trend and represent remnants of a shale terrace that has been dissected by southward flowing streams that began in the Book Cliffs. The southern extremities of these ridges (approximately the Grand Valley Canal) are the remnants of the shale cliffs that once formed the northern bank of the Colorado River (74).

With time, the Colorado River migrated southward in an approximately horizontal plane until it reached its present position. During this period, the river deposited what is now a cobble aquifer that extends from the present river location northward to, approximately, the Grand Valley Canal (Fig. 49). Migration of the Colorado River to the south decreased the gradient of southward flowing tributaries, and the valley was gradually filled with alluvial deposits transported by the tributaries. These tributary deposits buried the Colorado River bedload and flood plain deposits (74). It is the tributary alluvium, deposited during the Quaternary, that forms the source of most of the irrigated soils in the valley. In recent time, local washes have again cut into the alluvial deposits and into the Mancos shale at many locations. Recent downcutting into the Mancos shale bedrock is most prevalent

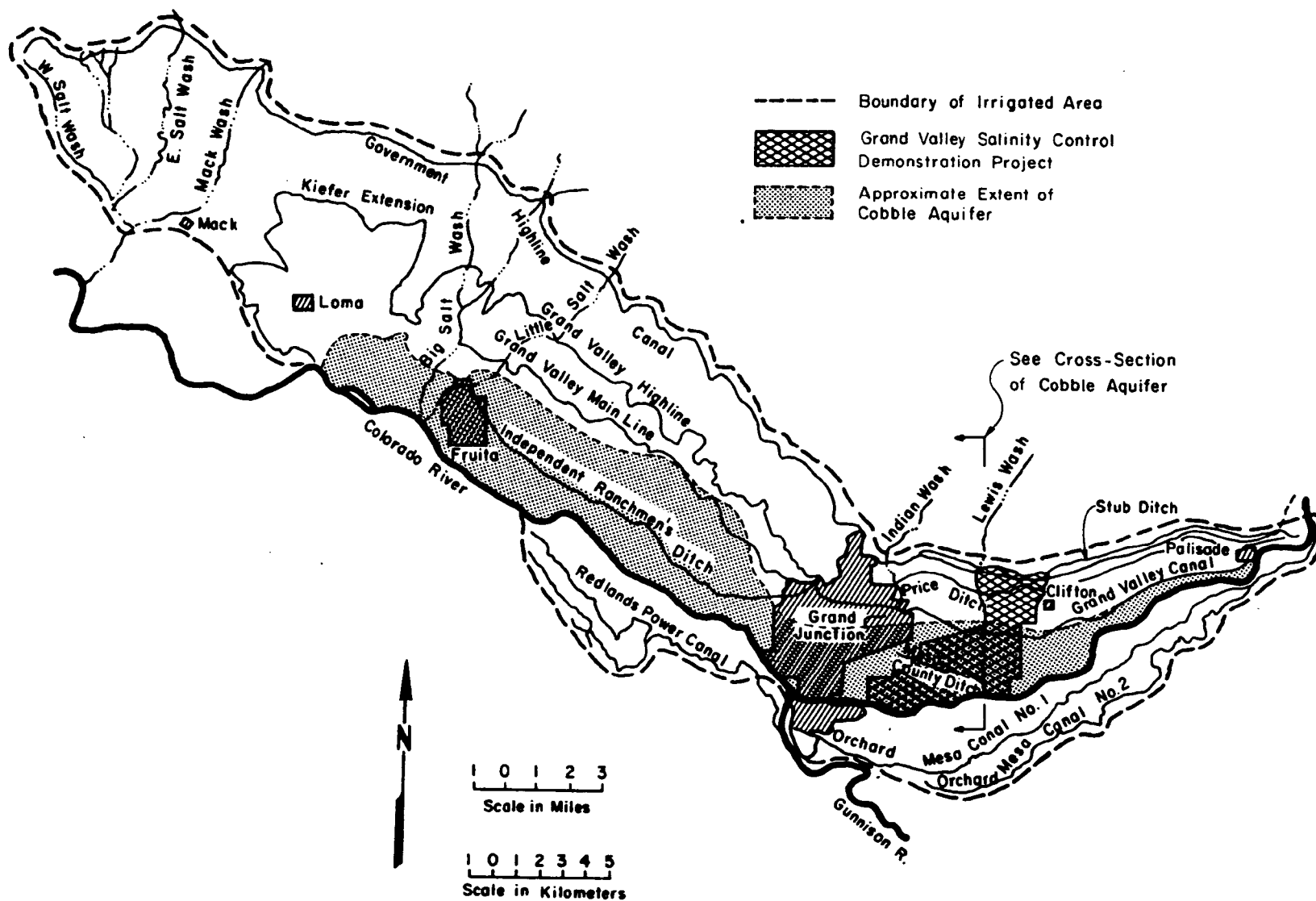


Figure 48. Natural washes, canals and boundary of irrigated lands in the Grand Valley.

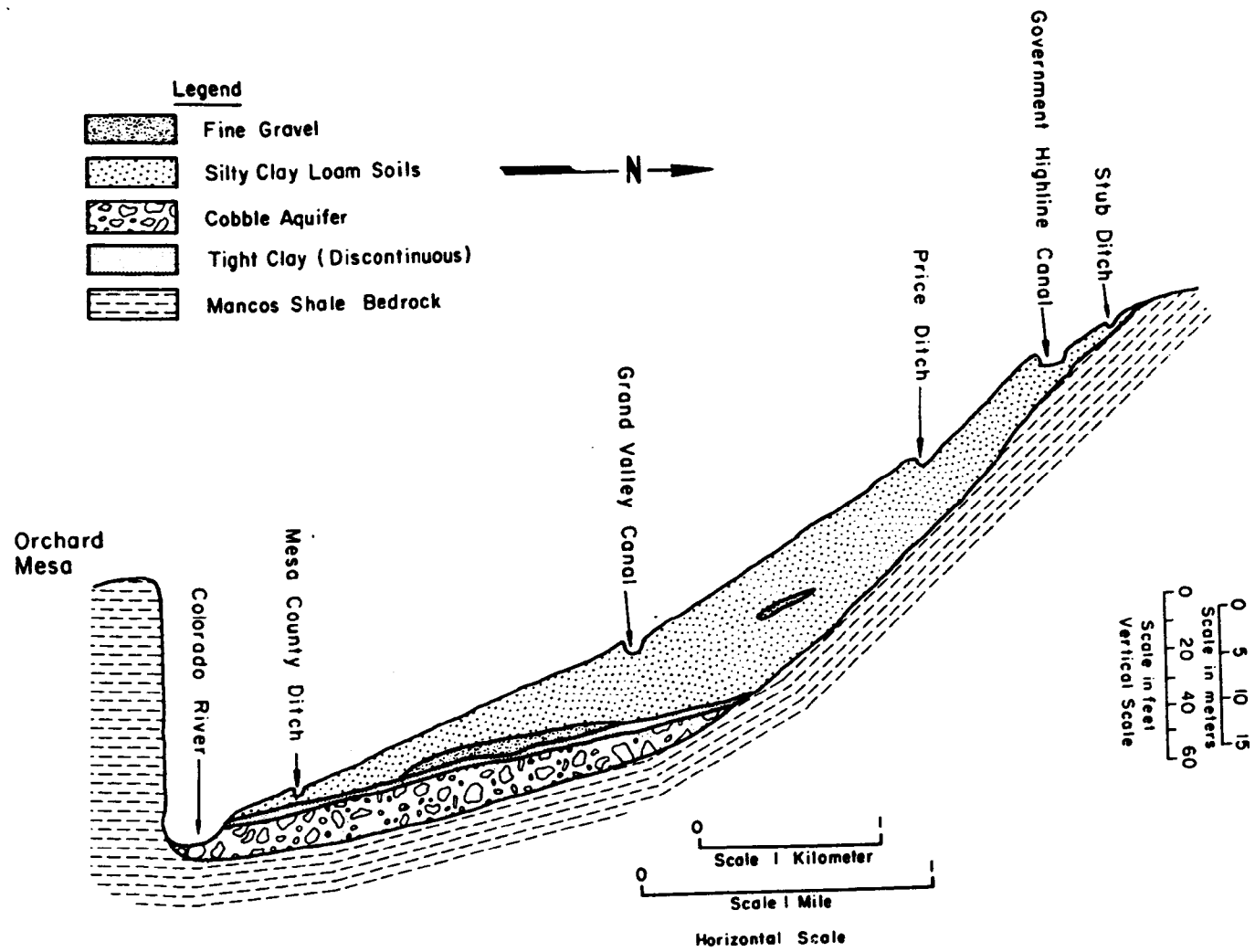


Figure 49. Cobble aquifer cross-section.

near the north edge of the irrigated region where the tributary deposits are relatively thin.

The alluvial deposits overlying the cobble aquifer and/or the Mancos shale are saline clays and silts derived mainly from Mancos shale in the Book Cliffs area and from shaly members of the Mesa Verde Group. Where the cobble aquifer is absent, the clay soils are in contact with a weathered shale zone, below which is the unweathered Mancos shale. The weathered shale can be recognized by its brownish-gray to brown color as compared to the darker gray of the unweathered shale. The weathered shale also exhibits joints, disintegration and separation along the bedding planes. These features account for the permeability of the weathered shale.

The cobble aquifer that underlies the tributary alluvium in much of the irrigated region of the valley is, locally, under artesian pressure, and the water table aquifer in the overlying alluvium is a perched aquifer. The two aquifers are not hydraulically independent, however, since there is sufficient permeability in the confining layer to permit interchange of waters. At some locations, the confining layer is apparently absent and there is direct hydraulic connection between the tributary alluvium and the cobble layer.

Ground water in the Quaternary alluvium exists because of seepage from canals and laterals and deep percolation from irrigation. This ground water acts as source for recharge of the cobble aquifer, particularly along the northern boundary of the cobble (74). Apparently the cobble is also recharged upstream by the Colorado River. Deep percolation from irrigation and seepage from the canals and distribution system return to the Colorado River only after passing through the soil formed from the Quaternary alluvium. The subsurface return flow, after passing through the soil, may then take one of several routes to the river. These routes include passage directly into natural washes or man-made drains with little or no contact with the Mancos Shale, movement through the weathered zone of the shale and into the washes or drains and movement into and through the cobble aquifer to the washes, drains, or river. The quality of these return flows depends upon the particular route taken as discussed in the following subsections.

Quality of Surface Waters

For purposes of general background, some of the chemical analyses of the irrigation water supply used in the research reported here are presented in Table 6. This water supply comes directly from the Government Highline Canal, which is only 300 feet north of Field I. The data show that the water is of good quality for purposes of irrigation. The variation in TDS throughout the irrigation season is roughly 300 to 700 ppm. Commonly, the canals divert water from the Colorado River beginning on April 1 and terminating on October 31.

Quality of Subsurface Waters

Soil Chemistry Test Plots --

In the previous sections of this document, it is reported that the dissolved solids concentration in the drainage water at the bottom of the soil profile at the Matchett farm site generally fell within the range of

TABLE 21. CONCENTRATION OF SALTS IN SOIL SOLUTION, MATCHETT FARM,
1976 (All concentrations in ppm)

Depth (cm)	Plot Number										
	1	2	3	4	5	6	7	8	9	10	11
0-30	1820	5308	3816	2836	1540	6588	10616	7680	11296	6612	4052
30-60	2052	1268	1928	1640	3080	7460	3044	2500	2232	9948	5576
60-90	2104	1292	2676	2464	4732	3548	3464	-	3276	3648	3736
90-120	3000	2588	3160	2704	4704	4748	3156	3260	3204	-	3348
120-150	2916	3272	3140	2828	3404		3716	3344		4988	3668
150-180	3192	3092	3148	3148	3080		3840	3760		3868	3240
180-240	2576	2992	3256	2904	3192		3520	3156		3276	3196
240-300	2976							3148			3260
	12	13	14	15	16	17	18	19	20	21	22
0-30	4948	7112	4572	6386	8124	8876	8088	2992	9084	1656	3235
30-60	1108	3404	8884	1472	1840	3028	2936	6576	6952	1096	920
60-90	3224	-	3364	4224	3208	2644	3028	4444	3700	940	1252
90-120	4488	3440	3792	3828	3388	4032	2448	3500	3672	3872	1720
120-150	6608	4112	3868	3308	3680	3708	3316	3848	4564	3944	5088
150-180	3224	4020	3092	3412	3336	3824	2904	3376	3160	2928	5408
180-240	3444	3608	3028	3548		3604	3008	3144		2968	2824
240-300		4200				3576					
	23	24	25	26	27	28	29	30	31	32	33
0-30	5876	3340	2536	4344	2602	7660	6248	6772	2000	7784	2032
30-60	1276	1936	2684	1812	1324	3396	1852	2232	900	2520	824
60-90	1480	3884	2844	2412	1876	3728	2120	1856	1440	2512	1040
90-120	4840	3308	3568	3612	2096	3796	4055	5024	1700	2496	1328
120-150	3420	3064	3208	2896	2760	3460	3600	3408	1820	3776	2176
150-180	-	3004	3104	3060	1964	2856	3424	2964	1648	2900	5237
180-240	2852		4268	2744	2660	2940	3132	2840	3112	2864	2944
240-300			3100	2940			3370	2828		3112	3444
	34	35	36	37	38	39	40	41	42	43	44
0-30	7172	2500	5076	1820	2048	2548	6372	6648	2116	5988	3590
30-60	1880	1140	1912	1120	1084	1156	2368	1628	1084	1916	1124
60-90	6660	1908	4820	4972	944	2532	2732	3704	1248	1267	992
90-120	5276	1164	3400	3648	1260	3888	3176	4164	4600	2416	2928
120-150	3272	3292	3212	3488	3944	4164	4224	3144	2580	2944	2736
150-180	3260	-	2976	3040	2732	3096	5008	2844	2736	2736	
180-240	3056	2716	4000	2960	2836	2956		2844		2488	
240-300	3096			3040	2752			2180			

(continued)

TABLE 21. (Continued)

Depth (cm)	Plot Number										
	45	46	47	48	49	50	51	52	53	54	55
0-30	6844	1268	1596	2288	1124	1092	1304	2196	1136	5676	2924
30-60	1132	2764	1296	1364	672	1040	860	1076	1280	4124	1664
60-90	1208	5312	3040	3008	2452	3060	4084	1268	3020	3312	4556
90-120	-	2772	3108		3340	3728	2976	2892	2932		3636
120-150	2956				3252	3444		3036	3272		
150-180	2440										
	56	57	58	59	60	61	62	63			
0-30	1192	1946	1176	2926	3160	3220	3204	3160			
30-60	1256	5324	1012	2972	2828	2956	2880	3328			
60-90		4104	3104	2784		3108					
90-120		3408									

3000 to 3900 ppm (see Table 13). Table 21 contains the dissolved solids concentrations of the soil solution as a function of depth for all of the plots at the Matchett experimental site. These data were collected in the fall of 1976. It is apparent that the concentrations in the lower part of the profile again fall within the range of 3000 to 3900 ppm. The significance of this observation is that the concentration remains in a rather narrow range even under a wide variety of irrigation and cropping treatments over a rather large sampling area. Again, this tends to verify the conclusion, derived from the model, that the concentration of waters leaving the soil profile (at ≈ 2 m) is insensitive to the rate or volume of deep percolation. Thus, the salt load leaving the soil profile is proportional to the volume of deep percolation and can be reduced most effectively by reducing the deep percolation.

Some of the test plots in Field III were constructed with lengths of approximately 60 m (200 feet), 90 m (300 feet), and 150 m (500 feet) (see Fig. 8). The TDS for some of the drainage samples collected from Field III are listed in Table 22. These data for the grain plots (49 to 58) correspond roughly with the data in Table 13, which means that no additional knowledge is gained regarding the salt pickup phenomena that are taking place as subsurface irrigation return flows continue their movement from a depth of 2 m in the soil profile, continue downward until reaching the Mancos shale bed, then moving overland until reaching the cobble aquifer, where it is displaced back into the Colorado River (Fig. 49). In contrast, the drainage water from the grass plots (59-63) showed very little quality degradation as compared with the salinity of the irrigation water supply. Unfortunately, Field III was underlain by fractured shale, whereas Fields I and II did not have this problem. As a consequence, large deep percolation loss rates were required before any subsurface flows would enter the drainage pipes that were located around the inside periphery of each plot. This was especially true for plots 59 to 63.

TABLE 22. TOTAL DISSOLVED SOLIDS OF DRAINAGE WATER FROM FIELD III, MATCHETT FARM, 1975

Plot	TDS ppm	Date collected	Plot	TDS ppm	Date collected
49	2908	8/28	59	956	8/01
50	3344	9/16	60	472	7/31
52	2960	9/11	62	588	7/27
58	2376	9/16	63	544	8/08

Natural Washes and Open Drains

There are a number of natural washes that traverse the Grand Valley (Fig. 48). These washes originate in the Book Cliffs north of the Grand Valley. Thunderstorm activity, principally during the months of July and August, results in flood flows transported by these washes in a generally southerly direction until they reach the Colorado River. These natural washes are used extensively for discharging canal spillage and tailwater runoff from irrigated lands. Summer flows and corresponding salinity concentrations reflect the usage of these natural washes as irrigation waste channels. Winter flows in these washes consist largely of subsurface flows into these channels, which have much higher salinity concentrations. These characteristics are illustrated in Table 23. These natural wash discharges frequently have salinity concentrations that are 50% greater than the usual salinity concentrations encountered below the crop root zone at a depth of 2 m.

TABLE 23. SALINITY OF NATURAL WASH DISCHARGES IN THE GRAND VALLEY

Natural Wash	12/17/75 EC, μ mhos	1/07/76 EC, μ mhos	1/22/76 EC, μ mhos	2/05/76 EC, μ mhos	3/03/76 EC, μ mhos
Lewis	4580	4480	4430	4350	4180
Indian	6090	5880	5920	5730	5090
Persigo	5370	5510	5420	5360	4810
Hunter	4720	5030	4850	4710	4340
Adobe	4650	4870	4460	4580	4260
Little Salt	4650	4800	4530	4360	2850
Big Salt West	3940	4020	3840	3560	3420
Big Salt East	3740	3930	4020	3890	3660

The monitoring network for the Grand Valley Salinity Control Demonstration Project is shown in Fig. 50. Some selected salinity data for open drains are listed in Table 24 to illustrate the variation in salinity concentrations in natural washes and open drains during the irrigation season as compared to

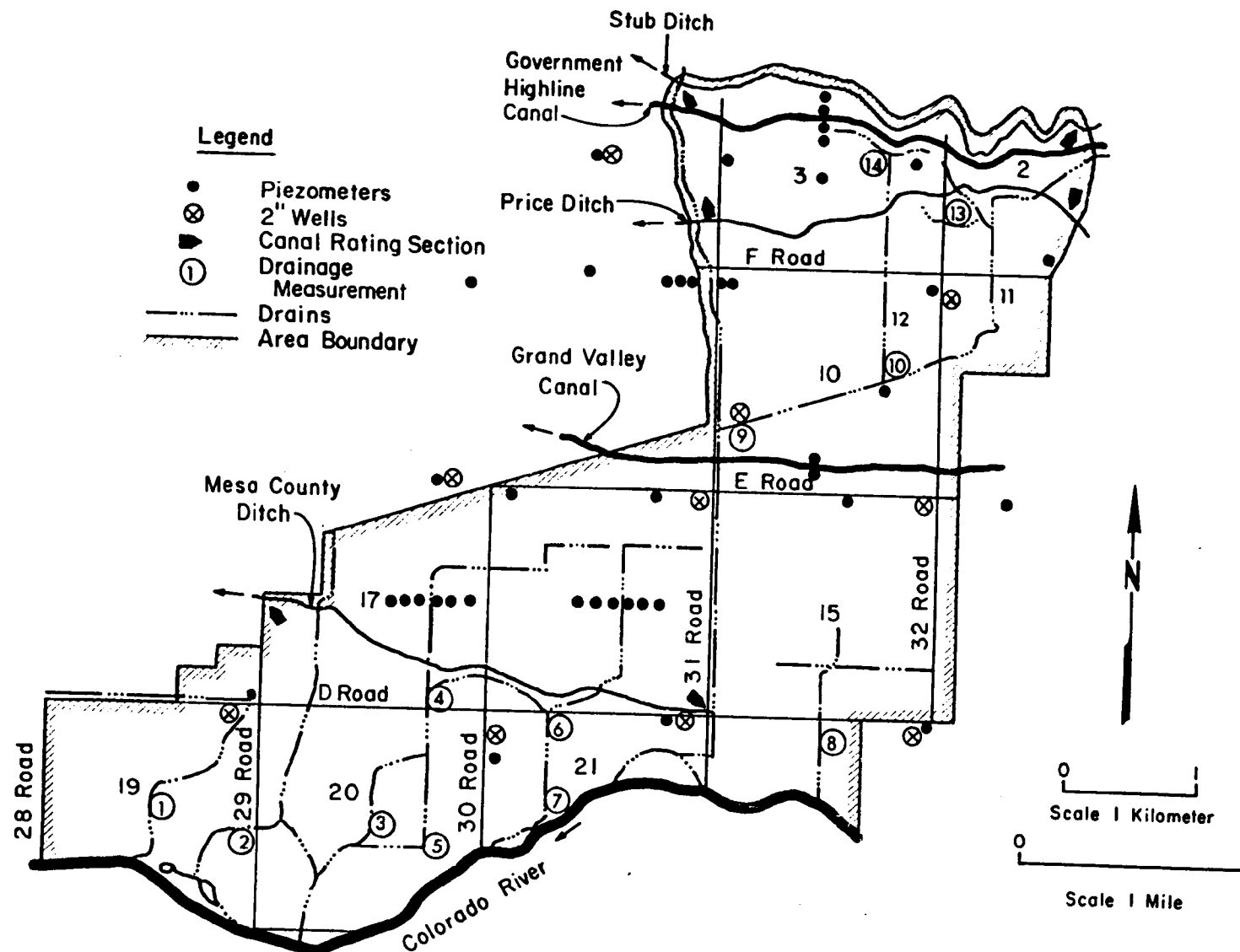


Figure 50. Monitoring network for the Grand Valley Salinity Control Demonstration Project.

TABLE 24. SALINITY OF OPEN DRAINS IN THE GRAND VALLEY SALINITY CONTROL DEMONSTRATION PROJECT AREA

Date	Flume No. 4		Flume No. 6		Flume No. 8		Lewis Wash		Indian Wash	
	EC	TDS	EC	TDS	EC	TDS	EC	TDS	EC	TDS
	μmhos	ppm	μmhos	ppm	μmhos	ppm	μmhos	ppm	μmhos	ppm
03/27/72	2567	1872	3065	2412	7248	7476	5452			
04/25/72	2268	1664	2571	1548	1773	2000	909	512		
06/06/72	1602	1216	3193	2768	1391	1080	515	376		
07/03/72	2108	1704	2391	1972	2571	2160	823	576		
08/07/72	2732	2328	2428	1912	2276	1832	1165	904		
09/04/72	2613	1980	4221	3804	2714	2256	1256	740		
10/03/72	3299	2584	2338	1644	2342	1700	1228	680		
11/07/72	6763	6764	6689	6576	7421	7456	4438	4216		
12/05/72	6728	6852	6624	6724	7234	7448	4960	4824		
01/08/73	6678	7060	6689	6860	7189	7492	4500	5196	5816	4458
02/05/73	6891	7128	5472	5536	7332	7596	5109	5120	5824	6004
03/05/73	6624	6836	6592	6872	7210	7608	5055	5096	5072	5056
04/02/73	6550	6796	6630	6808	7175	7368	5415	5368	5740	5812
05/02/73	1841	1592	1642	1420	2587	2288	846	556	5273	6320
06/01/73	1170	1008	1378	1216	1802	1584	565	468	5137	6064
07/02/73	1062	908	1453	1092	1816	1460	511	296	5032	5904
08/07/73	1336	892	1732	1268	2376	1980	853	364	5095	5452
09/04/73	1533	1088	2460	1880	2861	2364	1129	628	5142	5584
10/03/73	1671	1256	2060	1752	2314	2028	1131	728	5201	5800
11/08/73	4912	4702	4815	4676	5225	5660	1251	903	5129	5472
12/05/73	5712	6213	5611	6513	6262	7241	4174	4581	4951	5771
01/10/74	5626	5208	5626	5888	6068	6696	4105	3700	4551	4560
02/01/74	5314	6716	5475	6656	5788	7328	4247	4820	4913	5724
03/05/74	5036	6328	5425	6884	5899	7416	3587	4052	4748	5948
04/06/74	5867	6552	5580	6672	6511	7356	4694	4948	5356	5676
05/01/74	1459	944	2367	1648	2334	1724	690	440	5876	5768
06/06/74	1126	927	1488	1380	1448	1273	506	447	4960	6013
07/08/74	1351	1008	2208	2428	1676	1881	837	652	5647	5520
08/06/74	1576	1164	3065	2828	1931	1584	1016	700	4939	5756
09/02/74	1635	1488	1986	1532	2452	2104	1279	868	5202	5792
10/01/74	1719	1352	2565	2232	2041	1620	1256	860	2198	1732
11/05/74	5184	6360	5184	6644	6117	7376	3802	4140	2774	2620
12/06/74	6501	6152	5959	6328	6773	7112	4200	4216	5342	4544
01/07/75	5200	6624	5175	6844	5815	7388	3959	4640	4665	5028
03/05/75	6149	6404	6337	6752	6816	7308	4853	4936	5440	5320
04/08/75	5461	6672	5566	6684	5671	6116	4515	4680	4883	5152
05/06/75	1882	1360	1597	1132	2133	1664	1031	648	1819	1348
06/02/75	1207	832	1494	1316	1496	1248	630	544	696	940
07/07/75	1065	796	1314	968	2242	1716	522	260	1413	1076
08/04/75	1329	948	1961	1388	3203	2588	899	552	1655	1132
09/01/75	1695	1128	2223	1500	2517	1752	1199	664	1512	936
10/01/75	2100	1536	1900	1136	2213	1616	1258	776	1836	1332
11/05/75	6234	6064	6222	6095	6966	6836	3685	3252	4541	4168
12/03/75	6258	6260	6264	6284	6962	7060	4391	4320	5003	4736

(continued)

TABLE 24. (Continued)

Date	Flume No. 4		Flume No. 6		Flume No. 8		Lewis Wash		Indian Wash	
	EC	TDS	EC	TDS	EC	TDS	EC	TDS	EC	TDS
	μmhos	ppm	μmhos	ppm	μmhos	ppm	μmhos	ppm	μmhos	ppm
01/05/76	6492	6121	6384	6196	7161	6784	4851	4608	5320	5164
02/02/76	6450	6424	6414	6416	7021	6968	4740	4508	5480	5284
03/01/76	6406	6420	6411	6404	6984	7052	4980	4736	5544	5364
04/06/76	6502	6444	5610	5424	7124	7084	3081	2536	5273	4916
05/04/76	1370	776	2943	2244	4673	3948	860	476	1720	1176
06/01/76	1128	744	2081	1584	2686	2084	632	356	1319	956
07/06/76	1678	1204	3016	2508	1975	1468	803	480	1712	1252
08/02/76	1744	1240	2372	1836	2193	1628	1234	772	1367	892
09/03/76	1756	1112	2208	1183	2660	1908	1303	664	2190	1640
10/01/76	1747	1100	1989	1352	2785	2108	1187	620	2098	1512
11/03/76	6200	6184	5400	5160	6800	6780	4110	3820	4116	3708

winter base flows, which are essentially subsurface flows from groundwater. During the middle of the irrigation season, the open drain salinity levels are only slightly higher than the salinity of the irrigation water supply. Quite frequently in the winter, the TDS is double the salinity concentrations commonly found below the crop root zone. A comparison of EC with TDS in Table 24 shows that they are nearly equal for the higher salinity concentrations (i.e., 4000 micromhos or ppm, or greater).

Groundwater

The earliest known investigation of groundwater in the Grand Valley was reported by Miller (54) in 1916. Kruse (46) has reported the work of S. R. Olsen, who compared data reported by Miller and more recent investigators, to show that the salinity concentrations in the cobble aquifer have not changed significantly in the last sixty years. The following is quoted from Kruse (46):

"An important groundwater body in the Grand Valley is a gravel aquifer approximately parallel to the Colorado River. This water is one of the sources of salt contributing to the salt load in the river. Water in this aquifer is under pressure because of confining layers of shale below it and a relatively impermeable clay layer, although not continuous, above it. A hydraulic gradient exists indicating flow in the direction of the river. Water in some gravel pits adjacent to the river has been observed flowing to the river; water flowing into the aquifer is probably fed by deep percolation from fields at higher elevations north of the aquifer and by seepage from canals, laterals, and drains.

"In 1915, chemical analyses showed that the water in the aquifer had a Ca/Mg ratio of 0.5 as indicated in Fig. 51. Water from wells drilled into water-bearing shale north of the aquifer showed a Ca/Mg ratio of 0.41. Water from a well at Bethel Corner (H and 23 roads) showed a Ca/Mg ratio of 0.55 in 1954 and in 1973. Water from several

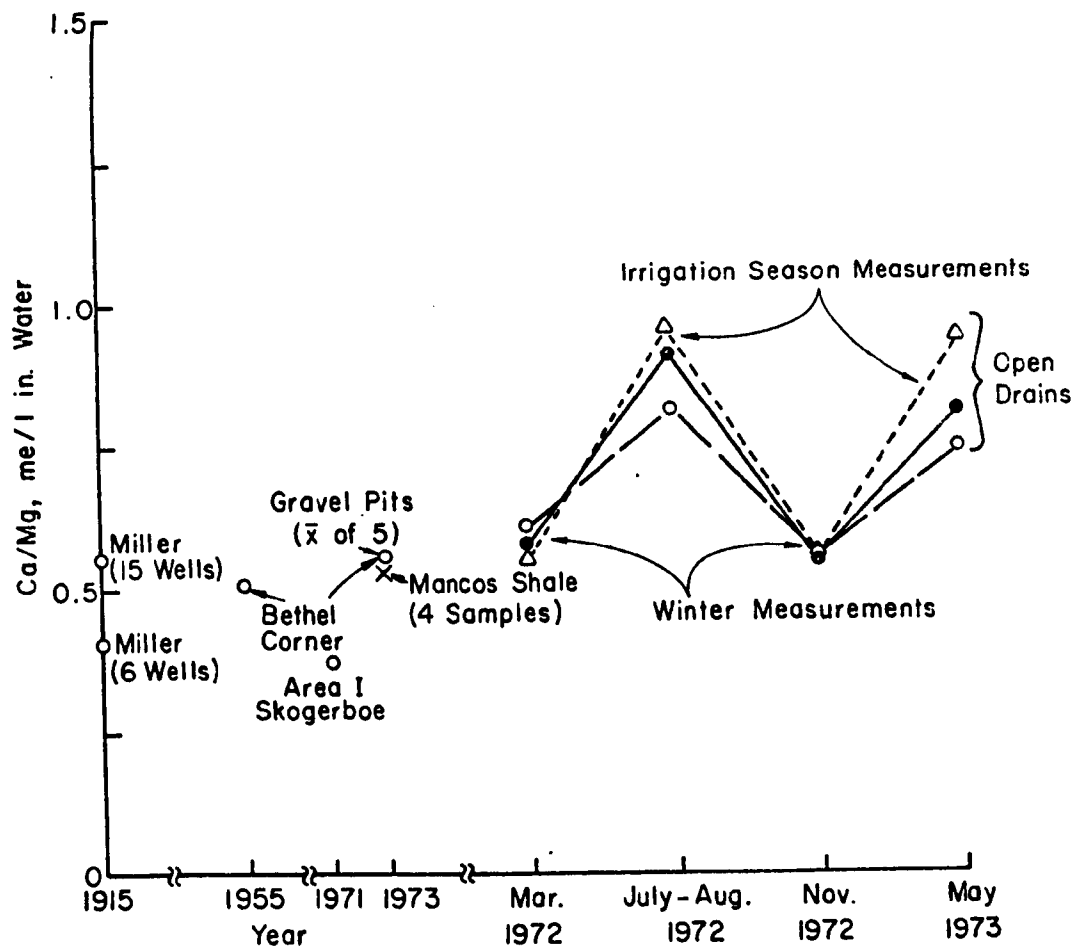


Figure 51. Calcium-magnesium ratios for selected ground and surface water samples in the Grand Valley. (Taken from S.R. Olsen as reported by Kruse, 46)

drains east of Grand Junction showed a Ca/Mg ratio of 0.58 during the winter when the canals were dry. Water from several gravel pits east and west of Grand Junction had a Ca/Mg ratio of 0.55. Water extracts of several shale samples had a Ca/Mg ratio of 0.5 as shown in Fig. 51. Water from a well within the city limits of Grand Junction has a Ca/Mg ratio of 0.66. This well is pumped continuously. Water from drains west of Grand Junction showed a Ca/Mg ratio of 1.2 during the winter season. Water from 12 wells east of Grand Junction had a Ca/Mg ratio of 0.50.

"Water in the gravel aquifer shows essentially a constant Ca/Mg ratio since 1915. This ratio appears to be constant because the water is in equilibrium with three solid phases, i.e., calcium carbonate (CaCO_3), gypsum ($\text{CaSO}_4 \cdot 2\text{H}_2\text{O}$), and magnesite (MgCO_3), and the partial pressure of CO_2 is near 0.011 atmospheres (in air $\text{PCO}_2 = 0.0003$ atm). The water is supersaturated with respect to calcite or aragonite if the pH is above 7; so the actual form and composition of the calcium carbonate present is unknown.

"Most of the water samples were in equilibrium and saturated with magnesite and gypsum. This criteria appeared to be necessary in most cases in order for water from other sources to show a Ca/Mg ratio similar to the water in the aquifer at Bethel Corner.

"Data for water in various wells north of the gravel aquifer indicate a characteristic Ca/Mg ratio of near 0.5 is reached by this water before it enters the gravel aquifer. This result indicates that the solid phases (gypsum, magnesite, and calcium carbonate) are present in shale and the alluvial material over the shale, but not necessarily in the surface soil material 0-3 feet in depth.

"Although the Ca/Mg ratio of water in the aquifer appears to be controlled by the solid phases present, the system has one degree of freedom to allow a soluble salt to vary in concentration, such as Na_2SO_4 or NaCl . The data indicate that such concentrations tend to vary within a narrow range rather than a wide range. These results will require further study for confirmation; but the data indicate tentatively that a reduction in the volume of water entering the aquifer will cause a proportional reduction in the salt load to the river."

The monitoring network shown in Fig. 50 includes numerous 2-inch diameter wells which reach the underlying Mancos shale formation. The location, depth and top elevation of these wells is listed in Table 25. The cross-section shown in Fig. 49 is taken along 31 Road which runs north-south and is parallel but 30 miles east of the Utah-Colorado state line. Selected salinity data for a 2-inch well shown in Fig. 49 is listed in Table 26. [The complete data is reported by Binder et al. (4).] This well is located near the upper portions of the irrigated lands. The TDS varies from roughly 6000 to 8000 ppm, which again is approximately twice the salinity concentration encountered at a depth of 2 m below the ground surface of croplands. Most of the data listed in Table 26 show that the TDS in ppm exceeds the EC in μmhos .

TABLE 25. LOCATION, DEPTH AND TOP ELEVATION OF TWO-INCH DIAMETER WELLS IN THE GRAND VALLEY SALINITY CONTROL DEMONSTRATION PROJECT

CSU Well No.	Location	Well Depth (ft)	Elevation (ft)
1	29 & D Roads	28.6	4603.65
2	30 & D Roads	31	4610.87
3	31 & D Roads	34	4622.13
4	31 & D Roads	22	4622.08
5	31 & D Roads	40	4622.22
6	32 & D Roads	39.5	4633.40
7	3110 E.25 Road	56	4676.94
8	3110 E.25 Road	50	4676.97
9	3110 E.25 Road	45.5	4676.82
10	32 & G.V. Canal	41	4667.11
11	3250 F Road	77	4717.74
12	31 & F Road	56	4715.89
13	31 & F.5 Road	57	4750.33
14	30 & F Road	50	4689.49
15	2950 E. Road	56	4641.07
16	29 & D.5 Road	42	4618.29
17	31 & D.5 Road	43	4641.36

TABLE 26. SELECTED SALINITY DATA FOR CSU WELL NO. 12 LOCATED NEAR THE INTERSECTION OF 31 AND F ROADS IN THE GRAND VALLEY SALINITY CONTROL DEMONSTRATION PROJECT AREA

Date Collected	EC μmhos	TDS ppm	Date Collected	EC μmhos	TDS ppm	Date Collected	EC μmhos	TDS ppm
10/30/69	7012	8240	01/05/72	6804	7144	11/28/73	5342	5852
11/26/69	6985	7440	02/01/72	6938	7168	02/01/74	5599	6924
02/05/70	6626	8016	04/25/72	6793	7292	03/06/74	5689	6984
06/08/70	6672	7492	05/02/72	7094	7684	06/06/74	5580	7060
05/12/71	6800		05/08/72	6999	7424	06/24/74	8126	7012
06/22/71	7300	7344	06/06/72	7061	7472	07/30/74	6767	7964
07/20/71	7000		07/05/72	6992	7348	08/26/74	6212	7536
08/02/71	6726	7596	08/01/72	6925	7476	10/02/74	5705	7148
08/19/71	7281	7572	09/04/72	6804	7260	11/05/74	5301	7016
08/31/71	7141	7532	10/03/72	6756	7044	12/06/74	6837	7352
09/14/71	7027		11/15/72	6773	6592			
09/23/71	7141	7532	12/05/72	6935	7248	01/07/75	5495	6832
09/28/71	7050	7612	01/02/73	6750	7172	03/05/75	6701	7040
10/12/71	7061	7764	01/29/73	6847	7180	04/01/75	5267	6740
10/27/71	6438	7204	03/05/73	6657	7280	05/06/75	6383	6776
11/09/71	6707	7208	04/02/73	6948	7408	06/03/75	6304	5708
11/23/71	6924	7020	06/11/73	5930	7380	07/08/75	6236	6228
12/08/71	6793	7100	07/02/73	6086	7300	08/05/75	6490	6236
12/21/71	6806	7080	08/07/73	6008	7256	09/02/75	6467	6156
			09/04/73	6150	7284	10/03/75	6468	6412

TABLE 26. (Continued)

Date Collected	EC μ mhos	TDS ppm	Date Collected	EC μ mhos	TDS ppm	Date Collected	EC μ mhos	TDS ppm
11/07/75	6397	6352	03/01/76	6400	6216	08/02/76	6426	6440
12/05/75	6522	6372	03/29/76	6425	6240	09/09/76	6479	6484
01/07/76	6456	6376	05/06/76	6482	6396	10/06/76	6978	6788
02/04/76	6362	6320	06/03/76	6331	6536	11/03/76	6300	6168
			07/06/76	6325	6488			

Salinity data for the 2-inch wells located along D Road (Fig. 50) are listed in Table 27. The TDS of these wells varies roughly from 5500 to 9000 ppm. There are numerous TDS measurements that exceed 8000 ppm. The salinity concentrations in the wells along D Road are only slightly greater than the salinity levels shown in Table 26 for CSU Well No. 12, which is located two miles north of D Road.

TABLE 27. SELECTED SALINITY DATA FOR WELLS LOCATED ALONG D ROAD IN THE GRAND VALLEY SALINITY CONTROL DEMONSTRATION PROJECT AREA

Date Collected	CSU Well No. 1 29 & D Roads		CSU Well No. 2 30 & D Roads		CSU Well No. 4 31 & D Roads		CSU Well No. 6 32 & D Roads	
	EC	TDS	EC	TDS	EC	TDS	EC	TDS
	μ mhos	ppm	μ mhos	ppm	μ mhos	ppm	μ mhos	ppm
05/25/71			7600	8262				
07/06/71								
08/02/71			7264	7816	6191	6364	7896	8804
09/23/71			7585	7964	6311	6544	8414	8640
10/27/71			7257	7872	6023	6308	7905	8524
11/23/71			7453	7664	6366	6248	8316	9096
12/21/71			7674	8332	6278	6312	8229	8440
02/01/72			7718	7556	6298	6212	8340	8904
03/21/72			7465	7860	6362	6424	8190	9100
03/27/72			7491	8184	6314	6508	7836	8404
04/25/72			7491	8180	6321	6424	8191	8880
05/30/72	6067	6088	7610	8140	6376	6500	8446	9040
06/27/72	6231	6148	7813	8284	6400	6572	8400	8964
07/25/72	6252	6300	7575	7920	6475	6592	8268	9060
08/29/72	6185	6292	7534	7512	6462	5204	8464	7332
09/26/72	6222	5916	7650	7684	6426	6888	8364	8664
10/31/72	5965	5960	7444	7980	9294	6360	8163	8760
11/27/72	6136	5544	7593	7656	6240	5824	8321	8208
12/18/72	6284	5776	7837	6284	6373	6421	8176	6323
01/29/73	6166	6100	7580	8068	6251	6476	8243	8776
02/26/73	6230	5872	7697	7844	6251	6248	8307	8688
03/26/73	6210	6080	7613	8064	6321	6388	8300	8772
04/27/73	5285	5992	6718	7828	5591	6460	6806	8640
05/30/73	5211	6116	6560	8128	5424	6564	6857	8724

(continued)

TABLE 27. (Continued)

Date Collected	CSU Well No. 1 29 & D Roads		CSU Well No. 2 30 & D Roads		CSU Well No. 4 31 & D Roads		CSU Well No. 6 32 & D Roads	
	EC	TDS	EC	TDS	EC	TDS	EC	TDS
	µmhos	ppm	µmhos	ppm	µmhos	ppm	µmhos	ppm
06/25/73	5406	6016	6507	7876	5481	6256	6902	8432
07/30/73	5436	6584	6801	8004	6688	6364	7015	8684
08/27/73	5580	6248	7061	8208	5806	6576	7084	8672
09/26/73	5493	5808	6371	7324	5484	6036	6879	7856
10/31/73	5643	5868	6763	6956	5899	6040	7556	7156
11/28/73	5500	6128	6651	7988	5501	6424	6769	8528
12/21/73	5483	6006	6579	7200	5293	5920	6373	6748
01/24/74	4961	4852	6058	5825	4969	4776	6481	5968
03/22/74	5585	6216	7299	8276	6068	6464	6952	8680
04/23/74	5526	5988	6826	7092	5831	6256	6934	8436
05/29/74	5406	6004	6834	8304	5490	6288	6609	8604
06/24/74	5322	6092	6845	7332	5694	6348	6610	7528
07/30/74	6270	6268	8066	8480	6310	6408	8013	8836
08/26/74	5472	6224	6756	8732	5767	6484	6902	8540
09/24/74	5287	6152	6220	8340	5495	6468	6324	8516
10/29/74	5145	6172	6595	8124	5356	6380	6281	8012
11/27/74	5317	6160	6635	6160	5137	5748	6507	7844
12/19/74	5818	5984	7528	7920	6344	6340	7316	7736
01/22/75	5433	6068	6614	7844	5270	6128		
02/26/75	5269	6148	5694	6540	5279	6016	6304	7688
03/24/75	5234	5888	6406	7872	5162	6060	5776	6704
04/22/75	5313	6108	5895	6852	5330	6180	6271	7976
05/27/75	6166	5892	7573	8096	5743	5736	7314	7808
06/30/75	5987	5832	7904	8072	6192	6164	7592	8108
07/28/75	5884	5816	7401	8296	6038	6032		
08/25/75	6049	5804	7927	8004	5997	5728		
09/24/75	6020	5640	7589	7448	6142	5520		
10/29/75			7666	7708	5957	5528		
11/26/75	6049	5692	7800	7788	6454	6024		
12/29/75	6033	5576	7747	7712	6212	5972		
01/26/76	6049	5620	7718	7596	6049	5728		
02/23/76	6064	5552	7733	7608	6096	5664		
03/29/76	6014	5508	7579	7648	5991	5676		
04/27/76	5928	5072	7684	7636	5904	5604		
05/25/76	5946	5688	7638	7612	6059	5912		
06/28/76	5819	5456	7666	7728	5684	5484		
07/28/76	5893	5540	7405	7368	5893	5524		
08/23/76	5980	5508	7794	7280	6171	5652		
09/22/76	5851	5400	7162	6976	5593	5296		
10/28/76	6266	5940	6597	6476	5416	5019		
11/03/76	5300	5048	7444	7512	5800	5660		

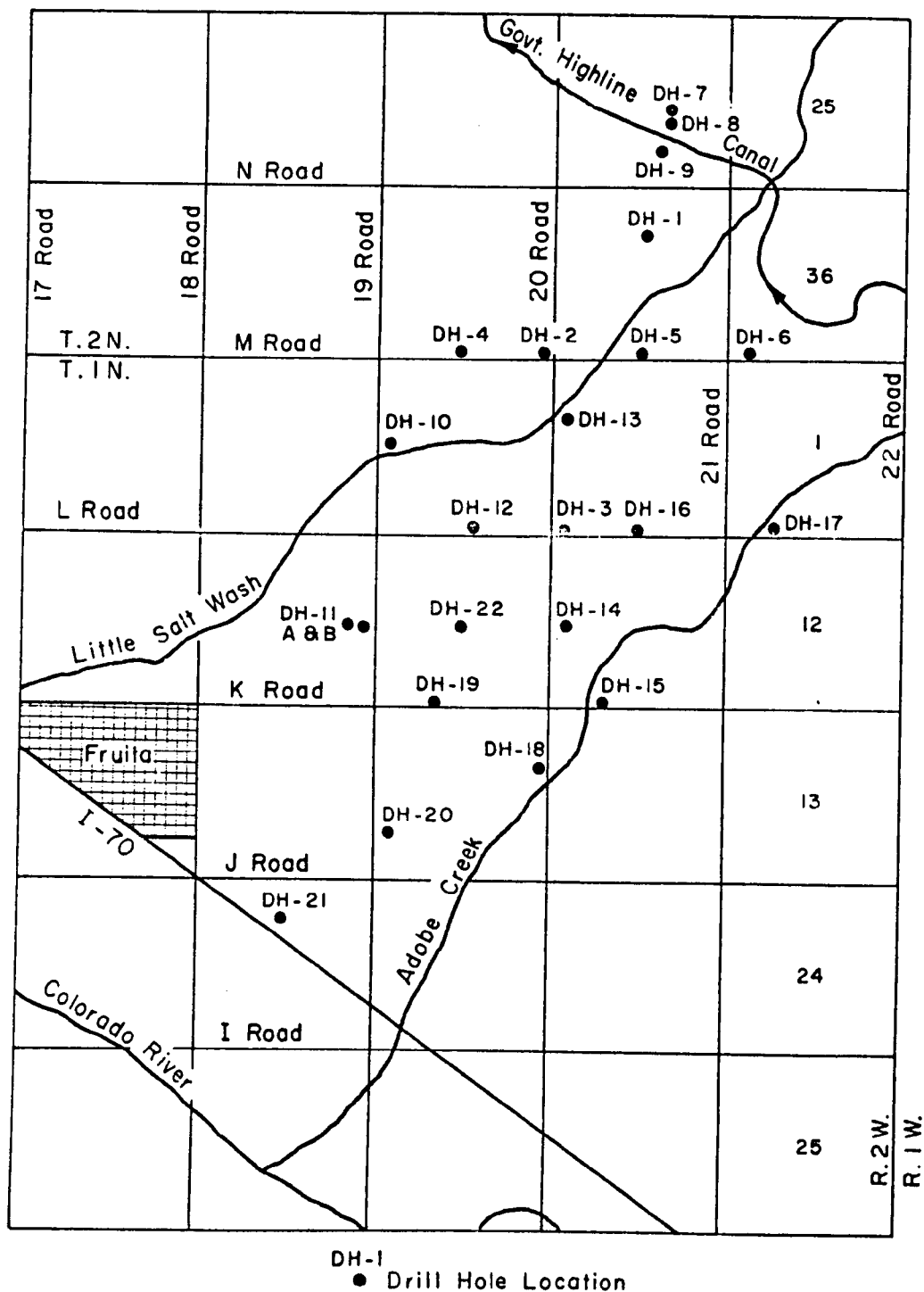


Figure 52. Location of wells installed by the Agricultural Research Service in western Grand Valley.

TABLE 28. SELECTED SALINITY DATA FOR WELLS INSTALLED BY THE AGRICULTURAL RESEARCH SERVICE (SEA) IN WESTERN GRAND VALLEY

ARS Well No.	Date Collected	pH	EC μmhos	meq/l							
				Ca	Mg	Na	K	HCO ₃	Cl	NO ₃	SO ₄
2	06/25/75	7.76	7,630	14.97	24.18	78.26	0.407	10.70	15.72	1.135	86.25
2	08/07/75	7.82	8,120	15.47	32.90	95.65	0.537	13.50	19.90	1.443	111.74
2	10/12/75	7.82	12,610	22.50	55.89	167.83	0.80	19.60	26.00	1.39	200.31
2	12/17/75	7.71	12,860	22.34	52.04	164.13	0.73	18.00	24.10	1.43	191.50
2	03/16/75	7.47	10,310	16.88	45.43	116.90	0.59	14.70	17.88	1.27	145.71
12	06/25/75	7.91	18,500	13.97	49.34	379.35	0.621	23.00	33.04	0.795	365.63
12	08/07/75	7.89	18,420	13.97	50.16	373.91	0.660	23.00	30.66	0.438	406.96
12	10/12/75	7.83	21,280	18.28	53.41	456.30	0.82	23.40	32.84	0.647	463.75
12	12/17/75	7.78	21,790	20.49	49.60	405.17	0.74	21.76	30.60	0.784	416.47
12	03/16/75	7.74	20,150	16.16	51.53	393.46	0.67	20.24	28.40	1.22	402.66
15	06/25/75	7.65	15,900	17.30	117.19	189.13	0.767	18.60	23.04	35.47	235.94
15	08/07/75	7.65	14,520	16.97	119.24	208.70	0.794	18.40	21.56	34.775	280.97
15	10/12/75	7.69	16,190	20.11	122.29	228.15	0.97	18.40	22.00	36.26	282.19
15	12/17/75	7.68	17,370	22.52	127.81	241.61	0.89	18.20	21.82	33.14	282.06
15	03/16/75	7.48	16,560	18.55	120.48	228.98	0.84	18.20	21.54	26.70	258.66
18-L	06/25/75	7.59	5,530	9.65	13.16	46.29	0.849	10.80	6.64	0.795	50.63
18-L*	08/07/75	7.76	5,110	10.48	13.16	43.70	0.852	11.80	6.86	0.623	49.72
18-L	10/12/75	7.86	5,480	14.18	14.58	49.22	1.02	12.36	6.88	0.824	57.81
18-L	12/17/75	7.29	6,530	15.51	20.39	58.65	1.21	11.96	7.30	3.02	70.87
18-L*	03/16/75	7.71	5,510	12.35	15.30	48.33	0.92	11.80	6.32	1.03	54.33
20-L	06/25/75	7.57	4,810	18.46	13.65	25.43	0.286	9.00	19.24	0.758	25.62
20-L	18/07/75	7.71	4,210	13.67	12.50	23.70	0.269	8.40	19.30	0.623	24.72
20-L	10/12/75	7.68	4,260	16.95	11.50	24.80	0.25	10.20	18.36	0.893	23.03
20-L	12/17/75	7.40	4,490	16.80	12.18	26.74	0.26	8.60	18.14	0.877	24.99
20-L	03/16/75	7.46	4,500	13.78	12.45	27.96	0.30	10.00	16.94	1.03	26.00

*L, 4" casing, shallow

The Scientific Education Administration (SEA), Agricultural Research has drilled a number of wells in the western portion of the Valley near the town of Fruita. The locations of these wells are shown in Fig. 52. Data from some of these wells (46,47,48) are listed in Table 28 for comparison with results cited in Tables 26 and 27. Some of the results are comparable (e.g., wells ARS(SEA)18-L and ARS(SEA)20-L). Some of the data included in Table 28 was selected because it represented the highest levels of salinity concentration encountered in the valley (e.g., wells ARS(SEA)2, ARS(SEA)12, and ARS(SEA)15). These wells have much higher Na^+ concentrations than the other wells. Thus, as subsurface irrigation return flows move through the groundwater reservoir, additional Na^+ is taken into solution. Since the soil moisture movement at a depth of 2 m is already saturated with gypsum, but the gypsum levels are even higher in the cobble aquifer, this would imply that secondary chemical reactions are taking place which allow additional sodium to be taken into solution. Unfortunately, these secondary chemical reactions are not described in the soil chemistry model used in this study.

PREDICTION OF SALT LOAD

The fact that the TDS concentrations in the drainage water at the bottom of the soil profile and the groundwater in the cobble aquifer, although markedly different, are relatively insensitive to the rates and volumes of discharge makes the prediction of salt load under various management or abatement alternatives a simple task. In other words, the salt load reaching the Colorado River is directly proportional to the volume of subsurface irrigation return flows because the salinity concentrations remain approximately constant below the crop root zone and in the cobble aquifer. The problem of predicting the subsurface return flow salinity is, therefore, reduced to determining the flow routes and discharge volumes for each flow route, which can then be combined with the salt concentrations corresponding to each flow route in order to calculate the salt load reaching the Colorado River.

REFERENCES

1. Ayars, J.E. Drainage of Irrigated Lands in Grand Valley. Unpublished M.S. Thesis, Colorado State University, Fort Collins, Colorado 80523, December, 1972. 150 pp.
2. Bhyiyan, S.K., E.A. Hiler, C.H.M. van Bavel and A.R. Aston. Dynamic Simulation of Vertical Infiltration into Unsaturated Soils. Water Resources Research, Vol. 7, No. 6, December, 1971. p 1597-1606.
3. Biggar, J.W. and D.R. Nielsen. Miscible Displacement and Leaching Phenomenon in Irrigation of Agricultural Lands. Edited by R.M. Hagan. Agronomy Monograph No. 11, 1967. p 254-274.
4. Binder, C.W., G. Bargsten, B.F. Mancuso, R.G. Evans, W.R. Walker, and G.V. Skogerboe. Grand Valley Salinity Control Demonstration Project Basic Field Data. Report AER77-78-CWB-GB-BFM-RGE-WRW-GVS8, Dept. of Agr. and Chem. Engr., Colorado State University, Fort Collins, Colorado 80523, June, 1978. 194 pp.
5. Bresler, E. A Model for Tracing Salt Distribution in the Soil Profile and Estimating the Efficient Combination of Water Quality and Quantity under Varying Field Conditions. Soil Science, Vol. 104, No. 4, October, 1967. p 227-233.
6. Bresler, E. Simultaneous Transport of Solutes and Water under Transient Unsaturated Flow Conditions. Water Resources Research, Vol. 9, No. 4, August, 1973. p 975-986.
7. Bresler, E. and R.J. Hanks. Numerical Method for Estimating Simultaneous Flow of Water and Salt in Unsaturated Soil. Soil Science Society of America Proceedings, Vol. 33, No. 6, November-December, 1969. p 827-832.
8. Brooks, R.H., J.O. Goertzen, and C.A. Bower. Prediction of Changes in the Compositions of the Dissolved and Exchangeable Cations in Soils upon Irrigation with High-Sodium Waters. Soil Science Society of America Proceedings, Vol. 22, No. 2, March-April, 1958. p 122-124.
9. Brooks, R.H. and A.T. Corey. Hydraulic Properties of Porous Media. Hydrology Paper No. 3, Colorado State University, Fort Collins, Colorado, March, 1964. 27 pp.

10. Bruce, R.R. Hydraulic Conductivity Evaluation of the Soil Profile from Soil Water Retention Relations. Soil Science Society of America Proceedings, Vol. 36, No. 4, July-August, 1972. p 555-561.
11. Bruce, R.R. and A. Klute. The Measurement of Soil Moisture Diffusivity. Soil Science Society of America Proceedings, Vol. 20, No. 4, October, 1956. p 458-460.
12. Bruce, R.R. and A. Klute. Measurements of Soil Diffusivity from Tension Plate Outflow Data. Soil Science Society of America Proceedings, Vol. 27, No. 1, January-February, 1965. p 18-21.
13. Brutsaert, W. The Adaptability of an Exact Solution to Horizontal Infiltration. Water Resources Research, Vol. 4, No. 4, August, 1968. p 785-789.
14. Brutsaert, W. The Permeability of a Porous Medium Determined from Certain Probability Laws for Pore-Size Distribution. Water Resources Research, Vol. 4, No. 2, April, 1968. p 425-434.
15. Brutsaert, W. A Solution for Vertical Infiltration into a Dry Porous Medium. Water Resources Research, Vol. 4, No. 5, October, 1968. p 1031-1038.
16. Cowan, I.R. Transport of Water in the Soil-Plant Atmosphere System. Journal of Applied Ecology, Vol. 2, 1965. p 221-239. Blackwell Scientific Publication, Oxford, United Kingdom.
17. Davidson, J.N., D.R. Baker, G.H. Brusewitz. Simultaneous Transport of Water and Adsorbed Solutes through Soil under Transient Flow Conditions. Transactions, American Society of Agricultural Engineers, 1975. p 535-539.
18. Davidson, J.M., L.R. Stone, D.R. Nielsen, and M.E. Larcie. Field Measurement and Use of Soil-Water Properties. Water Resources Research, Vol. 5, No. 6, December, 1969. p 1312-1321.
19. Deans, H.A. A Mathematical Model for Dispersion of the Direction of Flow in Porous Media. Society of Petroleum Engineers Journal, March, 1963. p 49-52.
20. Duke, H.R., E.G. Kruse, S.R. Olsen, D.F. Champion, and D.C. Kincaid. Irrigation Return Flow Water Quality as Affected by Irrigation Water Management in the Grand Valley of Colorado. Final Report to USEPA, Region VIII, Denver, Colorado, 1976. 123 p. EPA IAG D4-0545.
21. Duke, H.R. and H.R. Haise. Vacuum Extractors to Assess Deep Percolation Losses and Chemical Constituents of Soil Water. Soil Science Society of America Proceedings, Technical Note, Vol. 37, No. 6, November-December, 1973. p 963-964.

22. Dutt, G.R. Prediction of the Concentration of Solutes in Soil Solutions for Soil Systems Containing Gypsum and Exchangeable Ca and Mg. Soil Science Society of America Proceedings, Vol. 26, No. 4, July-August, 1962. p 341-343.
23. Dutt, G.R. and L.D. Doneen. Predicting the Solute Composition of the Saturation Extract from Soil Undergoing Salinization. Soil Science Society of America Proceedings, Vol. 27, No. 6, November-December, 1963. p 627-630.
24. Dutt, G.R., M.J. Shaffer, and W.J. Moore. Computer Simulation Model of Dynamic Bio-Physio-Chemical Processes in Soils. Technical Bulletin 196, Department of Soils, Water and Engineering, Agricultural Experiment Station, University of Arizona, Tucson, October, 1972. 101 pp.
25. Dyer, K.L. Unsaturated Flow Phenomena in Panoche Sandy Clay Loam as Indicated by Leaching of Chloride and Nitrate Ions. Soil Science Society of America Proceedings, Vol. 29, No. 2, April, 1965. p 121-126.
26. Freeze, R.A. The Mechanism of Natural Groundwater Recharge and Discharge, 1. One-dimensional, Vertical, Unsteady, Unsaturated Flow Above a Recharging or Discharging Groundwater Flow System. Water Resources Research, Vol. 5, No. 1, February, 1969. p 153-171.
27. Freeze, R.A. Three-Dimensional, Transient, Saturated-Unsaturated Flow in a Groundwater Basin. Water Resources Research, Vol. 7, No. 1, April, 1971. p 347-365.
28. Fried, J.J. and M.A. Combarous. Dispersion in Porous Media. Advances in Hydroscience, No. 1, 1971. p 169-282.
29. Frissel, M.J. and P. Poelstra. Chromatographic Transport Through Soils. 1. Theoretical Evaluation. Plant and Soil XXVI, No. 2, April, 1967. p 285-302.
30. Gardner, W.D. Calculation of Capillary Conductivity from Pressure Plate Outflow Data. Soil Science Society of America Proceedings, Vol. 20, No. 2, July, 1956. p 317-320.
31. Gardner, W.R. Dynamic Aspects of Water Availability to Plants. Soil Science, Vol. 89, No. 2, February, 1961. p 63-73.
32. Gardner, W.R. Relation of Root Distribution to Water Uptake and Availability. Agronomy Journal, Vol. 56, No. 1, January-February, 1964. p 41-45.
33. Gardner, W.R., D. Hillel, and Y. Benyamin. Post-Irrigation Movement of Soil Water. 1. Redistribution. Water Resources Research, Vol. 6, No. 3, June, 1970. p 851-861.
34. Glueckauf, E. Theory of Chromatography. Part 9. The "Theoretical Plate" Concept in Column Separations. Transactions, Faraday Society, London, Vol. 51, 1955. p 34-44.

35. Green, R.E., and J.C. Corey. Calculation of Hydraulic Conductivity: A Further Evaluation of Some Predictive Methods. Soil Science Society of America Proceedings, Vol. 35, No. 51, January, 1971. p 3-8.
36. Hanks, R.J. and S.A. Bowers. Numerical Solution of the Moisture Flow Equation for Infiltration into Layered Soils. Soil Science Society of America Proceedings, Vol. 26, No. 6, November-December, 1962. p 530-584.
37. Hanks, R.J. and S.A. Bowers. Influence of Variations in the Diffusivity-Water Content Relation on Infiltration. Soil Science Society of America Proceedings, Vol. 27, No. 3, May-June, 1963. p 263-265.
38. Hanks, R.J., A. Klute, and E. Bresler. A Numeric Method for Estimating Infiltration, Redistribution, Drainage, and Evaporation from Soil. Water Resources Research, Vol. 5, No. 5, October, 1969. p 1064-1069.
39. Hillel, P.V., D. Krentos and Y. Stylianou. Procedure and Test of an Internal Drainage Method for Measuring Soil Hydraulic Characteristics "In Situ". Soil Science, Vol. 114, No. 5, November, 1972. p 395-400.
40. Holburt, M.B. Salinity Control Needs in the Colorado River Basin. In: Proceedings, National Conference on Managing Irrigated Agriculture to Improve Water Quality, Grand Junction, Colorado, May, 1972. p 19-26.
41. Jensen, M.E. (ed.). Consumptive Use of Water and Irrigation Water Requirements. American Society of Civil Engineers, New York, N.Y. 1973. 215 p.
42. Kincaid, D.C. and D.F. Heermann. Scheduling Irrigations Using a Programmable Calculator. ARS-NC-12, ARS-USDA, February, 1974. p 55.
43. King, L.G. and R.J. Hanks. Irrigation Management for Control of Quality of Irrigation Return Flow. EPA-R2-73-265, U.S. Environmental Protection Agency, Washington, D.C. 307 p.
44. Klute, A. A Numerical Method for Solving the Flow Equation for Water in Unsaturated Materials. Soil Science, Vol. 73, No. 2, February, 1952. p 105-116.
45. Klute, A. Laboratory Measurement of Hydraulic Conductivity of Saturated Soil. Agronomy Monograph No. 9, Part 1, 1965. p 210-221.
46. Kruse, E.G. Alleviation of Salt Load in Irrigation Water Return Flow of the Upper Colorado River Basin. USDA-ARS FY 1974 Annual Report to Bureau of Reclamation, U.S. Department of Interior, 1974. 38 p.
47. Kruse, E.G. Alleviation of Salt Load in Irrigation Water Return Flow of the Upper Colorado River Basin. USDA-ARS FY 1975 Annual Report to Bureau of Reclamation, U.S. Department of Interior, 1975. 112 p.

48. Kruse, E.G. Alleviation of Salt Load in Irrigation Water Return Flow of the Upper Colorado River Basin. USDA-ARS FY 1976 Annual Report to Bureau of Reclamation, U.S. Department of Interior, 1976. 116 p.
49. Kyle, C.R. and R.L. Perine. Turbulent Dispersion in Porous Materials as Modeled by a Mixing Cell with Stagnant Zone. Society of Petroleum Engineers Journal, March, 1971. p 57-62.
50. Lai, S.H. and J.J. Jurinak. Numerical Approximation of Cation Exchange in Miscible Displacement through Soil Columns. Soil Science Society of America Proceedings, Vol. 35, No. 6, November-December, 1971. p 894-899.
51. Ludwick, A.E. and P.N. Soltanpour. Guide to Fertilizer Recommendations in Colorado. Cooperative Extension Service, Colorado State University, Fort Collins, Colorado 80523, January, 1975. 45 p.
52. McWhorter, D.B. Infiltration Affected by Flow of Air. Hydrology Paper No. 49, Colorado State University, Fort Collins, Colorado, May, 1971. 43 p.
53. Miller, D.G. The Seepage and Alkali Problem in the Grand Valley, Colorado. USDA Office of Public Roads and Rural Engineering, 1916. 48 p.
54. Miller, R.J., J.W. Biggar, and D.R. Nielsen. Chloride Displacement in Panoche Clay Loam in Relation to Water Movement and Distribution, Vol. 1, No. 1, 1965. p 63-73.
55. Millington, R.J. and J.P. Quirk. Transport in Porous Media. Transactions, 7th International Congress of Soil Science, Madison, Wisconsin, 1960. p 97-106.
56. Molz, F.J., I. Remson. Extraction Term Models of Soil Moisture Use by Transpiring Plants. Water Resources Research, Vol. 6, No. 5, October, 1970. p 1346-1356.
57. Molz, F.J., I. Remson, A.A. Fungaroli and R.L. Drake. Soil Moisture Availability for Transpiration. Water Resources Research, Vol. 4, No. 6, December, 1968. p 1661-1669.
58. Nielsen, D.R., J.W. Biggar, and K.T. Erh. Spatial Variability of Field-Measured Soil-Water Properties. Hilgardia, Vol. 42, No. 7, November, 1973. p 215-260.
59. Nimah, M.N. and R.J. Hanks. Model for Estimating Soil Water, Plant and Atmospheric Interrelations: I. Description and Sensitivity. Soil Science Society of America Proceedings, Vol. 37, No. 4, July-August, 1973. p 522-527.

60. Oster, J.D. and B.L. McNeal. Computations of Soil Solution Composition Variation with Water Content for Desaturated Soils. Soil Science Society of America Proceedings, Vol. 35, No. 3, May-June, 1971. p 436-442.
61. Oster, J.D. and J.R. Rhoades. Calculated Drainage Water Compositions and Salt Burdens Resulting from Irrigation with River Waters in the Western United States. Journal of Environmental Quality, Vol. 4, No. 1, 1975. p 73-79.
62. Parlange, J.-Y. Theory of Water Movement in Soils: I. One-dimensional Absorption. Soil Science, Vol. III, No. 2, 1971. p 134-137.
63. Parlange, J.-Y. Theory of Water Movement in Soils: 2. One-dimensional Infiltration. Soil Science, Vol. III, No. 2, 1971. p 170-174.
64. Penman, H.L., D.E. Angus and C.H.M. van Bavel. Microclimatic Factor Affecting Evaporation and Transpiration. Agronomy Monograph No. 11, Irrigation of Agricultural Lands, 1967. p 483-505.
65. Philip, J.R. The Theory of Infiltration: The Infiltration Equation and Its Solution. Soil Science, Vol. 83, No. 5, May, 1957. p 345-357.
66. Philip, J.R. The Theory of Infiltration: 6. Effect of Water Depth over Soil. Soil Science, Vol. 85, No. 5, May, 1958. p 278-286.
67. Reeve, R.C. and Doering, E.J. Engineering Aspects of the Reclamation of Sodic Soils with High-Salt Waters. In: Journal of the Irrigation and Drainage Division, American Society of Civil Engineers, Vol. 91, No. IR4, Proc. Paper 4588, December, 1965. p 59-72.
68. Reicosky, D.C., R.J. Millington, A. Klute and D.B. Peters. Patterns of Water Uptake and Root Distribution of Soybeans (*Glycine max.*) in the Presence of a Water Table. Agronomy Journal, Vol. 64, No. 3, May-June, 1972. p 292-297.
69. Remson, I., G.M. Hornberger, and F.J. Molz. Numerical Methods in Sub-surface Hydrology. Wiley-Interscience, 1971. 389 pp.
70. Richards, L.A. Capillary Conduction of Liquids through Porous Mediums. Physics, Vol. 1, No. 5, November, 1931. p 318-333.
71. Richtmyer, R.D. Difference Methods for Initial Value Problems. Interscience Publications, 1967, New York, 2nd Edition. 405 pp.
72. Rogerson, T.L. Half-minute Counts for Neutron Probes. Soil Science, Vol. 100, No. 5, November, 1968. p 359-360.
73. Rubin, J. Numerical Method for Analyzing Hysteresis-Affected Post-Infiltration Redistribution of Soil Moisture. Soil Science Society of America Proceedings, Vol. 31, No. 1, January-February, 1967. p 13-20.

74. Schneider, E.J. Surficial Geology of the Grand Junction-Fruita Area, Mesa County, Colorado. Unpublished MS Thesis, Department of Earth Resources, Colorado State University, Fort Collins, Colorado, 1975. 125 pp.
75. Skogerboe, G.V. and W.R. Walker. Evaluation of Canal Lining for Salinity Control in Grand Valley. EPA-R2-72-047, U.S. Environmental Protection Agency, Washington, D.C., 1972. 199 pp.
76. Smajstrala, A.G., D.L. Reddell, and E.A. Hiler. Simulation of Miscible Displacement in Soils. Paper No. 74-2015 presented at 1974 meeting, American Society of Agricultural Engineers, Stillwater, Oklahoma, June 23-26, 1974. 31 pp.
77. Stable, W.J. Comparison of Computed and Measured Moisture Redistribution Following Infiltration. Soil Science Society of America Proceedings, Vol. 33, No. 6, November-December, 1969. p 840-847.
78. Su, C. and R.H. Brooks. Soil Hydraulic Properties from Infiltration Tests. In: Proceedings, Watershed Management Symposium. Irrigation and Drainage Division, American Society of Civil Engineers, Logan, Utah, August 11-13, 1975. p 516-542.
79. Tanji, K.K. Solubility of Gypsum in Aqueous Electrolytes as Affected by Ion Association and Ionic Strengths Up to 0.15 m and at 25°C. Environmental Science and Technology, Vol. 3, No. 7, July, 1969. p 656-661.
80. Tanner, C.B. Measurement of Evapotranspiration in Irrigation of Agricultural Lands. Edited by R.M. Hagan et al. Agronomy Monograph No. 11, 1967. p 534-574.
81. Taylor, J.H. Irrigation Scheduling for Salinity Control. Unpublished MS Thesis, Colorado State University, Fort Collins, Colorado 80523, 1974. 93 pp.
82. Terkletaub, R.W. and K.L. Babcock. A Simple Method for Predicting Salt Movement through Soil. Soil Science, Vol. 111, No. 3, 1971. p 182-187.
83. Thomas, G.W. and N.T. Coleman. A Chromatographic Approach to the Leaching of Fertilizer Salts in Soils. Soil Science Society of America Proceedings, Vol. 23, No. 2, 1959. p 113-116.
84. Torres, A.J.J. An Analysis of Using Pan Evaporation Data for Estimating Potential Evapotranspiration. Technical Report, Colorado State University, Fort Collins, Colorado, 1975. 46 pp.
85. U.S. Salinity Laboratory. Diagnosis and Improvement of Saline and Alkali Soils. USDA. Agriculture Handbook No. 60, 1969. 160 pp.
86. van Bavel, C.H.M. Potential Evaporation: The Combination Concept and Its Experimental Verification. Water Resources Research, Vol. 2(3), 1966. p 455-467.

87. van Bavel, C.H.M., P.R. Nixon, and V.L. Hauser. Soil Moisture Measurement with the Neutron Method. United States Department of Agriculture, ARS. ARS-41-70, June, 1963. 39 pp.
88. van der Molen, W.H. Desalinization of Saline Soils as a Column Process. Soil Science, Vol. 81, No. 1, January, 1956. p 19-27.
89. van der Ploeg, R.R. and P. Benecke. Unsteady, Unsaturated, N-dimensional Moisture Flow in Soils: A Computer Simulation Program. Soil Science Society of America Proceedings, Vol. 38, No. 6, November-December, 1974. p 881-885.
90. Wang, F.C. and V. Lakshminarayana. Mathematical Simulation of Water Movement through Unsaturated Nonhomogeneous Soils. Soil Science Society of America Proceedings, Vol. 32, No. 3, May-June, 1968. p 329-334.
91. Warrick, A.W., J.W. Biggar, and D.R. Nielsen. Simultaneous Solute and Water Transfer for an Unsaturated Soil. Water Resources Research, Vol. 7, No. 5, October, 1971. p 1216-1225.
92. Whisler, F.D. and A. Klute. The Numerical Analysis of Infiltration Considering Hysteresis into a Vertical Soil Column at Equilibrium under Gravity. Soil Science Society of America Proceedings, Vol. 29, No. 5, September-October, 1965. p 489-494.
93. Willardson, L.S. and R.J. Hanks. Irrigation Management Affecting Quality and Quantity of Return Flow. EPA-600/2-76-226. U.S. Environmental Protection Agency, Ada, Oklahoma, 1976. 191 pp.

APPENDIX A
SOIL PROPERTIES AND EVAPOTRANSPIRATION DATA

TABLE A-1. SOIL PROPERTIES FOR BILLINGS SILTY CLAY LOAM, MATCHETT FARM
SOIL MOISTURE CHARACTERISTIC

$P_c/\rho g$ (cm water)	θ volume	S	Se
28	44	0.98	0.95
59	41	0.91	0.80
114	33.3	0.73	0.41
332	30.6	0.68	0.31
504	28.0	0.62	0.18
800	26.6	0.62	0.13

Bulk Density = 1.64 gm/cc

Saturated Moisture Content $\theta_s = 0.45$

Empirical Parameters

Brooks and Corey

$$\lambda = 0.651$$

$$S_r = 0.538$$

$$P_b/\rho g = 41.0 \text{ cm water}$$

Su and Brooks

$$P_i/\rho g = 96 \text{ cm water}$$

$$a = 0.24$$

$$b = 0.222$$

$$m = 0.428$$

TABLE A-2. INITIAL SOIL MOISTURE DISTRIBUTION USED FOR SIMULATIONS

Depth (cm)	θ (vol)	Depth (cm)	θ (vol)
0.0	0.19	122.0	0.35
15.2	0.19	137.2	0.33
30.5	0.28	152.5	0.32
45.7	0.33	167.7	0.33
61.0	0.33	183.0	0.34
76.2	0.33	198.2	0.34
91.5	0.34	213.5	0.36
106.7	0.35		

TABLE A-3. EQUATIONS USED TO CALCULATE EVAPOTRANSPIRATION

From - Scheduling Irrigations Using a Programmable Calculator -
ARS-NC-12, February 1974, ARS-USDA

Polynomial Constants for Crop Curves

K_{co} - crop coefficient

$$K_{co} = Ar^3 + Br^2 + Cr + D$$

Corn	$A = -1.583$	} Before effective cover r = fraction time from planting to effective cover
	$B = 2.756$	
	$C = -0.4276$	
	$D = 0.213$	

Corn	$A = 275 \times 10^{-8}$	} After effective cover r = number of days beyond effective cover date
	$B = 4688 \times 10^{-7}$	
	$C = 9.0$	
	$D = 0.915$	

$$K_s = \frac{\log[1 + 100(1 - D_p/D_t)]}{\log(101)}$$

D_p = soil water depletion

D_t = total available water in root zone at field capacity

$$D_{pi} = D_{pi-1} + K_c E_{tp} + E_{tr} - R_i$$

$$K_c + K_{co} K_s$$

K_s = adjusted E_t for losses due to surface evaporation

$$E_{tr} = K_r(0.9 - K_c)E_{tp}$$

$K_r = 0.8$ first day	} Follow irrigation or rainfall
0.5 second day	
0.3 third day	

$K_c = 0.9$ or more for 3 days after irrigation $E_{tr} = 0$

E_{tp} = potential evapotranspiration computed using Penman formula

R_i = rainfall

TABLE A-4. IRRIGATION SCHEDULE FOR THE CORN CROP USED IN THE SIMULATION
14-DAY IRRIGATION SCHEDULE AND 7-DAY IRRIGATION SCHEDULE

14-DAY IRRIGATION SCHEDULE								
Date	Julian Day	Dp (cm)	Dp plus Leaching Increment (cm)					
			1%	2%	5%	10%	20%	40%
5/24	144	6.60	6.67	6.73	6.93	7.26	7.29	9.24
6/07	158	2.62	2.65	2.67	2.75	2.88	3.14	3.67
6/21	172	3.81	3.85	3.89	4.00	4.19	4.57	5.33
7/05	186	5.72	5.78	5.83	6.01	6.29	6.86	8.01
7/19	200	6.86	6.93	7.00	7.20	7.55	8.23	9.60
8/02	214	7.44	7.51	7.59	7.81	8.18	8.93	10.42
8/16	228	8.86	8.95	9.04	9.30	9.75	10.63	12.40
8/30	242	8.86	8.95	9.04	9.30	9.75	10.63	12.40
9/13	256	7.49	7.56	7.64	7.86	8.24	8.99	10.49
9/27	270	6.38	6.44	6.51	6.70	7.02	7.66	8.93
10/11	284	5.16	5.21	5.26	5.42	5.68	6.19	7.22

7-DAY IRRIGATION SCHEDULE								
Date	Julian Day	Dp (cm)	Dp plus Leaching Increment (cm)					
			1%	2%	5%	10%	20%	40%
5/24	144	6.60	6.67	6.73	6.93	7.26	7.92	9.24
5/31	151	1.70	1.72	1.73	1.78	1.87	2.04	2.38
6/07	158	2.13	2.45	2.17	2.24	2.34	2.56	2.98
6/14	165	2.03	2.05	2.07	4.12	2.23	2.44	2.84
6/21	172	2.48	2.50	2.50	2.60	2.73	2.98	3.47
6/28	179	3.12	3.15	3.18	3.28	3.43	3.74	4.37
7/05	186	3.40	3.43	3.47	3.57	3.74	4.08	4.76
7/12	193	3.71	3.75	3.82	3.90	4.08	4.45	5.19
7/19	200	3.78	3.82	3.86	3.97	4.16	4.54	5.29
8/02	214	4.24	4.28	4.32	4.45	4.66	5.09	5.94
8/09	221	5.00	5.05	5.10	5.25	5.50	6.00	7.00
8/16	228	4.39	4.43	4.48	4.61	4.83	5.27	6.15
8/23	235	4.62	4.67	4.71	4.85	5.08	5.54	6.47
8/30	242	4.80	4.85	4.90	5.04	4.28	5.70	6.72
9/09	249	4.04	4.08	4.12	4.24	4.44	4.85	5.66
9/13	256	3.78	3.82	3.86	3.97	4.16	4.54	5.29
9/20	263	3.48	3.51	3.55	3.65	3.83	4.18	4.87
9/27	270	3.15	3.18	3.21	3.31	3.46	3.78	4.41
10/04	277	2.89	2.92	2.95	3.03	3.18	3.47	4.05
10/11	284	2.44	2.46	2.50	2.56	2.68	2.93	3.42

Corn planted May 24, 1975.

APPENDIX B
SIMULATED DATA

TABLE B-1. SIMULATION DATA FOR PLOT 23, MATCHETT FARM WITH $P_{CO_2} = 7 \text{ matm}$
DAY 166-196, 1975

Concentrations computed at a depth of 1.1 meters							
Julian Date	Ca ppm	Na ppm	Mg ppm	HCO ₃ ppm	Cl ppm	SO ₄ ppm	TDS ppm
166	915	60	100	123	333	1938	3469
168	790	58	72	111	339	1529	2919
170	785	61	72	113	345	1557	2942
172	739	120	71	119	429	1687	3165
174	736	132	71	120	450	1701	3210
176	737	209	77	122	491	1761	3397
178	738	216	77	122	487	1867	3407
180	740	220	78	123	490	1770	3421
182	741	222	78	123	494	1769	3427
184	742	223	78	123	496	1768	3430
186	744	225	78	123	500	1771	3441
188	745	227	79	123	505	1771	3450
190	747	226	79	122	510	1767	3451
192	739	225	78	123	497	1760	3422
194	746	243	81	123	488	1792	3472
196	747	249	81	123	484	1795	2379

TABLE B-2. SIMULATION DATA FOR PLOT 23, MATCHETT FARM, DAY 166-196, 1975.

Concentrations computed at a depth of 1.1 meters							
Julian Date	Ca ppm	Na ppm	Mg ppm	HCO ₃ ppm	Cl ppm	SO ₄ ppm	TDS ppm
166	975	60	101	304	333	1938	3711
168	820	57	75	290	338	1521	3113
170	826	61	75	296	345	1526	3129
172	771	121	73	275	429	1656	3325
174	772	134	74	292	450	1665	3387
176	769	212	79	282	491	1725	3558
178	773	220	80	299	487	1727	3586
180	776	224	81	309	490	1730	3610
182	779	227	81	316	494	1727	3624
184	781	227	82	322	496	1727	3625
186	784	229	82	326	500	1727	3648
188	786	231	82	332	505	1726	3662
190	786	231	83	336	510	1721	3667
192	779	229	81	329	497	1718	3633
194	779	247	83	293	488	1755	3624
196	781	253	84	303	484	1756	3661

TABLE B-3. TDS CONCENTRATIONS AND CHLORIDE CONCENTRATIONS IN CUMULATIVE LEACHATE AT 2.13 m FOR HYPOTHETICAL SIMULATION USING 7-DAY IRRIGATION SCHEDULE

2% LEACHING INCREMENT					
Julian Date	Cumulative Infiltration (cm)	Cumulative Leachate (cm)	Cl ppm	TDS ppm	TDS-Cl ppm
157	9.36	3.86	260	3256	2996
171	13.59	5.66	278	3296	3018
185	18.79	6.54	290	3318	3028
199	26.59	7.05	297	3332	3035
213	34.19	7.37	301	3338	3037
227	43.40	7.60	305	3351	3046
241	52.63	7.76	307	3355	3048
255	61.72	7.90	310	3356	3046
269	69.12	8.01	313	3357	3044
283	76.72	8.10	315	3362	3047
293	80.32	8.17	312	3357	3045
5% LEACHING INCREMENT					
Julian Date	Cumulative Infiltration (cm)	Cumulative Leachate (cm)	Cl ppm	TDS ppm	TDS-Cl ppm
157	9.60	4.08	262	3254	2992
171	14.00	5.89	280	3295	3015
185	19.19	6.82	291	3320	3029
199	27.23	7.35	299	3334	3035
213	35.11	7.67	303	3344	3041
227	44.77	7.92	306	3350	3044
241	54.25	8.11	311	3358	3047
255	63.55	8.29	310	3357	3047
269	74.14	8.53	308	3360	3050
283	77.90	8.91	302	3350	3048
293	81.58	9.19	304	3354	3050

(continued)

TABLE B-3. (continued)

20% LEACHING INCREMENT					
Julian Date	Cumulative Infiltration (cm)	Cumulative Leachate (cm)	Cl ppm	TDS ppm	TDS-Cl ppm
157	10.61	5.02	269	3276	3007
171	15.63	7.26	284	3320	3036
185	22.36	8.54	300	3349	3049
199	30.82	9.18	309	3373	3064
213	39.87	9.91	305	3375	3070
227	51.09	11.27	303	3385	3082
241	61.61	13.01	312	3411	3099
255	72.35	14.83	315	3424	3109
269	81.19	16.66	327	3446	3119
283	88.43	18.26	336	3471	3135
293	91.46	19.25	343	3467	3124
40% LEACHING INCREMENT					
Julian Date	Cumulative Infiltration (cm)	Cumulative Leachate (cm)	Cl ppm	TDS ppm	TDS-Cl ppm
157	12.40	6.23	278	3296	3018
171	17.98	8.90	295	3344	3049
185	26.12	10.32	311	3385	3074
199	36.04	12.34	306	3404	3098
213	46.47	15.24	317	3424	3107
227	59.42	18.52	326	3441	3115
241	72.14	22.25	346	3468	3122
255	84.44	25.97	373	3480	3107
269	94.83	29.18	400	3492	3092
283	103.41	32.07	429	3512	3083
293	107.40	33.76	447	3527	3080

TABLE B-4. TDS CONCENTRATIONS AND CHLORIDE CONCENTRATIONS IN CUMULATIVE LEACHATE AT 2.13 m FOR HYPOTHETICAL SIMULATION USING 14-DAY IRRIGATION SCHEDULE

2% LEACHING INCREMENT					
Julian Date	Cumulative Infiltration (cm)	Cumulative Leachate (cm)	Cl ppm	TDS ppm	TDS-Cl ppm
157	7.09	3.87	260	3256	2996
171	9.85	5.51	279	3291	3012
185	13.56	6.30	288	3314	3026
199	19.48	6.77	296	3328	3032
213	26.58	7.07	299	3338	3039
227	34.07	7.29	303	3343	3040
241	43.10	7.45	308	3354	3046
255	52.15	7.58	310	3356	3046
269	59.83	7.69	312	3362	3050
283	66.42	7.78	313	3366	3053
293	71.51	7.84	314	3368	3054
5% LEACHING INCREMENT					
Julian Date	Cumulative Infiltration (cm)	Cumulative Leachate (cm)	Cl ppm	TDS ppm	TDS-Cl ppm
157	7.74	4.46	264	3264	3000
171	10.54	6.13	284	3006	3022
185	14.41	6.93	294	3324	3030
199	20.49	7.40	300	3342	3042
213	27.62	7.70	306	3352	3046
227	35.45	7.92	309	3362	3053
241	44.78	8.09	311	3361	3050
255	54.07	8.24	313	3370	3057
269	61.93	8.39	313	3374	3061
283	68.67	8.65	307	3361	3054
293	74.10	8.95	303	3361	3058

(continued)

TABLE B-4. (continued)

20% LEACHING INCREMENT					
Julian Date	Cumulative Infiltration (cm)	Cumulative Leachate (cm)	Cl ppm	TDS ppm	TDS-Cl ppm
157	8.33	5.02	269	3276	3007
171	11.45	6.70	290	3318	3028
185	16.46	7.48	298	3336	3038
199	23.50	8.05	302	3352	3050
213	31.64	8.92	297	3352	3055
227	40.55	10.10	299	3365	3066
241	51.25	11.93	302	3391	3089
255	60.49	12.86	317	3416	3099
269	68.36	13.66	323	3432	3109
283	75.11	14.31	327	3444	3117
293	80.55	14.75	327	3444	3117
40% LEACHING INCREMENT					
Julian Date	Cumulative Infiltration (cm)	Cumulative Leachate (cm)	Cl ppm	TDS ppm	TDS-Cl ppm
157	9.52	6.16	278	3299	3021
171	13.22	8.00	297	3344	3047
185	18.60	9.23	304	3367	3063
199	26.64	10.93	303	3383	3080
213	36.15	13.47	312	3407	3095
227	46.59	16.22	323	3445	3122
241	59.04	19.79	343	3470	3127
255	71.49	23.44	364	3496	3132
269	82.00	26.64	388	3508	3120
283	90.94	29.38	409	3508	3099
293	98.14	30.94	420	3520	3100

TABLE B-5. CHLORIDE CONCENTRATION PROFILES (ppm) FOR HYPOTHETICAL SIMULATIONS USING 14-DAY IRRIGATION SCHEDULE

2% LEACHING INCREMENT					20% LEACHING INCREMENT					40% LEACHING INCREMENT				
Depth (cm)	Day 157	Day 199	Day 255	Day 293	Depth (cm)	Day 157	Day 199	Day 255	Day 293	Depth (cm)	Day 157	Day 199	Day 255	Day 293
15	195	146	111	96	15	161	122	105	88	15	145	110	100	82
30	302	239	155	108	30	282	188	131	97	30	256	155	117	92
46	525	439	211	149	46	482	332	151	118	46	439	252	125	104
61	659	730	435	277	61	621	669	241	162	61	587	433	161	124
76	578	787	767	547	76	582	699	403	246	76	579	587	226	151
91	510	727	1108	1012	91	522	724	665	439	91	532	675	358	213
107	411	508	903	1061	107	432	583	786	645	107	448	614	493	302
122	360	426	670	869	122	374	480	791	796	122	388	533	618	433
137	345	359	347	409	137	351	375	597	712	137	356	422	613	519
152	346	350	347	347	152	348	351	460	575	152	349	373	564	560
168	344	344	345	341	168	343	344	389	463	168	344	354	499	556
183	334	338	338	336	183	335	337	355	396	183	337	343	436	578
198	287	308	312	312	198	296	312	336	358	198	303	325	392	467
213	260	296	310	314	213	267	302	317	327	213	279	303	364	420

TABLE B-6. CHLORIDE CONCENTRATION PROFILES (ppm) FOR HYPOTHETICAL SIMULATIONS USING 7-DAY IRRIGATION SCHEDULE

2% LEACHING INCREMENT					20% LEACHING INCREMENT					40% LEACHING INCREMENT				
Depth (cm)	Day 157	Day 199	Day 255	Day 293	Depth (cm)	Day 157	Day 199	Day 255	Day 293	Depth (cm)	Day 157	Day 199	Day 255	Day 293
15	150	97	101	71	15	130	94	97	83	15	112	94	93	71
30	270	152	116	87	30	246	119	104	85	30	214	104	94	78
46	480	306	157	116	46	440	215	123	102	46	381	156	108	84
61	643	601	312	201	61	604	427	176	145	61	546	288	132	105
76	596	768	623	401	76	596	624	290	217	76	583	459	169	134
91	528	774	1052	814	91	540	734	532	392	91	550	616	260	186
107	422	539	956	1035	107	441	627	723	602	107	464	630	383	260
122	366	438	719	972	122	380	513	803	787	122	397	576	534	377
137	345	363	348	553	137	349	383	634	724	137	358	459	583	467
152	347	349	348	379	152	346	351	485	600	152	349	390	571	529
168	343	346	346	343	168	344	344	399	489	168	344	360	521	546
183	333	338	338	330	183	335	340	361	411	183	337	345	462	526
198	287	309	313	308	198	296	318	359	368	198	304	328	410	486
213	360	297	310	312	213	270	309	315	343	213	278	300	374	447

TABLE B-7. CHLORIDE CONCENTRATION PROFILES (ppm) FOR DAY 293 OF SECOND YEAR IN A 2-YEAR HYPOTHETICAL SIMULATION USING 20% LEACHING INCREMENT AND 14-DAY IRRIGATION SCHEDULE

Depth (cm)	No Winter Precipitation	With Winter Precipitation
15	88	88
30	98	98
46	117	117
61	148	145
76	179	166
91	229	188
107	284	193
122	401	227
137	494	262
152	573	326
168	620	406
183	621	483
198	584	540
213	527	564

TABLE B-8. TDS CONCENTRATION PROFILES (ppm) FOR 6-YEAR SIMULATION

Depth (cm)	Day 293	
	Year 1	Year 6
15	569	567
30	615	595
46	999	668
61	3638	790
76	3932	898
91	4166	1071
107	3922	3224
122	3734	3598
137	3396	3554
152	3320	3445
168	3395	3384
183	3390	3347
198	3469	3371
213	3444	3418

APPENDIX C
ANALYSIS OF FIELD DATA

TABLE C-1. CHEMICAL ANALYSIS OF SOIL SOLUTION EXTRACTED AT A DEPTH OF 1.1 METERS IN PLOT 23 ON THE MATCHETT FARM IN 1975

Julian Date	Ca ppm	Mg ppm	Na ppm	SO ₄ ppm	HCO ₃ ppm	Cl ppm	TDS ppm
169	647	106	250	1788	416	309	3516
171	674	89	185	1519	466	285	3218
172	656	111	263	1704	370	346	3450
174	627	86	163	1488	365	254	2983
176	620	101	174	1224	398	397	3217
180	601	113	262	1613	313	296	3198
185	629	84	162	1548	342	229	2994
191	616	96	176	1508	374	259	3250
197	593	102	203	1533	379	303	3597

TABLE C-2. pH ANALYSIS OF DRAINAGE WATER SAMPLES COLLECTED ON MATCHETT FARM, 1975

Julian Day	pCa	pMg	pSO ₄	pHCO ₃	pCO ₃	pCaCO ₃	pMgCO ₃	pCaSO ₄
<u>Plot 28</u>								
196	2.2822	2.7691	2.3805	2.1250	4.8540	7.1363	7.6232	4.6628
210	2.3389	2.8546	2.3324	2.2724	5.1014	7.4404	7.9561	4.6713
<u>Plot 29</u>								
196	2.2904	2.7415	2.3636	2.0538	4.7828	7.0732	7.5243	4.6541
196	2.2873	2.7156	2.3880	2.0051	4.8341	7.1215	7.5497	4.6754
<u>Plot 33</u>								
206	2.3074	2.6079	2.3235	2.2234	5.4524	7.7599	8.0603	4.6309
220	2.3628	2.6516	2.1795	2.8410	5.6700	8.0329	8.3217	4.5424
<u>Plot 34</u>								
208	2.3459	2.6186	2.2470	2.2686	5.0976	7.4435	7.7162	4.5929
211	2.3585	2.5781	2.3007	2.2639	5.1929	7.5514	7.7711	4.6592
212	2.3562	2.5880	2.2850	2.2713	5.1003	7.4566	7.6884	4.6412
216	2.3863	2.6090	2.2651	2.2790	5.3080	7.6943	7.9170	4.6515
220	2.3334	3.3693	2.2687	2.9293	5.9583	8.2918	9.3277	4.6022
<u>Plot 35</u>								
205	2.3627	2.6741	2.3054	2.2602	5.0892	7.4519	7.7633	4.6681
213	2.3330	2.7642	2.2879	2.3063	5.3353	7.6683	8.0995	4.6209
230	2.3429	2.7048	2.2813	2.2852	5.4142	7.7572	8.1191	4.6242
252	2.3622	2.7450	2.3407	2.2176	5.0466	7.4089	7.7917	4.7030

APPENDIX D

LISTING OF PROGRAM SORPT

PROGRAM SORPT

```

PROGRAM SORPT (INPUT,OUTPUT)
DIMENSION S(20),PC(20)
REAL L,L1
C
C * * DEFINITION OF SYMBOLES * * * * *
C
C S=SATURATION.
C PC=CAPILLARY PRESSURE.
C SR=RESIDUAL SATURATION.
C L=LAMBDA.
C R=SQUARE OF CORRELATION COEFFICIENT.
C PB=BUBBLING PRESSURE.
C E=ETA.
C RK=RELATIVE PERMEABILITY.
C FPC=(PB/PC)*L
C * * * * *
C
PRINT 1
1  FORMAT(1H1,/)
  READ 2,NP
2  FORMAT (I2)
100 READ 3,ION,N
3  FORMAT (15,15)
  DO 4 I=1,N
  READ 5,S(I),PC(I)
4  CONTINUE
5  FORMAT(2F10,4)
C
C FIRST ESTIMATION OF RESIDUAL SATURATION ASSUMING LAMBDA IS 2.
C
PC1=PC(1)
PC2=PC(2)
S1=S(1)
S2=S(2)
FPC1=(1./PC1)*(1./PC1)
FPC2=(1./PC2)*(1./PC2)
SR=(FPC2*S1-FPC1*S2)/(FPC2-FPC1)
IF(SR .LT. 0.0) SR=0.
PRINT101,SR
101 FORMAT(*FIRST SR CHECK=*,F10,4)
C
C NEXT ESTIMATION OF LAMBDA USING ESTIMATED RESIDUAL SATURATION.
C
PCL1=ALOG(PC1)
PCLN=ALOG(PC(N))
SEL1=ALOG((S(1)-SR)/(1.-SR))
SELN=ALOG((S(N)-SR)/(1.-SR))
L=-(SELN-SEL1)/(PCLN-PCL1)
J=0
K=0
DL=0.1
JR=0
R1=0.
R2=0.
R3=0.
SS=0.
SS2=0.
DO 6 I=1,N
SI=S(I)
SS=SS+SI
SS2=SS2+SI*SI
PRINT 102,L
6  CONTINUE
C
C CALCULATION OF CORRELATION COEFFICIENT.
C
7  CONTINUE
102 FORMAT(*FIRST CHECK ON L*,F10,4)

```

```

      SFPC=0.
      SPS=0.
      SFPC2=0.
      DO 8 I=1,N
      FPCI=(1./PC(I))*L
      SFPC=SFPC+FPCI
      SFPC2=SFPC2+FPCI*FPCI
      SPS=SPS+FPCI*S(I)
8     CONTINUE
      R=(SPS-SFPC*SS/N)**2/(SS2-SS*SS/N)/(SFPC2-SFPC*SFPC/N)
C
C     FIND BEST FIT LAMRDA.
C
      IF(JR.EQ. 1) P1=R
      IF(JR.EQ. 3) P3=R
      IF(K.EQ. 2) GO TO 22
      IF(R3.NE. 0.) GO TO 15
      IF(R2.NE. 0.) GO TO 13
      R2=R
      L1=L
      L=L1-OL
      GO TO 7
13     IF(R1.NE. 0.) GO TO 14
      R1=R
      L=L1+OL
      GO TO 7
14     R3=R
15     IF((R2-R1)*(R2-R3).LE. 0.0) GO TO 18
      GO TO 16
18     IF(R1.GT. R3) GO TO 19
      GO TO 20
19     R3=R2
      R2=R1
      JR=1
      L1=L1-OL
      L=L1-OL
      GO TO 7
20     R1=R2
      R2=R3
      JR=3
      L1=L1+OL
      L=L1+OL
      GO TO 7
16     C=(R1+R3-2.*R2)/(2.*OL*OL)
      B=(R3-R2-C*OL*OL)/OL
      L=L1
      L=L-R/(2.*C)
      OL=OL/10.
      R1=0.
      R2=0.
      R3=0.
      JR=0
      K=K+1
      GO TO 7
C
C     FIND BEST RESIDUAL SATURATION AND BUBBLING PRESSURE.
C
22     R=(SPS-SS*SFPC/N)/(SS2-SS*SS/N)
      PRINT 103,SS
      PRINT 104,N
      PRINT 105,SFPC
      PRINT 106,R
103    FORMAT(*SS=*,F10.5)
104    FORMAT(*N=*,F10.5)
105    FORMAT(*SFPC=*,F10.5)
106    FORMAT(*R=*,F10.5)
      SR=SS/N-SFPC/N/B
      PR=1./(R-SFPC/N-B*SS/N)**(1./L)
C
C     FIND ETA.
C

```

```

E=3.*L+2.
PRINT 31,IDN
31  FORMAT(1H ,* NR  *.I5,///)
    PRINT 32
32  FORMAT(1H ,20X,*S*,20X,*PC*,20X,*KR*,20X,*FPC*,//)
C
C  FIND RELATIVE PERMEABILITY AND FPC.
C
DO 33 I=1,N
WK=((S(I)-SR)/(1.-SR))*E/L
FPC=(PR/PC(I))*L
PRINT 34,S(I),PC(I),RK,FPC
33  CONTINUE
34  FORMAT(11X,F10.4,12X,F10.4,12X,E15.4,10X,F10.4,/)
    PRINT 35,E,L,SR,PR,R
35  FORMAT(///,10X,*ETA= *.F10.3,9X,*LAMBDA= *.F10.3,10X,*SR= *.F10.4,
110X,*PR= *.F10.2,///,10X,*CORRELATION= *.E16.6,////////)
    NR=NR+1
    IF(NR .NE. 0) GO TO 100
    STOP
END

```


APPENDIX E LISTING OF BIOLOGICAL-CHEMICAL PROGRAM **PROGRAM MOISTRE**

```

PROGRAM MOISTRE
  1(INPUT,OUTPUT,PUNCH,TAPE5,TAPE10)
C*****VERSION FOR U.S.B.R., APRIL 20,1971.
C***** MODIFIED FOR GARRISON DIVERSION UNIT MAR. 10, 1972          $$$$$$$$2
C***** MODIFIED FOR CYBER 70-28, MAY 2,1974
C***** MODIFIED TO CONFORM TO DOCUMENTATION, JAN. 13,1975          DOC
      DIMENSION HOR(4),Z(60),MON(50),DATE(50),AMT(50),TME(50),SF(60),
      2TO(60),TN(60),FN(60),ANT(60),K(60),O(60),S(60),E(60),F(60),U(60),
      3UH(366),KP3(6),TH(60),ADENT(50)
      DIMENSION AID(8)
      COMMON/PROP/KSAT,DSAT,C1,C2,C3,C4,TS ,TPB,SR          *****1
      COMMON/PROP1/OTS,DDSAT          MOD      1
      COMMON/PROP2/BET,ALP,AIRINF,ALM,EMP
      COMMON/XYZ/IDTE,MONTH,UH,KP3
      COMMON/CHK/ICHECK,ICROP
      COMMON/AJST/Q
      INTEGER O,P1,P2,Q,APPS,DATE,YEAR, DAY,CROP,TME,AA,9B,CC,ADENT,
  1START
      REAL K,IR,KP3,KSATD,KSAT          MOD      1
C-----READ PRINT OPTIONS, RUN PARAMETERS, WATER APPLICATIONS, PROFILE DATA
      READ 9156, IPUNCH,IRESTR,ISAVE,ITENTH,INFIL5,LLSTRT,MMSTOP,ISTOP, $$$$$$$$1
      1IDEF,FCAP,IPOPT,ICROP
      READ 100,AA,9B,CC,LL,MM,BBC,TBC,YEAR, CROP,M,      DELX,TS,TM,TD,SMDOC
C---- READ SOILS DATA FOR COMPUTING HYDRAULIC PROPERTIES, COMPUTE          MOD      1
C---- CONSTANTS          MOD      1
      IF(IPOPT.EQ.1) CALL CHAR          MOD      1
      IF(IPOPT.NE.1) CALL ACHAR
      READ 9861, ICODE,IYEAR,APPS,(AID(I),I=1,8)          *****1
      9861 FORMAT(I5,I5,I3,8A8)          *****1
      PRINT 9862, ICODE,IYEAR,APPS,(AID(I),I=1,8)          *****1
      9862 FORMAT(1H1,*ICODE= *,I2,* YEAR= *,I5,*APPS= *,I3,3X,8A8)          *****1
      PRINT 119          *****1
      READ 9863, (MON(I),DATE(I),ADENT(I),AMT(I),I=1,APPS)          *****1
      9863 FORMAT((10X,7(2I2,A1,F5.0)))          *****1
      PRINT 9864, (MON(I),DATE(I),AMT(I),ADENT(I),I=1,APPS)          *****1
      9864 FORMAT(30X,*DATE *,I2,*/,I2,7X,*AMOUNT=*,F6.2,* INCHES SOURCE=*,*****1
      1A1)          *****1
      READ 128,0
      READ 101,( IDENT,HOR(N),N=1,0)
C-----COMPUTATION OF TIME OF WATER APPLICATIONS
      START=0
      DO 29 L=1,APPS
      AMT(L)=AMT(L)*2.54          *****1
      29 TME(L)=DAY(DATE(L),START,MON(L))

C-----ESTABLISH MOISTURE DISTRIBUTION AND CONSTANTS
      DELTM=1./M
      CALL PROP(TS,TS,TD,KSATD,DSATD          //////////1
      DELT=DELTM
      Q=HOR(0)/DELX*1.1
      L=1
      G=DELX
C IF BBC EQUALS 0 THEN BBC IS TRANSIENT
      IF(BBC.EQ.1)BBC=TM
      IF(BBC.EQ.2)BBC=TS
      IF(TRC.EQ.1)TBC=TM
      IF(TBC.EQ.2)TBC=TS
      IR=1000.
      HED=CL=CHECK=ETS=ET=CI=FN(1)=DIF=CONST=0.0
      CL3=0.0
      CNA=CNI=DEFAMC=0.0          $$$$$$$$8
      X=10.*(-10.)
      TN(1)=TRC
      SF(1)=0.0
      DO 43 J=2,Q

```

```

      SF(J)=0.0
      TN(J)=SM
C      IF(J.EQ.Q)GO TO 43
C      TN(J+1)=SM
43    CONTINUE
      TN(Q)=RRC
      IF(CC.EQ.1) READ 9900, (TO(J),J=1,Q)
9900  FORMAT (AF10.5)
      DO 15 J=1,Q
      IF(CC.EQ.1)TN(J)=TO(J)
      TH(J)=TN(J)
15    CONTINUE
      DO 20 J=1,Q
      Z(J)=0.0
      IF(J.EQ.Q) TN(J+1)=TN(J)
      ANT(J)=TN(J)
20    CONTINUE
      DO 16 J=1,Q
16    CONST=CONST+TN(J)
      CONST=CONST-0.5*(TN(1)+TN(Q))

      IF(IRESTP.EQ.2) GO TO 8491
      IF(IRESTP.NE.1) GO TO 8493
C----- READ RESTART DATA FROM CARDS
      READ 9181,LYEAR,MONTH,IDTE,II,CL,CHECK,IR,L,HED
      READ 9182, CONST,CI,ETS,ET,CNA,CNI
      READ 9182, DEFAMC
      READ 9182, (TN(J),J=1,Q)
      READ 9182, (FN(J),J=1,Q)
      READ 9182, (ANT(J),J=1,Q)
      READ 9182, (Z(J),J=1,Q)
      GO TO 8492
C----- READ RESTART DATA FROM SAVED RESTART TAPE 10
8491  REWIND 10
      READ(10) LYEAR,MONTH,IDTE,II,CL,CHECK,IR,L,HED,CONST,CI,ETS,ET,
1    CNA,CNI,DEFAMC
      READ(10) (TN(J),J=1,Q)
      READ(10) (FN(J),J=1,Q)
      READ(10) (ANT(J),J=1,Q)
      READ(10) (Z(J),J=1,Q)
8492  PRINT 9155
      PRINT 9151,LYEAR,MONTH,IDTE,II,CL,CHECK,IR,L,HED,CONST,CI,ETS,ET,
1    CNA,CNI,DEFAMC
      PRINT 9152, (TN(J),J=1,Q)
      PRINT 9153, (FN(J),J=1,Q)
      PRINT 9154, (ANT(J),J=1,Q)
      PRINT 9172, (Z(J),J=1,Q)
8493  CONTINUE
      KFLAG=0
C----- POSITION TAPE 5 TO CORRECT POSITION FOR FIRST WRITE IF THIS IS A
C----- RESTART RUN AND UNIT 5 IS EQUIPED TO A SAVED MAG TAPE
      IF(IRESTR.EQ.1.AND.ISAVE.EQ.1) GO TO 8700
      IF(IRESTR.EQ.2.AND.ISAVE.EQ.1) GO TO 8700
      GO TO 8710
8700  REWIND 5
      IHI=INFIL5-1
      IF(IHI.LE.0) GO TO 8734
      DO 8733 I=1,IHI
      CALL SKIP(5)
8733  CONTINUE
8734  IF(ILL.EQ.LLSTRT) GO TO 8710
8701  DO 8705 I=1,10
      READ(5) IDUMY,KDAY
      IF(EOF(5))8800,8705
8705  CONTINUE
      IF(LLSTRT-KDAY-1)8802,8710,8701
C----- SET INDICES OF YEARLY LOOP
8710  ILG=LLSTRT
      IMI=MM
      IF(YEAR.EQ.ISTOP) IMI=MMSTOP
C-----DAYS WITHIN TOTAL RUN LENGTH LOOP
8700  DO 32 II=ILG,IMI

```

```

I=0
ICTDF=0
ICTDFD=0
DEFAM=0.0
DEFAMD=0.0
ISTCT=0
ISTCTD=0
XT=10.**(-10.)
CALL THEDATE(START,II)
C-----NOTE THAT THIS PROGRAM CAN ONLY BE RESTARTED ON FIRST OR SIXTEENTH.
IF(IDTE.F0.1.OR.IDTE.EQ.16.OR.KFLAG.EQ.0.OR.ICROP.EQ.3)11,8500
11 DO 3 J=1,Q
CALL CONUSE(CROP,DELX,J,U(J),II,ILO,IMI)
3 CONTINUE
U(2)=1.5*U(2)
IF(KFLAG.EQ.0) GO TO 8500
PRINT 9151, YEAR,MONTH,IDTE,II,CL,CHECK,IR,L,HED,CONST,CI,ETS,ET,
1 CNA,CNI,DEFAMC
PRINT 9152, (TN(J),J=1,Q)
PRINT 9153, (FN(J),J=1,Q)
PRINT 9154, (ANT(J),J=1,Q)
PRINT 9172, (Z(J),J=1,Q)
8500 IF(II.EQ.ILO) GO TO 10

C-----READ INITIAL DATA FOR NEW DAY FROM TAPE 4, EXCEPT ON DAY ONE
12 IF(II.EQ.1.AND.YEAR.EQ.1)GO TO 1
C BACKSPACE4
C READ(4)(TN(J),FN(J),CL,CHECK,IR,L,HED,ANT(J),J=1,Q)

C-----INITIALIZE HED AT START OF EACH DAY
1 IF(L.GT.APPS) GO TO 6330
IF(II.EQ.TME(L))30,34
6330 IF(HED.LT.0.01.AND.CNA.LE.0.05) GO TO 34
HED=HED+CNA
GO TO 6332
30 HED=HED+AMT(L)+CNA
6332 CNA=0.0
C IF(HED.LE.0.0)HED=AMT(L)
L=L+1
IR=100.
IR=1000.
PRINT 102,II,HED

C-----TIME INTERVALS WITHIN EACH DAY LOOP
34 DO 21 J=1,Q
21 TO(J)=TN(J)
C-----COMPUTE SIZE OF TIME INTERVAL, DELT
I=I+1
DELTO=DELT
IF(X.GE.0.1)X=10.**(-10.)
DELT=AMIN1(DELX*0.035/IR,DELTM)
IF(HED.GT.0.01.AND.KSATD*DELT.GT.HED) DELT=HED/KSATD
IR=10.**(-10.)
IF(X+DELT.LE.0.1)GO TO 4
DELT=0.1-X
4 CONTINUE
X=X+DELT
XT=XT+DELT+10.**(-10.)
Y=0.7

C-----EXAMINE UPPER BOUNDARY CONDITIONS
IF(HED.GT.0.01) GO TO 17

C-----NOTE--FIRST OF TWO PLACES STATEMENT FUNCTIONS ARE REFERENCED.
ZKCON=(TO(1)+TO(2))/2.
IF(IPOPT.NE.1) GO TO 670
CALL PROP (ANT(1),TN(1),TD,K(1),D(1))
CALL PROP (ANT(2),TN(2),TD,K(2),D(2))
K(1)=(K(1)+K(2))/2.
CALL ADIF(ANT(1),ANT(2),D(1))
GO TO 668
670 CALL APROP(ANT(1),ZKCON,TD,K(1),D(1))
668 CONTINUE
E(1)=1.0

```

```

        IF(D(1).LE.0.0)666,667
666  F(1)=0.0
      GO TO 18
667  F(1)=-K(1)*DELX/D(1)
      GO TO 18
17   TN(1)=TAC
      E(1)=0.0
      F(1)=TAC
      ZKCON=(TO(1)+TO(2))/2.
      IF(IPOPT.NE.1) GO TO 671
      CALL PROP (ANT(1),TN(1),TD,K(1),D(1))
      CALL PROP (ANT(2),TN(2),TD,K(2),D(2))
      K(1)=(K(1)+K(2))/2.
      CALL ADIF(ANT(1),ANT(2),D(1))
      GO TO 672
671  CALL APROP(ANT(1),ZKCON,TD,K(1),D(1))
672  CONTINUE

```

DOC
DOC
*****1

```

C-----COMPUTE E AND F FOR EACH NODE(J) FROM SURFACE TO DRAIN
18   N=1
      P1=2
      P2=HOR(N)/DELX+1.
35   DO 5 J=P1,P2
      S(J)=U(J)*DELT/DELX
      IF(J.EQ.0) TO(J+1)=TO(J)
C-----NOTE--SECOND OF TWO PLACES STATEMENT FUNCTIONS ARE REFERENCED.
      ZKCON=(TO(J)+TO(J+1))/2.
      IF(IPOPT.NE.1) GO TO 673
      CALL PROP (ANT(J),TN(J),TD,K(J),D(J))
      CALL PROP(ANT(J+1),TN(J+1),TD,K(J+1),D(J+1))
      K(J)=(K(J)+K(J+1))/2.
      CALL ADIF(ANT(J),ANT(J+1),D(J))
      GO TO 674
673  CALL APROP(ANT(J),ZKCON,TD,K(J),D(J))
674  CONTINUE
      A=(DELT*D(J))/(2.*DELX**2)
      C=(DELT*D(J-1))/(2.*DELX**2)
      B=1.+A+C
      W=A*TO(J+1)+(1.-A-C)*TO(J)+C*TO(J-1)+(K(J-1)-K(J))*2.*G*
1DELT/(2.*DELX**2)
      IF(TO(J)-S(J).GT.TD)GO TO 75
      ICTDF=ICTDF+1
      DEF=(TD-(TO(J)-S(J)))*DELX
      DEFAM=DEFAM+DEF
      DEFAMC=DEFAMC+DEF
      S(J)=TO(J)-TD
      W=W-S(J)
      Z(J)=Z(J)+(U(J)*DELT-S(J)*DELX)
      GO TO 76
75   W=W-S(J)
76   ET=ET+S(J)*DELX
      E(J)=A/(R-C*F(J-1))
      F(J)=(W+C*F(J-1))/(R-C*E(J-1))
5   CONTINUE
      IF(N.GE.0)GO TO 8
      N=N+1
      P1=P2+1
      P2=HOR(N)/DELX+1.
      GO TO 35

```

*****1

\$\$\$\$\$\$\$\$
\$\$\$\$\$\$\$\$
\$\$\$\$\$\$\$\$
\$\$\$\$\$\$\$\$

```

C-----COMPUTE THETA AND FLUX FOR EACH NODE(J) FROM DRAIN TO SURFACE
8   J=Q
      TN(J)=E(J)*TO(J+1)+F(J)
      TN(J+1)=TN(J)
      ANT(J)=TN(J)+Y*(TN(J)-TO(J))
      IF(ANT(J).GT.TS)ANT(J)=TS
      IF(ANT(J).LT.TD)ANT(J)=TD
      ANT(J+1)=ANT(J)
      IF(BRC.EQ.TS) TN(Q)=TS
      IF(BBC.EQ.TM) TN(Q)=TM
      J=Q-1

```

```

48  TN(J)=E(J)*TN(J+1)+F(J)
    ANT(J)=TN(J)+Y*(TN(J)-TO(J))
    IF(ANT(J).GT.TS) ANT(J)=TS
    IF(ANT(J).LT.TO) ANT(J)=TO
    FN(J)=(K(J)-(D(J)*(TN(J+1)+TO(J+1)-TN(J)-TO(J))/(2.*DELX)))*DELT
    FR=FN(J)/DELT
    FR=ABS(FR)
    IR=AMAX1(IR,FR)
    SF(J)=SF(J)+FN(J)
    IF(TN(J).LT.0.0.OR.TN(J).GT.TS) ISTCT=ISTCT+1
    J=J-1
    IF(J.GT.0) GO TO 48
    CL=CL+FN(Q-1)
    IF(Q.GE.7) CL3=CL3+FN(7)
    ETS=ETS+FN(1)
    IF(FN(1).LE.0.0.AND.HED.LE.0.01) GO TO 8793
    CI=CI+FN(1)
    HED=HED-FN(1)
C    IF(HED.LE.0.0) HED=0.0
    GO TO 23
8793 CNI=CNI-FN(1)
    CNA=CNA-FN(1)
    GO TO 23
23  CONTINUE

C-----WRITE ON TAPE 5 OR PRINT THETA AND FLUX AT 0.1 DAY INTERVALS
    IF(X.LT.0.1) GO TO 2
    WRITE(5) YEAR,II,XT,CI,CL,HED,ETS,DEFAMC,(J,TN(J),Z(J),SF(J),
1  U(J),J=1,Q)
    IF(ITENTH.NE.1) GO TO 8712
    PRINT 103
    PRINT 121,YEAR,II,XT,MONTH,IDTE,CL,CHECK,ETS,ET,DIF,CNA,CNI,HED,
1  CI,DEFAMC,I
    PRINT 105,(TN(J),J=1,Q)
    PRINT 9161,CL3
9161 FORMAT(4X,*CL AT 3.5 FEET THIS TENTH DAY*,F10.3)
    IF(ISTCT.NE.0) PRINT 9166,ISTCT
9166 FORMAT (10X,*UNSTABLE SOLUTION SITUATION ENCOUNTERED *, I8, * TIME
1ES THIS TENTH DAY*)
    IF(ICTDF.NE.0) PRINT 9170, ICTDF,DEFAM
9170 FORMAT (10X, *DEFICIT MOISTURE SITUATION ENCOUNTERED *, I8, * TIME
1S THIS TENTH DAY. AMOUNT IS *, F6.2, * CM*)
8712 CONTINUE
    ISTCTD=ISTCTD+ISTCT
    ISTCT=0
    ICTDFD=ICTDFD+ICTDF
    ICTDF=0
    DEFAMD=DEFAMD+DEFAM
    DEFAM=0.0
    DO 6 J=1,Q
    Z(J)=0.0
    6  SF(J)=0.0

    2  IF(XT.LT.1.0) GO TO 34

C-----COMPUTE "CHECK" TO VERIFY CL
    CONST1=0.0
    DO 19 J=1,Q
19  CONST1=CONST1+TN(J)
    CONST1=CONST1-0.5*(TN(1)+TN(Q))
    DIF=(CONST1-CONST)*DELX
    CHECK=ETS-DIF-ET

C-----WRITE FINAL VALUES FOR LAST (I) IN DAY (II) AS INPUTS FOR DAY (II+1)
C    WRITE(4) (TN(J),FN(J),CL,CHECK,IR,L,HED,ANT(J),J=1,Q)

C-----PRINT ONE OF TWO OPTIONS FOR DAILY OUTPUT
    IF(BB.EQ.1) GO TO 52
    PRINT 103
    PRINT 121,YEAR,II,XT,MONTH,IDTE,CL,CHECK,ETS,ET,DIF,CNA,CNI,HED,
1  CI,DEFAMC,I
    GO TO 31

```

```

52 PRINT 103
   PRINT 121,YEAR,II,XT,MONTH,IDTE,CL,CHECK,ETS,ET,DIF,CNA,CNI,HED, DOC
   1 CI,DEFAMC,I DOC
   PRINT 9160,CL3
9160 FORMAT(4X,*CL AT 3.5 FT*,F10.3)
   PRINT 105,(TN(J),J=1,Q)

31 IF(ISTCTD.NE.0) PRINT 9167,ISTCTD *****9
9167 FORMAT (10X,*UNSTABLE SOLUTION SITUATION ENCOUNTERED *, I8, * TIM*****9
   LES THIS DAY*) *****9
   IF(ICTDFD.NE.0) PRINT 9171,ICTDFD,DEFAMD $$$$$$$8
9171 FORMAT (10X, * DEFICIT MOISTURE SITUATION ENCOUNTERED *, I8, * TIM$$$$$$$$8
   LES THIS DAY. AMOUNT IS *, F6.2, * CM*) $$$$$$$8
32 CONTINUE
   ENDFILE 5 *****12
   II=II-1 *****14
C---- PRINT RESTART DATA AT END OF YEAR $$$$$$$3
   IF(IDTE.EQ.1.OR.IDTE.EQ.16) GO TO 4721 $$$$$$$3
   PRINT 9151, YEAR,MONTH,IDTE,II,CL,CHECK,IR,L,HED,CONST,CI,ETS,ET, $$$$$$$3
   1 CNA,CNI,DEFAMC $$$$$$$8
   PRINT 9152, (TN(J),J=1,Q) $$$$$$$3
   PRINT 9153, (FN(J),J=1,Q) $$$$$$$3
   PRINT 9154, (ANT(J),J=1,Q) $$$$$$$3
   PRINT 9172, (Z(J),J=1,Q) $$$$$$$8
9172 FORMAT ( X, * Z(J),J=1,Q* /, 7(9E13.6,/)) $$$$$$$8
C---- INCREMENT YEAR, SET DAY NUMBERS, CALCULATE MOISTURE DEFICIT, READ $$$$$$$1
C---- IRRIGATION APPLICATIONS, RESET ICHECK $$$$$$$1
C---- COMPUTE MOISTURE DEFICIT $$$$$$$1
4721 IF(IDEF.NE.1) GO TO 8738 $$$$$$$3
   SUMDEF=0.0 $$$$$$$1
   IF(TN(1).LT.FCAP) SUMDEF=(FCAP-TN(1))*DELX/2. $$$$$$$1
   DO 8736 J=2,Q $$$$$$$1
   IF(TN(J).LT.FCAP) SUMDEF=SUMDEF+(FCAP-TN(J))*DELX $$$$$$$1
8736 CONTINUE $$$$$$$1
   SUMDEF=SUMDEF/2.54 $$$$$$$1
   PRINT 9157, YEAR,MONTH,IDTE,II,SUMDEF $$$$$$$1
C---- INCREMENT YEAR, RESET ICHECK, SET INDICES FOR YEAR LOOP $$$$$$$1
8738 IF((YEAR+1).GT.ISTOP) GO TO 9300 $$$$$$$1
   YEAR=YEAR+1 $$$$$$$1
   ILO=LL $$$$$$$1
   IHI=MM $$$$$$$1
   IF(YEAR.EQ.ISTOP) IHI=MMSTOP $$$$$$$1
   ICHECK=0 $$$$$$$1
C---- READ IRRIGATION APPLICATION DATA $$$$$$$1
   READ 9861, ICODE,IYEAR,APPS,(AID(I),I=1,8) $$$$$$$1
   PRINT 9862,ICODE,IYEAR,APPS,(AID(I),I=1,8) $$$$$$$1
   PRINT 119 $$$$$$$1
   READ 9863, (MON(I),DATE(I),ADENT(I),AMT(I),I=1,APPS) $$$$$$$1
   IF(IDEF.EQ.1) AMT(1)=SUMDEF $$$$$$$1
   PRINT 9864,(MON(I),DATE(I),AMT(I),ADENT(I),I=1,APPS) $$$$$$$1
   DO 8739 L=1,APPS $$$$$$$1
   AMT(L)=AMT(L)*2.54 $$$$$$$1
8739 TME(L)=DAY(DATE(L),START,MON(L)) $$$$$$$1
   L=1 $$$$$$$1
   KFLAG=0 $$$$$$$1
   GO TO 7700 $$$$$$$1
9300 IF(IPUNCH.EQ.2) GO TO 9301 DOC
   IF(IPUNCH.NE.1) GO TO 99 DOC
C---- PUNCH RESTART DATA AT END OF RUN *****1
   PUNCH 9181, YEAR,MONTH,IDTE,II,CL,CHECK,IR,L,HED $$$$$$$1
   PUNCH 9182, CONST,CI,ETS,ET,CNA,CNI *****13
   PUNCH 9182, DEFAMC $$$$$$$8
   PUNCH 9182, (TN(J),J=1,Q) *****1
   PUNCH 9182, (FN(J),J=1,Q) *****1
   PUNCH 9182, (ANT(J),J=1,Q) *****1
   PUNCH 9182, (Z(J),J=1,Q) $$$$$$$8
   GO TO 99 $$$$$$$1
9181 FORMAT(I5, I3, I3, I4, 3E13.6, I3, E13.6) $$$$$$$1
9182 FORMAT(6E13.6) *****13
9301 REWIND 10 $$$$$$$1
   WRITE(10) YEAR,MONTH,IDTE,II,CL,CHECK,IR,L,HED,CONST,CI,ETS,ET, $$$$$$$1
   1 CNA,CNI,DEFAMC $$$$$$$1

```

```

WRITE(10) (TN(J),J=1,Q)
WRITE(10) (FN(J),J=1,Q)
WRITE(10) (ANT(J),J=1,Q)
WRITE(10) (Z(J),J=1,Q)
ENOFIL 10
99 STOP
8800 PRINT 8801
8801 FORMAT(5X, * END FILE FOUND ON TAPE 5 BEFORE DAY NO. LLSTRT-1 FOUND
10. EXECUTION TERMINATED *)
GO TO 99
8802 PRINT 8803
8803 FORMAT(5X, * DAY READ FROM TAPE 5 EQUALS OR IS GREATER THAN STARTI
ING DAY. EXECUTION TERMINATED *)
GO TO 99

C-----PRINT RUN PARAMETERS AND INITIAL CONDITIONS.
10 KFLAG=1
IF(AA.EQ.1)9.12
9 PRINT 109
PRINT 110
PRINT 9158,IPUNCH,IRESTR,ISAVE,ITENTH,INFIL5,LLSTRT,MMSTOP,ISTOP,
1 IDEF,FCAP,IPOPT
PRINT 119
PRINT 120,(TME(J),MON(J),DATE(J),AMT(J),ADENT(J),J=1,APPS)
PRINT 112
PRINT 105,(TH(J),J=1,Q)
PRINT 127
PRINT 107
PRINT 111,AA,BB,CC,LL,MM,BBC,TBC,YEAR, CROP,M,APPS,DELX,TS,TM,TD,
ISM
PRINT 113
PRINT 114,(IDENT,HOR(N),N=1,0)
IF(CROP,NE.3,OR.ICROP.EQ.3)GO TO 12
PRINT 115
PRINT 116,(KP3(I),I=1,6)
PRINT 117
PRINT 118,(UH(I),I=1,24)
PRINT 108
GO TO 12

100 FORMAT(5I5,2F5.0,3I5,5X,5F5.0)
101 FORMAT(2X,1A8,1F10.0)
102 FORMAT(/,2X,*WATER APPLIED. DAY NUMBER *,I4,*. AMOUNT = *F7.2,
1* CM,*)
103 FORMAT (/, X. 129H YEAR II XT MON DTE CL CHECK
1ETS ET DIF CNA CNI HED CI
2 DEFAMC NSTEPS)
104 FORMAT(45X,F6.5)
105 FORMAT(9X,10F12.6)
106 FORMAT(20X,I2,1X,I2,5X,F10.0,39X,A1)
107 FORMAT( 9X,* AA BB CC LL MM BBC TBC YEAR CROP M AP
IPS DELX TS TM TO SM*)
108 FORMAT(1H1)
109 FORMAT(1H1,3X,*PARAMETERS, CONSTANTS, AND INITIAL CONDITIONS USED
1IN THIS REPORT.*)
110 FORMAT(/,3X,*-----NOTE----- DIFFUSIVITY AND CONDUCTIVITY RELATIONS
1HIPS MUST BE INSERTED INTO SOURCE DECK.*,/)
111 FORMAT(9X,5I5,2F5.2,4I5,5F5.2)
112 FORMAT(/,7X,*INITIAL SOIL MOISTURE CONDITIONS.*)
113 FORMAT(/,7X,*SOIL IDENTIFICATION AND HORIZON DEPTHS.*)
114 FORMAT(9X,*IDENTIFICATION= *,A8,*. DEPTH= *,F5.1)
115 FORMAT(/,7X,*CONSUMPTIVE USE DATA.*)
116 FORMAT(9X,*PERCENTAGE OF ROOTS FOUND IN EACH OF TOP 6 FEET.*,
16F10.3)
117 FORMAT(9X,*CONSUMPTIVE USE CONSTANTS READ IN FROM DATA CARDS (IN
1 CM./ 15 DAYS) FOR SEMIMONTHLY PERIODS.*)
118 FORMAT(11X,24F5.2)
119 FORMAT(/,7X,*WATER APPLICATION DAYS, DATES, AND AMOUNTS.*)
120 FORMAT(9X,*DAY NUMBER*,I4,7X,*DATE *,I2,*/*,I2,7X,*AMOUNT=*,F6.2,*
1 CM. SOURCE = *,A1)
121 FORMAT (X, 2I4, F6.3, I3, I4, X, 10F10.4, I6)

```

```

126 FORMAT(25X,*UNSTABLE SOLUTION SUSPECTED*,I10,F8.6,I10,F20.4)
127 FORMAT(/,7X,*RUN PARAMETERS, AND BOUNDARY CONDITIONS,*)
128 FORMAT (I2)
9151 FORMAT(/, X, *RESTART DATA FOR YEAR *, I5, * MONTH * I2, * DAY * DOC
1, I2, * DAY NO. *, I3/ X, * CL= *, E13.6, * CHECK= *, E13.6, * IP=$$$$$$1
2 *, E13.6, * L= *, I3, * MED= *, E13.6/, X, * CONST= * E13.6, * C$$$$$$$1
3I= *, E13.6, * ETS= *, E13.6, * ET= *, E13.6/ X, * CNA= *, E13.6, * $$$$$$1
4 * CNI= *, E13.6, * DEFAMC= *, E13.6) $$$$$$1
9152 FORMAT( X, * TN(J),J=1,Q*/, 7(9E13.6,/)) $$$$$$1
9153 FORMAT( X, * FN(J),J=1,Q*/, 7(9E13.6,/)) $$$$$$1
9154 FORMAT( X, *ANT(J),J=1,Q*/, 7(9E13.6,/)) $$$$$$1
9155 FORMAT(/,X, *RESTART DATA AS READ FROM CARDS*) $$$$$$1
9156 FORMAT(9I5,F5.0,I5,I5)
9157 FORMAT(/, X,* DEPLETED MOISTURE FOR YEAR=*, I5, * MONTH=*,I3, * DADOC
ITE=*, I3, * (DAY NUMBER=*,I4, *) IS =*,F5.2, * INCHES*) $$$$$$1
9158 FORMAT(4X,*IPUNCH IRESTR ISAVE ITENTH INFIL5 LLSTP$$$$$$$1
1T MMSTOP ISTOP IDEF FCAP IPOPT*/, I8, 8I10, *MOD 1
2 F12.3, I8) MOD 1
END
SUBROUTINE CONUSE(CROP,DELX,J,U,K,LL,MM)
C-----CONSUMPTIVE USE SUBROUTINE
COMMON/XYZ/IDTE,MONTH,UH,KP3
COMMON/CHK/ICHECK,ICROP
DIMENSION MEANT1(12),MEANT2(12),KA1(12),KA2(12),KB1(12),KB2(12),
IP1(12),P2(12),KP(6),KP1(6),KP2(6,3),KP3(6),U1(366),UH(366)
DIMENSION FACTOR(24)
REAL MEANT1,MEANT2,KA1,KA2,KB1,KB2,KP,KP1,KP2,KP3
INTEGER CROP
*****2

C-----THIS ROUTINE RETURNS CONSUMPTIVE USE IN CM WATER/DEPTH SEGMENT/
C-----DELTA TIME

C---- ICROP=3 USED WHEN DAILY CONSUMPTIVE USE VALUES ARE READ
C-----MEAN TEMPERATURES (F) FOR FIRST HALF OF MONTH
DATA((MEANT1(I),I=1,12)=
$42.4,47.0,46.0,55.8,66.6,71.9,79.1,81.9,75.0,65.0,55.0,45.0),
C-----MEAN TEMPERATURES (F) FOR SECOND HALF OF MONTH
$((MEANT2(I),I=1,12)=
$47.0,48.1,58.8,62.5,73.9,73.8,82.6,77.6,75.0,65.0,55.0,41.6),
C-----CONSUMPTIVE USE CONSTANTS FOR BARLEY (FIRST HALF OF MONTH)
$((KA1(I),I=1,12)=
$0.50,1.58,1.17,3.00,1.22,0.44,0.00,0.00,0.00,0.00,0.00,0.12),
C-----CONSUMPTIVE USE CONSTANTS FOR BARLEY (SECOND HALF OF MONTH)
$((KA2(I),I=1,12)=
$0.80,0.50,3.00,2.65,0.44,0.00,0.00,0.00,0.00,0.00,0.00,0.12),
C-----CONSUMPTIVE USE CONSTANTS FOR MILO (FIRST HALF OF MONTH)
$((KB1(I),I=1,12)=
$0.00,0.00,0.00,0.00,0.00,0.00,0.14,1.29,2.20,2.20,0.10,0.10,0.10),
C-----CONSUMPTIVE USE CONSTANTS FOR MILO (SECOND HALF OF MONTH)
$((KB2(I),I=1,12)=
$0.00,0.00,0.00,0.00,0.00,0.00,0.74,1.67,2.20,2.20,0.10,0.10,0.10),
C-----PERCENT OF DAYLIGHT HOURS FOR FIRST HALF OF MONTH
$((P1(I),I=1,12)=
$3.31,3.65,4.04,4.47,4.84,5.03,4.94,4.63,4.22,3.80,3.42,3.22),
C-----PERCENT OF DAYLIGHT HOURS FOR SECOND HALF OF MONTH
$((P2(I),I=1,12)=
$3.54,3.17,4.31,4.47,5.16,5.03,5.27,4.94,4.22,4.06,3.42,3.43)
C-----ROOT DISTRIBUTION WITH DEPTH FOR BARLEY
DATA((KP(I),I=1,6)=0.40,0.24,0.19,0.13,0.04,0.00)
C-----ROOT DISTRIBUTION WITH DEPTH FOR MILO
DATA((KP1(I),I=1,6)=0.31,0.22,0.14,0.09,0.08,0.08)
DATA(ICHECK=0)
DATA (FACTOR=15.,16.,15.,13.,15.,16.,15.,15.,15.,16.,15.,15.,15.,
116.,15.,16.,15.,15.,15.,16.,15.,15.,15.,16.) *****2
*****2

C---- COMPUTE DEPTH IN FEET MOD 2
D=DELX*(J-1)/30.48 MOD 2

C-----READ U OFF DATA CARDS IF CROP=3.
IF(CROP.NE.3)GO TO 11
IF(J.NE.2)GO TO 9
ICOUNT=MONTH*2-0.5

```



```

      IF (IDTE.GE.14) ICOUNT=MONTH*2+0.5
9    IF (ICHECK.EQ.1) GO TO 20
      ICHECK=1
      N=LL-1
      IF (JCHECK.EQ.1) GO TO 7000
      READ 100.(KP3(I),I=1,6)
      DO 15 I=1,6
15   KP2(I,3) = KP3(I)
      JCHECK=1
      CALL AJST(KP3,DELX,ADJUST)
      ADJUST=ADJUST*DELX/30.48
      7000 CONTINUE
      IF (ICROP.EQ.3.AND.CROP.EQ.3) GO TO 201
      READ 102.ICODE,IYEAR,(U1(I),I=1,12)
      READ 102.ICODE,IYEAR,(U1(I),I=13,24)
102  FORMAT (2I5,12F5.0)
      PRINT 103.ICODE,IYEAR
103  FORMAT(7X,*CONSUMPTIVE USE CONSTANTS READ IN FROM DATA CARDS IN IN
      ICHES PER SEMIMONTHLY PERIOD, ICODE=*, I5, * IYEAR= *, I5)
      PRINT 104.(U1(I),I=1,24)
104  FORMAT (11X,24F5.2)
      DO 19 I=1,24
         U1(I)=U1(I)*2.54
         UM(I)=U1(I)
19   CONTINUE
20   U=U1(ICOUNT)
      GO TO 21
201  CONTINUE
C READ NUMBER OF DAYS OF ET
      LM=(MM-LL)+1
      READ 106.ICODE, IYEAR
106  FORMAT(2I5)
      READ 105.(U1(I),I=1,LM)
105  FORMAT(16F5.3)
      PRINT 107, ICODE,IYEAR
107  FORMAT(7X,*CONSUMPTIVE USE CONSTANTS READ IN FROM DATA CARDS IN IN
      ICHES PER DAY, ICODE= *,I5, * IYEAR= *,I5)
      PRINT 108.(U1(I),I=1,LM)
108  FORMAT(11X,10F5.3)
7001 DO 7002 I=1,LM
      U1(I)=U1(I)*2.54
      UM(I)=U1(I)
7002 CONTINUE
21   CONTINUE
      IF (ICROP.NE.3) U=U1(ICOUNT)
      KL=K-N
      IF (ICROP.EQ.3.AND.CROP.EQ.3) U=U1(KL)
      GO TO 7

11   DO 12 I=1,6
      KP2(I,1) = KP(I)
12   KP2(I,2) = KP1(I)
C----- CONVERT DELX (CM) TO ADJUST (FEET)
      ADJUST=DELX/30.48
      I=MONTH
      MOD      2
      MOD      2
C-----BRANCH ACCORDING TO CROP
      GO TO (1,2),CROP
C-----BRANCH ACCORDING TO HALF OF MONTH
1    IF (IDTE.LE.15) 3,4
2    IF (IDTE.LE.15) 5,6
C-----COMPUTE CONSUMPTIVE USE FROM CONSUMPTIVE USE FORMULA
3    U=KA1(I)*(MEANT1(I)*P1(I)/100.)*2.54      $ GO TO 7
C-----COMPUTE CONSUMPTIVE USE FROM CONSUMPTIVE USE FORMULA
4    U=KA2(I)*(MEANT2(I)*P2(I)/100.)*2.54      $ GO TO 7
C-----COMPUTE CONSUMPTIVE USE FROM CONSUMPTIVE USE FORMULA
5    U=KA1(I)*(MEANT1(I)*P1(I)/100.)*2.54      $ GO TO 7
C-----COMPUTE CONSUMPTIVE USE FROM CONSUMPTIVE USE FORMULA
6    U=KA2(I)*(MEANT2(I)*P2(I)/100.)*2.54
C-----ADJUST CONSUMPTIVE USE FOR LENGTH OF TIME INTERVAL
7    CONTINUE
      IF (ICROP.EQ.3 .AND.CROP.EQ.3) GO TO 200

```

```

      IF (IDTE.LE.15) 47,48
47  KIS=(MONTH*2)-1
      GO TO 49
48  KIS=MONTH*2
49  U=U/FACTOR(KIS)
C-----ADJUST CONSUMPTIVE USE FOR SIZE OF DEPTH SEGMENT AND ROOT DISTRIB-
C-----UTION
200 CONTINUE
      IFOOT=D+1
      IF (IFOOT.GT.6) U=0.0
      IF (IFOOT.LE.6) U=U*KP2(IFOOT,CROP)*ADJUST
      RETURN
100 FORMAT(6F10.0)
      END

```

INTEGER FUNCTION DAY

```

      INTEGER FUNCTION DAY (K,L,M)
      GO TO (1,2,3,4,5,6,7,8,9,10,11,12) M
1   DAY=K-L
2   DAY=K-L+31
3   DAY=K-L+59
4   DAY=K-L+90
5   DAY=K-L+120
6   DAY=K-L+151
7   DAY=K-L+181
8   DAY=K-L+212
9   DAY=K-L+243
10  DAY=K-L+273
11  DAY=K-L+304
12  DAY=K-L+334
      END

```

SUBROUTINE THEDATE

```

      SUBROUTINE THEDATE (K,L)
      COMMON/XYZ/IDTE,MONTH,UH,KP3
      M=K+L
      IF (M.GE.1.AND.M.LE.31) GO TO 1
      IF (M.GT.31.AND.M.LE.59) GO TO 2
      IF (M.GT.59.AND.M.LE.90) GO TO 3
      IF (M.GT.90.AND.M.LE.120) GO TO 4
      IF (M.GT.120.AND.M.LE.151) GO TO 5
      IF (M.GT.151.AND.M.LE.181) GO TO 6
      IF (M.GT.181.AND.M.LE.212) GO TO 7
      IF (M.GT.212.AND.M.LE.243) GO TO 8
      IF (M.GT.243.AND.M.LE.273) GO TO 9
      IF (M.GT.273.AND.M.LE.304) GO TO 10
      IF (M.GT.304.AND.M.LE.334) GO TO 11
      IF (M.GT.334.AND.M.LE.365) GO TO 12
1   IDTE=M
2   IDTE=M-31
3   IDTE=M-59
4   IDTE=M-90
5   IDTE=M-120
6   IDTE=M-151
7   IDTE=M-181
8   IDTE=M-212
9   IDTE=M-243
10  IDTE=M-273
11  IDTE=M-304
12  IDTE=M-334
      END

```

```

$ RETURN
$ RETURN
$ RETURN
$ RETURN
$ RETURN
$ RETURN
$ RETURN
$ RETURN
$ RETURN
$ RETURN
$ RETURN
$ RETURN

```

SUBROUTINE CHAR

```

SUBROUTINE CHAR
C-----
C----- PROGRAM TO READ INPUTS AND COMPUTE CONSTANTS FOR EVALUATING THE
C----- CONDUCTIVITY AND DIFFUSIVITY BY BROOKS COREY THEORY USING THE
C----- SPECIAL GENERALIZED FORM FOR SUBROUTINE PROP
C-----
COMMON/PROP/KSAT,DSAT,C1,C2,C3,C4,TS,TPB,SR
COMMON/PROP1/DTS,ODSAT
COMMON/PROP2/BET,ALP,AIRINF,ALM,EMP
REAL KSAT
C----- READ INPUTS
READ 9001,KSAT,REMP,AIRENT,TPB,SR,DTS,ODSAT
READ 9001,ALM,ALP,BET,AIRINF,EMP
C----- COMPUTE SATURATED DIFFUSIVITY AND CONSTANTS
DSAT=REMP*AIRENT*KSAT/(DTS-SR)
C3=2*REMP.3
C4=9EMP.2
C1=KSAT/((TS-SR)**C3)
C2=DSAT/((DTS-SR)**C4)
C----- LIST OUTPUT
PRINT 9500,KSAT,REMP,AIRENT,SR,ALP,BET,EMP,AIRINF,ALM,C1,C3
RETURN
C----- FORMATS
9001 FORMAT(8F10.5)
9500 FORMAT(1H1,49X,35H UNSATURATED FLOW PROGRAM (MOISTRE)//,5X,
1 69H CONDUCTIVITY RELATIONS TO BE BASED ON THE MET
2HOD OF BROOK AND COREY//,5X,12H INPUTS ARE-/,9X,25H SATURATED COND
3UCTIVITY =,F10.4,7H CM/DAY//,9X, 25H EMPIRICAL CONSTANT B =,
4F10.4//,9X, 25H AIR-ENTRY POTENTIAL =,F10.2, 3H CM/,
19X, 25H RESIDUAL SATURATION =,F10.5//,5X,
563H DIFFUSIVITY RELATIONS COMPUTED USING FUNCTION OF SU AND BROOKS
6//,5X,12H INPUTS ARE-/,9X,25H A =,F10.5//,9X,2
85H A =,F10.5//,9X,25H EMPIRICAL CONSTANT M =
1,F10.5//,9X,25H INFLECTION POTENTIAL =,F10.5,3H CM//,9X,25H LAMBDA
2 =,F10.5//,5X,19H RELATIONSHIP USED-//,9X,21H COND
3UCTIVITY(THETA)=,F14.5,13H * (THETA ** .F7.3, 9H ) CM/DAY//)
END

```

SUBROUTINE PROP

```

SUBROUTINE PROP(Z,ZK,TD,K,D)
C-----
C----- PROGRAM TO COMPUTE CONDUCTIVITY AND DIFFUSIVITY USING BROOKS AND
C----- COREY METHOD
C-----
C----- NOMENCLATURE
C----- Z =VOL.MOISTURE CONTENT AT WHICH DIFFUSIVITY COMPUTED
C----- ZK =VOL.MOISTURE CONTENT AT WHICH CONDUCTIVITY COMPUTED
C----- TD =VOL.MOISTURE CONTENT BELOW WHICH PROPERTIES ASSUMED AS 0.
C----- TS =VOL.MOISTURE CONTENT AT SATURATION
C----- KSAT =CONDUCTIVITY AT SATURATION (CM/DAY)
C----- DSAT =DIFFUSIVITY AT SATURATION (CM2/DAY)
C----- C1-C4 =CONSTANTS IN EQUATIONS
C----- K =CONDUCTIVITY AT CONTENT ZK (CM/DAY)
C----- D =DIFFUSIVITY AT CONTENT Z (CM2/DAY)
C----- EQUATIONS
C----- K(ZK)=C1*(ZK-SR)**C3
C----- D(Z)=C2*(Z-SR)**C4
C-----
COMMON/PROP/KSAT,DSAT,C1,C2,C3,C4,TS,TPB,SR
COMMON/PROP1/DTS,ODSAT
REAL K,KSAT
C----- CONDUCTIVITY COMPUTATION
IF(ZK.GE.TD) GO TO 10

```

11 K=0.0	
GO TO 100	
10 IF(ZK.GE.TS) GO TO 20	PROP 110
IF(ZK.LT.SR) GO TO 11	
K=C1*((ZK-SR)**C3)	
GO TO 100	
20 K=KSAT	PROP 140
GO TO 1000	PROP 150
C---- DIFFUSIVITY COMPUTATION	PROP 160
100 IF(Z.GE.TD) GO TO 110	PROP 170
111 D=0.0	
GO TO 1000	PROP 190
110 IF(Z.GT.DTS) GO TO 120	
IF(Z.LT.SR) GO TO 111	
D=C2*((Z-SR)**C4)	
GO TO 1000	PROP 220
120 D=DDSAT	
IF(DTS.EQ.TS) D=DDSAT	
1000 RETURN	PROP 240
END	PROP 250

SUBROUTINE AJST

SUBROUTINE AJST(KP3,DELX,ADJUST)	AJST 10
C----	AJST 20
C---- PROGRAM TO COMPUTE ADJUSTMENT FACTOR FOR CONSUMPTIVE USE	AJST 30
C----	AJST 40
DIMENSION KP3(6)	AJST 50
COMMON/AJST/Q	AJST 60
INTEGER Q	AJST 70
REAL KP3	AJST 80
U=U-KP3(1)*DELX	AJST 90
C---- CONVERT NODE SPACING FROM CM TO FT	AJST 100
DEL=DELX/30.48	AJST 110
U=0.0	AJST 120
C---- ENTER LOOP FOR ALL NODES	AJST 130
DO 100 I=2,Q	AJST 140
C---- COMPUTE DEPTH OF NODE IN FEET	AJST 150
D=DEL*(I-1)	AJST 160
C---- COMPUTE SUBSCRIPT FOR PROPER DEPTH ZONE	AJST 170
IFOOT=D+1	AJST 180
C---- TEST IF BEYOND ROOT ZONE	AJST 190
IF(IFOOT.GT.6) GO TO 110	AJST 200
C---- COMPUTE RELATIVE CONUSE REMOVED	AJST 210
U=U-KP3(IFOOT)*DEL	AJST 220
100 CONTINUE	AJST 230
C---- ADJUST CONUSE FOR REMOVAL AT TOP NODE	AJST 240
110 IFOOT=DEL+1	AJST 250
U=U-KP3(IFOOT)*DEL*0.5	AJST 260
ADJUST=1./U	AJST 270
RETURN	AJST 280
END	AJST 290

SUBROUTINE ADIF

```

SUBROUTINE ADIF(TZ,TK,D)
COMMON/PROP/KSAT,DSAT,C1,C2,C3,C4,TS,TPB,SR
COMMON/PROP1/DTS,DDSAT
COMMON/PROP2/BET,ALP,AIRINF,ALM,EMP
REAL KSAT
IF(TZ.GT.SR.AND.TZ.LT.TS.AND.TK.LE.SR) GO TO 4
IF(TK.GT.SR.AND.TK.LT.TS.AND.TZ.LE.SR) GO TO 7
IF(TZ.EQ.TS.AND.TK.LE.SR) GO TO 5
IF(TK.EQ.TS.AND.TZ.LE.SR) GO TO 6
GO TO 10
5 TZ=TS-.0001
GO TO 4
6 TK=TS-0.0001
GO TO 7
4 CALLSIMP(TZ,SR,AVD)
D=AVD/(TZ-TK)
GO TO 100
7 CALLSIMP(TK,SR,AVD)
D=AVD/(TK-TZ)
GO TO 100
10 IF(TZ.GT.SR.AND.TZ.LT.TS.AND.TK.GT.SR.AND.TK.LT.TS) GO TO 12
GO TO 32
12 IF(TZ.GT.TK) GO TO 15
IF(TK.GT.TZ) GO TO 18
20 A=((1./(TS-SR))*((2./ALM)+3.))*KSAT*EMP*AIRINF
B=(1./((1./(ALP*TS))*EMP))*((1./(RET*TS))*((BET*EMP/ALP).)
C=((TK-SR))*((2.+(2./ALM))-EMP))*((TS-TK))*((BET*EMP/ALP))
D=A*B*C*(((TK-SR)/(TS-TK))*((BET/ALP))+1.0)
GO TO 100
15 CALLSIMP(TZ,TK,AVD)
D=AVD/(TZ-TK)
GO TO 100
18 CALLSIMP(TK,TZ,AVD)
D=AVD/(TK-TZ)
GO TO 100
32 IF(TZ.EQ.TS.AND.TK.GT.SR.AND.TK.LT.TS) GO TO 33
IF(TK.EQ.TS.AND.TZ.GT.SR.AND.TZ.LT.TS) GO TO 34
IF(TK.EQ.TS.AND.TZ.EQ.TS) GO TO 21
GO TO 22
21 TK=TS-0.0001
GO TO 20
33 TZ=TS- 0.0001
IF(TZ.LE.TK) GO TO 20
GO TO 15
34 TK=TS-0.0001
IF(TK.LE.TZ) GO TO 36
GO TO 18
36 TK=TZ
GO TO 20
22 IF(TZ.LE.SR.AND.TK.LE.SR) GO TO 25
GO TO 100
25 D=0.0
100 RETURN
END

```

```

SUBROUTINE SIMP(SZ,SK,SVD)
COMMON/PROP/KSAT,DSAT,C1,C2,C3,C4,TS,TPB,SR
COMMON/PROP1/DTS,DDSAT
COMMON/PROP2/BET,ALP,AIRINF,ALM,EMP
REAL KSAT,INTEG
F(Z)=(Z-SR)**((2.+(2./ALM))-EMP)
F2(Z)=(TS-Z)**((BET*EMP)/ALP)
FUNC(Z)=F(Z)*F2(Z)*(((Z-SR)/(TS-Z))*(BET/ALP))+1.0)
A=((1./(TS-SR))*((2./ALM)+3.))*KSAT*EMP*AIRINF
B=(1./((1./(ALP*TS))*EMP))*((1./(BET*TS))*((BET*EMP)/ALP))
CONST=A*B
C THIS SECTION COMPUTES INTEGRAL VALUES USING SIMPSON RULE
H=(SZ-SK)/2.0
N=1
ENDS=FUNC(SZ)+FUNC(SK)
TWO=0.0
FOUR=FUNC(SK+H)
OLDINT=H/3.0*(ENDS+4.0*FOUR)
C EVALUATION LOOP
25 H=H/2.0
N=2*N
TWO=TWO+FOUR
FOUR=0.0
T=SK+H
DO 26 I=1,N
FOUR=FOUR+FUNC(T)
26 T=T+H+H
INTEG=H/3.0*(ENDS+2.0*TWO+4.0*FOUR)
C CHECK FOR CONVERGENCE OR EXCESSIVE NUMBER OF ITERATIONS
IF(ABS(OLDINT-INTEG).LT.1.0E-6.OR.N.GT.10000) GO TO 10
OLDINT=INTEG
GO TO 25
10 SVD=CONST*INTEG
RETURN
END

```

PROGRAM USCHEM

```

C
C-----UNSATURATED CHEMISTRY PROGRAM USBR VERSION 1.2.0--NOV 1974
C
DIMENSION X(7,25)

COMMON/BYPAS/NRYPAS,IDYSTR,IDYSTP,ILO,IMI,INFIL1,ICONT1,JPAS
COMMON/ARLE/TITLE(10),SMONTH,MM,0,IPRINT,JPRINT,INK,IPUNCH,ISTOP,
1ITEST,IREADP,IMASS,IADD(25),IORNAP(25),HOR(9),TOTN(99),YEAR
2AIRR(9),IRR(25),TT(60),FERT(7),OFERT(3),NORGIN,NFERTIN,NTEMPIN,
3ITOT,JTOT,IPTOT,NT
COMMON/XX2/A1,A2,A3,X
COMMON/AFG/ENH3,II,LLL,IOP,ANETLIM(25)
COMMON/YYY/START,IDTE,MONTH,I,ILAP
COMMON/XXY/ICHECK,ICOUNT,CONV,PK,PK1,CROP,FACT
COMMON/XXX/DELX,DELT,MS,WTART,BD(25),TEN(25),CHECK(25),MOISIN
1(25),CMH201(25),MOISOUT(25),ANO3(25),ANH3(25),UREA(25),ORN
2(25),CA(25),ANA(25),AMG(25),HCO3(25),CL(25),CO3(25),SO4(25),
3E5(25),C5(25),SAS(25),XX5(25),CASO(25),AGSO(25),BNH4(25),
4EC(25),CN1(25),SAMT(25),RN(25),RC(25),TEM(25),CAL(25),Q,SRO
1P,XTRACT,SUMNO3,THOR(4),TO,IDAY,U9(25),CH,CH1,TRERUN,ISWCH,CUMSUM,

```

ISUMOUT,REDUCE,IIK(25),AZE(25),PP(10)	25
COMMON/1/XTRACT(25),AKCS(25),AKCM(25)	26
COMMON/TRNIT/U(25),ACTCA(25),IOPN,ISETN(25)	28
COMMON/SALT/SEPTIO(25),SBYPAS	29
COMMON/CO2/PCO2(25),IPC02	30
INTEGER Q,Q,START,CROP,TO,SMONTH,YEAR,TITLE,SBYPAS	31
REAL MOISIN,MOISOUT	32
DATA (CONV=11.221367)	33
DATA (AKCS=25*0.707),(AKCM=25*0.67)	34
REWIND 3 \$REWIND 8 \$REWIND 9 \$REWIND 10	35
C-----SET INITIAL VALUES	36
ICHECK = 0 \$CMH201(1) = 1.0	37
JPAS=0	38
DO 693 IJ=1,7	39
DO 693 JI=1,25	40
693 X(IJ,JI) = 1.E+6	41
C-----READ TITLE CARD	44
READ 88,TITLE	45
C-----READ CONTROL CARDS	46
READ 105,DELX,DELT,RSN ,CH,CH1,A1,A2,REDUCE,PK,PK1,FACT,	47
1LL,MM,0,CROP,TO,NT,IPRINT,JPRINT,INK,IRERUN,IPUNCH,IREADP,ITEST,	49
2START,SMONTH,YEAR,ISTOP,IMASS,IPRINTI,IPRINTJ,NBYPAS,SBYPAS,IDYSTR	
1,IDYSTR,INFIL2,INFIL1,ICONT1,ICONT2,IOP,IOPN,IPC02,IREK	51
C----- SET DAY NUMRERS (ILO,IHI) FOR SUR. EXECUTE	52
C----- RESET LL,MM IF OUTSIDE LIMITS FOR TAPE1	53
IF(1LL.LT.IDYSTR) LL=IDYSTR	54
IF(MM.GT.IDYSTR) MM=IDYSTR	55
ILO=LL	56
ILAP = ILO	
IHI=MM	57
IF(YEAR.NE.ISTOP) IHI=IDYSTR	58
C----- POSITION TAPE2 TO PROPER RECORD FOR WRITE	
REWIND 2	60
NSKIP=INFIL2-1	61
IF(NSKIP.LE.0) GO TO 9012	62
DO 9011 I=1,NSKIP	63
CALL SKIP(2)	
9011 CONTINUE	65
9012 IF(ICONT2.EQ.1) GO TO 9014	
NSKIP=ILO-IDYSTR	67
IF(NSKIP.LE.0) GO TO 9014	68
DO 9013 I=1,NSKIP	69
READ (2) I1	70
9013 CONTINUE	71
9014 CONTINUE	72
C-----COMPUTE NO. OF TIME INTERVALS PER DAY	73
LLL= 1./DELT + 0.5	74
IF(IPRINTI.NE.0) CALL PRNT(IPRINTI,IPRINTJ)	75
IF(NBYPAS.EQ.1) GO TO 9000	76
C-----READ TEMPERATURE HORIZON DEPTHS	77
READ 107, (THOR(J),J=1,TO)	78
9000 CONTINUE	79
C-----READ COMPONENT HORIZON DEPTHS	80
READ 100,(HOR(J),J=1,0)	81
IF(NBYPAS.EQ.1) GO TO 9001	82
C-----STORE TEMPERATURE PROFILE DATA ON TAPE 8	83
DO 800 J=1,NT	84
READ 801,(TT(I),I=1,TO)	85
	86
	87
	88

WRITE(8) (TT(I),I=1,TO)	89
800 CONTINUE	90
	91
9001 CONTINUE	92
C-----READ IRRIGATION WATER ANALYSIS	93
READ 100, ANH3(1), ANO3(1), CA(1), ANA(1), AMG(1), HCO3(1), CL(1), CO3(1)	94
1, SO4(1)	95
	96
C-----STORE TRANSFORMED IRRIGATION WATER ANALYSIS	97
ORN(1)=UREA(1)=SAMT(1)=0.0	98
CALL UNITS1(1)	99
AIRR(1)=ANH3(1) SAIRR(2)=ANO3(1) SAIRR(3)=CA(1) SAIRR(4)=ANA(1)	100
AIRR(5)=AMG(1) SAIRR(6)=HCO3(1) SAIRR(7)=CL(1) SAIRR(8)=CO3(1)	101
AIRR(9)=SO4(1)	102
	103
C-----COMPUTE TOTAL NUMBER OF COMPONENT HORIZONS	104
Q=HOR(0)/DELX+1.1	
IF(SRYPAS.EQ.1) READ 1100, (SERATIO(N9), U(N9), ACTCA(N9), N9=2,Q)	
IF(ISN.EQ.1) READ 1101, (ISETN(N9), N9=2,Q)	
IF(ITEST.EQ.1) 782, 783	106
782 READ 784, (CMH201(J), MOISIN(J), MOISOUT(J), TEN(J), U(J), J=1,Q)	107
	108
C-----PRINT HEADING	109
783 IF(IRERUN.EQ.0) PRINT 201	110
	111
C-----SET COUNTERS	112
N=2 SL=1 SK1 = 1	113
	114
C-----CALL OUTPT TO ZERO INITIAL VALUES	115
CALL OUTPT(K1)	116
IF(IRERUN.EQ.0) 22, 701	117
	118
C-----READ INITIAL SOIL ANALYSES	119
22 READ 100, ANH3(1), ANO3(1), UREA(1), CA(1), ANA(1), AMG(1), HCO3(1)	120
1, CL(1), CO3(1), SO4(1), EC(1), XX5(1), CAL(1), BD(1), SAMT(1), CN1(1)	121
	123
C-----PRINT INITIAL SOIL ANALYSES	124
PRINT 200, L, ANH3(1), ANO3(1), UREA(1), SAMT(1), CA(1), ANA(1), AMG(1),	125
1HCO3(1), CL(1), CO3(1), SO4(1)	126
READ 101, XTRCT(1), PCO2(1), AKCS(1), AKCM(1)	
	127
C-----COMPUTE SEGMENT NUMBER OF COMPONENT HORIZON	128
KK=HOR(L)/DELX+1.1	129
	130
C-----STORE INITIAL SOIL ANALYSES IN PROPER COMPONENT ARRAYS	131
DO 23 J=N+KK	132
ANH3(J)=ANH3(1) SAN03(J)=ANO3(1) SUREA(J)=UREA(1)	133
CA(J)=CA(1) SANA(J)=ANA(1) SAMG(J)=AMG(1)	134
HCO3(J)=HCO3(1) SCL(J)=CL(1) SC03(J)=CO3(1)	135
SO4(J)=SO4(1) SEC(J)=EC(1) SXX5(J)=XX5(1)	136
CAL(J)=CAL(1) SBD(J)=BD(1) SSAMT(J)=SAMT(1)	137
CN1(J)=CN1(1)	138
XTRCT(J)=XTRCT(1) SPC02(J)=PCO2(1)	
IF(IKEX.EQ.0) GO TO 23	
AKCS(J)=AKCS(1)	
AKCM(J)=AKCM(1)	
23 CONTINUE	140
	141
	142
C-----CHECK FOR LAST SEGMENT	143
IF(KK.EQ.0) 20, 21	144
	145
C-----RESET COUNTERS	146
21 N=KK+1	147
L=L+1	148
GO TO 22	149
	150
C-----PRINT HEADING	151
20 PRINT 202	152
GO TO 703	153
701 CONTINUE	154
	155

C-----FCR & RERUN. READ FROM TAPE3 OR FROM CARDS	156
IF (IREADP.EQ.0)	157
1 READ (3) ICOUNT,NFERTIN,NORGIN,NTEMPIN,(ANH3(J),ANO3(J),UREA(J)	158
1,CA(J),ANA(J),AMG(J),HC03(J),CL(J),C03(J),S04(J),EC(J),XX5(J),CAL(159
2J),RD(J),SAMT(J),CN1(J),ORN(J),RN(J),RC(J),E5(J),C5(J),SAS(J),CASO	160
3(J),AGSO(J),BNH4(J),XTRCT(J),ANETLIM(J),AZE(J),IIK(J),	161
4PC02(J),AKCS(J),AKCM(J),J=2,Q)	
IF (IREADP.NE.0)	162
1 READ 505. ICOUNT,NFERTIN,NORGIN,NTEMPIN,(ANH3(J),ANO3(J),UREA(J)	163
1,CA(J),ANA(J),AMG(J),HC03(J),CL(J),C03(J),S04(J),EC(J),XX5(J),CAL(164
2J),RD(J),SAMT(J),CN1(J),ORN(J),RN(J),RC(J),E5(J),C5(J),SAS(J),CASO	165
3(J),AGSO(J),BNH4(J),XTRCT(J),ANETLIM(J),AZE(J),IIK(J),	166
4PC02(J),AKCS(J),AKCM(J),J=2,Q)	
	167
C-----SET INITIAL VALUES	168
703 DO 1 J=2,Q	169
IF (IRERUN.EQ.0) 780,781	170
780 ORN(J)=RC(J)=RN(J)=CHECK(J)=0.0	171
SAS(J)=BNH4(J)=0.0	172
CMH201(J)=XTRCT(J)*RD(J)*DELX	173
	174
EC(J)=EC(J)/1.E5	175
	176
C-----CALL UNIT CONVERSION SUBROUTINE	177
CALL UNITSI(J)	178
	179
C-----PRINT TRANSFORMED DATA	180
PRINT 200, J,ANH3(J),ANO3(J),UREA(J),SAMT(J),CA(J),ANA(J),AMG(J),	181
1HC03(J),CL(J),C03(J),S04(J)	182
781 IF (IRERUN.EQ.1) CHECK(J)=1.0	183
1 CONTINUE	184
	185
C-----READ FERTILIZER APPLICATION DATES	186
READ 104,ITOT,(IADD(K),K=1,ITOT)	187
	188
IF (NBYPAS.EQ.1) GO TO 9002	189
C-----READ ORGANIC-N APPLICATION DATES	190
READ 104,JTOT,(IORNAP(K),K=1,JTOT)	191
	192
9002 CONTINUE	193
C-----READ IRRIGATION WATER APPLICATION DATES	194
READ 104,IRTOT,(IRR(K),K=1,IRTOT)	195
	196
C-----STORE FERTILIZER APPLICATIONS ON TAPE 9	197
DO 802 I=1,ITOT	198
READ 100,(FERT(J),J=1,7)	199
WRITE(9) (FERT(J),J=1,7)	200
802 CONTINUE	201
	202
IF (NBYPAS.EQ.1) GO TO 9003	203
C-----STORE ORGANIC APPLICATIONS ON TAPE 10	204
DO 803 I=1,JTOT	205
READ 100,(OFERT(J),J=1,3)	206
WRITE(10) (OFERT(J),J=1,3)	207
803 CONTINUE	208
9003 CONTINUE	209
	210
C-----SET SEGMENT ONE VALUES EQUAL TO ZERO	211
16 ANH3(1)=ANO3(1)=CA(1)=ANA(1)=AMG(1)=HC03(1)=UREA(1)=CL(1)=C03(1)=	212
1S04(1)=0.0	213
IF (IRERUN.NE.0) 508,720	214
508 REWIND 8	215
REWIND 9	216
REWIND 10	217
IF (NTEMPIN.EQ.0) GO TO 522	218
IF (NBYPAS.EQ.1) GO TO 9004	219
	220
C-----SPACE TAPE8 FORWARD THE PROPER NO. OF RECORDS	221
DO 510 I=1,NTEMPIN	222
510 READ (8)	223
	224
9004 CONTINUE	225

522	IF(NFERTIN.EQ.0) GO TO 550	226
C-----	SPACE TAPE9 FOREWARD THE PROPER NO. OF RECORDS	227
	DO 511 I=1,NFERTIN	228
511	READ (9)	229
		230
550	IF(NORGIN.EQ.0) GO TO 513	231
		232
	IF(NBYPAS.EQ.1) GO TO 9005	233
C-----	SPACE TAPE10 FOREWARD THE PROPER NO. OF RECORDS	234
	DO 512 I=1,NORGIN	235
512	READ (10)	236
		237
	9005 CONTINUE	238
	GO TO 513	239
720	REWIND 8	240
	REWIND 9	241
	REWIND 10	242
	NFERTIN = NORGIN = NTEMPIN = 0	243
513	CONTINUE	244
	ISWCH = 1	
	IF(IPRINTJ.NE.0) CALL PPNT1(IPRINTI,IPRINTJ)	246
		247
C-----	CALL SUBROUTINE TO EXECUTE PROGRAM FOR EACH DAILY TIME INTERVAL	248
	CALL EXECUTE	249
		250
C-----	CHECK FOR END OF RUN	251
	ENDFILE 2	252
	IF(MOD(IDAY,IDYSTP).EQ.0) 726,721	253
726	IF(YEAR.EQ.ISTOP) GO TO 721	254
		255
C-----	RESET COUNTERS	256
	ICOUNT = 0 SYEAR = YEAR + 1 SLL = 1	257
	ILO=IDYSTR	258
	ILAP = ILO	259
	IHI=IDYSTP	
	IF(YEAR.EQ.ISTOP) IHI=4M	260
	IF(ICONT1.EQ.0) GO TO 720	261
	REWIND 10	
C-----	READ IRRIGATION WATER APPLICATION DATES FOR NEXT YEAR	
	READ 104,IRTOT, (IRR(K),K=1,IRTOT)	
C-----	READ LAST ORGANIC-N APPLICATION FOR NEXT YEAR	
	READ 100,(OFERT(J),J=1,3)	
	IOCOU = JTOT - 1	
	JPAS = 0	
	DO 1321 I=1,IOCOU	
1321	READ (10)	
	WRITE(10) (OFERT(J),J=1,3)	
	REWIND 10	
	GO TO 720	264
721	CONTINUE	265
C 721	ENDFILE 2	266
C	ENDFILE 15	267
	NTEMPIN=NTEMPIN-1	268
	ICOUNT=ICOUNT-1	269
		270
C-----	EITHER PUNCH A RERUN DECK OR WRITE RERUN (RESTART) DATA ON TAPE3	271
	IF(IDAY.EQ.IDYSTP) ICOUNT = NFERTIN = NORGIN = NTEMPIN = 0	272
	IF(IPUNCH.EQ.0) 502,503	273
502	REWIND 3	274
	WRITE (3) ICOUNT,NFERTIN,NORGIN,NTEMPIN,(ANH3(J),ANO3(J),UREA(J)	275
	1,CA(J),ANA(J),AMG(J),HCO3(J),CL(J),CO3(J),SO4(J),EC(J),XX5(J),CAL(276
	2J),BD(J),SAMT(J),CN1(J),ORN(J),RN(J),RC(J),ES(J),C5(J),SA5(J),CASO	277
	3(J),AGSO(J),BNH4(J),XTRCT(J),ANETLIM(J),AZE(J),IIK(J),	278
	4PCO2(J),AKCS(J),AKCM(J),J=2,Q)	
	GO TO 561	
503	PUNCH 505, ICOUNT,NFERTIN,NORGIN,NTEMPIN,(ANH3(J),ANO3(J),UREA(J)	279
	1,CA(J),ANA(J),AMG(J),HCO3(J),CL(J),CO3(J),SO4(J),EC(J),XX5(J),CAL(280
	2J),BD(J),SAMT(J),CN1(J),ORN(J),RN(J),RC(J),ES(J),C5(J),SA5(J),CASO	281
	3(J),AGSO(J),BNH4(J),XTRCT(J),ANETLIM(J),AZE(J),IIK(J),	282
	4PCO2(J),AKCS(J),AKCM(J),J=2,Q)	283

C 561	REWIND 2	284
C	REWIND 3	285
C----	PRINT RESTART DATA	286
561	PRINT 9100, IDAY, YEAR, ICOUNT, NFERTIN, NORGIN, NTEMPIN, Q	287
	PRINT 9101, (ANH3(J), ANO3(J), UREA(J)	288
	1, CA(J), ANA(J), AMG(J), HCO3(J), CL(J), CO3(J), SO4(J), EC(J), XX5(J), CAL(J)	289
	2(J), BD(J), SAMT(J), CN1(J), ORN(J), RN(J), RC(J), ES(J), CS(J), SAS(J), CASO	290
	3(J), AGSO(J), BNH4(J), XTRCT(J), J=2, Q)	291
9100	FORMAT(1H1, 5X, *RESTART DATA FROM DAY=*, I4, * YEAR=*, I5//, 5X,	292
	1 * ICOUNT=*, I5, * NFERTIN=*, I5, * NORGIN=*, I5, * NTEMPIN=*, I5//,	293
	2 5X, *(ANH3(J), ANO3(J), UREA(J), CA(J), ANA(J), AMG(J), HCO3(J), CL(J), C	294
	303(J), SO4(J), EC(J), XX5(J), CAL(J) * // 5X, * BD(J), SAMT(J), CN1(J), OR	295
	4N(J), RN(J), RC(J), ES(J), CS(J), SAS(J), CASO(J), AGSO(J), BNH4(J), XTRCT(296
	5J), J=2, Q) WHERE Q= * I3)	297
9101	FORMAT(6E13.5/6E13.5/6E13.5/6E13.5/2E13.5)	298
	STOP	299
		300
98	FORMAT(10A8)	301
100	FORMAT(16F5.0)	302
104	FORMAT(16I5)	
105	FORMAT(11F5.0/16I5/16I5)	304
106	FORMAT(11I5)	305
107	FORMAT(5F5.0)	306
200	FORMAT(I5, 11F10.3)	307
201	FORMAT(//1X*INITIAL SOIL ANALYSES(MEQ/L OF SOIL EXTRACT)--(ORG=	308
	1UG/GM OF SOIL)*//2X*HZN*	309
	1 7X*NH3*7X*NO3*6X*UREA*7X*ORG*8X*CA*8X*NA*8X*Mg*6X *HCO3*8X*CL	310
	1*7X*CO3*7X*SO4*)	311
202	FORMAT(//1X*TRANSFORMED SOIL ANALYSES(UG/SEGMENT OF SOIL)*//2X*SEF	312
	1* 7X*NH3*7X*NO3*6X*UREA*7X*ORG*8X*CA*8X*NA*8X*Mg*6X *HCO3*8X*CL	313
	1*7X*CO3*7X*SO4*)	314
505	FORMAT(4I5/, (6E13.5/6E13.5/6E13.5/6E13.5/*E13.5, I5/3E13.5))	315
101	FORMAT(F5.0, F10.0, 2F5.0)	
784	FORMAT(5F10.0)	
801	FORMAT(2X, F8.0, 7F10.0)	317
1100	FORMAT(3F5.0)	318
1101	FORMAT(80I1)	
	END	

SUBROUTINE COMBINE

SUBROUTINE COMBINE(IDAY, IPRINT, JPRINT)		COMBINE
		COMBINE
		COMBINE
COMMON/SALT/SERATIO(25), SBYPAS		
COMMON/3/IFLBYPAS, ISEGST		1
COMMON/8YPAS/NBYPAS, IDYSTR, IDYSTP, ILO, IHI, ZDUM(3)		
COMMON/SABLE/SUMS(3)		3
COMMON/EEE/PSUM, DIFNH4, DIFNO3, TPLANT		4
COMMON/XXY/ICHECK, ICOUNT, ZDUM1(5)		
COMMON/YYY/START, IDTE, MONTH, III, LL		6
COMMON/AFG/ENH3, II, LLL, IOP, ANETLIM(25)		7
		COMBINE
C-----	THIS SUBROUTINE CALLS THE COMPUTATIONAL SUBROUTINES AND ASSEMBLES	COMBINE
C-----	THEIR DELTA VALUES	COMBINE
COMMON/XXX/DELX, DELT, MM, WTART, BD(25), TEN(25), CHECK(25), MOISIN		8
1(25), CMH201(25), MOISOUT(25), ANO3(25), ANH3(25), UREA(25), ORN		9
2(25), CA(25), ANA(25), AMG(25), HCO3(25), CL(25), CO3(25), SO4(25)		10
3), ES(25), CS(25), SAS(25), XX5(25), CASO(25), AGSO(25), BNH4(25),		11
4EC(25), CN1(25), SAMT(25), RN(25), RC(25), TEM(25), CAL(25), Q, CRO		12
1P, SPACE(36), ISWCH, CUMSUM, SUMOUT, REDUCE		
COMMON/GIRL/UREA1, UREA2, DNH31, DNH32, DNO31, DNO32, CA1, ANA1, AMG1,		14
1HCO31, CL1, CO31, SO41, KKK, PPPP(4)		
COMMON/CO2/PCO2(25), IPCO2		

DIMENSION CONVERT(25),EXNH3(25),EXCA(25),EXANA(25),EXAMG(25),	16
1DELNO3(25),DELNH3(25),DELOGRN(25),DELUPEA(25),EXHCO3(25),EXCO3(25)	17
2,EXSO4(25),EXCL(25),EXBNH4(25),FLNO3(25),FLNH3(25),FLUREA(25),FLCA	18
3(25),FLANA(25),FLAMG(25),FLHCO3(25),FLCL(25),FLCO3(25),FLSO4(25),	19
4PLNO3(25),PLNH4(25),DELBH4(25),ANET1(25),ANET2(25),ANET3(25),ADDI	20
5T(25),ADDIT1(25),DELRN(25),DELCRC(25)	21
INTEGER Q,SBYPAS	23
REDUCE = 1.0	25
IFLAYPA=0	
NOW = 2	
IF(ISEGST.EQ.1) NOW = 1	
IFACT = REDUCE	28
ISSET = IFACT + 2 \$F = 1.0	29
IF(II.EQ.LLL) K=2	30
C-----COMPUTE DELTA VALUES FOR EACH SOIL SEGMENT	31
50 DO 1 I=NOW,Q	32
C-----CALL SHUT-OFF SUBROUTINE	33
C CALL CHK(L1,L2,L3,I,EXNH3(I),EXCA(I),EXANA(I),EXAMG(I),DELNO3(I),	34
C 1DELNH3(I),DELOGRN(I),DELUPEA(I))	35
C IF(II.EQ.1.OR.ISSET.LE.IFACT)3,4	36
3 L1=L2=L3=0	37
4 CONTINUE	38
C-----SET A UNIT CONVERSION CONSTANT	39
CONVERT(I) = DELX*RD(I)	40
C	41
C-----IF SO INDICATED	42
C-----ENTER SECTION TO COMPUTE AMOUNT OF LIME WHICH HAS PRECIPITATED	43
IF(IOP.EQ.0) GO TO 205	44
C	45
C-----COMPUTE AMOUNT OF LIME IN SYSTEM EXCLUSIVE OF SOLID STATE	46
C-----UNITS ARE UG OF CACO3 PER SEGMENT OF SOIL	47
ASUM1 = CA(I)*2.497 + CASO(I)*CMH2O1(I)*100.09E3 + E5(I)*100.09E6*	48
1CONVERT(I) + XX5(I)*100.09E6*CONVERT(I)	49
205 CONTINUE	50
IF(SBYPAS.EQ.1) GO TO 333	51
C-----CALL THE EXCHANGE SUBROUTINE	52
IF(L1.EQ.0) CALL XCHANGE(I,EXNH3(I),EXCA(I),EXANA(I),EXAMG(I),EXHC	53
103(I),EXCO3(I),EXSO4(I),EXCL(I),EXBNH4(I))	54
GO TO 334	55
333 CALL SALTRP(CONVERT(I),ANH3(I),BNH4(I),I)	56
EXNH3(I) = EXBNH4(I) = 0.0	57
334 IF(IOP.FQ.0) GO TO 206	
C	59
C-----AGAIN COMPUTE LIME IN SYSTEM EXCLUSIVE OF SOLID STATE	60
ASUM2 = CA(I)*2.497 + CASO(I)*CMH2O1(I)*100.09E3 + E5(I)*100.09E6*	61
1CONVERT(I) + XX5(I)*100.09E6*CONVERT(I)	62
C	63
C-----ADD OR SUBTRACT ANY DIFFERENCE IN LIME TO SOLID STATE LIME STORAGE	64
ANETLIM(I) = ANETLIM(I) + ASUM1 - ASUM2	65
C	66
C-----COMPUTE POROSITY OF SOIL SEGMENT, ASSUME PARTICLE DENSITY IS 2.65	67
POR = 1. - RD(I)/2.65	68
C	69
C-----COMPUTE UG OF CACO3 WHICH CAN PRECIPITATE IN PORE SPACE	70
APOR = DELX*POR*2.828E6	71
C	72
C-----COMPARE UG OF LIME PRECIPITATED WITH UG OF CACO3 NECESSARY TO	73
C-----FILL THIS SPACE	74
C-----ASSUME DENSITY OF CACO3 (CALCITE) IS 2.828	75
C	76
C-----IF PORE SPACE HAS BEEN EXCEEDED, PRINT DAY, SEGMENT, MASS OF CACO3	77
C-----WHICH CAN PRECIPITATE IN PORE SPACE, AND MASS OF CACO3 WHICH HAS	78
C-----PRECIPITATED	79
IF(ANETLIM(I).GE.APOR) PRINT 201,III,I,APOR,	80
1ANETLIM(I)	81

206	CONTINUE	82
	IF (L1.NE.0) EXNH3(I)=EXCA(I)=EXANA(I)=EXAMG(I)=EXHC03(I)=EXC03(I)=	83
	1EXS04(I)=EXBNH4(I)=EXCL(I)=0.0	84
		85
	IF(NRYPAS.EQ.1) GO TO 9008	86
C-----	CALL THE NITROGEN TRANSFORMATION SUBROUTINE	87
	IF (L2.EQ.0) CALL TRNSFM(I,CONVERT(I),DELUREA(I),DELOGRN(I),DELNH3(I),	88
	1I),DELNO3(I),DELBH4(I),DELRN(I),DELC(I),II)	89
		90
9008	CONTINUE	91
	IF (IFLAYPA.EQ.1) GO TO 8000	92
C-----	CALL THE FLOW SUBROUTINE	93
	CALL FL(I,FLN03(I),FLNH3(I),FLUREA(I),FLCA(I),FLANA(I),	94
	1,FLAMG(I),FLMC03(I),FLCL(I),FLC03(I),FLS04(I))	95
8000	CONTINUE	96
	IF (II.NE.1) GO TO 20	97
	IF (ISET.LE.IFACT) GO TO 20	98
		99
	IF (NRYPAS.EQ.1) GO TO 9009	100
C-----	CALL THE PLANT NUTRIENT UPTAKE SUBROUTINE	101
	IF (IDTE.EQ.1.OR.IDTE.EQ.16.OR.IDAY.EQ.LL) CALL UPTAKE(II,PLN03(I),	102
	1PLNH4(I),DELT,DELX)	103
20	CONTINUE	
61	CON = AN03(I)/CMH201(I)	111
	CON1 = ANH3(I)/CMH201(I)	112
C-----	TEST FOR LOW N03 CONCENTRATION	113
	IF (CON.LT.0.2) 62,63	114
62	ADDIT(I) = 0.0	115
	GO TO 64	116
63	ADDIT(I) = PLN03(I)	117
		118
C-----	TEST FOR LOW NH4 CONCENTRATION	119
64	IF (CON1.LT.0.2) 65,66	120
65	ADDIT(I) = 0.0	121
	GO TO 67	122
66	ADDIT1(I) = PLNH4(I)	123
67	CONTINUE	124
C-----	COMPUTE NET CHANGES FOR NH4, UREA, AND N03	125
	ANET1(I) = DELNH3(I) + FLNH3(I) + EXNH3(I) + ADDIT1(I)	126
	ANET2(I) = DELUREA(I) + FLUREA(I)	127
	ANET3(I) = DELNO3(I) + FLN03(I) + ADDIT(I)	128
		129
		130
9009	CONTINUE	131
C-----	TEST TO DETERMINE IF SEGMENT ONE IS BEING CONSIDERED	132
	IF (KKK.EQ.1) 77,1	133
77	SNH31=DNH31 \$SN031=DN031 \$SREA1=UREA1 \$SA1=CA1 \$SNA1=ANA1	134
	SMG1=AMG1 \$SC031=HC031 \$SL1=CL1 \$S031=C031 \$RO41=S041	135
1	CONTINUE	136
		137
		138
		139
C-----	TEST TO DETERMINE IF ADDITIONAL TIME STEPS ARE BEING USED	140
	IF (ISET.LE.IFACT) GO TO 16	141
		142
	IF (NRYPAS.EQ.1) GO TO 9010	143
C-----	TEST TO DETERMINE IF MASS IN SYSTEM WILL BE EXCEEDED	144
	DO 5 I=2,0	145
	IF (ANH3(I) + ANET1(I).LT.0.0) GO TO 14	146
	IF (UPEA(I) + ANET2(I).LT.0.0) GO TO 14	147
	IF (AN03(I) + ANET3(I).LT.0.0) GO TO 14	148
5	CONTINUE	149
	GO TO 16	150
		151
C-----	USE SMALLER TIME STEPS IF NECESSARY	152
14	ISET = 1 SF = IFACT	153
		154
9010	CONTINUE	155
C-----	UPDATE THE MASSES IN STORAGE	156
16	DO 6 I=NOH,0	157
	ANH3(I) = ANH3(I) + ANET1(I)/F SUPEA(I) = UREA(I) + ANET2(I)/F	158

C-----CALL SURROUTINE TO OUTPUT LEACHATE VALUES	226
CALL OUTPT(K)	227
	228
C-----CALL MASS BALANCE ROUTINE FOR NITROGEN	229
IF(NRYPAS.EQ.1) GO TO 9013	230
IF(ISWCH.EQ.1.AND.II.EQ.JPRINT) CALL MCHECK	231
9013 CONTINUE	232
	233
	234
C-----RETURN TO SURROUTINE EXECUTE	235
RETURN	236
	237
	238
	239
100 FORMAT(15,14E9.3)	240
201 FORMAT(1X*THE SOIL POROSITY EQUALED ZERO DUE TO PRECIPITATED LIME	241
10N DAY NO.*.15./1X*DEPTH SEGMENT NO.*.15./10X*POROSITY ALLOWS*2X.	242
2E10.3.2X*UG OF LIME TO PPRECIPITATE*, 5X,E10.3.2X*UG OF LIME HAVE	243
3PRECIPITATED*)	244
END	

SUBROUTINE XCHANGE

SUBROUTINE XCHANGE(J,EXNH3,EXCA,EXANA,EXAMG,EXHC03,EXC03,EXS04,EXCXCHANGE	
1L,EXRNH4)	XCHANGE
C-----THIS IS THE EXCHANGE SUBROUTINE	XCHANGE
	XCHANGE
COMMON/IP/CAS(25),AMGS(25)	
	XCHANGE
COMMON/AION/U	
COMMON/TPNIT/ISTR(25),ACTCA(25),IOPN,ISETN(25)	
COMMON/XXX/DELX,DELT,MM,START,BD(25),TEN(25),CHECK(25),MOISIN	XCHANGE
1(25),CMH202(25),MOISOUT(25),ANOZ(25),ANH2(25),UPEA(25),OPN	
2(25),CZ(25),ANZ(25),AMZ(25),HCO2(25),CY(25),CO2(25),SO2(25	XCHANG1
3),EZ(25),CX(25),SAZ(25),XXZ(25),CASZ(25),AGSZ(25),BNH2(25),XCHANG1	
4EY(25),CN1(25),SAMT(25),RN(25),RC(25),TEM(25),CAZ(25),Q.CROXCHANG1	
1P.XTPACT,SUMNO3,THOR(4),TO,IDAY,U3(25),CH,CH1,IRERUN,SPC(4),IIK(25	
1),AZE(25)	
COMMON/1/XTRCT(25),AKCS(25),AKCM(25)	
COMMON/CO2/PCO2(25),PCO2	
	XCHANG1
DIMENSION CMH201(25)	XCHANG1
	XCHANG1
DATA(TES=1.E-100)	
	XCHANG1
C-----SET EXCHANGE CONSTANTS	
DA = AKCS(J)	
D = AKCM(J)	
C-----SET SEGMENT VOLUMES	XCHANG1
CMH201(J)=CMH202(J)	XCHANG2
C-----COMPUTE MOISTURE CONTENT ON A PERCENT BASIS	XCHANG2
B1 = CMH201(J)/(BD(J)*DELX)	XCHANG2
B1 = B1*100.	XCHANG2
	XCHANG2
C-----COMPUTE SEGMENT VOLUMES BASED ON INITIAL SOIL ANALYSES	XCHANG2
IF(CHECK(J).EQ.0.0) CMH201(J)=XTRCT(J)*DELX*BD(J)	XCHANG2
	===== 2
	XCHANG2
C-----CONVERT UNITS FROM UG/SEGMENT TO MOLES/LITER	XCHANG2
	XCHANG2
C-----RESET STORAGE LOCATIONS FOR USE IN THIS ROUTINE	XCHANG3
1005 ANH4 = ANH2(J)/CMH201(J)/14000.	XCHANG3
A = CZ(J)/CMH201(J)/40080.	XCHANG3
S = ANZ(J)/CMH201(J)/22990.	XCHANG3
F = AMZ(J)/CMH201(J)/24320.	XCHANG3
HCO3 = HCO2(J)/CMH201(J)/61000.	XCHANG3
CO3 = CO2(J)/CMH201(J)/60000.	XCHANG3

```

      ANO3(I) = ANO3(I) + ANET3(I)/F  SCA(I) = CA(I) + FLCA(I)/F + EXCA(I)  159
      ANA(I) = ANA(I) + FLANA(I)/F + EXANA(I)  SAMG(I) = AMG(I) + FLAMG(I)  160
      1)/F + EXAMG(I)  161
      HCO3(I) = HCO3(I) + FLHCO3(I)/F + EXHCO3(I)  $CL(I) = CL(I) + FLCL  162
      1(I)/F + EXCL(I)  163
      CO3(I) = CO3(I) + FLCO3(I)/F + EXCO3(I)  $SO4(I) = SO4(I) + FLSO4(I)  164
      1(I)/F + EXSO4(I)  165
      BNH4(I) = BNH4(I) + EXBNH4(I) + DELBNH4(I)/F  $ORN(I) = ORN(I) + DELORG  166
      1N(I)/F  $RN(I) = RN(I) + DELRN(I)/F  $RC(I) = RC(I) + DELRC(I)/F  167
31  IF(I.EQ.2)36,37  180
C-----UPDATE MASSES CONTAINED ON SOIL SURFACE
36  ANH3(1) = ANH3(1) - SNH31/F$ANO3(1) = ANO3(1) - SNO31/F  1
      UREA(1) = UREA(1) - SREA1/F$CA(1) = CA(1) - SA1/F  182
      ANA(1) = ANA(1) - SNA1/F$AMG(1) = AMG(1) - SMG1/F  183
      HCO3(1) = HCO3(1) - SCO31/F  $CL(1) = CL(1) - SL1/F  184
      CO3(1) = CO3(1) - SO31/F$SO4(1) = SO4(1) - RO41/F  185
37  CONTINUE  186
      IF(NRYPAS.EQ.1) GO TO 9011  187
C-----CHECK AND CORRECT FOR ANY NEGATIVE VALUES
      IF(BNH4(I).LT.0.0) CALL NEGN(BNH4(I),ANO3(I),EXBNH4(I),ANH3(I),
      1ORN(I),0.0,0.0,0.0,CONVERT(I),3)
      IF(ANH3(I).LT.0.0) CALL NEGN(ANH3(I),ANO3(I),EXNH3(I),ADDIT1(I),
      1ORN(I),BNH4(I),ANH3(I-1),CONVERT(I),1)
      IF(ANO3(I).LT.0.0) CALL NEGN(ANO3(I),0.0,0.0,ADDIT(I),0.0,0.0,
      10,ANO3(I-1),CONVERT(I),2)
      IF(UREA(I).LT.0.0) CALL NEGN(UREA(I),0.0,0.0,0.0,0.0,0.0,0.0,UREA(I-1)
      1,CONVERT(I),4)
      IF(I.EQ.0) 30,9011
C-----KEEP TRACK OF TOTAL-N LEACHED FROM SYSTEM  170
30  SUMOUT = SUMOUT + (DNO32 + DNH32 + UREA2)/F
      SUMS(1) = SUMS(1) + DNO32/F
      SUMS(2) = SUMS(2) + DNH32/F  175
      SUMS(3) = SUMS(3) + UREA2/F  176
9011 CONTINUE  177
      IF(ORN(I).LT.0.0) ORN(I) = 0.0
      IF(CA(I).LT.0.0) CA(I) = 0.0  194
      IF(ANA(I).LT.0.0) ANA(I) = 0.0  195
      IF(AMG(I).LT.0.0) AMG(I) = 0.0  196
      IF(HCO3(I).LT.0.0) HCO3(I) = 0.0  197
      IF(CL(I).LT.0.0) CL(I) = 0.0  198
      IF(CO3(I).LT.0.0) CO3(I) = 0.0  199
      IF(SO4(I).LT.0.0) SO4(I) = 0.0  200
      IF(NRYPAS.EQ.1) GO TO 9012  201
C-----KEEP TRACT OF PLANT UPTAKE OF N  202
      IF(ISET.LE.IFACT)17,18  203
17  PL1 = ADDIT(I)/IFACT  SPL2 = ADDIT1(I)/IFACT  204
      TPLANT = TPLANT + PLNH4(I)/IFACT + PLNO3(I)/IFACT  205
      L1=L2=L3=0  206
      GO TO 25  207
18  PL1 = ADDIT(I)  SPL2 = ADDIT1(I)  208
      TPLANT = TPLANT + PLNH4(I) + PLNO3(I)  209
25  PSUM = PSUM + PL1 + PL2  210
      IF(ANH3(I).EQ.0.0) DIFNH4 = DIFNH4 + PL2  211
      IF(ANO3(I).EQ.0.0) DIFNO3 = DIFNO3 + PL1  212
9012 CONTINUE  213
      IF(ISET.LT.IFACT) GO TO 6  214
      IF(MOD(IDAY,IPRINT).EQ.0.AND.II.EQ.JPRINT)2,6  215
C-----PRINT VALUES FOR THE COMPONENTS (UG/SEGMENT) AND SEGMENT VOLUMES  216
C----- (PL)  217
2  VNH3 = RNH4(I)*14.0E6*CONVERT(I)  218
      ESP = SAS(I)/EC(I)*100.  219
      PRINT 100,I,ANH3(I),ANO3(I),UREA(I),ORN(I),CA(I),ANA(I),AMG(I),  220
      1HCO3(I),CL(I),SO4(I),VNH3,CMH201(I),ESP,PCO2(I)  221
6  CONTINUE  223
      ISET = ISET + 1  224
      IF(ISET.LE.IFACT) GO TO 50  225

```

```

      H = CY(J)/CMH201(J)/35460.
      G = SOZ(J)/CMH201(J)/96100.
      ANO3 = ANOZ(J)/CMH201(J)/14000.
      ET = EZ(J)      SCT = CX(J)      SSAT = SAZ(J)      SXXT=XXZ(J)
      RNH4 = RNHZ(J)
      IF(CHECK(J).EQ.0.0) GO TO 2
      AGSO = AGSZ(J)  SCASO = CASZ(J)
      G = G - AGSO - CASO
      A = A - CASO
      F = F - AGSO
2     CONTINUE
      EC = EY(J)      S CAL = CAZ(J)
      IF(CHECK(J).EQ.0.0)200,201

C-----CALL THE EQUILIRIUM EXCHANGE SUBROUTINE IF THIS IS THE FIRST
C-----TIME INTERVAL

200  CALL EQEXCH(A,F,S,H,G,HCO3,C03,EC,ANH4,ET,CT,SAT,
      1CASO,AGSO,BNH4,U,ANO3,DA,D)
      ET = ET/2.
      CT = CT/2.
      A = A/2.
      F = F/2.
      XXT = XXT/2.E5
201  CONTINUE
      DNH4=0.22
      R = B1
      IF(CHECK(J).NE.0.0) U=SQRT(2.0*(A+F+G+C03)+0.5*(S+HCO3+H+ANH4+ANO3
      1))
      IF(CHECK(J).EQ.0.0)299,298
299  B = XTRACT(J)*100.
      IF(CAL)1001,602,603
602  IIK(J) = 1
      AZE(J) = 3.46737E-5
      GO TO 604
603  IIK(J) = 2
      ZE = (A*HCO3**2*EXP(-7.033*U/(1.0+U)))
      AZE(J) = ( R**1.68)*ZE
604  RATIO=B/R1
      A=A*RATIO      SG=G*RATIO
      F=F*RATIO      SH=H*RATIO
      S=S*RATIO      SCASO = CASO*RATIO
      AGSO=AGSO*RATIO      $ANH4=ANH4*RATIO
      C03 = C03*RATIO
      HCO3 = HCO3*RATIO
298  R = 1.E5/B1
      IF(IPC02.EQ.1) GO TO 300
      ZE = AZE(J)/(B1 **1.68)
      PC02(J) = ZE/1.778E-6
      GO TO 301
300  ZE = PC02(J)*1.778E-6
301  IK = IIK(J)
24  A1=A
      IF(XXT)4,4,26
4    U=SQRT(2.0*(A+F+G)+0.5*(S+H+HCO3+ANH4+ANO3))
      AA=EXP (-9.366*U/(1.0+U))
      IF(2.4E-5-A*G*AA)26,18,18
26  X=0.0
      U=SQRT(2.0*(A+F+G)+0.5*(S+H+HCO3+ANH4+ANO3))
      9B=A+G
      EX=(9.366*U)/(1.0+U)
      CC=A*G-(2.4E-5)*EXP (FX)
      R=SQRT(9B*9B-4.0*CC)
      X=(-9B+R)/2.0
      CAS1=4.897E-3-CASO
      DEL=R*XXT-CAS1
      IF(DEL-X)27,28,28
27  X=XXT*B
      XXT=0.0
      CAS1=0.0
      A=A+X
      G=G+X

```


U=SQRT(2.0*(A+F+G)+0.5*(S+H+HC03+ANH4+4NO3))	
AA=EXP (-9.366*U/(1.+U))	
7 BR=- (4.9E-3+AA*A+AA*G)	XCHAN10
CC=AA*A*G-4.9E-3*CASO	XCHAN10
XXX=BB*BR-4.0*AA*CC	XCHAN10
IF (XXX) 35.35.36	XCHAN10
35 X1=0.0	XCHAN10
GO TO 37	XCHAN10
36 X1=(-BR-SQRT (XXX))/(2.0*AA)	XCHAN10
37 CASO=CASO+X1	XCHAN10
A=A-X1	XCHAN10
G=G-X1	XCHAN10
GO TO 44	XCHAN11
18 IF (G) 1.1.6	XCHAN11
6 IF (A) 1.1.7	XCHAN11
1 IF (CASO) 44.44.7	XCHAN11
28 A=A+X	XCHAN11
G=G+X	XCHAN11
XXT=XXT-X/B	XCHAN11
CASO=CASO+CAS1	XCHAN11
XXT=XXT-CAS1/B	XCHAN11
44 A2=A	XCHAN11
IF (S) 80.181.80	XCHAN12
181 IF (SAT) 80.515.80	XCHAN12
80 IJ=2	XCHAN12
404 IF (SAT-ET) 402.403.403	XCHAN12
402 Z=SAT/10.	XCHAN12
Z1=Z	XCHAN12
GO TO 5	XCHAN12
403 Z=ET/10.	XCHAN12
Z1=Z	XCHAN12
5 EX=EXP ((-2.341*U)/(1.0+U))	XCHAN12
AA=-4.0*DA*DA*RB	XCHAN13
RR=4.0*RB*(EX+2.0*DA*DA*ET*RB-DA*DA*S)	XCHAN13
CC=4.0*EX*(A*SAT*RB)-4.0*DA*DA*RB*ET*(B*ET+2.0*S)-DA*DA*S*S	XCHAN13
NO=SAT*EX*(4.0*A*SAT*RB)+2.0*DA*DA*ET*S*(2.0*RB*ET+S)	XCHAN13
EE=SAT*SAT*A*EX-DA*DA*S*S*ET*ET	XCHAN13
81 ZZ=-(((AA*Z+BB)*Z+CC)*Z+DD)*Z+EE)	XCHAN13
ZZZ=(((4.0*AA*Z+3.0*BB)*Z+2.0*CC)*Z+DD)	XCHAN13
IF (ABS(ZZ).LT.TES.OR.ABS(ZZZ).LT.TES) GO TO 515	XCHAN13
ZZ=ZZ/ZZZ	XCHAN13
IF (ABS(ZZ).LT.TES.OR.ABS(Z) .LT.TES) GO TO 515	XCHAN13
ZZZ=ZZ/Z	XCHAN14
Z=Z+ZZ	XCHAN14
IF (ABS(ZZZ)-.001) 83.83.81	XCHAN14
83 A=A+R*Z	XCHAN14
IF (A) 510.510.512	XCHAN14
552 SAT=SAT-2.*Z	XCHAN14
551 ET=ET+Z	XCHAN14
550 S=S+2.*R*Z	XCHAN14
510 A=A-R*Z	XCHAN14
Z=-Z1	XCHAN14
GO TO 81	XCHAN15
512 S=S-2.*R*Z	XCHAN15
IF (S) 550.550.513	XCHAN15
513 ET=ET-Z	XCHAN15
IF (ET) 551.551.514	XCHAN15
514 SAT=SAT+2.0*Z	XCHAN15
IF (SAT) 552.552.515	XCHAN15
515 A3=A	XCHAN15
RR=A+R*(CT+D*ET)+D*F	XCHAN15
AA=8*(1.0-D)	XCHAN15
CC=(A*CT-D*F*ET)	XCHAN16
R=SQRT (BB*BB-4.0*AA*CC)	XCHAN16
Y=(-RB+R)/(2.0*AA)	XCHAN16
A=A+R*Y	XCHAN16
F=F-R*Y	XCHAN16
ET=ET-Y	XCHAN16
CT=CT+Y	XCHAN16
A4=A	XCHAN16
AA = 8*(1.0-DNH4)	XCHAN16
BB = ANH4 + 8*(SAT+DNH4*PNH4) + DNH4*S	XCHAN16
	XCHAN17

CC = ANH4*SAT - DNH4*S*BNH4	XCHAN17
R=SQRT(RR*BB-4.0*AA*CC)	XCHAN17
Y=(-RR+P)/(2.0*AA)	XCHAN17
BNH4 = RNH4 - Y	XCHAN17
SAT = SAT + Y	XCHAN17
ANH4 = ANH4 + R*Y	XCHAN17
S = S - R*Y	XCHAN17
IF(G)790,790,791	XCHAN17
791 IF(F)790,790,792	XCHAN17
792 AA=EXP(-9.366*U/(1.+U))	XCHAN18
BB=-(5.9E-3+AA*F+AA*G)	XCHAN18
CC=AA*F*G-5.9E-3*AGSO	XCHAN18
XXXX=BB*BB-4.0*AA*CC	XCHAN18
IF(XXXX)793,793,794	XCHAN18
793 X1=0.0	XCHAN18
GO TO 795	XCHAN18
794 X1=(-BB-SQRT(XXXX))/(2.0*AA)	XCHAN18
795 AGSO=AGSO+X1	XCHAN18
F=F-X1	XCHAN18
G=G-X1	XCHAN19
790 CONTINUE	XCHAN19
GO TO (600,601),IK	XCHAN19
601 AA=4.0	XCHAN19
BB=4.*(HC03+A)	XCHAN19
CC=HC03**2+4.*A*HC03	XCHAN19
DD=A*HC03**2-ZE*EXP (7.033*U/(1.+U))	XCHAN19
IF(HC03-A)61,61,62	XCHAN19
61 Z=-HC03/4.	XCHAN19
GO TO 650	XCHAN19
62 Z=-A/2.	XCHAN20
650 Z1=Z	XCHAN20
63 ZZ=-(((AA*Z+BB)*Z+CC)*Z+DD)	XCHAN20
ZZZ=(((3.0*AA*Z+2.0*BB)*Z+CC)	XCHAN20
IF(ABS(ZZ).LT.TES.OR.ABS(ZZZ).LT.TES) GO TO 600	XCHAN20
ZZ=ZZ/ZZZ	XCHAN20
IF(ABS(ZZ).LT.TES.OR.ABS(Z) .LT.TES) GO TO 600	XCHAN20
ZZZ=ZZ/Z	XCHAN20
Z=Z+ZZ	XCHAN20
IF(ABS(ZZZ)-.001)64,64,63	XCHAN20
64 A=A+Z	XCHAN21
HC03=HC03+2.*Z	XCHAN21
IF(HC03)752,752,651	XCHAN21
752 HC03=HC03-2.*Z	XCHAN21
A=A-Z	XCHAN21
Z=-Z1	XCHAN21
GO TO 63	XCHAN21
651 IF(A) 752,752,753	XCHAN21
753 CAL=CAL-Z	XCHAN21
600 IF(IX.EQ.2) GO TO 606	
ZX=(A*HC03**2*EXP(-7.033*U/(1.+U)))	
IF(ZX-ZE)606,605,605	XCHAN22
605 IK=2	XCHAN22
AZE(J) = (B1 **1.68)*ZX	
606 DEL=A-A1	XCHAN22
IF(DEL+CH1)24,48,48	XCHAN22
48 IF(DEL+CH1)49,49,24	XCHAN22
49 DEL=A-A2	XCHAN22
IF(DEL+CH1)24,50,50	XCHAN22
50 IF(DEL+CH1)51,51,24	XCHAN22
51 DEL=A-A3	XCHAN22
IF(DEL+CH1)24,52,52	XCHAN22
52 IF(DEL+CH1)8,8,24	XCHAN23
8 DEL=A-A4	XCHAN23
IF(DEL+CH1)24,66,66	XCHAN23
66 IF(DEL+CH1)67,67,24	XCHAN23
1000 CONTINUE	XCHAN23
67 CONTINUE	XCHAN23
IF(CHECK(J).EQ.0.0) CMH201(J) = CMH202(J)	XCHAN23
ANH4 = ANH4*CMH201(J)*14000.	XCHAN23
ACTCA(J) = A*10.**(-2.036*U/(1.+U))	
A = (A + CASO)*CMH201(J)*40080.	
S = S*CMH201(J)*22990.	XCHAN23

```

F = (F + AGSO) * CMH201(J) * 24320.
HC03 = HC03 * CMH201(J) * 61000.
H = H * CMH201(J) * 35460.
C03 = C03 * CMH201(J) * 60000.
G = (G + AGSO + CASO) * CMH201(J) * 96100.
IF (CHECK(J).EQ.0.0) * 00.401
400 ANHZ(J) = ANH4      SCZ(J) = A
    ANZ(J) = S      $AMZ(J) = F
    HCOZ(J) = HC03      SCOZ(J) = C03
    CY(J) = H      $SOZ(J) = G
    BNHZ(J) = BNH4
    CHECK(J) = CHECK(J) + 1.
401 CONTINUE

IHK(J) = IK
C----- COMPUTE DELTA VALUES FOR COMPONENTS
EXNH3 = ANH4 - ANHZ(J)      SEXCA = A - CZ(J)
EXANA = S - ANZ(J)      SEXAMG = F - AMZ(J)
EXHC03 = HC03 - HCOZ(J)      SEXC03 = C03 - COZ(J)
EXCL = H - CY(J)      SEXSO4 = G - SOZ(J)
EXBNH4 = BNH4 - BNHZ(J)
EZ(J) = ET      SCX(J) = CT
SAZ(J) = SAT      SXXZ(J) = XXT
CASZ(J) = CASO      $AGSZ(J) = AGSO
CAZ(J) = CAL      $EY(J) = EC
ISTR(J) = U * 2
CAS(J) = CASZ(J) * CMH201(J) * 136180.
AMGS(J) = AGSZ(J) * CMH201(J) * 120420.

C----- RETURN TO SUBROUTINE COMBINE
RETURN
1001 STOP
END

```

SUBROUTINE EQEXCH

```

SUBROUTINE EQEXCH(CA,AMG,SOS,CL,S0,MC03,C03,EC,ANH4,E5,C5,SAS,CAS0EQEXCH
1,AGS0,BNH4,U,ANO3,D1,D)
C-----THIS SUBROUTINE COMPUTES THE AMOUNTS OF IONS CONTAINED ON THE EX- EQEXCH
C-----CHANGE COMPLEX (BASED ON INITIAL SOIL ANALYSIS) EQEXCH
EQEXCH
EQEXCH
DA = 1.414/D1
DNH4=0.22
CAS0=0.0 EQEXCH1
U=SQRT(2.0*(CA+AMG+S0+C03)+0.5*(SOS+MC03+CL+ANH4+ANO3)) EQEXCH1
AGS0=0.0
42 ACT2=EXP(-9.366*U/(1.0+U)) EQEXCH1
IF (S0) 1000,713,712 EQEXCH1
712 AA=ACT2*ACT2 EQEXCH1
BB=ACT2*(10.8E-3+(ACT2*(AMG+CA-S0))) EQEXCH1
CC=28.91E-6+(ACT2*(AMG*.9E-3+(CA*5.9E-3)-(S0*10.8E-3))) EQEXCH1
DD=-S0*28.91E-6 EQEXCH1
800 Z=S0/2. EQEXCH1
850 Z1=Z EQEXCH2
863 ZZ=-(((AA*Z+BB)*Z+CC)*Z+DD) EQEXCH2
ZZZ=((13.0*AA*Z+2.0*BB)*Z+CC) EQEXCH2
ZZ=ZZ/ZZZ EQEXCH2
ZZZ=ZZ/Z EQEXCH2
Z=Z+ZZ EQEXCH2
IF (ABS(ZZZ)-.001)840,840,863 EQEXCH2
840 SQT=S0 EQEXCH2
S0=Z EQEXCH2
IF(S0)710,710,711 EQEXCH2
710 SC=SQT EQEXCH3
Z=Z1 EQEXCH3
GO TO 863 EQEXCH3

```

711	CASX=SO*CA*ACT2/(4.9E-3+ACT2*SO)	EQEXCH3
	CX=CA-CASX	EQEXCH3
	AGSX=SO*AMG*ACT2/(5.9E-3+ACT2*SO)	EQEXCH3
	AMX=AMG-AGSX	EQEXCH3
	UU=SQRT(2.*(CX+AMX+SO+C03)+0.5*(SOS+HC03+CL+ANH4+AN03))	
	IF(ARS(UU/U-1.)-1.0E-4) 40,40,41	
41	U=UU	EQEXCH3
	SO=SOT	EQEXCH4
	GO TO 42	EQEXCH4
40	CAS0=CASX	EQEXCH4
	AGS0=AGSX	EQEXCH4
	CA=CX	EQEXCH4
	AMG=AMX	EQEXCH4
713	ACT1=SQRT(ACT2)	EQEXCH4
	ACTM=SQRT(ACT1)	EQEXCH4
	ACTM=SQRT(ACTM)	EQEXCH4
	CA=CA*2.	EQEXCH5
	AMG=AMG*2.	EQEXCH5
	E5=EC/((ACTM*SOS/(DA*SQRT(ACT1*CA)))+1.+(D*ACT1*AMG/(ACT1*CA)))	EQEXCH5
	SA5=ACTM*SOS*E5/(SQRT(ACT1*CA)*DA)	EQEXCH5
	C5=EC-E5-SA5	EQEXCH5
	BNH4 = (SA5*ANH4)/(SOS*DNH4)	EQEXCH5
1000	RETURN	EQEXCH5
	END	EQEXCH5

SUBROUTINE EXECUTE

SUBROUTINE EXECUTE		EXECUTE
C-----SUBROUTINE TO EXECUTE PROGRAM FOR EACH DAILY TIME INTERVAL		EXECUTE
COMMON/BYPAS/NBYPAS, IDYSTR, IDYSTP, ILO, IMI, INFIL1, ICONT1, JPAS		EXECUTE
COMMON/ABLE/TITLE(10), SMONTH, MM, 0, IPRINT, JPRINT, INK, IPUNCH, ISTOP,		EXECUTE
1ITEST, IREADP, IMASS, IADD(25), IORNAP(25), HOR(9), TOTN(99), YEAR		EXECUTE
2AIRR(9), IRR(25), TT(60), FERT(7), OFERT(3), NORGIN, NFERTIN, NTEMPIN,		EXECUTE
3ITOT, JTOT, IRTOT		EXECUTE
COMMON/XX2/A1, A2, A3, X		EXECUT1
COMMON/YYY/STAPT, IDTE, MONTH, I, LL		EXECUT1
COMMON/XXY/ICHECK, ICOUNT, CONV, PK, PK1, CROP		EXECUT1
COMMON/AFG/ENH3, II, LLL		EXECUT1
COMMON/XXX/DELX, DELT, MS, WTART, BD(25), TEN(25), CHECK(25), MOISIN		EXECUT1
1(25), CMH201(25), MOISOUT(25), AN03(25), ANH3(25), UREA(25), ORN		EXECUT1
2(25), CA(25), ANA(25), AMG(25), HC03(25), CL(25), C03(25), S04(25)		EXECUT1
3), E5(25), C5(25), SA5(25), XX5(25), CAS0(25), AGS0(25), BNH4(25),		EXECUT1
4EC(25), CN1(25), SAMT(25), RN(25), RC(25), TEM(25), CAL(25), 0, SRO		EXECUT1
1P, XTRACT, SUMN03, THOR(4), TO, IDAY, U(25), CH, CH1, IRERUN, ISWCH, CUMSUM,		EXECUT1
1SUMOUT		EXECUT2
		EXECUT2
		EXECUT2
		EXECUT2
		EXECUT2
DIMENSION X(7,25)		EXECUT2
		EXECUT2
INTEGER Q, 0, START, CROP, TO, SMONTH, YEAR		EXECUT2
REAL MOISIN, MOISOUT		EXECUT2
C---- POSITION TAPE1 (INPUT FROM MOISTURE FLOW PROGRAM) TO PROPER		EXECUT2
C---- RECORD		EXECUT2
IF(ITEST.NE.0) GO TO 9007		EXECUT2
IF(ICONT1.EQ.1) GO TO 8000		EXECUT2
REWIND 1		EXECUT2
8009 NREC=ILO-IDYSTR		EXECUT2
IF(NREC.LE.0) GO TO 9007		EXECUT2
DO 9004 I=1, NREC		EXECUT2
DO 9003 IK=1, LLL		EXECUT2
READ(1) I1		EXECUT2
9003 CONTINUE		EXECUT2
9004 CONTINUE		EXECUT2
GO TO 9007		EXECUT2
8000 IF(JPAS.EQ.1) GO TO 8002		EXECUT2
JPAS=1		EXECUT2
REWIND 1		EXECUT2
NSKIP=INFIL1-1		EXECUT2

IF(NSKIP.LE.0) GO TO 8009	\$\$\$\$ Q2
DO 8001 I=1,NSKIP	\$\$\$\$ R2
CALL SKIP(1)	
8001 CONTINUE	\$\$\$\$ T2
GC TO 8009	\$\$\$\$ U2
8002 READ(1) I1	\$\$\$\$ V2
IF(EOF(1))9007,8003	
8003 PRINT 8004, YEAR	\$\$\$\$ X2
8004 FORMAT(/, 5X, * ERROR- END OF FILE NOT FOUND ON TAPE 1 AT START OF	\$\$\$\$ Y2
1 YEAR NO. *, 15/, 5X, * EXECUTION TERMINATED *)	\$\$\$\$1A2
CALL EXIT	\$\$\$\$2A2
9007 CONTINUE	\$\$\$\$ L2
	EXECUT2
	EXECUT2
C-----LL = STARTING DAY, MM = TERMINATION DAY	EXECUT2
DC 4 I=ILO,IHI	\$\$\$\$ 2
IF(NAYPAS.EQ.1) GO TO 9010	\$\$\$\$ A2
IF(MOD(I-IMASS).EQ.0) ISWCH = 1	EXECUT3
9010 CONTINUE	\$\$\$\$ A3
	EXECUT3
C-----STORE DAILY INTERNAL VALUES ON TAPE15	EXECUT3
C WRITE (15)	EXECUT3
C 1(I,J, ANH3(J),AN03(J),UREA(J),CA(J),ANA(J),AMG(J),HCO3(J),CL(J)	EXECUT3
C 1),CO3(J),SO4(J),EC(J),XX5(J),CAL(J),BO(J),SAMT(J),CNI(J),ORN(J),	EXECUT3
C 2RN(J),RC(J),E5(J),C5(J),SA5(J),CASO(J),AGSO(J),BNH4(J),J=1,Q)	EXECUT3
	EXECUT3
C-----CALL SUBROUTINE TO COMPUTE DAY OF MONTH	EXECUT3
CALL THEDATE(START,I,SMONTH,0)	EXECUT4
IDAY = I	EXECUT4
	EXECUT4
C-----CHECK FOR FERTILIZER APPLICATION DATE	EXECUT4
DO 3 K=1,ITOT	EXECUT4
IF(I.EQ.IADD(K))301,3	EXECUT4
3 CONTINUE	EXECUT4
GO TO 5	EXECUT4
	EXECUT4
C-----READ FERTILIZER APPLICATIONS FROM TAPE 9	EXECUT4
301 READ(9) DEPTH,AANH3,AAN03,AUREA,ACA,AS04,AC03	EXECUT5
NFERTIN = NFERTIN + 1	EXECUT5
	EXECUT5
C-----IF SURFACE APPLICATION, BRANCH TO 600. OTHERWISE GO TO 601	EXECUT5
IF(DEPTH.EQ.0,600,601	EXECUT5
600 CCC = CONV	EXECUT5
606 IS = 1 SIDEPH = 1	EXECUT5
GO TO 602	EXECUT5
601 IDEPTH = DEPTH/DELX + 1	EXECUT5
IF(IDEPTH.LT.2) IDEPTH = 2	EXECUT5
IS = 2	EXECUT6
CCC = DELX/DEPTH*CONV	EXECUT6
602 SAVE1 = AANH3*CCC*0.7777	EXECUT6
SAVE2 = AAN03*CCC*0.2258	EXECUT6
SAVE3 = AUREA*CCC*0.4466	EXECUT6
SAVE4=ACA*CCC	EXECUT6
SAVE9=AC03*CCC	EXECUT6
SAVE10=AS04*CCC	EXECUT6
	EXECUT6
DO 302 J = IS,IDEPTH	EXECUT6
	EXECUT7
C-----ADD THE FERTILIZER TO THE PROPER ARRAYS	EXECUT7
ANH3(J) = ANH3(J) + SAVE1	EXECUT7
AN03(J) = AN03(J) + SAVE2	EXECUT7
UREA(J) = UREA(J) + SAVE3	EXECUT7
CA(J)=CA(J)+SAVE4	EXECUT7
CO3(J)=CO3(J)+SAVE9	EXECUT7
SO4(J)=SO4(J)+SAVE10	EXECUT7
	EXECUT7
C-----STORE ACCUM AMOUNTS OF FERTILIZER ADDED	EXECUT7
CUMSUM = CUMSUM + SAVE1 + SAVE2 + SAVE3	EXECUT8
CUMCA=CUMCA+SAVE4	EXECUT8
CUMCO3=CUMCO3+SAVE9	EXECUT8

302	CUMS04=CUMS04+SAVE10	EXECUT8
5	IF(NRYPAS.EQ.1) GO TO 9006	\$\$\$ A8
	DO 8 K=1,JTOT	EXECUT8
		EXECUT8
C-----	CHECK FOR ORGANIC-N APPLICATION DATE	EXECUT8
	IF(I.EQ.IORNAP(K))7,8	EXECUT8
7	CONTINUE	EXECUT8
		EXECUT8
C-----	READ ORGANIC-N APPLICATION	EXECUT9
	READ (10) DEPTH,ACN1,SSAMT	EXECUT9
	NORGIN = NORGIN + 1	EXECUT9
		EXECUT9
C-----	TRANSFORM AND STORE VALUES	EXECUT9
	IDEPTH = DEPTH/DELX + 1	EXECUT9
	IF(IDEPTH.LT.2) IDEPTH = 2	EXECUT9
	CCC = DELX/DEPTH*CONV	EXECUT9
		EXECUT9
	DO 303 J=2,IDEPTH	EXECUT9
		EXECUT9
C-----	STORE ORGANIC-N APPLICATION INTO PROPER ARRAYS	EXECU10
	SAMT(J) = SAMT(J) + SSAMT*CCC	EXECU10
		EXECU10
C-----	STORE ACCUM AMOUNT OF ORGANIC-N ADDED	EXECU10
C	SAVE = SSAMT*CCC*0.4/ACN1	EXECU10
	SAVE = SSAMT*CCC	EXECU10
	CUMSUM = CUMSUM + SAVE	EXECU10
303	CN1(J) = ACN1	EXECU10
	GO TO 17	EXECU10
8	CONTINUE	EXECU10
		EXECU11
C-----	COMPUTE TEMPERATURE READ-IN DATE	EXECU11
17	IF(MOD(I,7).EQ.0.OR.I.EQ.ILO) 580,581	EXECU11
		EXECU11
C-----	CALL TEMPERATURE INPUT SUBROUTINE	EXECU11
580	CALL TEMP SNTMPIN = NTEMPIN + 1	EXECU11
581	CONTINUE	EXECU11
9006	CONTINUE	\$\$\$A11
	IF(MOD(I,INK).EQ.0) K = 2	EXECU11
		EXECU11
C-----	ENTER LOOP TO EXECUTE PROGRAM FOR EACH TIME INTERVAL	EXECU11
		EXECU12
C-----	HERE LLL IS THE NO. OF TIME INTERVALS PER DAY	EXECU12
		EXECU12
C-----	THE PROGRAM MAY OR MAY NOT CALL ALL OF THE COMPUTATIONAL SUB-	EXECU12
C-----	ROUTINES FOR EACH INTERVAL	EXECU12
		EXECU12
C-----	ALL CRITICAL ROUTINES ARE CALLED AT LEAST ONCE PER DAY	EXECU12
		EXECU12
	DO 10 II=1,LLL	EXECU12
		EXECU13
C-----	READ INPUT DATA ON TAPE1 FROM MOISTURE FLOW PROGRAM	EXECU13
	IF(ITEST.EQ.0) READ(1)(I1,I2,I3,I3,CMH201(J),MOISIN(J),MOISOUT(J),	\$\$\$A13
	1 TEN(J),U(J),J=1,Q)	\$\$\$R13
	IF(II.EQ.1.AND.CMH201(1).GT.0.0)790,795	EXECU13
		EXECU13
C-----	CHECK TO SEE IF THIS IS AN IRRIGATION DAY	EXECU14
790	DO 792 L8 = 1,IRTOT	EXECU14
	IF(I.EQ.IRR(L8))793,792	EXECU14
		EXECU14
C-----	ENTER ROUTINE TO ADD IRRIGATION WATER COMPONENTS	EXECU14
793	SAVE1=AI RR(1)*CMH201(1) SSAVE2=AI RR(2)*CMH201(1)	EXECU14
	SAVE4=AI RR(3)*CMH201(1) SSAVE5=AI RR(4)*CMH201(1)	EXECU14
	SAVE6=AI RR(5)*CMH201(1) SSAVE7=AI RR(6)*CMH201(1)	EXECU14
	SAVE8=AI RR(7)*CMH201(1) SSAVE9=AI RR(8)*CMH201(1)	EXECU14
	SAVE10=AI RR(9)*CMH201(1)	EXECU14
	ANH3(1)=ANH3(1)+SAVE1 SAN03(1)=ANO3(1)+SAVE2	EXECU15
	CA(1)=CA(1)+SAVE4 SANA(1)=ANA(1)+SAVE5	EXECU15
	AMG(1)=AMG(1)+SAVE6 SHC03(1)=HC03(1)+SAVE7	EXECU15
	CL(1)=CL(1)+SAVE8 SCO3(1)=C03(1)+SAVE9	EXECU15
	SO4(1)=SO4(1)+SAVE10	EXECU15
C-----	STORE ACCUM AMOUNTS OF COMPONENTS	EXECU15

```

CUMSUM=CUMSUM+SAVE1+SAVE2      $CUMCA=CUMCA+SAVE4      EXECU15
CUMANA=CUMANA+SAVE5            $CUMAMG=CUMAMG+SAVE6      EXECU15
CUMHC03=CUMHC03+SAVE7          $CUMCL=CUMCL+SAVE8      EXECU15
CUMC03=CUMC03+SAVE9            $CUMS04=CUMS04+SAVE10     EXECU15
PRINT 207,CMM201(1),I
GO TO 795
792 CONTINUE                    EXECU16
795 CONTINUE                    EXECU16
IF(MOD(IDAY,IPRINT).EQ.0.AND.II.EQ.JPRINT)400,401  EXECU16
400 PRINT 206,YEAR,I,II        EXECU16
PRINT 205                      EXECU13
401 CONTINUE                   EXECU13
C-----CALL COMPRINE SUBROUTINE EXECU16
CALL COMPRINE(IDAY,IPRINT,JPRINT) EXECU16
10 CONTINUE                   EXECU16
4 CONTINUE                   EXECU16
RETURN                       EXECU16
205 FORMAT( 1X*PREDICTED AMOUNTS(UG/SEGMENT OF SOIL)--(SEGVOL=CC WATEEXECU17
1R/SEG SOIL)*//2X*SEG*      EXECU17
14X*NM4-N*4X*NO3-N*3X*UREA-N*6X*ORN*7X*CA*7X*NA*7X*MG*5X*HC03*7X*CL
1 5X*S04* 3X*RNH4-N*3X*SEGVOL*6X*ESP*1X*PC02(ATM)*
206 FORMAT(//1X*YEAR= *,I4,10X*DAY= *,I4,10X*TIME INTERVAL= *
1,I4)
207 FORMAT(///10X*AN IRRIGATION OF*,F6.1,*CM WAS APPLIED ON DAY NUMBER
1*,I5//)
END
EXECU17

```

SUBROUTINE OUTPT

```

SUBROUTINE OUTPT(K)
C-----THIS SUBROUTINE WRITES PREDICTED TOTAL AND DELTA AMOUNTS FOR THE
C-----COMPONENTS AND VOLUMES ON TAPE2 (UNITS ARE EXPRESSED IN UG/UNIT
C-----AREA AND ML/UNIT AREA).
DIMENSION AMT(10),AMT1(10),DEL(10)
INTEGER Q,Q0,START,CROP,TO
INTEGER YEAR
REAL MOISOUT
COMMON/SABLE/SUMS(3)
COMMON/XXX/DELX,DELT,MS,WTART,BD(25),TEN(25),CHECK(25),MOISIN
1(25),CMM201(25),MOISOUT(25),AN03(25),ANH3(25),UREA(25),CON
2(25),CA(25),ANA(25),AMG(25),HC03(25),CL(25),C03(25),S04(25)
3),E5(25),C5(25),SAS(25),XX5(25),CASO(25),AGSO(25),BNH4(25)
4EC(25),CNI(25),SAMT(25),RN(25),RC(25),TEM(25),CAL(25),Q CR)
1P,XTRACT,SUMNO3,THOR(4),TO,IDAY,U(25),CH,CH1,IRERUN
COMMON/ARLE/TITLE(10),SMONTH,MM,O,IPRINT,JPRINT,INK,IPUNCH,ISTOP,
1ITEST,IREADP,IMASS,IADD(25),IORNAP(25),HOR(9),TOTN(99),YEAR,
2AIRR(9),IRR(25),TT(60),FERT(7),OFERT(3),NORGIN,NFERTIN,NTEMPIN,
3ITOT,JTOT,IRTOT,NT
COMMON/IP/CAS(25),AMGS(25)
C-----ESTABLISH STATEMENT FUNCTION
SUBA(X,Y) = X*Y
IF(K.EQ.1) 1,2
C-----ZERO INITIAL VALUES
1 SUMOUT = SUMOUT1 = 0.0
DO 3 I=1,10
3 AMT(I) = AMT1(I) = 0.0
GO TO 5
2 Y = CMM201(Q)
Z = MOISOUT(Q)

```

Y = Z/Y	
IF(Y.GT.1) Y=0.99	
C-----SUM THE COMPONENTS	OUTPUT 3
AMT(1) = SUMS(1)	OUTPUT 3
AMT(2) = SUMS(2)	OUTPUT 3
AMT(3) = SUMS(3)	OUTPUT 3
A = SUBA(CAS(Q),Y)	OUTPUT 3
B=SUBA(AMGS(Q),Y)	OUTPUT 4
AMT(4) = AMT(4) + SUBA(CA(Q),Y)	
AMT(5) = AMT(5) + SUBA(ANA(Q),Y)	OUTPUT 4
AMT(6) = AMT(6) + SUBA(ANG(Q),Y)	
AMT(7) = AMT(7) + SUBA(HCO3(Q),Y)	OUTPUT 4
AMT(8) = AMT(8) + SUBA(CL(Q),Y)	OUTPUT 4
AMT(9) = AMT(9) + SUBA(CO3(Q),Y)	OUTPUT 4
AMT(10) = AMT(10) + SUBA(SO4(Q),Y)	
C-----SUM THE VOLUMES OUT	OUTPUT 4
SUMOUT = SUMOUT + MOISOUT(Q)	OUTPUT 4
IF(K.EQ.2)4.5	OUTPUT 5
C-----COMPUTE DELTA VALUES FOR COMPONENTS	OUTPUT 5
4 DO 6 I=1.10	OUTPUT 5
6 DEL(I) = AMT(I) - AMT1(I)	OUTPUT 5
C-----COMPUTE DELTA VALUE FOR VOLUME OUT	OUTPUT 5
DELN = SUMOUT - SUMOUT1	OUTPUT 5
C-----WRITE SUMMATIONS AND DELTA VALUES ON TAPE2	OUTPUT 5
WRITE(2) YEAR,IDAY,SUMOUT,DELN,(AMT(I),DEL(I),I=1.10)	OUTPUT 6
C-----RESET VALUES FOR DELTA DETERMINATIONS	2222 6
DO 7 I=1.10	OUTPUT 6
7 AMT1(I) = AMT(I)	OUTPUT 6
SUMOUT1 = SUMOUT	OUTPUT 6
5 K=3	OUTPUT 6
C-----RETURN TO MAIN PROGRAM	OUTPUT 6
RETURN	OUTPUT 7
100 FORMAT(1X,12E10.3)	OUTPUT 7
END	OUTPUT 7

INTEGER FUNCTION DAY

INTEGER FUNCTION DAY(K,M)		DAY
L = 0		DAY
GO TO (1,2,3,4,5,6,7,8,9,10,11,12,13) M		DAY
12 DAY=K-L	\$ RETURN	DAY
1 DAY=K-L+31	\$ RETURN	DAY
2 DAY=K-L+62	\$ RETURN	DAY
3 DAY=K-L+90	\$ RETURN	DAY
4 DAY=K-L+121	\$ RETURN	DAY
5 DAY=K-L+151	\$ RETURN	DAY 1
6 DAY=K-L+182	\$ RETURN	DAY 1
7 DAY=K-L+212	\$ RETURN	DAY 1
8 DAY=K-L+243	\$ RETURN	DAY 1
9 DAY=K-L+274	\$ RETURN	DAY 1
10 DAY=K-L+304	\$ RETURN	DAY 1
11 DAY=K-L+335	\$ RETURN	DAY 1
13 DAY=K-L+365	\$ RETURN	DAY 1
END		DAY 1

IDAY
IDAY
IDAY
IDAY
IDAY
IDAY
IDAY
IDAY
IDAY 1

[illegible]

198

HC03(J) = HC03(J)*CMH201(J)*61.0	UNITS12
C03(J) = C03(J)*CMH201(J)*30.0	UNITS12
CL(J) = CL(J)*CMH201(J)*35.46	UNITS12
S04(J) = S04(J)*CMH201(J)*48.05	UNITS12
ORN(J) = ORN(J)*BD(J)*DELX	UNITS12
SAMT(J) = SAMT(J)*BD(J)*DELX	UNITS12
RETURN	UNITS12
ENTRY UNITS2	UNITS12
C-----CONVERT FROM UG/SEGMENT TO MEQ/LITER	
ANH3(J) = ANH3(J)/(CMH201(J)*14.0)	UNITS13
ANO3(J) = ANO3(J)/(CMH201(J)*14.0)	UNITS13
UREA(J) = UREA(J)/(CMH201(J)*28.0)	UNITS13
CA(J) = CA(J)/(CMH201(J)*20.04)	UNITS13
ANA(J) = ANA(J)/(CMH201(J)*22.99)	UNITS13
AMG(J) = AMG(J)/(CMH201(J)*12.16)	UNITS13
HC03(J) = HC03(J)/(CMH201(J)*61.0)	UNITS13
C03(J) = C03(J)/(CMH201(J)*30.0)	UNITS13
CL(J) = CL(J)/(CMH201(J)*35.46)	UNITS14
S04(J) = S04(J)/(CMH201(J)*48.05)	UNITS14
ORN(J)=ORN(J)/BD(J)/DELX	UNITS14
RETURN	UNITS14
END	UNITS14

SUBROUTINE FL

```

SUBROUTINE FL(J,FLN03,FLNH3,FLUREA,FLCA,FLANA,FLAMG,FLHC03,FLCL,
1FLC03,FLS04)
COMMON/XXX/DELX,DELT,MM,START,BD(25),TEN(25),CHECK(25),MOISIN
1(25),ORMOIS(25),MOISOUT(25),BNO3(25),BNH3(25),BREA(25),ORN
2(25),BA(25),BNA(25),BMG(25),BCO3(25),BL(25),BO3(25),BO4(25)
3),E5(25),C5(25),SAS(25),XX5(25),CASO(25),AGSO(25),BNH4(25),
4EC(25),CN1(25),SAMT(25),PN(25),RC(25),TEM(25),CAL(25),Q,CRO
SP,XTRACT,SUMNO3,THOR(4),TO,IDAY,US(25),CH,CH1,IRERUN,ISWCH,CUMSUM,
6SUMOUT,RSPLA(60)
COMMON/GTRL/UREA1,UREA2,DNH31,DNH32,DNO31,DNO32,CAL,    ANA1,
1AMG1,HC031,CL1,C031,SC041,KCOUNT,LSET1,LSET2,LSET3
DIMENSION ANH3(25),ANO3(25),UREA(25),CA(25),ANA(25),AMG(25),HC03(2
15),CL(25),C03(25),S04(25)
INTEGER Q
REAL MOISIN,MOISOUT
IF(J.NE.2) GO TO 1
DO 18 I=1,Q
ANH3(I) = BNH3(I)  $ANO3(I)=BNO3(I)  $UREA(I)=BREA(I)  $CA(I)=BA(I)
1)  $ANA(I)=BNA(I)  $AMG(I)=BMG(I)  $HC03(I)=BCO3(I)  $CL(I)=BL(I)
2  $C03(I) = BO3(I)  $S04(I) = BO4(I)
18 CONTINUE
ORMOIS(Q+1) = ORMOIS(Q)
ANH3(Q+1) = ANH3(Q)  $ANO3(Q+1) = ANO3(Q)
UREA(Q+1) = UREA(Q)  $CA(Q+1) = CA(Q)
ANA(Q+1) = ANA(Q)  $AMG(Q+1) = AMG(Q)
HC03(Q+1) = HC03(Q)  $CL(Q+1) = CL(Q)
C03(Q+1) = C03(Q)  $S04(Q+1) = S04(Q)
1 CONTINUE
IF(ORMOIS(1).LT.0.0) ORMOIS(1) = 0.0
IF(MOISIN(J).LT.0.0) 2,3
2 COEFIN = MOISIN(J)/ORMOIS(J)
GO TO 4
3 IF(ORMOIS(J-1).GT.0.0) GO TO 14
COEFIN = 0.0
GO TO 15
14 COEFIN = MOISIN(J)/ORMOIS(J-1)
15 CONTINUE
4 IF(MOISOUT(J).LT.0.0) 5,6
5 COEFOUT = MOISOUT(J)/ORMOIS(J+1)
GO TO 7
6 COEFOUT= MOISOUT(J)/ORMOIS(J)
7 IF(COEFIN.LT.0.0) 8,9

```

```

8      K = J
      GO TO 10
9      K = J-1
10     IF (COEFOUT.LT.0.0) 11,12
11     L = J-1
      GO TO 13
12     L = J
13     KCOUNT = K SIF (COEFIN.LT.0.0.AND.K.EQ.2) KCOUNT = 1
      IF (ABS(COEFIN).GT.1.0) COEFIN = ABS(COEFIN)/COEFIN*0.99
      IF (ABS(COEFOUT).GT.1.0) COEFOUT = ABS(COEFOUT)/COEFOUT*0.99
      IF (J.NE.2.AND.LSET2.EQ.1) GO TO 101
      DN031 = COEFIN*AN03(K)
      GO TO 102
101    DN031 = DN032
102    DN032 = COEFOUT*AN03(L)
      IF (J.NE.2.AND.LSET1.EQ.1) GO TO 103
      DNH31 = COEFIN*ANH3(K)
      GO TO 104
103    DNH31 = DNH32
104    DNH32 = COEFOUT*ANH3(L)
      IF (J.NE.2.AND.LSET3.EQ.1) GO TO 105
      UREA1 = COEFIN*UREA(K)
      GO TO 106
105    UREA1 = UREA2
106    UREA2 = COEFOUT*UREA(L)
      CA1 = COEFIN*CA(K)  $CA2 = COEFOUT*CA(L)
      ANA1 = COEFIN*ANA(K)  $ANA2 = COEFOUT*ANA(L)
      AMG1 = COEFIN*AMG(K)  $AMG2 = COEFOUT*AMG(L)
      HCO31 = COEFIN*HCO3(K)  $HCO32 = COEFOUT*HCO3(L)
      CL1 = COEFIN*CL(K)  $CL2 = COEFOUT*CL(L)
      CO31 = COEFIN*CO3(K)  $CO32 = COEFOUT*CO3(L)
      SO41 = COEFIN*SO4(K)  $SO42 = COEFOUT*SO4(L)
      FLN03 = DN031 - DN032
      FLNH3 = DNH31 - DNH32
      FLUREA = UREA1 - UREA2
      FLCA = CA1 - CA2
      FLANA = ANA1 - ANA2
      FLAMG = AMG1 - AMG2
      FLHCO3 = HCO31 - HCO32
      FLCCL = CL1 - CL2
      FLC03 = CO31 - CO32
      FLSD4 = SO41 - SO42
      LSET1 = LSET2 = 0
      RETURN
      END

```

SUBROUTINE PRNT

```

      SUBROUTINE PRNT(IPRINTI,IPRINTJ)
C-----THIS SUBROUTINE PRINTS CONTROL AND INPUT DATA
      COMMON/ABLE/TITLE(10),SMONTH,MM,0,IPRINT,JPRINT,INK,IPUNCH,ISTOP,
1ITEST,IREADP,IMASS,IADD(25),IORNAP(25),HOR(9),TOTN(99),YEAR,9999,
2AIRP(9),IRR(25),TT(60),FERT(7),OFERT(3),NORGIN,NFERTIN,NTEMPIN,
3ITOT,JTOT,IRTOT,NT
      COMMON/XX2/A1,A2,A3,X
      COMMON/YYY/START,IDTE,MONTH,I,LL
      COMMON/XXY/ICHECK,ICOUNT,CONVPK,PK1,CROP
      COMMON/XXX/DELX,DELT,MS,WTART,BD(25),TEN(25),CHECK(25),MOISIN
1(25),CMH201(25),MOISOUT(25),AN03(25),ANH3(25),UREA(25),ORN
2(25),CA(25),ANA(25),AMG(25),HCO3(25),CL(25),CO3(25),SO4(25),
3,E5(25),C5(25),S45(25),XX5(25),CASO(25),AGSO(25),BNH4(25),PRNT
4EC(25),CN1(25),SANT(25),RN(25),RC(25),TEN(25),CAL(25),Q,SROPRNT
IP,XTRACT,SUMNO3,THOR(+),TO,IDAY,U(25),CH,CH1,IRERUN,ISWCH,CUMSUM,PRNT
ISUMOUT,REDUCE
      INTEGER TITLE,SMONTH,START,0,TO,YEAR

```

```

      PRNT 2
      PRNT 3
      PRNT 4
      PRNT 5
      PRNT 6
      PRNT 7
      PRNT 8
      PRNT 9
      PRNT 10
      PRNT 11
      PRNT 12
      PRNT 13
      PRNT 14
      PRNT 15
      PRNT 16
      PRNT 17
      PRNT 18
      PRNT 19
      PRNT 20
      PRNT 21

```

C-----PRINT TITLE	PRNT 22
PRINT 100,TITLE	PRNT 23
IF(IPRINT1.EQ.2) GO TO 1	PRNT 24
	PRNT 25
	PRNT 26
	PRNT 27
C-----PRINT BASIC CONTROL CARD PARAMETERS	PRNT 28
PRINT 101, SMONTH,XTRACT,START,CROP,LL,PK,MM,PK1,DELX,CH,DELT,	PRNT 29
1CH1.0,A1,TO,A2,ISTOP,YEAP,REDUCE	PRNT 30
	PRNT 31
C-----PRINT I-O CONTROL PARAMETERS	PRNT 32
PRINT 102, IPRINT,IREADP,JPRINT,ITEST,INK,IMASS,IRERUN,IPRINTI,	PRNT 33
1IPUNCH,IPRINTJ	PRNT 34
1 RETURN	PRNT 35
ENTRY PRNT1	PRNT 36
	PRNT 37
C-----SKIP PAGE	PRNT 38
PRINT 103	PRNT 39
	PRNT 40
C-----PRINT TEMPERATURE HORIZONS	PRNT 41
PRINT 104, (THOR(J),J=1,TO)	PRNT 42
PRINT 109	PRNT 43
REWIND 8	PRNT 44
	PRNT 45
C-----PRINT TEMPERATURES	PRNT 46
DO 10 J=1,NT	PRNT 47
READ (8) (TT(I),I=1,TO)	PRNT 48
10 PRINT 105, J, (TT(I),I=1,TO)	PRNT 49
REWIND 8	PRNT 50
	PRNT 51
C-----SKIP PAGE	PRNT 52
PRINT 103	PRNT 53
	PRNT 54
C-----PRINT WATER ANALYSIS HEADING	PRNT 55
PRINT 107	PRNT 56
	PRNT 57
C-----PRINT IRRIGATION WATER ANALYSIS	PRNT 58
PRINT 108, (AIRR(I),I=1,9)	PRNT 59
	PRNT 60
C-----PRINT IRRIGATION APPLICATION DATES	PRNT 61
PRINT 110, (IRR(I),I=1,IPTOT)	PRNT 62
	PRNT 63
	PRNT 64
C-----PRINT FERTILIZER APPLICATION DATES	PRNT 65
PRINT 111, (IADD(I),I=1,ITOT)	PRNT 66
PRINT 112	PRNT 67
REWIND 9	PRNT 68
DO 2 I=1,ITOT	PRNT 69
READ (9) (FERT(J), J=1,7)	PRNT 70
FNH4 = FERT(2)*CONV*0.7777 \$FNO3=FERT(3)*CONV*.2258	PRNT 71
FUREA = FERT(4)*CONV*.4466 \$FCA = FERT(5)*CONV	PRNT 72
FSO4 = FERT(6)*CONV \$FCO3 = FERT(7)*CONV	PRNT 73
	PRNT 74
	PRNT 75
C-----PRINT FERTILIZER APPLICATIONS	PRNT 76
2 PRINT 113,I,FERT(1),FNH4,FNO3,FUREA,FCA,FSO4,FCO3	PRNT 77
REWIND 9	PRNT 78
REWIND 10	PRNT 79
PRINT 109	PRNT 80
	PRNT 81
C-----PRINT ORGANIC APPLICATION DATES	PRNT 82
PRINT 114, (IORNAP(J),J=1,JTOT)	PRNT 83
PRINT 115	PRNT 84
DO 3 I=1,JTOT	PRNT 85
READ (10) (OFERT(J),J=1,3)	
FCORN = OFERT(3)*CONV	
	PRNT 87
C-----PRINT ORGANIC APPLICATIONS	PRNT 88
3 PRINT 113, I,OFERT(1),OFERT(2),FORM	PRNT 89
REWIND 10	PRNT 90
	PRNT 91
C-----PRINT COMPONENT HORIZON DEPTHS	PRNT 92
PRINT 106, (HOR(J),J=1,0)	PRNT 93

PRINT 103		PRNT 94
RETURN		PRNT 95
100 FORMAT(1H1//.3RX,10AR//)		PRNT 96
101 FORMAT(56X*CONTROL CARD SUMMARY*/57X*(BASIC PARAMETERS)*/35X		PRNT 97
1*STARTING MONTH	==,I5,10X*TRACT ==,F5.1,/35X	PRNT 98
1*STARTING DAY	==,I5,10X*CROP ==,I5/35X	PRNT 99
2*RELATIVE STARTING DAY	==,I5,10X*UPTAKE(N03) ==,F5.2,/35X	PRNT 100
3*RELATIVE TERMIN DAY	==,I5,10X*UPTAKE(NH4) ==,F5.2,/35X	PRNT 101
4*SOIL SEGMENT SIZE	==,F5.1,* CM*7X.*CONVERG1 ==,F5.2,/35X	PRNT 102
5*TIME INTERVAL SIZE	==,F5.2,* DAYS*5X*CONVERG2 ==,F5.3/35X	PRNT 103
6*NO. OF COMPONENT HRZNS	==,I5,10X*CHECK1 ==,F5.1/35X	PRNT 104
7*NO. OF TEMP HRZNS	==,I5,10X*CHECK2 ==,F5.1/35X	PRNT 105
8*ISTOP	==,I5,10X*YEAR ==,I5/35X	PRNT 106
9*REDUCE	==,F5.0/////	PRNT 107
102 FORMAT(55X*(I-O CONTROL PARAMETERS)*/35X		PRNT 108
1*IPRINT	==,I5,10X*IREADP ==,I5/35X	PRNT 109
2*JPRINT	==,I5,10X*ITEST ==,I5/35X	PRNT 110
3*INK	==,I5,10X*IMASS ==,I5/35X	PRNT 111
4*IRERUN	==,I5,10X*IPRINTI ==,I5/35X	PRNT 112
5*IPUNCH	==,I5,10X*IPRINTJ ==,I5/////	PRNT 113
103 FORMAT(1H1)		PRNT 114
104 FORMAT(//15X*WEEKLY TEMPERATURE DATA*13X*HORIZON DEPTH(CM)*		PRNT 115
1/46X,6(3X,F6.1))		PRNT 116
105 FORMAT(20X,I3,2X*TEMPERATURE(DEG C)*2X,6F9.1)		PRNT 117
106 FORMAT(//10X*COMPONENT HORIZON DEPTHS(CM)* , 6X,6(3XF6.1))		PRNT 118
107 FORMAT(10X*IRRIGATION WATER ANALYSIS(PDM)/10X*NH4*7X*N03*7X*CA		PRNT 119
1X*NA *7X*MG *6X*HCO3*7X*CL *7X*CO3*7X*S04*)		PRNT 120
108 FORMAT(3X,9F10.2//)		PRNT 121
109 FORMAT(//)		PRNT 122
110 FORMAT(10X*IRRIGATION APPLICATION DATES*/8X,25I5)		PRNT 123
111 FORMAT(//10X*FERTILIZER APPLICATION DATES*/8X,25I5)		9999 124
112 FORMAT(//10X*FERTILIZER APPLICATIONS(UG)*/10X*DEPTH*5X*NH4*5X*N03*		9999 125
15X*UREA*5X*CA*5X*S04*5X*CO3*)		PRNT 126
113 FORMAT(2X,I5,7F8.1)		PRNT 127
114 FORMAT(10X*ORGANIC-N APPLICATION DATES*/8X,25I5)		PRNT 128
115 FORMAT(//10X*ORGANIC-N APPLICATIONS(UG)*/10X*DEPTH*5X*C/N*5X*ORN*)		9999 129
END		PRNT 130
		PRNT 131

SUBROUTINE CHK

SUBROUTINE CHK(I1,L2,L3,J,EXNH3,EXCA,EXANA,EXAMG,DELNO3,DELNH3,DELCHK		2
10RGN,DELUREA)		CHK 3
C-----THIS SUBROUTINE DETERMINES IF THE NITROGEN TRANSFORMATION AND/OR		CHK 4
C-----ION EXCHANGE SUBROUTINES NEED BE CALLED FOR THIS TIME STEP (BASED		CHK 5
C-----ON CRITERIA READ FROM DATA CARDS)		CHK 6
		CHK 7
		CHK 8
COMMON/RYPAS/NRYPAS,IOYSTR,IOYSTP,ILO,IHI,INFIL1,ICONT1,JPAS		**** A8
COMMON/XXX/DELX,DELT,MS,WTART,80(25),TEN(25),CHECK(25),MOISIN		CHK 9
1(25),CMM201(25),MOISOUT(25),AN03(25),ANH3(25),UREA(25),ORN		CHK 11
2(25),CA(25),ANA(25),AMG(25),HCO3(25),CL(25),CO3(25),S04(25)		CHK 12
3),E5(25),C5(25),S45(25),XX5(25),CASO(25),AGS0(25),BNH4(25),CHK		CHK 13
4EC(25),CN1(25),SAMT(25),RN(25),RC(25),TEM(25),CAL(25),Q,SROCHK		CHK 14
IP,XTRACT,SUMN03,THOR(4),TO,IDAY,U(25),CH,CHI,IRERUN		CHK 15
COMMON/XX2/A1,A2,A3,X		CHK 16
		CHK 17
REAL MOISIN, MOISOUT		CHK 18
		CHK 19
DIMENSION X(7,25)		CHK 20
		CHK 21
L1 = L2 = L3 = 0		CHK 22
IF(ABS(EXNH3).LT.A1.AND.ABS(EXCA).LT.A1)1,2		CHK 23
1 IF(ABS(EXANA).LT.A1.AND.ABS(EXAMG).LT.A1)3,2		CHK 24
3 IF(ABS(X(2,J) - ANH3(J)).LT.A1)4,2		CHK 25
4 IF(ABS(X(5,J) - CA(J)).LT.A1)5,2		CHK 26
5 IF(ABS(X(6,J) - ANA(J)).LT.A1)6,2		CHK 27
6 IF(ABS(X(7,J) - AMG(J)).LT.A1)7,2		CHK 28

7	L1 = 1	CHK	29
	2 IF(NRYPAS.EQ.1) GO TO 9007	****	A29
	IF(ARS(DELN03).LT.A2.AND.ARS(DELNH3).LT.A2)8.9	CHK	30
8	IF(ABS(DELOGN).LT.A2.AND.ABS(DELUREA).LT.A2)10.9	CHK	31
10	IF(ARS(X(1.J) - AN03(J)).LT.A2)11.9	CHK	32
11	IF(ARS(X(2.J) - ANH3(J)).LT.A2)12.9	CHK	33
12	IF(ARS(X(4.J) - ORN(J)).LT.A2)13.9	CHK	34
13	IF(ARS(X(3.J) - UREA(J)).LT.A2)14.9	CHK	35
14	L2 = 1	CHK	36
	9007 CONTINUE	****	A36
9	IF(ARS(MOISIN(J)).GT.A3.OR.ABS(MOISOUT(J)).GT.A3)15.16	CHK	37
16	L3 = 1	CHK	38
15	X(1.J) = AN03(J) SX(2.J) = ANH3(J)	CHK	39
	X(3.J) = UREA(J) SX(4.J) = ORN(J)	CHK	40
	X(5.J) = CA(J) SX(6.J) = ANA(J)	CHK	41
	X(7.J) = AMG(J)	CHK	42
	RETURN	CHK	43
	END	CHK	44

SUBROUTINE SKIP

	SUBROUTINE SKIP(IUNIT)	SKIP	10
C----		SKIP	20
C----	CYBER 74-28	SKIP	30
C----	PROGRAM TO SKIP FROM PRESENT LOGICAL FILE TO NEXT LOGICAL FILE	SKIP	40
C----	IUNIT=LOGICAL UNIT NUMBER	SKIP	50
C----		SKIP	60
10	READ(IUNIT) IDUM	SKIP	80
	IF(EOF(IUNIT))20.10	SKIP	90
20	RETURN	SKIP	100
	END		

SUBROUTINE BACK

	SUBROUTINE BACK(IUNIT)	BACK	10
C----		BACK	20
C----	CYBER 74-28	BACK	30
C----	PROGRAM TO BACK FROM PRESENT LOGICAL FILE TO END OF PREVIOUS	BACK	40
C----	LOGICAL FILE (IE.JUST BEFORE END-OF-FILE MARK)	BACK	41
C----	IUNIT=LOGICAL UNIT NUMBER	BACK	50
C----		BACK	60
10	BACKSPACE IUNIT		
	READ(IUNIT)	BACK	80
	IF(EOF(IUNIT))30.20	BACK	90
20	BACKSPACE IUNIT	BACK	100
	GO TO 10	BACK	110
30	BACKSPACE IUNIT	BACK	120
	RETURN	BACK	130
	END	BACK	140

TECHNICAL REPORT DATA
(Please read Instructions on the reverse before completing)

1. REPORT NO. EPA-600/2-79-148		3. RECIPIENT'S ACCESSION NO.	
4. TITLE AND SUBTITLE IRRIGATION PRACTICES AND RETURN FLOW SALINITY IN GRAND VALLEY		5. REPORT DATE August 1979 issuing date	
7. AUTHOR(S) Gaylord V. Skogerboe, David B. McWhorter, and James E. Ayars		6. PERFORMING ORGANIZATION CODE	
9. PERFORMING ORGANIZATION NAME AND ADDRESS Agricultural and Chemical Engineering Department Colorado State University Fort Collins, Colorado 80523		8. PERFORMING ORGANIZATION REPORT NO.	
12. SPONSORING AGENCY NAME AND ADDRESS Robert S. Kerr Environmental Research Laboratory Office of Research and Development U. S. Environmental Protection Agency Ada, Oklahoma 74820		10. PROGRAM ELEMENT NO. 1B8770	
		11. CONTRACT/GRANT NO. Grant No. S-800687	
		13. TYPE OF REPORT AND PERIOD COVERED Final	
		14. SPONSORING AGENCY CODE EPA/600/15	
15. SUPPLEMENTARY NOTES 216 pages, 52 fig., 42 tab., 93 ref.			
16. ABSTRACT <p>This study was undertaken to evaluate the relationships between leachate volume and chemical quality. A numerical model of soil moisture and salt transport was used. Field data were collected on 63 research plots located in the Grand Valley, Colorado. From the calibration of the moisture flow model using infiltration data, water content profiles and storage change data, it was concluded that soil moisture flow could be adequately modeled for the Grand Valley. From comparisons of field and simulated data used in evaluating the soil chemistry model, it was concluded that TDS concentrations were adequately modeled but that individual ionic species concentrations were not. The TDS profile calculated at the beginning and end of the growing season show the salt concentration in the profile below the root zone to be relatively constant. This region acts as a buffer and causes the salt concentration of the return flow to be relatively constant. This means the reductions in salt loading are directly proportional to reductions in the volume of return flow.</p>			
17. KEY WORDS AND DOCUMENT ANALYSIS			
a. DESCRIPTORS	b. IDENTIFIERS/OPEN ENDED TERMS	c. COSATI Field/Group	
Fluid infiltration, Irrigation, Saline soils, Salinity, Seepage, Water distribution, Water loss, Water pollution, Water Quality	Colorado River, Furrow irrigation, Grand Valley, Irrigation practices, Return flow, Salinity control	98C	
18. DISTRIBUTION STATEMENT Release to Public	19. SECURITY CLASS (This Report) Unclassified	21. NO. OF PAGES 218	
	20. SECURITY CLASS (This page) Unclassified	22. PRICE	